Simulation and Optimization of Optical Amplifiers in Optical Communication Networks

A Thesis

Submitted in fulfillment of the requirement for the award of degree

of

DOCTOR OF PHILOSOPHY

Submitted by

SURINDER SINGH

Regd. No.: 9041252

Supervisor

Dr. R. S. KALER

Department of Electronics and Communication Engineering

Thapar University, Patiala (Punjab) India

DEPARTMENT OF ELECTRONICS AND COMMUNICATION ENGINEERING

THAPAR UNIVERSITY

PATIALA-147001

October, 2007

CERTIFICATE

I, Surinder Singh hereby certify that the work which is being presented in this thesis entitled **"Simulation and Optimization of Optical Amplifiers in Optical Communication Networks"** in partial fulfillment of requirements for the award of degree of Doctor of Philosophy in Electronics and Communication Engineering from Thapar University, Patiala, is an authentic record of my own work carried under the supervision of Dr. R. S. Kaler.

The matter presented in this thesis has not been submitted in any other University/ Institute for the award of any degree.

(Surinder Singh)

Signature of the Student Date: 14 Oct, 2007

This is certified that the above statement made by the candidate is correct to the best of my knowledge.

(Dr. R. S. Kaler)
Guide & Professor of ECED
Thapar University, Patiala
Date:

Abstract

For several years now, optical fiber communication systems are being extensively used all over the world for telecommunication, video and data transmission purposes. Fiber optics has made a revolutionary change in commercial telecommunications over the past few decades. The demand for transmission over the global telecommunication network will continue to grow at an exponential rate and only fiber optics will be able to meet the challenge. Multimedia optical networks are the demands of today to carry out large information like real time video services. Presently, almost all the trunk lines of existing networks are using optical fiber. This is because the usable transmission bandwidth on an optical fiber is so enormous (as much as 50 THz) as a result of which, it is capable of allowing the transmission of many signals over long distances. However, attenuation is the major limitation imposed by the transmission medium for long-distance high-speed optical systems and networks. So with the growing transmission rates and demands in the field of optical communication, the electronic regeneration has become more and more expensive. The powerful optical amplifiers came into existence, which eliminated the costly conversions from optical to electrical signal and vice versa.

Due to the need of longer and longer unrepeated transmission distances and ultra fast broadband transmission, the advanced transmission schemes have to be investigated. So, it is imperative to investigate into the feasibility of unrepeated transmission and ultra fast broadband transmission over long distances. In order to achieve these goals *i.e.* broadband and repeaterless transmission of an optical communication system, it is of utmost importance to optimize the optical amplifier and have placement in optical networks.

The semiconductor optical amplifiers (SOAs) have attracted much attention as they are cost effective as compared to erbium doped fiber amplifiers for long haul optical communication system. The semiconductor optical amplifiers (SOAs) have wide gain spectrum, low power consumption, ease of integration with other devices and low cost. But as gain saturation problem arises in multichannel optical system, it limits the system performance.

This thesis is mainly concerned with the use of optical amplifiers (SOAs and EDFAs) in multichannel wavelength division multiplexing (WDM) optical communication system

and network. The aim of investigation is to increase the transmission distance, flexibility and cascadability of optical networks by optimizing optical amplifiers (SOAs, EDFAs).

The cascaded utilization of the semiconductor optical amplifier (SOA) is not possible for long transmission distance due to gain saturation problem which arises from cross gain modulations (XGM), cross phase modulation (XPM) and four wave mixing (FWM) etc. Therefore, these nonlinearities of SOA produce crosstalk and power penalty problems in long haul WDM optical communication system.

In order to utilize the SOA for long haul WDM transmission link, the structural optimization is performed by developing the SOA model based on the analysis for multichannel WDM optical communication system. Therefore it is essential to optimize structural parameters of SOA in order to reduce the power penalty and bit error rate problem which arises due to gain saturation. The optimization is made by simulation of multichannel WDM optical transmission link with cascaded SOA. The effect of amplified spontaneous emission (ASE) noise is also minimized for adequate amplification factor. It is observed that differential phase shift keying (DPSK) system has large capacity as compared to on off keying (OOK) system by using cascaded optimizing SOA for 1050 km transmission distance.

The simulative optimization of confinement factor and differential gain is done for reducing cross gain modulation of SOA for improving transmission distance at 40 Gb/s and 80 Gb/s. The soliton RZ-DPSK WDM signals with high capacity up to 0.4 Tb/s is transmitted up to a distance of 4550 km successfully by using optimized semiconductor optical amplifiers with spectral efficiency of 0.4 bit/s/Hz. It is observed from the XPM analysis that by increasing the carrier lifetime, width and thickness while reducing confinement factor, differential gain and bias current in the SOA structure, mitigate the crosstalk due to the cross phase modulations. It is shown that the SOA model obtained on basis of XPM is attractive, when used as pre-amplifiers and in-line amplifier for long haul links up to 5250 km for 10 × 40 Gb/s soliton DPSK WDM signals. These results provide useful information for designing of long WDM transmitter links at higher capacity by using low cost SOA.

The placement of SOA is investigated for long haul WDM and DWDM (dense wavelength division multiplexing) transmission of RZ-DPSK signal. It is shown that post-power compensation method is superior than pre- and symmetrical-power compensation methods. By using optimum span scheme based on post-power compensation method, it is possible to transmit ten channels at 10 Gb/s up to transmission distance of 68908 km

for channel spacing of 100 GHz. Further by optimization of the optical phase modulator bandwidth *i.e.* 5.5 GHz for 400 mA bias current, the maximum transmission distance approaches to 17227 km for 10 × 10 Gb/s DWDM signals for channel spacing of 20 GHz by using same optimum span scheme.

The improvement of receiver sensitivity and bandwidth of a SOA pre-amplifier model is developed by reducing ASE noise extremely low *i.e.* 22.3 μW for 0.1 mW input power. The minimum receiver sensitivity of -69.9 dBm is observed at BER floor of 4.6×10^{-10} for PIN receiver at 10 Gb/s. Also improvement of receiver sensitivity of -19.2 dBm and -46.5 dBm is observed for PIN receiver and DPSK receiver at 40 Gb/s. It has been shown that the gain variation increases with the increase of input light power and is also observed that tolerance of input wavelength power is more than 100 nm. The SOA optical pre-amplifier is found to be more relaxed from optical alignment and anti-reflection coating and eliminates the need of optical filter.

Due to limited bandwidth of the SOA, there is requirement of EDFAs for larger bandwidth optical communication system. We are using different approaches to gain flattening in EDFAs without using additional components *i.e.* gain flattening filter, dispersion shift fiber and periodic gratings etc. The gain flattening can be achieved by connecting two EDFAs with opposite gain characteristic *i.e.* peak gain of first EDFA for a given wavelength and another EDFA has a valley gain with same wavelength. The overall power penalty can be reduced by using 3rd pre-amplifier EDFA. Therefore, by using gain flattening approach, the maximum transmission distance up to 490 km can be achieved for sixteen channels at 40 Gb/s with channel spacing of 200 GHz. Another approach by using optical super Gaussian notch filter, the transmission distance is improved up to 504 km for 16 × 40 Gb/s WDM for non return to zero (NRZ) signals.

The wavelength converter leads to the increase the cascadability and capacity of future optical networks. The nonlinearities of SOA like four wave mixing (FWM) and cross phase modulation (XPM) is utilized for improving the performance of wavelength converter based on FWM and XPM. The effect of FWM and XPM in SOA is improved by structural parameter optimization of SOA. This can be done in such a manner that the SOA never saturates and produces maximum FWM and XPM signals with minimum gain fluctuations. It is shown that 50 nm up and down wavelength conversion is possible for the NRZ-DPSK by using FWM in SOA. The Q factor improvement observed is 1.74 dB for signal-to-pump ratio of -5 dB at 0 dBm pump signal for 50 nm up converter. Ten stage cascaded wavelength conversion over 1302 km single mode transmission is possible for

10 Gb/s NRZ-DPSK by using FWM in the SOA. The wavelength conversion based XPM in the SOA-MZ1 configuration has wide band *i.e.* more than 15 nm up and down conversions with conversion efficiency more than -9 dB. It is observed that high active region length and bias current in the SOA leads to XPM in the SOA-MZ1 configuration.

The performance of optical communication network topologies *i.e.* bus, ring, star, and tree is compared for 10 Gb/s DPSK signal in the presence of optimized SOA at minimum signal input power. The bus network topology supported maximum 27 users. For ring network topology, the maximum nodes are more than 29. The number of users supported can be increased by decreasing splice and insertion loss in star network topology. It is evaluated that tree network topology offers maximum numbers of users with minimum utilization of optimized SOAs and optical couplers. Therefore, tree network topology in the presence of optimized SOAs provided low cost solution for connecting metropolitan area networks.

Therefore, this study establishes the optimization of optical amplifiers in the fiber optical communication networks resulting in the revolutionary growth of internet traffic for terrestrial fiber backbone networks. Also, the number of users and transmission distance can be increased by improving the power budget or reducing the losses in the network by using these optical amplifiers. Most of the research findings of this thesis have been published in various international referred journals (Chapters 2, 3, 4, 5, 6 and 7) as per the list at pages (237-238).

Acknowledgement

I am highly indebted to my thesis supervisor Prof. R.S. Kaler, Department of Electronics and Communication Engineering, Thapar Engineering Campus, Thapar University, Patiala, Punjab, India for giving me the opportunity to work under his supervision. He had encouraged me in my period of distress and anxiety and guided me to accomplish this research work.

I am extremely thankful to Dr. Abhijit Mukherjee, Hon'ble Director of Thapar University, Patiala, for allowing me to use all necessary infrastructure and facilities needed for successful accomplishment of this research work.

I must acknowledge the staff of Electronics and Communication Engineering, Thapar Institute of Engineering and Technology, Patiala (Dr Sushil Mittal, Dr.A.K. Chatterjee, Dr. Sanjay Sharma) for their support and help.

I am extremely thankful to the referees of various Journals who critically examined my papers. Their suggestions and comments have really helped in me bringing this thesis to the present shape.

I also wish to extend my thanks to Dr. Harpal Singh (Principal), Dr. Savina Bansal (Head), Dr. Ashok Kumar Goel and other colleagues of my college for their insightful comments and constructive suggestions to improve the quality of this research work. I want to pay my hearty gratitude to Ms. Swati Gupta, Mr Sanjeev Kumar and Mr. Darshan Singh for their valuable views and encouragement.

I acknowledge my parents for their blessings and support who had kept me free from my duties at home so that I can devote maximum time to my research work. Finally, words are not adequate to express my deep gratitude to my wife 'Lovkesh' for her patience, support, and active assistance in many ways.

I sincerely thank all the persons who have helped and supported me directly or indirectly in the course of this research work.

(Surinder Singh)

vii

TABLE OF CONTENTS

LIST OF FIGURES

LIST OF TABLES

LIST OF SYMBOLS

λ	Wavelength of light
c	Velocity of light
q	Charge of electron
h	Plank constant
hf	Energy of photon
E	Photon energy
N_1 , N_2	Population densities of lower and upper state
N	Carrier density
R_{spon}	Rate of spontaneous emission
R_{stim}	Rate of stimulated emission
R_{abs}	Rate of absorption
R_{nr}	Nonradiative recombination rate
K_B	Boltzmann constant
T	Absolute temperature
$\rho_{em}(\omega)$	Spectral density of photons
$f_c(E_2)$, $f_v(E_1)$	Occupations probability electrons in conduction and valence bands
ρ_{cv}	Joint density of the states
g	Optical gain of SOA
g_o	Small signal gain of SOA
G	Amplification factor of SOA
G_o	Unsaturated amplifier gain of SOA
Γ	Confinement factor of SOA
a	Differential gain of SOA
V	Active region volume of SOA
I	Bias current of SOA
τ	Carrier lifetime of SOA
Δf	Optical bandwidth of the amplifier

α_{int}	Input/Output insertion loss of SOA
α_p	Material loss of SOA
N_t	Transparency carrier density of SOA
L	Length of semiconductor optical amplifier
t_a	Thickness of active region of SOA
P_{in}, P_{out}	Input and output power of SOA
P_s	Saturation power
P_{out}^s	Output saturation power
P_{ASE}, P_{sp}	Spontaneous emitted power at the output of SOA
i_{sp}	Photocurrent equivalent to spontaneous emission power
F_n	Noise figure of SOA
N_{shot}	Shot noise
N_{s-sp}	Signal to spontaneous beat noise, spontaneous to
N_{sp-sp}	Spontaneous beat noise
N_{th}	Thermal noise
B_e	Electrical bandwidth
B_o	Optical filter bandwidth after SOA pre-amplifier
m	Number of polarization modes
η_{in}, η_{out}	SOA input and output coupling efficiencies
L_l	Optical loss between the amplifier and the receiver
I_s	Photocurrent equivalent of amplifier input power
N_{sp}	Population inversion factor
t, z	Time and position along the propagation direction of light
J	Injection current density
$N(t,z)$	Carrier density as the function of time and position
$g(t,z)$	Gain coefficient of the SOA
M	Total number of channels
w, t_{eff}, α_w	Width, effective thickness and loss of waveguide

$\overline{N}$, P_L	Rate of change of carrier density and power coefficient
Δg	Small dynamic variation of gain
$P_{penalty}$	Power penalty
ΔP_1	Power variations
$\sigma^2_{\Delta g(t,z)}$	Variance of gain variation
$\Delta g_m(t,z)$	Mean value of small gain fluctuation
E_b	Energy per bit
N_o	Part of input signal instead of ASE generated by the SOA
L_1 , L_2	Lengths of SMF and DCF
D_1 , D_2	Dispersion parameters for SMF and DCF
$\partial D_1/\partial\lambda$, $\partial D_2/\partial\lambda$	Second order dispersion parameters for SMF and DCF
$\Phi(t)$	Phase shift induced by signal in SOA
β	Line_width enhancement factor
$\Delta\Phi(t,z)$	Differential phase error as the function of time and position of photon
η	Quantum efficiency of PIN photodetector
N_p	Number of photons per bit
$P_{Optimum}$	Power penalty for optimum span scheme
P_{Equal}	Power penalty for equal span scheme
$P_{Convention\ al}$	Power penalty for conventional span scheme
A,	Nonradiative recombination,
B	Spontaneous emission
C	Auger recombination terms
χ	Saturation parameter of EDFA
b_{eff}^2	Effective radius of the doped region
τ_1	Metastable lifetime of the doped fiber
n_t	Average ion density of doped fiber
$g(\lambda), \alpha(\lambda)$	Gain and absorption coefficients of doped fiber

$\sigma_{em}(\lambda), \sigma_{abs}(\lambda)$	Emission and absorption cross-sections of doped fiber
$\Gamma(\lambda)$	Overlap integral between the optical mode inside the fiber and the erbium doping profile
v_1, v_2	Frequencies of input signal
N_u	Number of users

LIST OF ACRONYMS

OA	Optical amplifier
SOA	Semiconductor Optical Amplifier
TWA	Travelling wave amplifier
FPA	Fabry-perot amplifier
EDFA	Erbium doped fiber amplifier
InGaAlAsP	Indium gallium aluminium arsenide phosphide
SRS	Stimulated Raman scattering
SBS	Stimulated Brillouin scattering
RZ	Return to zero
CSRZ-DPSK	Carrier sense return zero differential phase-shift keying
NRZ-DPSK	Non-return to zero differential phase shift keying
ASE	Amplified spontaneous emission
DFA	Distributed fiber amplifier
DRA	Distributed Raman amplifier
XGM	Cross gain modulation
FWM	Four wave mixing
XPM	Cross phase modulation
TDM	Time division multiplexing
WDM	Wavelength division multiplexing
FEC	Forward error check
MAN	Metropolitan area network
WAN	Wide area network
FDDI	Fiber distributed data interface
BER	Bit error rate
OSNR	Optical signal to noise ratio
OOK	On-Off keying
MZ1	Mach-Zehnder interferometer
DWDM	Dense wavelength division multiplexing
FWHM	Full wave half maxima
PBRS	Pseudorandom binary sequence
CW	Continuous wave
Q	Quality

SMF	Single mode fiber
DCF	Dispersion compensating fiber
IM DD	Intensity modulated direct detection
NRZ	Non return to zero
APD	Avalanche photodiode
TE	Transverse electric
TM	Transverse magnetic
PMD	Polarization mode dispersion
ITU	International telecommunication union

Chapter 1
Introduction

1.1 Introduction

Information revolution implies that multimedia networks need high bandwidth for real-time communication services. At present, optical fiber is the only transmission medium offering such large bandwidth with low loss communication links. One of the foundations of this information society is high capacity optical fiber communications, which has been one of the fastest growing industries since the 1980s and is the key technology to fulfill the demands for bandwidth for broadband systems. The early optical fiber had a very high attenuation up to 1000 dB/km and could not be used for commercial fiber optical communication systems. In 1970, the scientists at Corning Glass Works were successful in producing a fiber with 20 dB/km loss which opened the doors for optical fiber communications. Now a day, the optical fibers with losses up to 0.2 dB/km are commercially available.

In fiber optic communication, there is degradation of transmission signal with increased distance. By the use of optoelectronic repeater, this loss limitation can be overcome. In optoelectronic repeater, optical signal is first converted into electric signal and then after amplification it is regenerated by transmitter. But such regeneration becomes quite complex and expensive for wavelength division multiplexing systems. So, to remove loss limitations, optical amplifiers are used which directly amplify the transmitter optical signal without converting it into electric forms. The optical amplifiers are used in linear mode as repeaters, optical gain blocks and optical pre-amplifiers. The optical amplifiers are also used in nonlinear mode as optical gates, pulse shaper and routing switches. The optical amplifiers are mainly used for amplification of all channels simultaneously in WDM light wave system called as optical in-line amplifiers. The optical amplifiers are also bit rate transparent and can amplify signals at different wavelengths simultaneously. The optical amplifier increases the transmitter power by placing an amplifier just after the transmitter called power booster. The transmission distance can also be increased by putting an amplifier just before the receiver to boost the received power. The optical amplifier magnifies a signal immediately before it reaches the receiver called as optical pre-amplifier.

1.2 Principle of Optical Amplifiers

The interaction of light with matter takes place in discrete packet of energy or quanta called photons. Atom exists only in certain discrete energy state, absorption and emission of light cause them to make a transition from one discrete energy state to another state and related to difference of energy E between the higher energy state E_2 and lower energy state E_1 as shown in figure (1.1). When photon energy E is incident on atom, it may be excited into higher energy state E_2 through absorption of photon called absorption as shown in figure (1.1a). As atom in energy state E_2 is not remain stable, atom returns to lower energy state in random manner by generating a photon as shown in figure (1.1b). This is called spontaneous emission.

The stimulated emission occurs, when incident photon having energy $E = hc/\lambda$ interact with electron in upper energy state causing it to return back into lower state with creation of second photon as shown in figure (1.1c), where h is Plank constant, c is velocity of light and λ is the wavelength of light [Mynbeav and Scheiner, 2003]. The light amplification occurs, when incident photon and emitted photon are in phase and release two more photons. The continuation of this process effectively creates avalanche multiplication and the amplified coherent emission is obtained.

To achieve optical amplification, the population of upper energy level has to be greater than that of lower energy level *i.e.* $N_1 > N_2$, where N_1, N_2 are population densities of lower and upper state. This condition is known as population inversion. This can be achieved by exciting electron into higher energy level by external source called pumping.

1.3 Types of Optical Amplifiers

The optical amplifiers are classified on the basis of device characteristics *i.e.* whether it is based on linear characteristic (Semiconductor optical amplifier and Rare-earth doped fiber amplifiers) or non-linear characteristic (Raman amplifiers and Brillouin amplifiers). Optical amplifiers are also classified on the basis of structure *i.e.* whether it is semiconductor based (Semiconductor optical amplifiers) or fiber based (Rare earth doped fiber amplifiers, Raman and Brillouin amplifiers).

1.3.1 Semiconductor Optical Amplifiers

The semiconductor optical amplifiers (SOAs) use the principle of stimulated emission to amplify an optical information signal. The optical input signal carrying original data

enters into the semiconductor active region through coupling. The coupling is required because the mode field diameter of single mode beam is 9.3 μm while size of active region is less in order of tenth of micrometers [Mynbeav and Scheiner, 2003]. The injection current delivers the external energy to pump the element at conduction band. The input signal stimulates the transition of electrons down to valence band and emits photons having same energy and wavelength as the input signal, so the amplified optical signal is obtained. The SOA is of two types; fabry-perot amplifier (FPA) and travelling wave amplifier (TWA). The fabry-perot amplifier **(**FPA) configuration is same as fabry-perot laser. In this, the light entering the active region is reflected several times from cleaved face and is amplified as it leaves the cavity. The travelling wave amplifier is an active medium without reflective facets. So that the input signal is amplified by a single passage through active region. The practical active region without reflective facets was made by covering the facets of semiconductor material by antireflection coating, tilting the active region with respect to facet and by using buffer material between active region and facet to reduce reflectance R as small as 10^{-4} [Mahony *et al.*,1998].

The stimulating emission can dominate only if the condition of population inversion is satisfied. For SOA this condition is realized by doping the p-type and n-type cladding layer so heavily that the Fermi level separation the band gap under forward bias of p-n junction. The rates of spontaneous emission, stimulated emission and absorption can be written as

$$R_{spon} = AN_2$$

$$R_{stim} = BN_2\rho_{em}$$

$$R_{abs} = B^{'}N_2\rho_{em} \tag{1.1}$$

Where A, B and $B^{'}$ are constants. ρ_{em} is the spectral density of photons. Also, N_2 is the atomic density of excited state. In thermal equilibrium, the atomic densities are distributed according to Boltzmann statistics [Saleh and Teich, 1991], *i.e.*

$$\frac{N_2}{N_1} = \exp\left(\frac{-E}{K_BT}\right) \equiv \exp\left(\frac{-hf}{K_BT}\right) \tag{1.2}$$

Where K_B is Boltzmann constant and T is the absolute temperature. Since N_1 and N_2 do not change with time in thermal equilibrium, the upward and downward transition rate should be equal

$$AN_2 + BN_2\rho_{em} = B^{'}N_1\rho_{em} \tag{1.3}$$

By using equation (1.2) in (1.3), the spectral density ρ_{em} becomes

$$\rho_{em} = \frac{A/B}{\left(B^{'}/B\right)\exp\left(\frac{hf}{K_B T} - 1\right)} \tag{1.4}$$

The stimulated emission and absorption rates can be obtained in similar manner and are given by

$$R_{stim}(\omega) = \int_{E_c}^{\infty} B(E_1, E_2) f_c(E_2)[1 - f_v(E_1)]\rho_{cv}\rho_{em}\partial E_2 \tag{1.5}$$

$$R_{abs}(\omega) = \int_{E_c}^{\infty} B(E_1, E_2) f_v(E_1)[1 - f_c(E_2)]\rho_{cv}\rho_{em}\partial E_2 \tag{1.6}$$

Where $f_c(E_2)$ and $f_v(E_1)$ are the occupation probability electrons in conduction and valence bands. Also, $\rho_{em}(\omega)$ is the spectral density of photons and ρ_{cv} is joint density of the states (number of states per unit volume per unit energy) E_c is the energy of conduction band.

When injected carrier density in active layer exceeds a certain value known as transparency value, population inversion is realized and active region exhibits optical gain. An input signal propagating inside the active layer would then amplify as $exp(gz)$, where g is gain coefficient. In this g is proportional to $R_{stim} - R_{abs}$. When g is the function of injected carrier density N, then peak value of gain g_p depends upon N which is given by empirical approach as

$$g_p(N) = a(N - N_t) \tag{1.7}$$

Where N_t is the transparency value of a carrier density and a is called the differential gain. Typical value of N_t and a for InGaAsP amplifiers are in the range $1.0 - 1.5 \times 10^{18}$ cm^{-3} and $2 - 3 \times 10^{-16}$ cm^{-3}, respectively [Agrawal and Dutta, 1993].

The small signal gain is given by

$$g_o = (\Gamma \alpha / V)(I \tau / q - N_t) \tag{1.8}$$

Where Γ is the confinement factor, α is the differential gain, V is the active volume, I is the bias current, q is the charge of electron and N_t is the transparency carrier density. Also τ is carrier lifetime represents the total recombination time of charge carrier in absence of stimulated recombination.

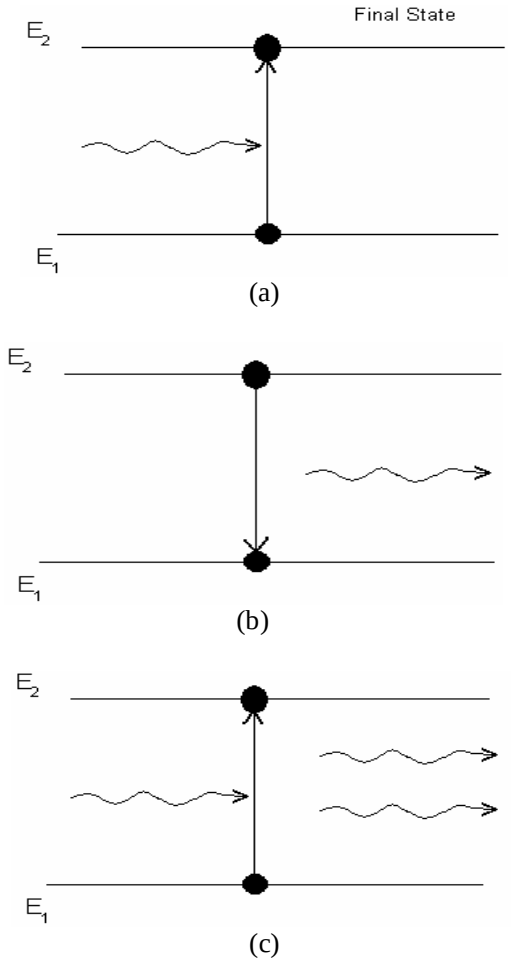

Figure 1.1: Absorption, spontaneous emission and stimulated emission process.

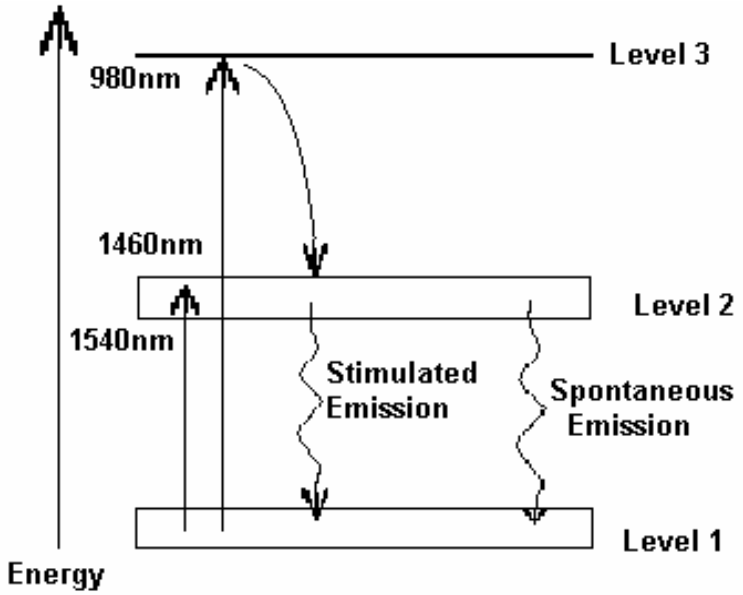

Figure 1.2: Energy level diagram for different levels in doped fiber amplifier.

It is defined as $R_{spon} + R_{nr} = (N/\tau)$, where N is carrier density and R_{nr} is nonradiative recombination rate. R_{spon} and R_{nr} increase nonlinearly with N such that

$$R_{spon} + R_{nr} = AN + BN^2 + CN^3$$

Where A is nonradiative coefficient due to recombination at defects or traps, B is the spontaneous radiative recombination coefficient, and C is the Auger coefficient. The carrier lifetime then becomes N dependent and it is obtained by using $\tau = A + BN + CN^2$.

1.3.2 Fiber Amplifiers

The fiber amplifiers also act as power amplifier, repeater, and a pre-amplifier. The gain medium comprises a length of single mode fiber connected to WDM coupler, which provides low insertion loss at both signal and pump wavelength [Agarwal, 2001]. The excitation occurs through optical pumping laser along with optical input signal within the coupler. The stimulated emission process occurs inside the fiber gain medium. The amplified optical signal is emitted from the other end of fiber made from heavily doped ions depending upon type of fiber amplifiers *i.e*. rare-earth doped fiber amplifier, Raman fiber amplifier and Brillouin fiber amplifier.

1.3.2.1 Rare Earth Doped Fiber Amplifier

Different rare-earth ions such as erbium, holmium, neodymium, praseodymium, thulium and ytterbium can be used to realize fiber amplifiers operating at different wavelength covering from visible to infrared region. In the rare earth doped fiber amplifier, erbiums dopant in silica based single mode fiber is used and is called erbium doped fiber amplifier (EDFA). A piece of fiber gain medium is an active medium that is heavily doped with ions of erbium. In this, population inversion is stronger due to large number of erbium ions that fall into level 2 from various upper levels as shown in figure (1.2). When the optical information passes through such a highly populated erbium doped fiber, it would stimulate transition of erbium ions from level 2 to level 1 and generates photon of same wavelength, direction and phase as applied photon [Diagonnet *et al.*,1993].

The EDFA consists of three basic components: length of erbium doped fiber, pump laser and wavelength selective coupler to combine the signal and pump wavelengths as shown in figure (1.3). The optimum fiber length used depends upon the pump power, input signal power, amount of erbium doping and pumping wavelength. Erbium doped fiber amplifiers (EDFAs) can be extensively used in optical fiber communication systems due

to their compatibility with optical fiber. It has low insertion loss, low crosstalk, high gain, polarization insensitive and low noise figure [Desurvire *et al.*,1989]. An EDFA has a comparatively wide wavelength range of amplification making it useful as transmission amplifier in wavelength division multiplexing systems. Theoretically EDFA is capable of amplifying all the wavelengths ranging from 1500 to 1600 nm. However practically there are two windows of wavelength. These are C and L band. The C band ranges from 1530 nm to 1560 nm and L band from 1560 nm to 1610 nm. The semiconductor laser pumping source at 980 nm wavelength has proved to be the best in terms of efficiency (more than 10 dB gain per mW pump power) and better noise performance [Giles and Desurvire, 1991]. It is typically evaluated that the noise figure lies in between 4-5 dB and efficiency between 40-50 % for forward pumping. Similarly, the equivalent noise figure for backward pumping is 6-7 dB and efficiency between 60-70 %. The pumping light wavelength was 1480 nm for both case [Yoneda and Okshi, 1992]. But at this wavelength, the population inversion is not strong as compared to 980 nm wavelength. The praseodymium-doped fluoride fiber amplifier is similar to EDFA but operated at 1300 nm with noise figure 3-5 dB showing best performance.

Thulium-doped fiber amplifiers have extended transmission bandwidth of optical fibers beyond the range available from the EDFA [Kasamatsu *et al.*, 2001].

1.3.2.2 Raman Amplifier

Raman optical amplifiers differ in principle from EDFAs or conventional lasers in that they utilize stimulated Raman scattering (SRS) to create optical gain. In this scattering, some pump photons give up their energy to create other photons of reduced energy at a lower frequency, the remaining energy is absorbed by silica molecules which end up in an excited vibrational state. Here optical phonons participate in scattering process. The principle can also be expressed by taking example of spring that is stretched from *b* to *a*. if we put energy into the spring, the entire spring moves. Some energy however scatters. This scattered energy is at a longer wavelength (lower power) which boosts signals at that wave length throughout the fiber. Therefore, if we pump the power at 1450 nm with a gain of 100 nm, signals at 1550 nm receive a boost in power.

The Raman scattering process becomes stimulated if the pump power exceeds a threshold value. The SRS can occur in both forward as well as backward direction in optical fibers. The beating of the pump with scattered light in these two directions creates a frequency component at the beat frequency ω_p-ω_s, which acts as a source that derives molecular

vibrations. Since amplitude of scattered wave increases in response to these oscillations, a positive feedback loop sets in. The spectrum of the Raman gain depends on the decay time associated with excited vibrational state. This decay time is 1 ns for gas or liquid, resulting in a Raman gain band width of 1 GHz. In case of optical fibers the band width exceeds 10 THz.

Figure (1.4) shows population inversion in Raman fiber. The broadband and multipeak nature of the spectrum is due to the amorphous nature of glass. As a result, the stokes frequency ω_s can differ from pump frequency ω_p over a wide range. The maximum gain occurs when Raman shift (ω_p-ω_s) is about 13 THz. Another major peak occurs near 15 THz while minor peaks at 35 THz. The peak value of Raman gain is about 10^{-13} m/W at a wavelength of 1 μm. SRS is especially useful because of its extremely large bandwidth. Raman gain is used for compensating fiber losses.

Raman amplifiers are simple devices that use the intrinsic properties of silica fiber to create amplification, enabling the transmission fiber to become a distributed amplifier such that the gain in the fiber overcomes the loss of signal along the fiber. Raman amplification is based on stimulated Raman scattering (SRS), a non-linear effect of optical fiber in which gain is produced at lower energy wavelengths when excited (or pumped) with higher energy (at approximately 100 nm shorter wavelength) light.

The position of the gain bandwidth within the wavelength domain can be determined by selection of the pump wavelength. Thus, Raman amplification can be achieved in every region of the transmission window of the optical transmission fiber and thus push a fiber's capacity beyond C-band.

In the long haul space, we may replace existing erbium-doped fiber amplifier (EDFA) by combination of EDFAs and distributed Raman amplifiers (DRAs). The DRAs deliver broader and flatter gain spectrums with lower effective noise figure. These devices also reduced eye closure and have higher tolerance to transients. Based on the advantages above, DRA transmission is poised to grow as the next generation of long haul networks gets funded. Additionally, since these amplifiers work well with EDFAs, they can be used in conjunction with EDFAs to eliminate the number of amplifier sites and regenerators needed.

A fiber based Raman amplifier uses SRS when an intense pump beam propagates through it. The SRS is different from stimulated emission in one aspect, in this the incident pump photon gives up its energy to create another photon of reduced energy at a lower

frequency; the remaining energy is absorbed by the medium in the form of molecular vibrations that is optical phonons. This occurs when a sufficiently large pump wave is co-launched at a lower wavelength than the signal to be amplified. The Raman gain depends strongly on the pump power and the frequency offset between pump and signal. Amplification occurs when the pump photon gives up its energy to create a new photon at the signal wavelength, plus some residual energy, which is absorbed as phonons (vibrational energy) as shown in figure (1.5). As there is a wide range of vibrational states above the ground state, a broad range of possible transitions provide the gain. Generally, Raman gain increases almost linearly with wavelength offset between signal and pump peaking at about 100 nm and then dropping rapidly with increased offset.

In Raman amplifier, standard single mode optical fiber can be used generally. The main features of the Raman amplification were that it realized the continuous amplification along the fiber, it is bidirectional in nature and offers more stability, insensitivity to reflections [Senior, 1992]. The saturation optical power level was very high as it depends on the pump power [Aoki *et al.*, 1988]. The main disadvantage of this amplifier is that the pump power requirement is relatively high in comparison to SOA and EDFA.

1.3.2.3 Brillouin Fiber Amplifier

The operating principle of this amplifier is same as the Raman amplifier except that the optical gain is obtained by the stimulated Brillouin scattering (SBS). In this, each pump photon creates signal photon and the remaining energy is used to excite an acoustic phonon. The amplification occurs only when the signal beam propagates in the direction opposite to that of the pump beam (backward pumping). Brillouin gain spectrum is extremely small with bandwidth < 100 MHz [Senior, 1992]. The narrow bandwidth of this amplifier makes it less suitable as power amplifier, pre-amplifier or in-line amplifier in the light wave systems. This amplifier uses for channel selection by allowing amplification of a particular channel without boosting other nearby channels as shown figure (1.6).

1.4 Comparison between Optical Amplifiers

For SOAs and EDFAs, the gain is greater than 20 dB while for Raman fiber amplifiers gain is restricted to lower values [Agarwal, 1992]. The SOAs need an electrical bias supply at levels of around 50 mA while the supply requirement is much more stringent in erbium and Raman fiber amplifiers because of the high pump power laser requirement.

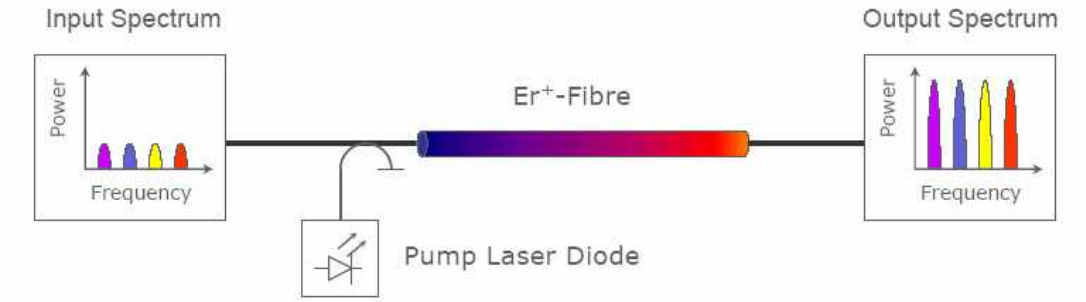

Figure 1.3: Typical Erbium doped fiber amplifier configuration.

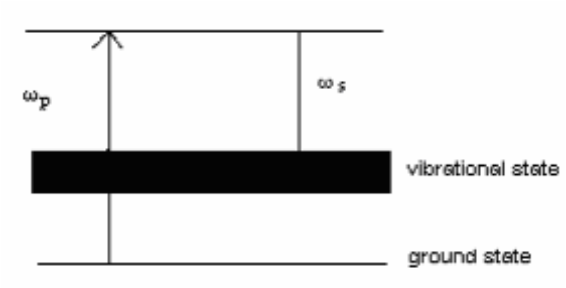

Figure 1.4: Population inversion in Raman amplifier.

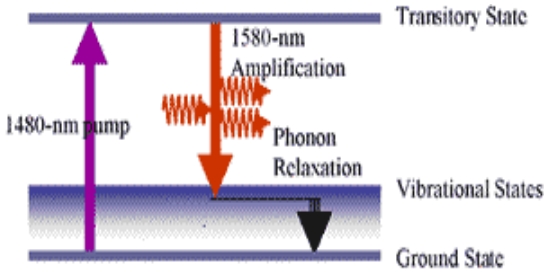

Figure 1.5: Energy states during SRS.

The SOA gain spectrum depends upon the band gap of material used, bias current and reflectivity of facets. The difference in signal and pump frequency (stokes shift) for SBS (Brillouin amplifiers) is smaller by three order of magnitudes compared with SRS (Raman amplifier) [Senior, 1992]. Inter modulation distortion and saturation induces crosstalk in WDM systems which are negligibly small in fiber amplifiers as compared to SOAs. For both SOAs and EDFAs, the saturated output power is typically a few milliwatts. In Raman and Brillouin amplifiers, the saturated output power could be much higher as it is limited only by pump power. The comparison characteristic and main features of optical amplifiers are given in table (1.1) [Senior, 1992; Agarwal, 1992; Mahony *et al*., 1998; Mynbeav and Scheiner, 2003]. Further, a representative gain spectral curve is shown in figure (1.6).

1.5 Literature Review

The idea of doping optical fibers with rare earth ions to realize amplifiers was investigated by Koestner and Snitzer [1964]. The first fiber amplifiers were pumped by flash lamps and operated in a pulsed mode. In the mid-1980s, the group led by D.N. Payne [Payne *et al.*, 1987] at the University of Southampton, developed a technology of rare earth ions deposition in single-mode silica fibers and the first EDFA was reported in 1987. The SOAs came into existence after generation of lasers in 1962 [Agarwal, 1992]. Both SOAs and Raman amplifiers were developed for practical use in 1980. The fourth generation of light wave systems made use of optical amplification for increasing repeater spacing and bit rate of wavelength division multiplexing systems. In most WDM systems, fiber losses were compensated periodically by using erbium doped fiber amplifiers spaced 60-80 km apart and amplifiers became commercial by 1990. The current emphasis of WDM light wave systems increased the system capacity by amplifying all channels by using single amplifier covering spectral region from 1.45 to 1.62 μm. Bergano *et al.* [1996] successfully demonstrated transmission of 640 Gb/s over 7200 km by using a re-circulating loop while Vareille *et al.* [1999] demonstrated the transmission capacity of 340 Gb/s over 6380 km on a straight-line test bed. Erwin *et al.* [2001] demonstrated 24,000 km transmission of dispersion-managed solitons at 40 Gb/s. The optical amplifiers have become an integral part of almost all fiber-optic communication installed after 1995. Upgradation of existing system is required for their excellent performance characteristics such as low insertion loss, high gain, large bandwidth, low noise and crosstalk, input/output signal levels.

1.5.1 Nonlinearities in Optical Amplifier

There are so many nonlinear effects present in the optical amplifiers which restrict it to use for various applications in optical communication systems even the gain bandwidth product of optical amplifiers are quite high. There are nonlinearities in the optical amplifiers such as gain saturation, four wave mixing, cross gain modulation and phase noises which effect the optical communication system.

1.5.1.1 Gain Saturation

The power of the signal is increased with the increase in active region length of SOA. When power becomes too high, the gain coefficient starts to decrease, thus reducing the power of the signal undergoing amplification. This effect is called the gain saturation. This effect due to high optical power involves all electrons from the conduction band so that a further increase in the number of external photons will not stimulate any further transition of electrons down to valence band. Hence, it will not produce additional stimulated photons. In gain saturation of SOA, g is reduced when P becomes comparable to saturation power P_s

$$g = \frac{\partial P}{\partial z} = \frac{g_o}{1 + P/P_s}$$

Where g_o is the small signal gain. P is input signal power and P_s is the saturation power.

1.5.1.2 Four Wave Mixing and Cross Gain Modulation

In WDM networks, several channels amplify simultaneously so that the crosstalk may take place between the channels. Two type of crosstalk occur in SOAs; Interchannel and cross saturation. Interchannel crosstalk occurs when two wavelength channels enters a SOA. There is a nonlinear interference producing new signals at beat frequencies and they are amplified more as compared to the original signal. This effect is called as four wave mixing in the SOA. The cross saturation occurs when SOA works in saturation mode and channels change from ON to OFF, the gain undergoes opposite change. This is called as cross gain saturation or cross gain modulation (XGM) in the SOA. This change in gain results in variations in the amplification of another signal because again, all signals share the same gain produced by one active medium. This change depends upon the rate of gain variations which follows input bit rate. For SOAs, the carrier lifetime is around 1 ns. All bit rates less than 1 Gb/s will cause severe crosstalk [Mynbeav and Scheiner, 2003]. While in EDFA, the crosstalk is not important because the carrier

lifetime is about 10 ms, it means bit rate above 100 kHz will not cause crosstalk. To reduce crosstalk in the SOA, it is desirable to increase the saturation power and decrease the lifetime of carriers. The RZ differential phase-shift keying (DPSK) modulation format has attracted intense research interests [Xu *et al.*, 2003] as the signal power is constant for this format, so this format is applied to SOA-based WDM transmission link as it reduces the cross gain modulation (XGM) effect accordingly.

The intensity of noise is suppressed by a gain saturated SOA in spectrum-sliced WDM system [Zho *et al*., 2002]. The high noise suppression ratio and large bandwidth were obtained by increasing the bias current of saturated SOA. For optimum operation of the SOA, an increase in gain of 13.5 dB was obtained for intensity-noise limited system at bit rate of 2.488 Gb/s.

1.5.1.3 Polarization Sensitivity of SOA

The gain of the SOA is polarization dependent due to the rectangular shape and crystal structure of the active region. The gain of SOA was varied from 5 to 7 dB due to polarization [Agarwal, 1992]. Olsson *et al*. [1987] investigated to reduce the polarization dependence in the SOA. It was required to make active region square in cross section, connecting two SOAs in series or in parallel to compensate for the orthogonal polarization unequal gain. A double pass of signal through the same active region was also reducing the polarization dependent gain. Hence, polarization dependent gain was reduced to 0.5 dB for the SOA. The optical amplifier magnifies the signal noise along with the signal and also generates its own noise. The noise figure for the SOA was 6 to 9 dB [Agarwal, 2001]. Morito *et al.* [2003] have setup the SOA module which exhibited a high saturation output power of +17 dBm together with a low noise figure of 7 dB, large gain of 19 dB, and low polarization sensitivity of 0.2 dB for optical signals of 1550 nm wavelength.

1.5.1.4 Phase Noises of SOA

The variations of intensity of an optical signal in the SOA medium change the refractive index of the SOA. This variations of the refractive index lead to a nonlinear phase shift of the signal, giving rise to self phase modulation (SPM). Wei *et al.* [2005] reported that phase noise impact is less at higher bit rates. They suggested that saturated induced SPM can be significantly reduced by increasing the bit rate and carrier lifetime of the SOA for single channel DPSK signal amplification. The phenomenon in which the variations of

intensity of one optical signal can change the refractive index of the SOA and modulate the phase of other optical signals co propagating in the same SOA is known as cross phase modulation (XPM). This effect did not discuss in earlier literature for the SOA.

Optical noise in an EDFA is termed as ASE (amplified spontaneous emission). The actual signal degradation came from beating signal generated at noise-noise and noise-signal interference [Mynbeav and Scheiner, 2003]. The noise-to-noise beating can be removed by using narrow band filter. The noise is also higher for counter propagating pump system. The splicing loss occurs due to the mismatch of core diameter of single mode fiber *i.e.* 8 and 10 μm and the core diameter of erbium doped fiber varies *i.e.* 2.8 to 5.2 μm [Senior, 1992]. The noise figure for the EDFA was 3.5 to 9 dB less than that of the SOA. There are several techniques used to flatten the gain of EDFA.

1.5.2 Gain-Bandwidth of Optical Amplifier

The gain bandwidth product of the optical amplifiers must be large for optical communication system in order to transmit of multimedia information signals. The FPA exhibits peak gain called gain ripple at resonance and gain can be increased with increase in reflectance. In the case of FPA, reflectance can be increase up to certain limit. If R =0 in the FPA, then gain of amplifier is gain of the TWA. To achieve high gain in the TWA, it was required to make an active region long enough. Therefore, gain saturation problem is existing in the TWA. The bandwidth of the FPA is small but gain is large. The TWA has larger bandwidth but smaller gain. The bandwidth for FPA was 0.0086 nm and bandwidth of TWA was 40 nm [Mynbeav and Scheiner, 2003]. The FPA construction is also complex and costly as compared to the TWA construction. Jennen *et al.* [2001] developed the SOA model that shown accurate result for both single channel and WDM transmission at low saturated levels. Jennen *et al.* [2001] noted that the SOA used had minimal signal gain of 12 dB, a noise figure of 10 dB and a saturated output power of 12 dBm. Bjorlin and Brower [2002] demonstrated experimental setup showing that the noise figure was strongly affected by the reflectivity of the mirrors. The signal' s spontaneous beat-noise on enhancement (χ) could be eliminated by choosing proper mirror reflectivities. The highest power of SOAs that had been reported to posses is P_s (saturation power) values of +17 dBm for single polarization device [Dagenais *et al.*, 2003]. Therefore, SOA can be utilized for transmission of small number of channels.

Due to limited bandwidth of SOA, the fiber amplifiers are used for broadband optical communication systems. The erbium doped fiber amplifiers are very attractive because they operate in the wavelength region near 1.55 μm, in this region the fiber attenuation is minimum [Agarwal, 2001]. The EDFA amplified simultaneously all channels when a WDM signal was amplified. The shape of the gain spectrum was affected by the amorphous nature of silica and by presence of other codopants within the fiber core such as Germania and Alumina. The EDFA whose core was doped with Germania, its gain spectrum is quite broad and has a double-peak structure [Pederson *et al.*, 1991]. The gain bandwidth of such codopants EDFA typically exceeds 35 nm. The gain of EDFA depends upon erbium-ions concentration, amplifier length, and core radius and pump power [Agarwal, 2001]. The gain of modern EDFA range from about 20 dB to 40 dB depending on as they act as a booster or a pre-amplifier as noted by Diagonnet *et al.* [1993]. The Raman amplifier exhibited advantages of self-phase matching between pump and optical signal together with a broad gain- bandwidth. Aoki *et al.* [1988] investigated Raman gain of 20 dB for silica fiber with broad spectral bandwidth of up to 40 nm by using suitable doping of fiber.

1.5.2.1 Gain Flattening

Gain depends upon the wavelength of the input signal and is restricted by the width of radiating energy bands. Actually gain curve fluctuates between 1530 and 1560 i.e. there are two peaks at these frequencies as shown in figure (1.6) and hence is highly undesirable. We should have a flat gain for the range of operating wavelength *i.e.* 1530-1560 nm and 1560-1610 nm. This property of EDFA amplifier is called gain flatness. Various filters are designed to flatten the gain in these ranges.

The gain clamping is the fixed drop in gain from fluctuating gain to achieve stable gain. Giuliani and Alessandro [2000] proposed gain clamped SOA which offered advantages over the conventional SOA. They found that the response of the SOA was linear and suffer less from crosstalk related effects. Gain clamping was achieved by fabricating two distributed Bragg (DBP) mirrors on both ends of the amplifier [Wolfson *et al.*, 1998; Giuliani and Alessandro, 2000]. For the SOA in TWA fashion, reflections must be avoided which leads to an implementation with angle strip and facet antireflection coating [Kelly *et al.*, 2000].

Bononi and Barbieri [1999] designed a gain-clamped DFA (distributed fiber amplifier) for the selection of pump power, laser wavelength and laser cavity loss with specific

number of WDM signals, power per channel and gain. In eight channels WDM transmissions by using gain clamped DFA, 12 dB gain was required for -3 dBm input signal power per channel. It was found that a pump power of 21.5 dBm and a laser placed at 1530 nm ensured a worst-case over shoot less than 0.25 dB.

Cockrane *et al.* [1990] noted in the EDFA that the gain was the function of wavelength and two-fold gain fluctuates at 1530 and 1560 nm as shown in figure (1.6). The EDFA gain was flattened by using various methods to obtain good gain bandwidth product. A combination of several long periodic fiber gratings were acting as the optical filter which can flatten the gain within 1 dB over the 40 nm bandwidth in wavelength range of 1530-1570 nm [Wysocki *et al.*, 1997]**.** The notch filter was used to flattening of gain over wavelength with length of active fiber ranging from 20 to 50 meters as optimal length. The gain also depends upon the pumping power for population inversion. A noise figure of 3.2 dB was measured in 30 m long EDFA which is pumped at 0.98 μm with power of 11 mW [Ono *et al.*, 1999]. When this EDFA amplifier was cascaded in two stages, a flat gain of 0.5 dB was achieved at wavelength range of 1544-1561 nm. Ono *et al.* [1999] demonstrated the gain flattening technique by using passive filter-based method. The optical filter when placed before the amplifier increased the noise while placing it after the amplifier reduced the output power.

Zimmerman and Spiekman [2004] studied various gain flattening methods such as the hybrid Al-codoped and Al/P- codoped EDFAs, the gain equalizer filters and hybrid Raman and EDFAs by gain simulation of the amplifier. They found that the utilization of gain equalizer filter was the most applicable technique for gain broadening of the EDFAs but the hybrid Raman amplifier and EDFAs had the maximum accessible bandwidth without any power consumption in optical filter.

Therefore, there is need to optimize the SOA for reducing amplified spontaneous noise power, gain saturation in optical communications for improving gain and bandwidth.

1.5.3 Optical Amplifiers in Long Distance Communication and Ultra high Capacity

At present stage, there are two competing technologies that allow increasing the overall data rate in an optical link, time division multiplexing (TDM) *i.e.* higher bit rate per channel and wavelength division multiplexing (WDM) *i.e.* more channels per channel per fiber. As an example, 10 Gb/s line or by using four channels at different wavelengths, each operated at 2.5 Gb/s or with 16 channels running at 622 Mb/s. The higher the total

data rate, the more difficult the system design will emerge due to the electronic bottleneck. On the other hand, it is easier to achieve high link capacity with WDM system than with a single wavelength system operated at higher bit rate. This comes out to be cost effective solution for providing broadband optical communication systems and networks.

The group velocity dispersion (GVD) [Faquir Jain, *et al.,* 2001] is an undesirable, but unavoidable characteristic of the fiber *i.e.* light pulses broadens in time as they propagate through it. Its effect is to place an upper limit on the information capacity of the communication systems. The performance of broadband optical communication systems and networks can be improved by higher order dispersion compensation by differential time delay with enhanced bandwidth and transmission distance [Sharma *et al.,* 1997, 1998, 2000]. The optical filter design was based on thin-film interface for multichannel optical communication system at 1550 nm [Sinha *et al.*, 2003]. This will make small size of overall system.

The SOA is used as a functional device in the area of long haul optical communication. The nonlinearities in optical amplifiers *i.e.* ASE noise power, gain saturation, cross gain modulation (XGM), four wave mixing (FWM) and cross phase modulation (XPM) limits its use for long distance optical fiber communication as an in-line amplifier. It also shows limitation for use as pre- and booster amplifiers.

Olsson *et al.* [1989] demonstrated coherent detection system at 400 Mb/s up to distance of 372 km using four in-line amplifier transmissions with penalty of 1.5 dB. Various researches reported solution to overcome the problem in saturation region. Choi *et al.* [2002] reported 8 × 10 Gb/s transmission over 240 km. Spiekman *et al.* [2000] reported 8 × 20 Gb/s transmission over 160 km with SOAs span of 47.9 km, by optimizing transmission system design parameters. Spiekman *et al.* [2003] reported 8 × 40 Gb/s transmission over 160 km. The SOA is used for in-line amplification of both single and multichannel systems. The SOAs are used as functional device in the area of long-haul optical transmission demonstrated [Jennen *et al.,* 2001].

Xu *et al.* [2003] reported 8 × 40 Gb/s transmission over 160 km. Kim *et al.* [2001] demonstrated 4 × 10 Gb/s transmission over 500 km by using SOA as in-line amplifiers with wavelength modulation technique. Sun *et al.* [1999] reported error free transmission of 32 × 2.5 Gb/s DWDM (dense wavelength division multiplexing) channels over 125 km by using cascaded in-line semiconductor optical amplifiers.

Xu *et al.* [2004] reported a dispersion management scheme for reducing SOA induced crosstalk in WDM links up to distance 420 km with 70 km SOA spacing to carrying 100 Gb/s WDM RZ-OOK (return zero on-off keying) signals. In conventional on-off keying (OOK) modulation format (such as non return to zero and return to zero etc.), the cross gain modulation (XGM) effect of SOA limits the transmission performance of the WDM system [Choi *et al.*, 2002]. As RZ-DPSK signals are more tolerant to cross gain modulation in SOA than OOK signals [Cho and Khurgin, 2003]. The RZ differential phase-shift keying (DPSK) modulation format has attracted intense research interests [Xu. C *et al*., Apr. 2003] as the signal power is constant for this format, so this format applied to SOA-based WDM transmission link reduces the cross gain modulation (XGM) effect accordingly. In addition, RZ-DPSK could provide 3 dB reductions in required received OSNR for given bit error rate (BER) [Xu. C *et al*., Apr. 2003].

Onishchukov *et al*. [1999] reported the error-free transmission of single-channel DBPSK (differential binary phase shift keying) format at 1300 nm over 500 km using SOA as in-line amplifier. Li *et al*. [2004] reported the transmission of 8 × 10 Gb/s signals over 1050 km by using cascaded SOAs and the DPSK modulation format with 400 GHz channel spacing.

Zimmerman and Spiekman [2004] demonstrated transmission of 32 WDM channels modulated at 10 Gb/s across four SOAs as in-line amplifiers with the spans of 40 km standard fiber. They observed an optical signal to noise ratio (OSNR) of 20 dB, an average Q factor of 16.8 dB for optimum gain. Also the cross gain modulation distortion due to gain compression in SOAs deteriorates the quality by 1.2 dB. The BER was less than 10^{-11} for all channels.

For long distance with high capacity, the amplification is done with L-band EDFA. The L-band EDFA doubles the capacity of WDM transmission system. Rotwitt *et al.* [1993] noted the spectral gain profile leading to a reduction in bit error rates due to timing jitter of the arrival times of the signal pulses. They found reductions in bit error rates up to 4 dB in transmission lines of 9000 km length with signal wavelength of 1534 and 1554 nm. At 1554 nm, there is a need of insertion of additional components in order to reduce propagation of amplifier spontaneous emission noise. An optimum relation between the pulse width and fiber dispersion showed that optimum system operation will always be limited by timing jitter. The bit rate distance product was 55 Gb/s.Mm.

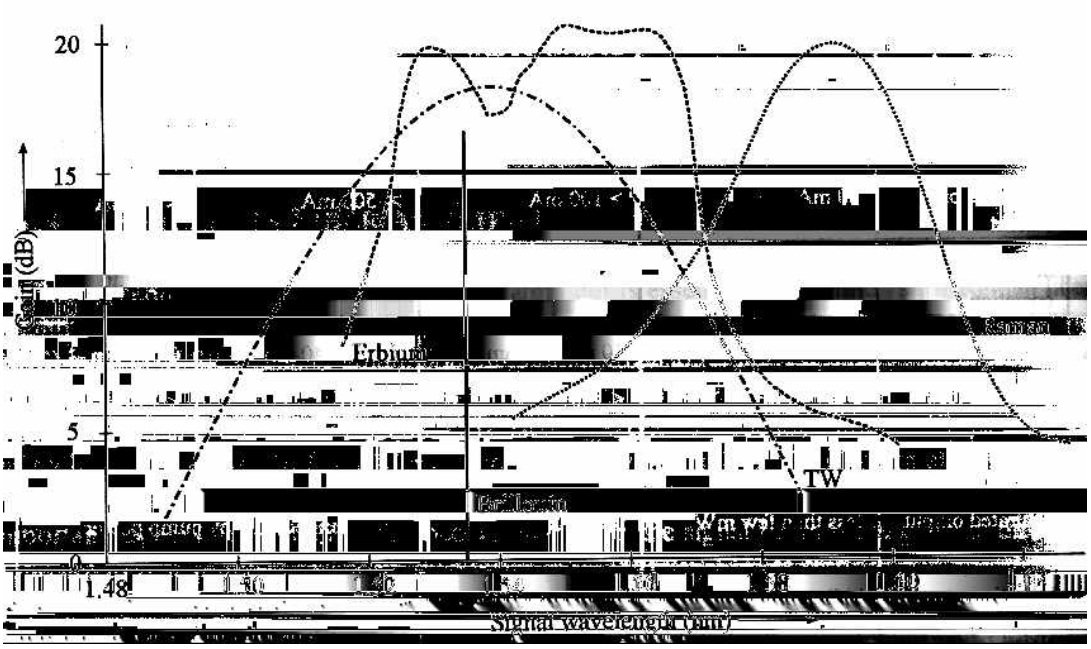

Figure 1.6: Typical gain curves for various optical amplifiers.

Table 1.1

Comparison of optical amplifiers (NA: not applicable).

Property	**SOA**	**EDFA**	**Raman Amplifiers**	**Brillouin Amplifier**
Unsaturated device gain	>20dB	>20dB	5 - 15dB	>25dB
Optical pump power	NA	20 – 50mW	100 – 200mW	<10mW
Optical pump wavelength	NA	820nm, 980nm 1400 – 1500nm	Stokes shift below signal	
Electrical bias current	50mA	>100mA	>500mA	<50mA
Wavelength of operation	any	1525 – 1565nm	Any, but subject to pump	
Bandwidth	20 – 50nm	10 – 40nm	20 – 40nm	0.001nm
Coupling loss	5 – 6dB	<1dB	<1dB	<1dB
Polarization sensitivity	> few dB	0dB	0dB	0dB
Saturated output	> few mW	few mW	Limited only by pump power	
Directions	bidirectional	bidirectional	bidirectional	unidirectional
Noise	low	low	Very low	Very low

When ASE seeding is applied by feedback reflector at the input end to reduce ASE then gain improvement of 6 dB was noted in single wavelength operation at 1588 nm, [Nilson *et al.*, 1998].

An expression was derived for the exponationed approximation of the power transients in a single EDFA for the evolution of 1 dB transient response times. Tancevski and Rush [1998] presented a numerical simulation of a realistic point-to-point optical communication links involving twenty channels WDM transmission through the cascaded 35 amplifiers. Tancevski and Rush [1998] found that an L-band EDFA required long fiber lengths (> 100m) to keep the inversion level low in wavelength range of 1570-1610 nm.

Hwang and Cho [2001] demonstrated two stage designs for WDM system. The first stage pumped at 980 nm for short length of doped fiber and the second stage using bidirectional pump at 1480 nm with long doped fiber (200 meters). An optical isolation was used between these stages, which passed ASE from first stage but blocked the backward propagation of ASE into first stage.

Zimmerman and Spiekman [2004] investigated fibers having peak absorption greater than 30 dB/m while maintaining the pumping efficiency and satisfactory noise performance. These fibers allow shortening of the fiber by as much as 3 times as compared to standard EDF that is optimized for the DWDM.

Raman amplification, combined with EDFAs increased the maximum reachable distance and the span length. Raman amplification was also used to substantially reduce the impact of fiber nonlinearities [Carena *et al.*, 2001]. There were many recent developments in the DWDM (dense wavelength division multiplexing) at 40 Gb/s transmission over distance up to about 9000 km. Rasmussen *et al.* [2004] demonstrated error free DWDM transmission of 40 channels at 40 Gb/s with 100 GHz spacing over a regenerator distance of 10,000 km. It was possible by using the CSRZ-DPSK (carrier sense return to zero differential phase-shift keying) enhanced FEC and all Raman amplified span with 100 km. So, bit rate-distance product of 400 Gb/s was noted. Table (1.2) shows the major progress of long distance transmission by using cascaded optical amplifiers during last years.

1.5.4 Sensitivity of Optical Receiver with Optical Amplifiers

Among a group of optical receivers, a receiver is said to be more sensitive if it achieve the same performance with less optical power incident on it. The performance criterion for

digital receivers is depending upon bit error rate. Therefore, it requires the improved receivers sensitivity and bandwidth for greater transmission capabilities.

The APD (avalanche photodiode) receivers give a high sensitivity of -29.5 dBm at 10 Gb/s and has advantage over the PIN receivers at bit rates up to several Gb/s [Kasper, 1987], but at higher bit rates, the gain bandwidth product of APD has limited sensitivity. PIN receivers offer a greater potential bandwidth but a poorer sensitivity [Gimlett, 1988].

The optical pre-amplifiers have been used for improvement of receiver sensitivities of optical receivers by placing them before photodetector. The work regarding receiver sensitivity was first reported with -37.2 dBm by using EDFA (erbium doped fiber amplifier) at 10 Gb/s [Saito *et al.*, 1991] and -38.8 dBm by using two-cascaded EDFA [Gnauck and Giles, 1992].

The SOAs have advantage of having low cost and are compact as optical pre-amplifier in comparison with EDFAs. Olsson *et al.* [1989] demonstrated the SOA pre-amplifier receiver with sensitivity of -34.3 dBm at 4 Gb/s without any optical filter. Dreyer *et al.*[2002] reported an improvement in receiver sensitivity of -32.5 dBm at 10 Gb/s by using high gain SOA with polarization sensitivity of 1.1 dB ± 0.4 dB followed by a 0.6 nm optical filter. SOA optical pre-amplifiers are used in 40 Gb/s optical networks, where APD cannot be used. Mason *et al.* [2002] demonstrated a receiver sensitivity of -17 dBm at 40 Gb/s by using SOA-PIN integrated receiver excluding an optical filter.

Yamatoya and Koyama [2001] proposed an optical pre-amplifier using an inverted-ASE signal from a saturated SOA, which has an advantage over conventional SOA optical pre-amplifiers *i.e.* relaxed requirement on anti reflecting coating, fiber alignments of an SOA, optical narrow band pass filter and tolerance for a wavelength of input signal light. Yamatoya and Koyama [2004] demonstrated the minimum receiver sensitivity was -32.7 dBm with including 0.1 nm optical filter by using pre-amplifier which has optical gain bandwidth over 60 nm and also ASE power was 267 μW for input light power 10 μW.

1.5.5 Optical Amplifiers in Broadcast Networks

The broadcast networks can be classified as active or passive networks. When the signal is optoelectronically regenerated or amplified, the network is active broadcast network otherwise it is passive broadcast network. Ethernet and token bus are the examples of passive broadcast network, while token ring is an active broadcast network. In passive broadcast networks, the transmitted optical power is spilt for distribution among the receivers [Gerla and Fratta, 1988]. Therefore, increase in the number of users implies that

each receiver will get reduced amount of optical power for fixed transmitted power level. These reductions in received optical power level will worse the receiver performance. To keep the receiver performance acceptable, the number of users has to be limited. Therefore, we require the optical amplifiers to keep same number of users with acceptable performance of receiver.

Optical multiplexing and switching technique was used for increasing the capacity [Marrakchi and Dekker, 1994]. In wavelength division multiplexing system optical spectrum is sliced in multiple channels. These channels are centered at different wavelength due to which information does not interface with each other. Implementation of WDM system requires couplers, wavelength multiplexer and demultiplexers, tunable or fixed wavelength source and detector capable of operating over the entire wavelength range. As implementation of encoders/decoders and time division multiplexers/ demultiplexers at Tb/s is very difficult in TDM and CDM (code division multiplexing), the WDM implementation was easily possible and provided large bandwidth. The complexity of switched network can be avoided by using broadcast network topologies [Brackett *et al.*, 1990].

Many issues were taken into care for implementation of WDM broadcast networks. In WDM, the system must have large number of users in topology to utilize the available bandwidth [Green, 1993]. The number of fibers used in network topology must be minimum. The transmitter to receiver loss is minimum in the topology, so that the number of users supported can be increased. Also, minimize the number of couplers, multiplexers, transmitters, receivers and optical amplifiers, input power in the topology. The optical network advancement will need to integrate on photonic chip for low power requirement [Fiddy M., 2005]. A step towards this requirement was achieved by using artificial material for optical switches and buffers.

Huang and Jain [2004] reported that the performance of integrated InGaAs-InP quantum wire laser modulator is superior over quantum well laser for 1550 nm. Similarly, the post-amplifier implies that OA (optical amplifier) is used just after the transmitter. It is also possible that OA is integrated with the source to form a high power optical source. In this application, OA with high saturation power is desirable to reduce the effect of gain saturation. The DFAs (doped fiber amplifier) can be used for this application because of their high saturation power level [Rottwitt *et al.*, 1993] but such a high power optical source would be bulky. When OA is used as pre-amplifier, it is placed just before the receiver. This can also be integrated with the receiver to form a high sensitivity receiver

module. The OA in this application produced low noise. The in-line amplifiers were used in the optical fiber link itself. The DFA (doped fiber amplifier) are better for this application because these can be easily spliced but it is more expensive than the SOA.

1.5.6 Placement of Optical Amplifiers and Related Issues in Optical Networks

The placement issue of optical amplifiers will estimate the number of users and transmission distance in the optical communication systems and networks. Earlier, the broadcast optical networks support very few users (64 users) [Cheet *al*., 1992]. It is also reported that the receiver performance of optical network was varied with or without using optical amplifiers. In absence of OAs, the Gaussian filter in the receiver reduced noise by removing noise outside the frequency band of interest and increased the bandwidth resulting in reduction of inter symbol interference[Blahut, 1983].

The optical amplifier can be used in passive broadcast networks for increasing the number of users supported. The optimal utilization of OAs can be achieved by (i) proper placement of OAs in a given network topology (ii) Modifying the existing topologies to utilize the OAs effectively. Wagner *et al.* [1987] implemented the bus topology in optical fiber network and supported limited number of users (typically < 24) [Wagner *et al*., 1987]. This was due to non uniform distribution of power among users. So the optical amplifier can be used to keep the distribution of received power level uniform. This results in increase in number of supportable users. The use of SOAs in single channel bus network makes uniform distribution users.

Dual bus topology was used for implementation of distributed queue dual bus metropolitan area network (MAN). There was limited number of nodes supported by network. Koai and Olshanshky [1993] proposed photonic dual bus by using OAs (with unsaturated gain of 12 dB and saturation power level of 4 dBm). This photonic dual bus supported 100 nodes spanning hundred of kilometers with OAs and suitable for wide area network or MAN.

Optical fiber has been used for connecting consecutive nodes in rings. Ross *et al.* [1986, 1989] proposed fiber distributed data interface (FDDI) which is a ring network designed with fiber. The passive optical rings can provide high reliability because failure of node does not break the ring. But these have power budget problem limiting the number of nodes used. This problem can be overcome to a great extent by using optical amplifiers. Goldstein *et al.* [1991] proposed a passive ring which had distributed erbium doped fiber

amplifier. The 300 km ring at 2.5 Gb/s can not support a single user without an amplifier but 450 users can be supported with the distributed amplification [Goldstein *et al.*, 1991]. In the star topology, optical power is equally distributed at output ports. Therefore, it can support the maximum number of users without OAs as compared to any other topology. Chen *et al.* [1992] reported that the number of users supported by star is small (typically <64). Many modified topologies which use star coupler and OAs has been proposed [Irshid and Kaverhrad, 1993; Chen *et al.*, 1992; Chen and Guo, 1994]. These topologies can support higher number of users as compared to passive star topology. The star topology can be either tranmissive or reflective star or both. In reflective star coupler, input and output port were same. The user transmits the signal in given port and receives the signal from the same port for other users [Duthie *et al.*, 1987]. The propagation direction of transmitted and received signals were opposite in the port. Chen *et al.* [1992] proposed two schemes of distributed reflective star coupler which used erbium doped fiber amplifiers (EDFAs). In the first scheme, m numbers of $m \times m$ star coupler were used. This implementations of $m \times m$ coupler required $m/4$ EDFAs and $6m/4 + (m/2)\log_2(m/4)$ number of 2×2 couplers. Therefore, the reflective star made up of m number of $m \times m$ star coupler could support $N_u = m^2$ number of users. In second scheme, $2m$ number of $m \times m$ coupler were used to implement a distributed reflective star coupler which could support $N_u = m^2$ number of users. Another star coupler configuration by using EDFAs for WDM/FDMA network has also been proposed [Irshid and Kaverhrad, 1993]. In this, there was one central coupler of dimensions $m_c \times m_c$. All other couplers were auxiliary couplers. The network size was easily expandable by using auxiliary stars until all the ports of central star were filled. The recirculation signals which can produce interference can be minimized by suitable matching the band pass filters (BPFs) and band stop filters (BSFs). Chen and Guo [1994] modify this coupler; it was $mm_c \times mm_c$ centralized star coupler. This scheme supported more number of users than $m(m_c\text{-}1) \times m(m_c\text{-}1)$ coupler. The number of required 2×2 coupler is less than that of the star coupler [Irshid and Kaverhrad, 1993] for $m \geq 32$ and it did not require a BPF and BSF. As each user must be connected to centralized star coupler, there was large fiber requirement. The fiber requirement can be reduced by making the star coupler distribution.

Table 1.2

Major Progress of transmission distance by using optical amplifiers.

Year	Type of Amplifier/ Using Additional Component	Bite Rate Channel Spacing	Transmission Distance	References
1987	Brillouin Amplifier	100 Mb/s	30 km	Olsson and Ziel
1989	SOA	400 Mb/s	372 km	Olson *et al.*[1989]
1991	Fiber Amplifier/ Circulating loop	5 Gb/s	14000 km	Bergano *et al.* [1991]
1993	EDFA	1.8 Gb/s	15000 km	Rotwitt *et al.* [1993]
1993	SOA	4 × 10 Gb/s	40 km	Nakano *et al.* [1993]
1994	EDFA	16 × 2.5 Gb/s	1420 km	Chraplyvy *et al.[*1994]
1995	SOA	10 Gb/s	500 km	Mecozzi *et al.* [1995]
1997	EDFA	2.5 Gb/s	9000 km	Otani *et al.* [1997]
1997	SOA	10 Gb/s	3500 km	Settelmbe *et al.* [1997]
1999	SOA	80 Gb/s	50 km	Bischoff *et al.* [1999]
1999	EDFA/ Carrier suppressed RZ pulse	8 × 40 Gb/s (400 GHz)	367 km	Miyamoto *et al.* [1999]
2000	SOA	8 × 20 Gb/s	160 km	Spiekman *et al.* [2000]
2003	SOA	8 × 40 Gb/s	160 km	Xu *et al.* [2003]
2004	SOA/ RZ	10 × 10 Gb/s	420 km	Xu and Jacob [2004]
2004	SOA	8 × 10 Gb/s	1050 km	Li *et al.* [2004]
2005	EDFA	320 Gb/s (100 GHz)	320 km	Chung and Chung [2005]

Table 1.3

Progress in placement of optical amplifiers in networks.

Topology	Bit Rate	No. of user without Amp.	No. of users /with No. of SOAs	Repeater distance	Reference
Bus	20 Mb/s	20	Increase depend upon dynamic range transmitted and received levels	0.5 km	Wagner *et al.*[1987]
Dual Bus	100 Mb/s	Limited number of nodes in network	100 nodes span hundred km	2.5 km	Koai and Olshansky, [1993]
FDDI Ring	100 Mb/s	300 km ring at 2.5 Gb/s does not support single users	450 users possible/ With a distributed amplifier	2 km	Ross *et al.* [1986 and 1989]; Goldstein *et al.* [1991]
Star	1 Gb/s	64	128/128, 256/256, 1024/1024	1 km	Singh *et al.* [1996 and 1997]
Tree	1 Gb/s	64	124/4, 256/16, 1024/256	1 km	Singh *et al.* [1996 and 1997]

This can be achieved by putting the $1\times m$ and $m\times 1$ coupler with the group of m users. The fiber was required only to connect the $1\times m$ and $m\times 1$ coupler to $m_c \times m_c$ star coupler, so the fiber utilization was reduced. The doped fiber can also be used in distributed star couplers to increase the number of supportable users. But the SOA can be easily integrated with integrated optic implementation.

The SOAs are also better suited as post- or pre-amplifiers since these can be integrated with either transmitter or receivers chips. However the SOA as pre-amplifier provides the low cost solution for this topology.

The tree-net topology provided large geographical area coverage with fewer amounts of fiber and was easily expendable. The capacity of these networks was increased by making use of WDM. The tree-net topology is consisting of star as main topology and folded bus as auxiliary topology. In a purely passive tree-net, the number of user supported was limited by spilt and distribution loss in star couplers. The number of user can be increased by using SOAs. In tree-net with b branches and n number of users per branch, the total number of supported users was $N_u = bn$ [Gerla and Fratta, 1998]. The power loss in tree-net topology network could be reduced by realizing the star portion as multistage star coupler [Green, 1993]. The table (1.3) shows the comparison in placement of optical amplifiers in optical network topologies. It had been observed that gain saturation in SOAs affect the performance of tree-net. It reduced the number of users supported as compared to unsaturated SOAs. The gain fluctuation in SOAs further deteriorated the performance. The star topology supported maximum number of users without SOAs star network and tree-net required less number of SOAs as compared to the star for a fixed number of supportable users [Singh *et al.,* 1996, 1997].

The nonlinearities (FWM, XGM, and XPM) of optical amplifiers are utilized for formation of wavelength converters. The wavelength converters are the main related issues of optical networks. All optical wavelength converters have become the key components of future broadcast optical networks [Durhuus *et al.*, 1996]. Wavelength converters remove wavelength blocking in optical cross connects in wavelength division multiplexed (WDM) networks and increase the flexibility and capacity of network for fixed set of wavelength [Durhuus *et al.,* 1996].

The electro-optic converter is a straightforward solution for conversion. But electro-optic converter has limitations such as large power consumption and complexity. Wavelength conversions based on semiconductor optical amplifiers (SOAs) and semiconductor lasers

have been focus on research interests during the last few years [Kovacevic and Acampora, 1996; Durhuus *et al.*, 1996]. Semiconductor optical amplifiers are used in cross gain modulation mode (XGM), cross phase modulation (XPM) and four wave mixing (FWM) mode for wavelength conversions. Seo *et al.* [2002] reported that all optical up conversion use cross gain modulation of the SOA with high conversion efficiency. But, it requires a large input optical power to saturate the gain of the SOA.

In four wave mixing, the amplitude and phase information remains transparent to signal format [Durhuus *et al.*, 1996; Ludwig and Raybon, 1994]. Four wave-mixing (FWM) converters include multi wavelength conversion and fiber dispersion compensation capabilities [Ludwig and Raybon, 1994].

Hsu *et al.* [2004] showed that with the help of assist beam, a BER of 10^{-9} can achieved with power penalty of 2.5 dB for wavelength conversion. Durhuus *et al.* [1996] showed that wavelength conversion at 2.5 Gb/s has penalty of 0.7 dB by using cross gain modulation in SOA. The wavelength converter baser on cross gain modulation has permitted transmission distance of 50 km by using normal dispersion shift (NDS) fiber with 3 dB penalty for 5 Gb/s [Durhuus *et al.*, 1996]. The bit error rate (BER) of this converter varied from 10^{-3} to 10^{-10} of received power. By using 10 Gb/s, the signal was found to be totally corrupted after 25 km due to chirp. As reported [Perino *et al.*, 1994], the transmission over 121 km with dispersion shifted fiber is possible at 10 Gb/s after wavelength conversion. Kim *et al.* [1996] demonstrated that 10 Gb/s NRZ (non return to zero) signals could be successfully transmitted over 80 km within 2 dB power penalty at 10^{-12} BER due to self phase modulation and negative chirp induced by the phase modulation in SOAs.

FWM based wavelength conversion is limited when it used in On-Off keying (OOK) based transmission system. Therefore, there is need of increasing signal power for given pump power to maintain the OSNR (optical signal to noise ratio) which resulted in variations of the SOA gain causing induce distortion on converted signal. Lu *et al.* [2000] investigated the typical signal-to-pump ratio needed to maintain around -9 dB to achieve a trade off between signal OSNR and pattern effect. It was noted that RZ-DPSK provided 3 dB reduction in required received OSNR for a given bit error rate [Xu *et al.*, 2003]. It has also been shown that RZ-DPSK has continuous pulse sequence and will eliminate the pattern effect to the converted signal when FWM in SOA used and will improve OSNR of converted signal.

The extinction ratio degradation problem is also presented in the XGM scheme. Also conversion efficiency for this FWM scheme is not very high. So it is difficult to retain a large signal-to-noise ratio (SNR) for converted signal in cascaded wavelength converters. So to overcome the problems of XGM and FWM scheme, the SOA converters can be used in cross phase modulation (XPM) mode. Majumder *et al.* [2003] reported XPM based SOA Mach-Zehnder interferometer (SOA-MZ1) wavelength converter. They have optimized the bias current, optical filter bandwidth, and pump intensity in the SOA-MZI arrangements to achieve high signal-to-noise ratio.

1.6 Selection of Study Area

In the fiber optic communication, there is degradation in transmission signal with the increase in distance. The number of users can be increased by increasing the power budget or reducing the losses in the network by using optoelectronic regenerators. In optoelectronic regenerators, the optical signal is first converted into electric current and then regenerated by using a transmitter. But such regenerators become quite complex and expensive for wavelength division multiplexing systems. This reduces the reliability of networks as regenerator in an active device. Therefore, upgradation of multichannel WDM network will require optical amplifier. To remove loss limitations and to amplify the signal, the optical amplifiers are used which directly amplify the transmitter optical signal without conversion to electric forms as in-line amplifiers. The optical amplifiers are mainly used for WDM (Wavelength division multiplexing) light wave systems as all channels can amplify simultaneously. Optical amplifier increases the transmitter power by placing an amplifier just after the transmitter and just before the receiver.

As the need of long haul unrepeated transmission distances and ultra fast broadband transmission is increasing, the advanced transmission methods have to be investigated. So, there is a demand to investigate the unrepeated all optical transmission and ultra fast broadband transmission over long distances. In order to achieve these objectives *i.e.* broadband and repeaterless transmission of an optical communication system, it is of utmost importance to optimize the optical amplifier and then placement in optical networks.

Therefore, it is of utmost important to study, analyze and optimize the optical amplifiers in WDM optical communication network to improve the power budget for increasing the number of supported users.

1.7 Objectives

The semiconductor optical amplifiers (SOAs) have attracted much attention as cost effective compared to erbium doped fiber amplifiers for long haul optical communication system. But as gain saturation problems arises due to cross gain modulation (XGM), the cross phase modulation (XPM) and four wave mixing in multichannel optical system limits the system performance and the cascaded utilization of the SOA is not possible for long transmission distance. The crosstalk and power penalty problem arises in long haul dense wavelength division multiplexing using cascaded SOA due to XGM and XPM. So there is a need for proper placement of SOAs for long haul optical communication systems.

Due to limited bandwidth of the SOA, there is requirement of erbium doped fiber amplifiers (EDFAs) for broadband communication systems. In past years, various techniques and methods were presented to flatten the gain of optical amplifiers to push the bit rate and transmission distance higher and higher.

Wavelength converters are the key components for increasing the flexibility and capacity of broadcast optical networks. The nonlinear effects like cross phase modulation (XPM) and four wave mixing (FWM) are the powerful elements for improving the performance of wavelength converters.

All broadcast network topologies show improvement in the number of users in the presence of semiconductor optical amplifiers. But the real model of SOA utilization is not simulated in the literature for low power requirement. This thesis focuses on the investigation of minimizing the nonlinearities in the semiconductor optical amplifiers due to XGM, XPM and gain flattening problems of EDFA for increasing the capacity and flexibility of optical communication networks with the following objectives:

1. To investigate the optical amplifiers (SOA, EDFA) for effective performance with dispersion and fiber nonlinearities.

2. To improve the power budget in WDM optical communication network with placement of optimized optical amplifier.

3. To investigate placements and other related issues of optical amplifiers in WDM optical communication networks.

4. To analyze and compare the different topologies with placement of Optical amplifier in optical communication networks and formulation of topology for optimize performance.

1.8 Organization of the Thesis

The thesis has been organized into eight chapters. Contents of each chapter are briefly described as under:

- Ø After introducing the comprehensive literature review and the introduction in Chapter 1, SOA modeling and analysis for multichannel WDM optical communication systems and transmission performance of 20 × 10 Gb/s WDM signals using cascaded optimized SOAs with OOK and DPSK modulation formats have been presented in Chapter 2. It has been shown that the DPSK system has larger transmission capacity as compared to OOK system. By using cascaded optimized SOAs, the maximum transmission distances are 1190 km in RZ-DPSK system and 1050 km in RZ-OOK systems.
- Ø Chapter 3 is based on optimization of SOA structural parameters for multichannel WDM transmission with DPSK systems by reducing the cross gain modulation (XGM) and cross phase modulation (XPM) of the SOA for improving the capacity and transmission distance. We have successfully simulated the 10 × 40 Gb/s soliton RZ-DPSK WDM signals over 1050 km with spectral efficiency approaching 0.4 bit/s/Hz using optimized semiconductor optical amplifiers (SOAs) as in-line amplifier. With slight increase in differential gain 200 atto cm^2, the maximum transmission distance observed is 4550 km with quality of received signal more than 15 dB and having nil power penalties for 10 × 40 Gb/s. The ten-channel at 80 Gb/s WDM transmission is possible up to the transmission distance of 910 km by using the optimized SOAs as in-line and pre-amplifier with soliton RZ- DPSK modulation format at 200 GHz channel spacing. By reducing cross phase modulation the maximum transmission distance observed is 5220 km with good quality and nil power penalty for 10 × 40 Gb/s soliton RZ-DPSK WDM signals for the first time.
- Ø Chapter 4 deals with the improvement in power budget for long haul WDM and DWDM transmission of RZ-DPSK signals by using optimum placement of the optimized semiconductor optical amplifiers. It is found that the post-power

compensation method is superior to pre- and symmetrical-power compensation methods. The ten channels at 10 Gb/s WDM transmission of 68908 km by using the optimized SOAs as in-line and pre-amplifier with DPSK modulation format at 100 GHz channel spacing with the optimum span scheme. It is also numerically simulated that the ten channels at 10 Gb/s dense wavelength division multiplexing (DWDM) transmission faithfully over 17,227 km using 70 km span of single mode fiber (SMF) and dispersion compensating fiber (DCF) by using optimum span scheme at channel spacing of 20 GHz.

- Chapter 5 deals with improvement of receiver sensitivity and bandwidth by using polarization insensitive semiconductor optical amplifier for greater transmission capabilities. It has been shown that the receiver sensitivity is -69.9 dBm at bit error rate (BER) of 10^{-10} for 10 Gb/s and for the 40 Gb/s bit rate the improved receiver sensitivity is -19.2 dBm with PIN receiver. Our proposed SOA optical pre-amplifier gives large tolerance of an input light wavelength more than 100 nm.
- Chapter 6 pertains to study and evaluation of gain flattening approach of EDFA for WDM transmission systems. By using proposed gain flattening approach and optical super Gaussian notch filter, the peak and valley gain is flattened. It is possible to achieve the transmission of sixteen channels at 40 Gb/s wavelength division multiplexing (WDM) over a transmission distance of 490 km by single mode fiber and dispersion compensating fiber at a span of 70 km with channel spacing of 200 GHz by using this approach. The higher bit rate distance product of 313.6 Tb/s km is achieved.
- Chapter 7 provides the wavelength converters for optical communication networks based on four wave mixing and cross phase modulation in semiconductor optical amplifiers. The SOA parameters evaluated can be utilized for design of wide band wavelength converter and better conversion efficiency. We have simulated 50 nm up and down wavelength conversion for non-return to zero differential phase shift keying (NRZ-DPSK) signal by using four wave mixing in a semiconductor optical amplifier (SOA) at 10 Gb/s. Ten stage cascaded wavelength conversion over 1302 km single mode transmission is possible for 10 Gb/s NRZ-DPSK format by using FWM in the SOA. The wavelength conversion using XPM in the SOA-MZI configuration with wide band more than 15 nm up and down conversions is reported, for the first time.

The conversion efficiency of this converter is more than 11 dB at signal-to-pump power of -9 dB.

- Chapter 8 examines the performance of optical communication network topologies in presence of optimized semiconductor optical amplifiers. The performance of bus, ring, star and tree network topologies for 10 Gb/s DPSK signal in presence of optimized semiconductor optical amplifiers is compared for minimum signal input power. The tree network topology offers maximum number of users with minimum utilization of SOAs and optical couplers.
- Finally, the Chapter 9 highlights the conclusions and recommendations of the thesis and provides the future scope of the work.

Chapter 2

SOA Modeling and Analysis for Multichannel WDM Optical Communication Systems

2.1 Introduction

This chapter focuses on the SOA modeling and analysis for multichannel WDM optical communication systems, which is related to the first objective of the research work. As we have discussed in previous chapter that the most of literature is limited up to transmission distance of 1050 km at 100 Gb/s by using SOA [Li *et al.*, 2004]. Also the structural optimization of the SOA has been ignored. Here, the bias current optimization of the SOA is done to observe the performance of multichannel WDM optical communication systems. It is evaluated that the DPSK system has larger capacity as compared to OOK system in presence of cascaded SOAs.

2.1.1 SOA Analysis for Single Channel

Semiconductor optical amplifiers (SOAs) are more prospective device for optical fiber transmission systems as compared to fiber amplifiers due to their compact size, ultra wideband gain spectrum, low power consumption, ease of integration with other devices and low cost [Mahony, 1988; Gustavsson *et al.*, 1992; Iannone *et al.*,1996]. In order to utilize the SOA for different application like wavelength converter, switching, in-line and pre-amplifiers, there is a need of optimization of SOA for these applications. So the gain saturation and ASE noise power of SOA is analyzed here for single channel. In gain saturation, g is reduced when P becomes comparable to saturation power P_s, the amplification factor G decreases with an increase in the signal power. From [Agrawal, 2002]

$$g = \frac{\partial P}{\partial z} = \frac{g_o}{1 + P/P_s} \tag{2.1}$$

Where the small signal gain g_o is given by

$$g_o = (\Gamma \alpha / V)(I \tau / q - N_t) \tag{2.2}$$

Where Γ is the confinement factor, α is the differential gain, V is the active volume, I is the bias current, τ is the carrier lifetime, q is the charge of electron and N_t is the transparency carrier density.

The unsaturated amplifier gain is

$$G_o = g_o L$$

Where L is the length of semiconductor optical amplifier. Using initial condition, $P(0) = P_{in}$ together with $P(L) = P_{out} = GP_{in}$,relation for large signal amplification gain is obtained:

$$G = \frac{P_{out}}{P_{in}} \tag{2.3}$$

When a semiconductor amplifier works in the saturation mode, the power of the input is above the saturation value. The gain is given by

$$G = G_o \exp\left(-\frac{(G-1)P_{out}}{G \quad P_s} \right) \tag{2.4}$$

This equation shows that the amplification factor G decreases from its unsaturated value G_o when P_{out} becomes comparable to P_s [Agrawal, 2002]. The output saturation power of 30% is defined as the output power for which the amplifier gain G is reduced by 3 dB from its unsaturated value G_o and given by

$$P_{out}^s = \frac{G_o \log_e 2}{G_o - 2} P_s \tag{2.5}$$

Here P_{out}^s is smaller than P_s by about 30% , so we need $G_o \geq 2$ in practice. Also P_{out}^s becomes nearly independent of G_o for $G_o > 20$ dB [Agrawal, 2002]. For the SOA model, as G decrease from G_o , the amplification factor G at bias current 300 mA is reduced by 3 dB, it shows negative value for higher input signal, which is inadequate. So, gain saturation not only reduces the amplifier gain, but also leads to nonlinear effects that can increase the crosstalk in a multichannel transmission system [Franz and Jain, 1996]. From [Olsson, 1989], the spontaneous emitted power at the output of semiconductor optical amplifier is written as

$$P_{ASE} = P_{Sp} = N_{sp}(G-1)hfB_o \tag{2.6}$$

Therefore, photocurrent equivalent to spontaneous emission power [Spiekman, 2003] is

$$i_{sp} = \frac{P_{sp}q}{hf} = N_{sp}(G\text{-}1)qB_o \tag{2.7}$$

Where N_{sp} is population inversion factor. The shot noise N_{shot} , signal to spontaneous beat noise N_{s-sp} and spontaneous to spontaneous beat noise N_{sp-sp} are depended on photoequ-

-ivalent current given by [Olsson, 1989; Yamatoya and Koyama, 2004]

$$N_{shot} = 2B_e q i_{sp}$$

$$N_{s-sp} = \frac{4GI_s \eta_{in} \eta_{out}^2 i_{sp} L_l^2 B_e}{B_o}$$

$$N_{sp-sp} = \frac{i_{sp}^2 B_e (2B_o - B_e)}{mB_o^2} \tag{2.8}$$

Where B_e is the electrical bandwidth, m is the number of polarization modes, I_s is the photo current equivalent of amplifier input power, η_{in} and η_{out} are the amplifier input and output coupling efficiencies, L_l is the optical loss between the amplifier and the receiver and N_{th} is the thermal noise, So the total noise

$$N_{tot} = N_{shot} + N_{s-sp} + N_{sp-sp} + N_{th} \tag{2.9}$$

Also noise figure from [Agrawal, 2002] is given by

$$F_n = 2N_{sp}(G-1) \tag{2.10}$$

From above analysis, it is concluded that at low value of bias current for SOA, the amplification factor as in equation (2.3) goes on decreasing with the increase in input signal power. Even, when the amplified spontaneous emission (ASE) noise power in equation (2.6), the total noise in equation (2.9) and the noise figure are quit low and the output power drop occurs. It is also found that for high value of bias current for SOA, the ASE noise power from equation (2.6), the total noise from equation (2.9) and the noise figure from equation (2.10) has boosted due to the increase in gain even when input power is more than saturation power. These lead to the increase in interchannel crosstalk in multichannel transmission system. So for optimum bias current and the optimal gain is obtained at reasonable noise figure from equation (2.10).

2.1.2 Multichannel Crosstalk Analysis for SOAs

Due to cross gain modulation in the SOA, there is crosstalk among WDM channels. There may be degradation in quality of received signals. In order to decrease the gain a fluctuation, the gain has to be reduced otherwise this will cause power penalty of received signals.

In order to optimize the SOA, we considered the multichannel WDM case. In this, the rate equation governs the carrier density in the SOA gain region [Xu *et al.*, 2003]

$$\frac{\partial N(t,z)}{\partial t} = \frac{J}{qt_a} - \frac{N(t,z)}{\tau} - a\left(N(t,z) - N_t\right)\frac{\sum_{i=1}^{M} P_i(t,z)}{h\nu w t_{eff}} \tag{2.11}$$

Where t is the time, z is the position along the propagation direction of light, J is the injection current density, $N(t,z)$ is the carrier density, t_a is the thickness of active region, τ is the carrier recombination time, a is the differential gain, N_t is the transparency carrier density, M is the total number of channels, $P_i(t,z)$ is the power in the ith channel, hf is the energy of photon, w is the width of waveguide, t_{eff} is the effective thickness of the waveguide and $\Gamma = t_a / t_{eff}$ is the confinement factor.

The gain coefficient of the amplifier is given by

$$g(t,z) = \left[N(t,z) - N_t\right] a\Gamma L \tag{2.12}$$

The crosstalk can be suppressed by keeping the gain coefficient constant. By replacing J with I/wL, multiplying $a\Gamma L$ on both sides of equation (2.11) and rearranging items, the equation becomes

$$\frac{\partial\left(N(t,z) - N_t\right)a\Gamma L}{\partial t} = \frac{I\tau\, a\Gamma}{wqt_a} - \frac{N(t,z)a\Gamma L}{\tau} - a^2\Gamma L\left(N(t,z) - N_t\right)\frac{\sum_{i=1}^{M} P_i(t,z)}{h\nu w t_{eff}} \tag{2.13}$$

Where I is the bias current of the SOA. Because at steady state, $\partial N_t / \partial t = 0$. Normalizing the power to saturation power P_s

$$Q_i(t,z) = \frac{a\tau\, P_i(t,z)}{h\nu w t_{eff}}$$

For SOA model below, variation of the normalized total optical power for all channels

$$P(t,z) = \sum_{i=1}^{M} Q_i(t,z) \tag{2.14}$$

As with variation in time, the distance moved by photon varies. Therefore, $t_1 = t/\tau$ and $z_1 = z/L$ is considered here. By substituting the gain coefficient and total power from equation (2.12) and (2.14) to (2.13), we have

$$\frac{\partial g(t,z)}{\partial t_1} = \frac{I\, a\Gamma}{wqt_a} - \frac{N(t,z)a\Gamma L}{\tau} - \frac{g(t,z)}{\tau}P(t,z) \tag{2.15}$$

Rearranging the equation (2.15)

$$\frac{\partial g(t,z)}{\partial t_1}+\frac{g(t,z)}{\tau}P(t,z)=\frac{a\Gamma}{\tau}\left[\frac{I\,\tau}{wqt_a}-N(t,z)L\right] \tag{2.16}$$

This is a first-order differential equation; its solution for time varying is

$$g(t_1,z_1)=\exp\left(-\int_{-\infty}^{t_1}\frac{P(t,z)}{\tau}dt\right)\int_{-\infty}^{t_1}\left[\begin{array}{l}\frac{a\Gamma}{\tau}\left[\frac{I\,\tau}{wqt_a}-N(t,z)L\right]\\ \times\exp\left(\int_{-\infty}^{t_1}\frac{P(t,z)}{\tau}dt\right)dt\end{array}\right] \tag{2.17}$$

Solution of this equation with variation in time and position from equation (A8) in appendix is

$$g(t_1,z_1)=\frac{a\Gamma}{\tau P_L}\left[\frac{I\tau}{wqt_a}\exp\left(\frac{\Delta P_1}{\tau}\right)+\sum_{n=1}^{M}\frac{(-1)^n}{P_L^{n-1}}L\,\overline{N}^n(t_n,z_n)\exp\left(\frac{\Delta P_n}{\tau}\right)\right] \tag{2.18}$$

Where ΔP and $N(t_n,z_n)$ is the time variation of power and carrier density. Also taking derivative of power coefficient, $P_L=\partial P(t_1,z_1)/\tau\partial t_1$ for reducing complexity of the system and derivative of carrier density, $\overline{N}=\partial N(t_1,z_1)/\partial t_1$.

The variation of gain is

$$g(t_1,z_1)=g(t,z)+\Delta g \tag{2.19}$$

Where Δg is the small dynamic variation of $g(t_1,z_1)$ around $g(t,z)$. The power varies from $P(t,z)$ to $P(t_1,z_1)$ for variation in time and position. Substituting (2.19) in (2.16), and at steady state $\partial g/\partial t_1=0$. Then, we have

$$\frac{\partial\Delta g}{\partial t_1}+\frac{\Delta g}{\tau}P(t_1,z_1)=\frac{a\Gamma}{\tau}\left[\frac{I\,\tau}{wqt_a}-N(t,z)L\right]-g(t,z)\frac{P(t_1,z_1)}{\tau} \tag{2.20}$$

Δg is small gain variation which can be found by solving first order differential equation (2.20)

$$\Delta g(t_1,z_1)=\exp\left(-\int_{-\infty}^{t_1}\frac{P(t_1,z_1)}{\tau}dt_1\right)\left[\begin{array}{l}\int_{-\infty}^{t_1}\frac{a\Gamma}{\tau}\left[\frac{I\,\tau}{wqt_a}-N(t,z)L\right]\times\\ \exp\left(\int_{-\infty}^{t_1}\frac{P(t_1,z_1)}{\tau}dt_1\right)dt_1-g(t,z)\times\\ \int_{-\infty}^{t_1}\frac{P(t,z)}{\tau}\exp\left(\int_{-\infty}^{t_1}\frac{P(t_1,z_1)}{\tau}dt_1\right)dt_1\end{array}\right] \tag{2.21}$$

Solution of the equation (2.19) from equation (A13) of appendix is

$$\Delta g(t_1,z_1)=\frac{a\Gamma I}{wqt_a P_L}\exp\left(\frac{\Delta P_1}{\tau}\right)+\frac{1}{\tau}\sum_{n=1}^{M}\frac{(-1)^n}{P_L^n}\exp\left(\frac{\Delta P_n}{\tau}\right)\times \left[a\Gamma L\,\overline{N}^n(t_n,z_n)-g\,\overline{P}^{n-1}(t_{n-1},z_{n-1})\right] \tag{2.22}$$

By substituting the value of gain coefficient and rearranging parameters. From appendix equation (A14) the equation becomes as

$$\Delta g(t_1,z_1)=\frac{a\Gamma}{\tau P_L}\left[\frac{I\tau}{wqt_a}\exp\left(\frac{\Delta P_1}{\tau}\right)+\sum_{n=1}^{M}\frac{(-1)^n}{P_L^{n-1}}L\exp\left(\frac{\Delta P_n}{\tau}\right)\times \left[\overline{N}^n(t_n,z_n)-(N(t,z)-N_t)\overline{P}^{n-1}(t_{n-1},z_{n-1})\right]\right] \tag{2.23}$$

Equation (2.18) shows that for multichannel WDM signals, the SOA gain directly depends upon the bias current of the SOA. The variation in gain leads to crosstalk. As deduced from equation (2.23), the small dynamic variation in gain depends upon the variation of bias current, lifetime, confinement factor and power of the input signals.

As from equation (2.23), if longer is the lifetime taken then smaller will be gain variation which produces interchannel crosstalk same as reported in [Xu *et al.*, 2003]. Similarly, if we decrease the bias current, it results reduction in gain fluctuation *i.e.* less crosstalk. But by reducing the injection current, amplification factor goes on decreasing. As from equation (2.23) by increasing the confinement factor, the SOA-induced crosstalk increases. Also equation (2.23) shows that with increase in launched power leads to increase in the crosstalk.

2.1.3 Power Penalty Analysis of SOA for Multichannel

The rate equation of optical power in the SOA region [Xu *et al.*, 2003] is

$$\frac{\partial P_i(t,z)}{\partial z}=a\Gamma(N(t,z)-N_t)P_i(t,z)-\alpha_w P_i(t,z) \tag{2.24}$$

Where α_w is the waveguide loss. The unsaturated amplifier gain for multichannels is represented by

$$P_{out}=P_{in}g(t,z)L \tag{2.25}$$

The power penalty in presence of impairment is defined as the amount of increase in signal power required (in dB) to maintain the same bit error rate as in the absence of that impairment. The power penalty in presence of impairment is written as

$$P_{penalty}(dB)=10\log_{10}\frac{P_{in}}{P_{out}} \tag{2.26}$$

This $P_{penalty}$ amount of power required with same bit error rate as in the absence of the impairment. Power penalty varies with time and position inside the active region of the SOA. By rearranging the equation (2.24), we have

$$P_i(t,z) = \frac{\partial P_i(t,z)}{\partial z} \Big/ a\Gamma\left(N(t,z) - N_t\right) - \alpha_w \tag{2.27}$$

Substituting equation (2.25) and (2.27) in (2.26)

$$P_{penalty}(dB) = \frac{\partial P_i(t,z)/\partial z}{a\Gamma\left(N(t,z) - N_t\right) - \alpha_w}\left(1 - g(t,z)L\right) \tag{2.28}$$

Using equation (2.12) in (2.28), we have

$$P_{penalty} = \frac{\partial P_i(t,z)/\partial z}{a\Gamma\left(N(t,z) - N_t\right) - \alpha_w} - L^2\left(N(t,z) - N_t\right)\frac{\partial P_i(t,z)/\partial z}{\left(N(t,z) - N_t\right) - \alpha_w} \tag{2.29}$$

Due to a small variation in power, there is a variation in gain Δg . So there is also change in penalty occur in equation (2.29) as

$$\Delta P_{penalty} = \frac{\partial \Delta P_i(t,z)/\partial z}{a\Gamma\left(\Delta N(t,z) - N_t\right) - \alpha_w} - L^2\left(\Delta N(t,z) - N_t\right)\frac{\partial \Delta P_i(t,z)/\partial z}{\left(\Delta N(t,z) - N_t\right) - \alpha_w} \tag{2.30}$$

From equation (2.30), it shows that confinement factor and differential gain are inversely proportional to power penalty. As we increase the confinement factor the power penalty goes on decreasing but the quality of signal should be recognizable for power margin and forwarded error check maximum up to 15 dB. Also shown from the equation as we increase the input power the power penalty goes on increasing.

2.1.4 Bit Error Rate Estimation due to XGM in SOA

Gain variation Δg as the function of time and position of the photon

$$\Delta g(t,z) = \Delta g_1(t,z) + \Delta g_2(t,z) \ldots\ldots\ldots + \Delta g_i(t,z) \ldots\ldots + \Delta g_I(t,z) \tag{2.31}$$

The variance of gain variation is

$$\sigma^2_{\Delta g(t,z)} = \sum_{i=1}^{k} \frac{\left(\Delta g_i(t,z) - \Delta g_m(t,z)\right)^2}{k} \tag{2.32}$$

Where $\Delta g_m(t,z)$ is the mean value of small gain fluctuation and k is integer.

$$\sigma^2_{\Delta g(t,z)} = \sum_{i=1}^{k} \frac{1}{k}\left[\begin{array}{l} \dfrac{a\Gamma I}{wqt_a P_L}\exp\left(\dfrac{\Delta P_{1i} - \Delta\Delta_{1m}}{\tau}\right) \\ + \dfrac{1}{\tau}\sum_{n=1}^{M}\dfrac{(-1)^n}{P_L^n}\exp\left(\dfrac{\Delta P_{ni} - \Delta\Delta_{nm}}{\tau}\right) \\ \times\left[\begin{array}{l} a\Gamma L\left\{\overline{N}_i^n(t_{ni},z_{ni}) - \overline{N}_m^n(t_{nm},z_{nm})\right\} - (g_i - g_m) \\ \times\left\{\overline{P}_i^{n-1}(t_{(n-1)i},z_{(n-1)i}) - \overline{P}_m^{n-1}(t_{(n-1)m},z_{(n-1)m})\right\} \end{array}\right] \end{array}\right]^2 \tag{2.33}$$

Where subscript m is denoted as the mean value. By using Gaussian approximation and estimate the BER through the differential gain Q factor same as [Wei and Zhang, 2005]

$$Q_{\Delta\Phi} = \frac{\Pi}{2\sqrt{\sigma^2_{\Delta g(t,z)} + \frac{N_o}{E_b}}} \tag{2.34}$$

When power penalty occurs, then BER as

$$Q_{\Delta\Phi} = \frac{\Pi}{2\sqrt{\frac{N_o}{E_b} - \sigma^2_{\Delta g(t,z)}}} \tag{2.35}$$

The bit error is estimated as

$$BER \approx erfc\left(\frac{Q_{\Delta\Phi}}{2}\right) \approx \exp\left[-\frac{\Pi}{8\left(\sigma^2_{\Delta g(t,z)} + \frac{N_o}{E_b}\right)}\right] \tag{2.36}$$

When there is no cross gain modulation, then BER for DPSK is

$$BER = \frac{1}{2}\exp\left[-\frac{E_b}{N_o}\right] \tag{2.37}$$

So from equation (2.35) and (2.36), we conclude that bit error rate degradation occurs due to cross gain modulation among the WDM channels.

2.2 Transmission Performance of 200 Gb/s WDM Signals by using Cascaded Optimized SOAs with OOK and DPSK Modulation Formats

With the growing transmission rates, the demands in the field of optical communication, electronic regeneration has become more and more expensive. The powerful optical amplifiers came into existence, which eliminated the costly conversions from optical to electrical signal and vice versa. When SOAs work in saturation region, it has high nonlinearities, which restrains it from use in long-haul wavelength division multiplexing transmission system. Most of the researchers have used conventional SOAs for long distance communication as already discussed in the section 1.5.3 of Chapter 1. It is observed from the pervious literature that the maximum transmission distance is 1050 km with capacity 8 × 10 Gb/s by using differential phase shift keying (DPSK) modulation format at channel spacing 400 GHz. Using OOK system, the maximum transmission

distance reported is 420 km with 100 Gb/s bit rate. In this section, the work reported in [Xu *et al.*, 2004; Li *et al.*, 2004] is extended to further optimize SOA for increasing the transmission distance and channel capacity at 10 Gb/s.

2.2.1 SOA Model

The standard InGaAlAs travelling wave SOA with negligible residual facet reflectivity is taken as the amplifier model in our simulation. After solving equation (2.23) and simulative optimization, the relevant parameters are as follows: the length is 750 μm, the width of active layer is 2 μm, its thickness is 0.2 μm and confinement factor is 0.4. The transparency carrier density in the SOA is taken to be 1.5×10^{18} cm^{-3} and the differential gain of 2×10^{-16} cm^2. The carrier recombination time τ at this density is estimated to be 300 ps given the saturation power P_s = 21.36 mW. The optimum injection current evaluated is 400 mA same as reported in [Yamatoya and Koyama, 2004]. The optical bandwidth of SOA is 40 nm and considered spontaneous emission factor is 2. The input and output coupling losses of SOAs are taken as 3 dB.

2.2.2 Validation of SOA Model

In order to determine and optimize the SOA parameters, the simulations have been carried out for SOA in-line amplifier for optimizing the parameters by using setup shown in figure (2.1). The DPSK signal formed by encoding a continuous wave (CW) Lorentzian light source with different power and data in terms of RZ-DPSK format launched into optical phase modulation. The RZ data was pseudorandom binary sequence (PBRS) with word length 2^{10}-1 at 10 Gb/s. The full wave half maxima (FWHM) line_width of the CW light source is 1 MHz. The low pass Bessel filter have 3 dB bandwidth of 5 GHz for generation of data source in terms of RZ format. After that this DPSK signal is launched into SOA as in section 2.2.2. At the output, a raised cosine optical filter with a bandwidth 50 GHz is used. The output of filter is fed to DPSK receiver for detection of signal. The time domain simulation is carried out with simulation bandwidth 0.466 THz and centre wavelength 1550.38 nm.

Figure (2.2) shows the results of our SOA in-line amplifier model. This gives the variation of amplification factor with the increase in input signal power for different value of bias current (mA). It is measured that for 300 mA, the amplification factor goes to negative value which is not characteristic of an amplifier, but for 500 mA current, good amplification factor is obtained for -20 dBm input signal power.

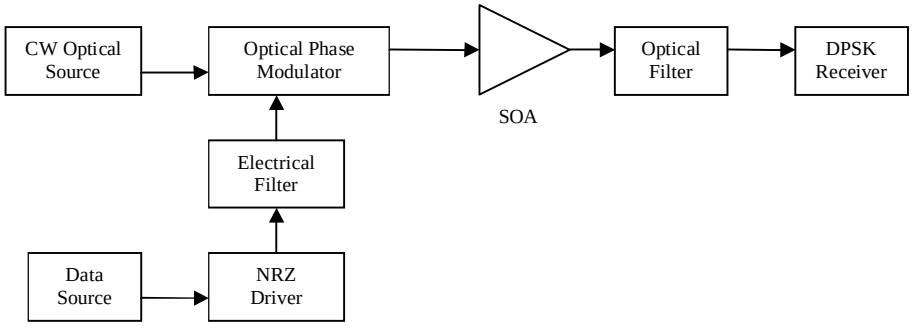

Figure 2.1: Setup for measuring the SOA response.

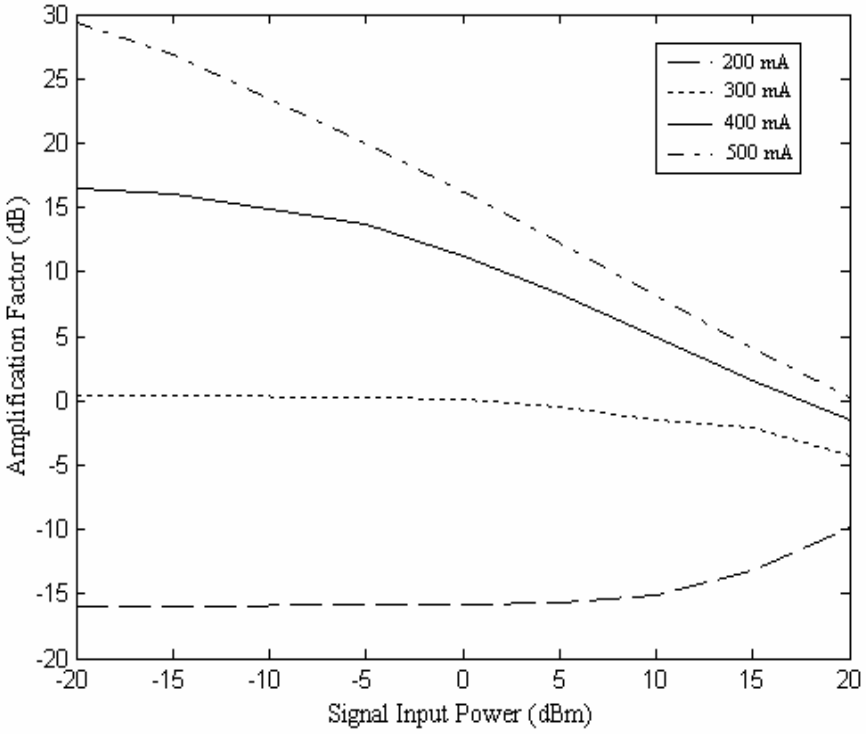

Figure 2.2: Amplification factor varies with signal input power at different bias currents.

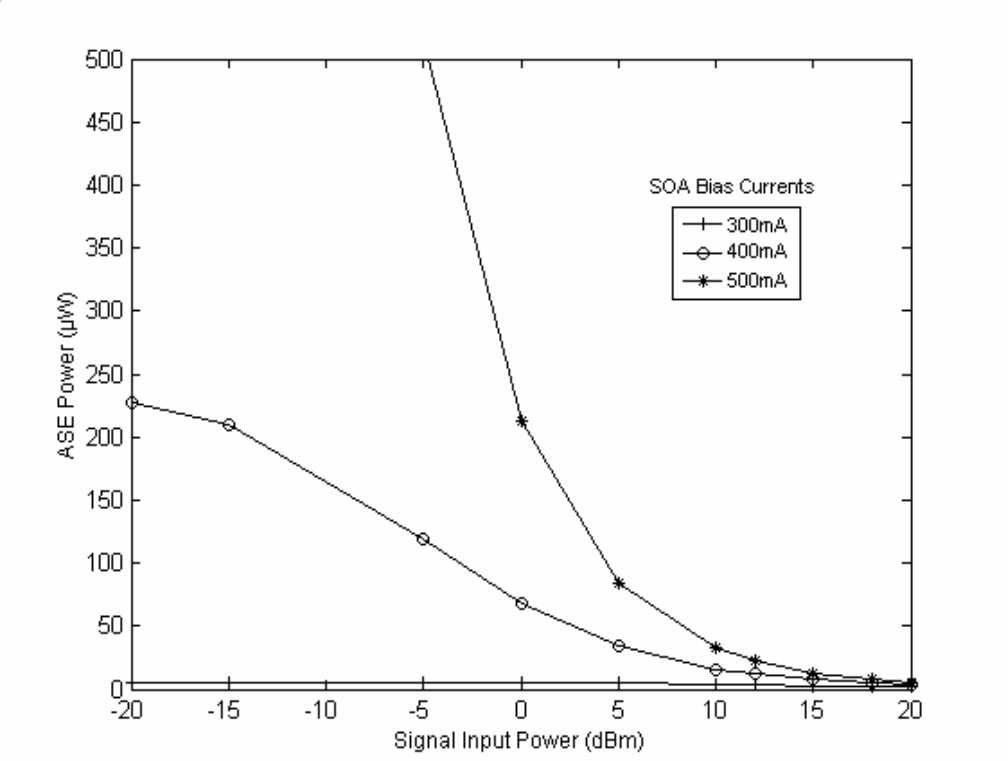

Figure 2.3: Amplified spontaneous power versus signal input power for different bias currents.

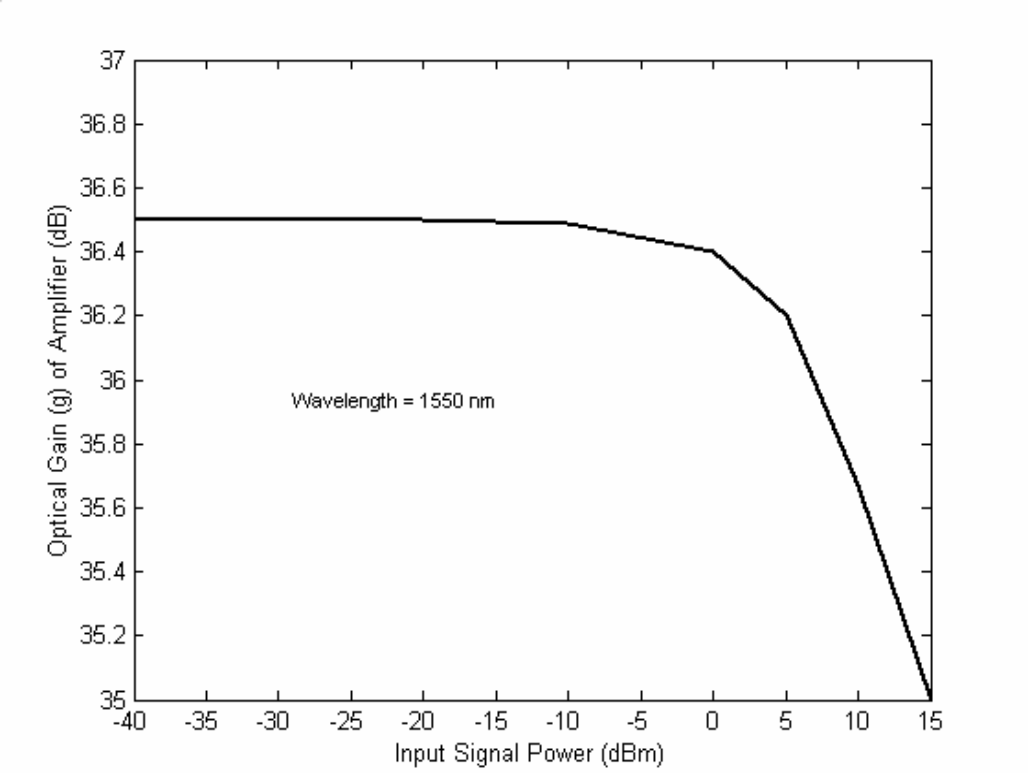

Figure 2.4: Gain of SOA varies with signal input power for 400 mA injection current.

It is also observed that amplification factor goes on decreasing with increase in input power. The ASE noise power is measured as shown in figure (2.3). The ASE noise power for 500 mA is 4457 μW for input -20 dBm which is too large and is not to suit the amplifier as reported in case [Yamatoya *et al.*, 2004]. For 300 mA bias current, the ASE noise power is very low as compared to current 500 mA. But at 300 mA, the amplification factor is negative which is not suitable. For 400 mA, ASE noise power is 227 μW at -20 dBm that is less as compared to current 500 mA and ASE reported in [Yamatoya *et al.*, 2004] with sufficient amplification factor. Therefore, 400 mA bias current is optimal bias current and at this bias current, constant gain of 36.5 dB observed up to saturation as shown in figure (2.4). Such a high constant gain has large tolerance of an input light wavelength.

The crosstalk in SOA in-line amplifier model is found for two or more channels. So simulations are carried out for setup as in figure (2.6) with two channels DPSK signal without single mode and dispersion shift fiber. We measure the crosstalk of these channels by varying the input signal power for different bias current (mA) as shown figure (2.5). It is observed that with the increase in bias current the crosstalk increases, which shows a good agreement with above analysis. It is also noted that at 400 mA, the crosstalk is -10.314 dB with input power -15 dBm at 100 GHz channel spacing, which shows an improvement over the result reported in [Choi *et al.*, 2002].

It is also observed that with increase the launched power, there is increase in the interchannel crosstalk for different bias current. As a result low crosstalk, low noise figure and ASE noise power with good agreement of amplification factor is obtained at 400 mA bias current of the SOA in-line amplifier. This is in agreement with the results reported in [Yamatoya *et al.*, 2004], as faster response was obtained at higher bias current.

2.2.3 20 × 10 Gb/s RZ-DPSK WDM Signal Transmission

The transmission performance of WDM signals with DPSK modulation format is analyzed by using cascaded SOAs. Figure (2.6) shows a schematic setup of 20 × 10 Gb/s DPSK WDM system. Twenty Lorentzian laser sources in the wavelength range 1550.38 nm to 1557.63 nm (100 GHz channel spacing) are modulated by each optical $LiNbO_3$ phase modulator with return to zero (RZ) format. The input of each transmission channel is -15 dBm. Therefore, the design carries 200 Gb/s WDM RZ signals over the transmission distance of 1190 km with 70 km SOA spacing.

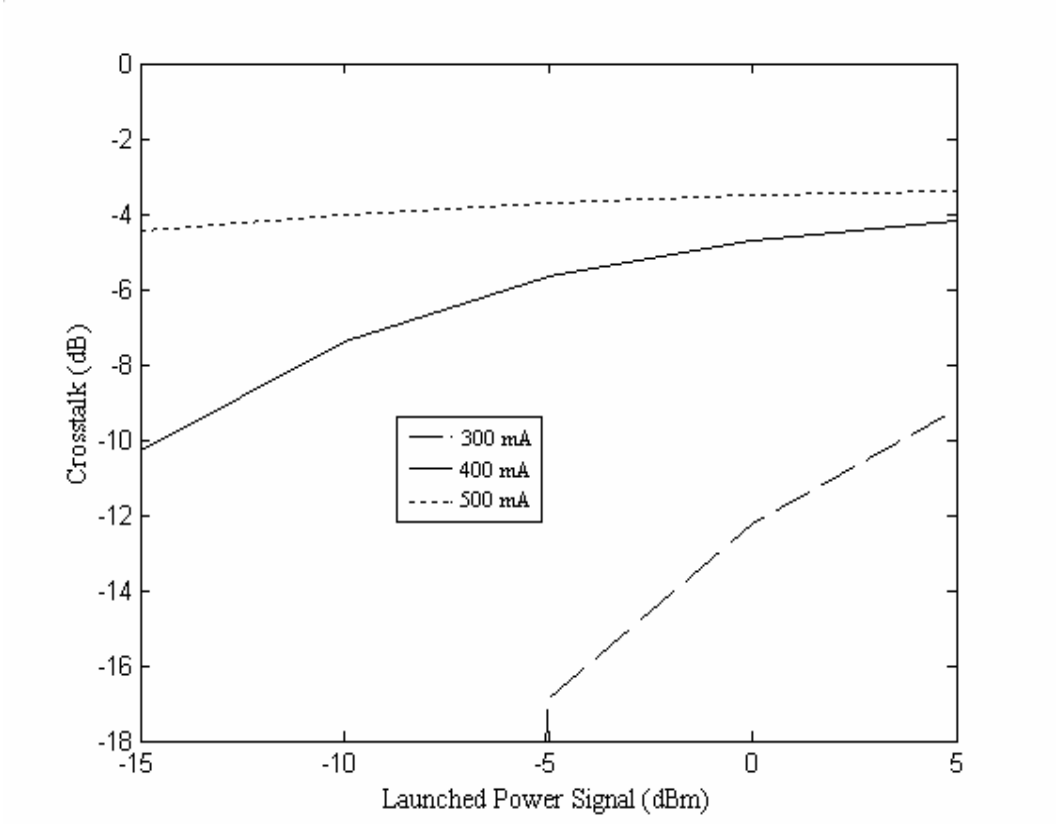

Figure 2.5: Crosstalk variation with launched power of SOA for different bias current.

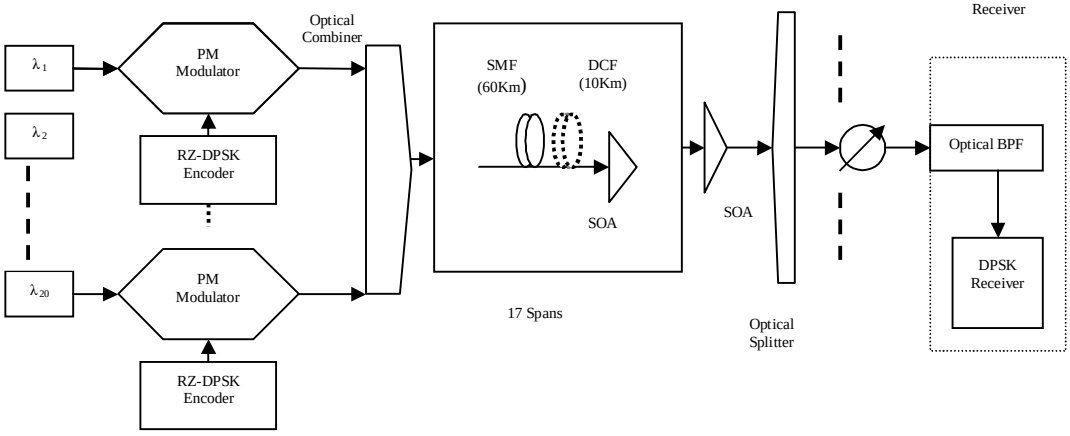

Figure 2.6: Schematic diagram of transmission system of 20 × 10 Gb/s RZ-DPSK WDM signals.

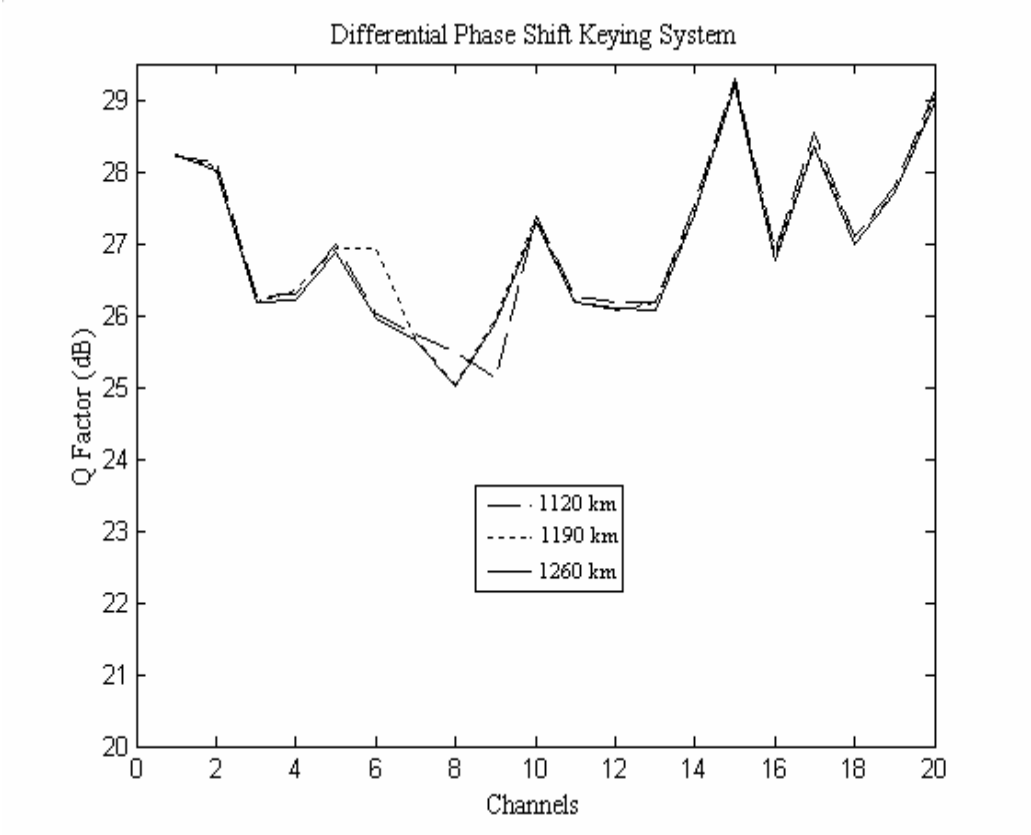

Figure 2.7: Q factor variations with channels for different transmission distances.

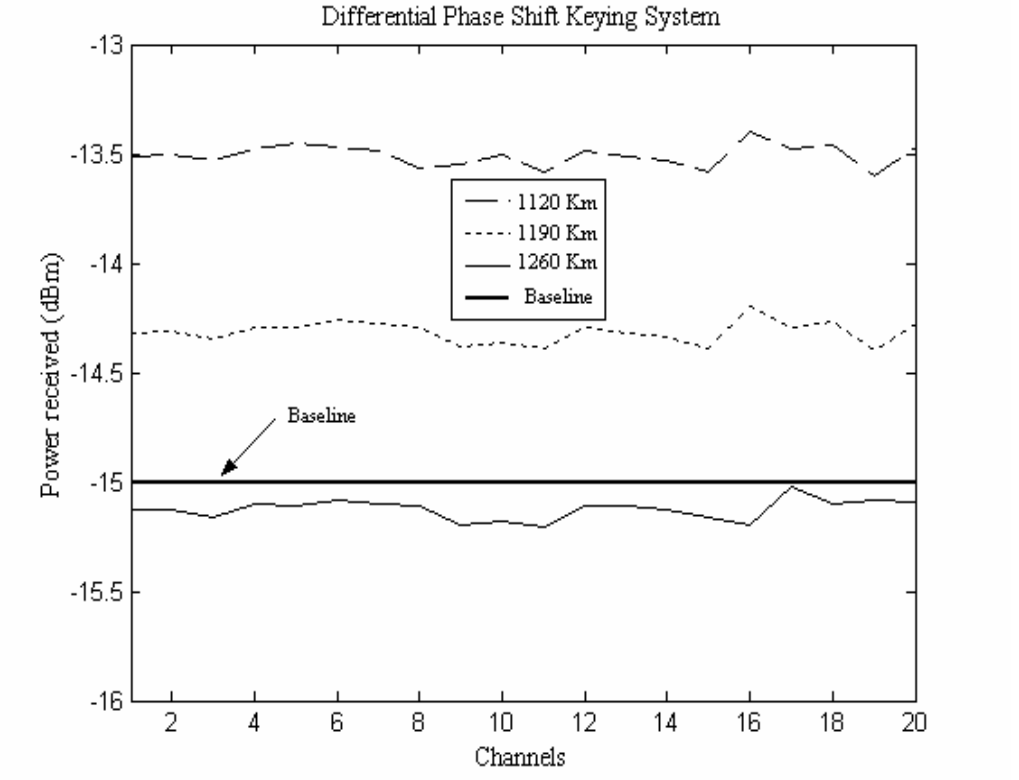

Figure 2.8: Optical power versus different channels for different transmission distances.

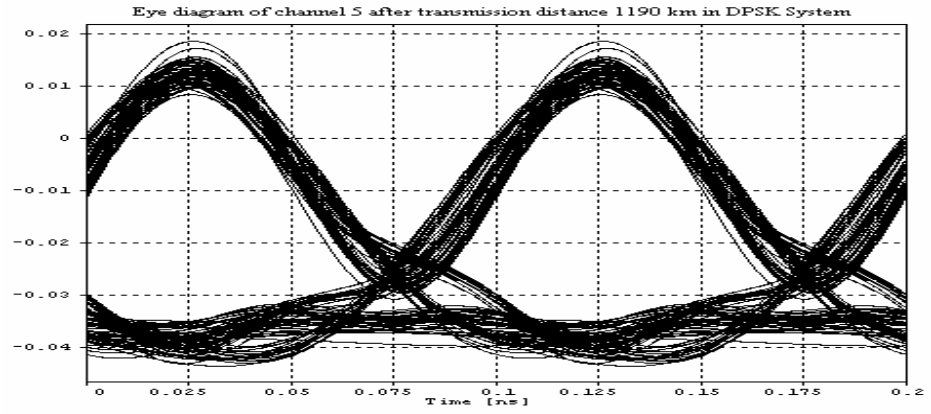

Figure 2.9a: Eye diagram after distance 1190 km of channel no. 5.

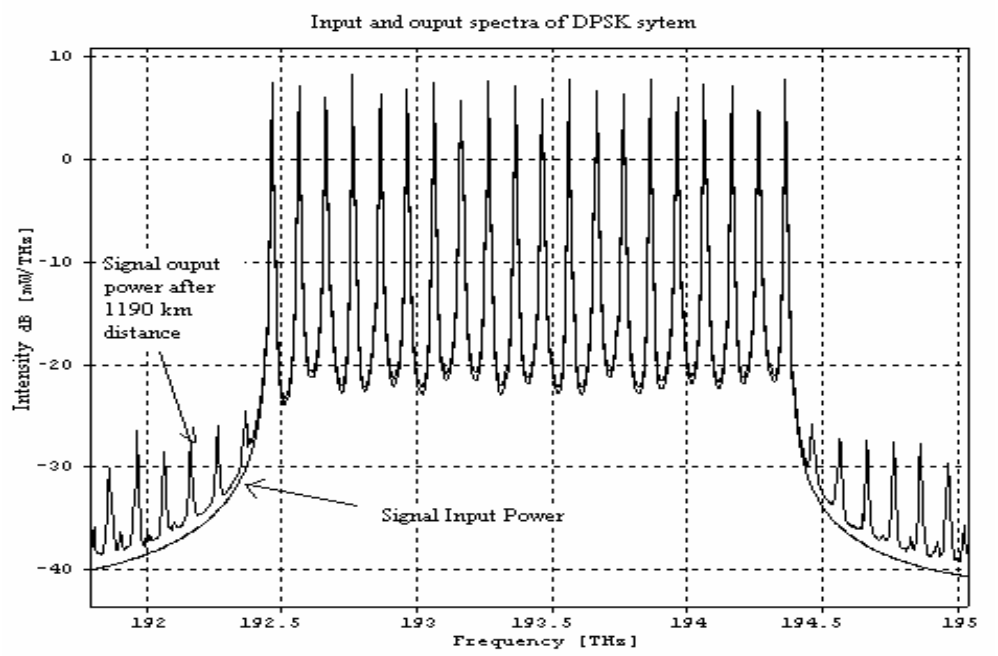

Figure 2.9b: Optical spectrum for twenty channels at different frequency before and after transmission distance 1190 km.

Each of the span consists of a 60 km standard single mode fiber (SMF), one or more DCF (dispersion compensating fiber) [Agrawal, 2002] and a SOA at the end. For SMF, the values dispersion parameter D at the operating wavelength is 17 ps/km-nm. The corresponding value for DCF is six times greater with opposite sign in order to achieve dispersion management for fiber link. The loss of SMF is 0.2 dB/km and loss of DCF is 0.55 dB/km. The time domain simulations have been carried out for this setting as shown in figure (2.6) with bandwidth 3.25 THz and centre frequency 193.417 THz.

The dependence of Q factor for different channels is measured as shown in figure (2.7). The quality is observed for the transmission 1120 km, 1190 km and 1260 km, which shows almost the same and more than 15 dB. But power received is not same for all these transmission distance as shown in figure (2.8). For transmission distance of 1120 km, approximately -13.5 dBm powers are observed for all channels. But for transmission distance 1260 km, there is power penalty approximately of 0.15 dB for all channels. For 1190 km distance, the power received is more than input power by 0.6 dB rounds off for all channels.

The eye diagram for distance 1190 km with P_{out} = -14.29 dBm for channel number 5 is shown in figure (2.9a). The optical spectrum of twenty channels for input and output signal power after transmission distance 1190 km is shown in figure (2.9b).

2.2.4 20 × 10 Gb/s RZ-OOK WDM Signal Transmission

The transmission performance of WDM signals with OOK modulation format is analyzed by using the cascaded SOAs. Figure (2.10) shows a schematic setup of 20 × 10 Gb/s OOK WDM system. Twenty Lorentzian laser sources in the wavelength range 1550.38 nm to 1557.63 nm (100 GHz channel spacing) are modulated by each optical $\sin^2$ Mach Zehnder amplitude modulator with return to zero (RZ) format. The input of each transmission channel is -15 dBm. Therefore, the design carries 200 Gb/s WDM RZ-OOK signals over 1050 km with 70 km SOA spacing. Each of the span consists of a 60 km standard single mode fiber (SMF), one or more DCF and a SOA at the end. The same dispersion parameter and loss is taken for SMF and DCF as in section 2.2.4. The corresponding value for the DCF is six times greater with an opposite sign. The time domain simulations have been carried out for this setup as shown in figure (2.10) with bandwidth 5.256 THz and centre wavelength 1550.3 nm.

In order to measure the performance of RZ-OOK WDM signal transmission, the quality and received power is noted. The Q factor is measured for different channels as shown in

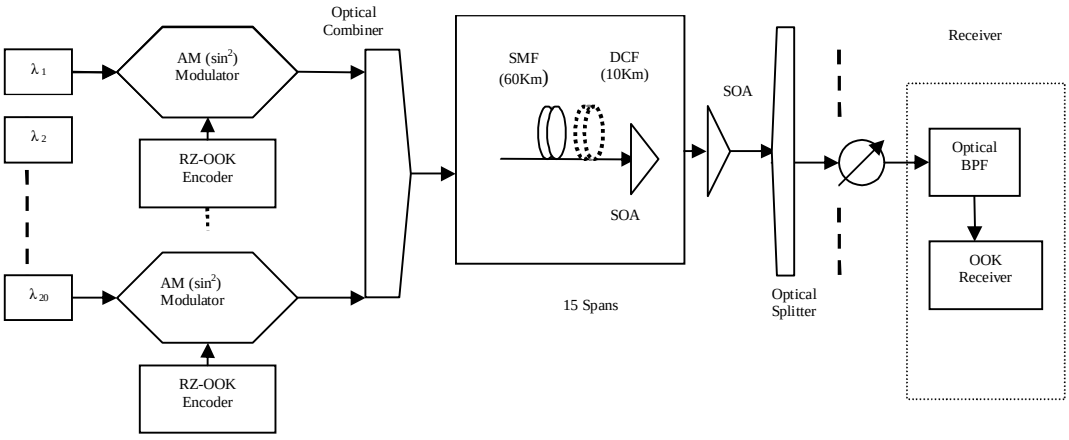

Figure 2.10: Schematic diagram of transmission system of 20 × 10 Gb/s RZ-OOK WDM signals.

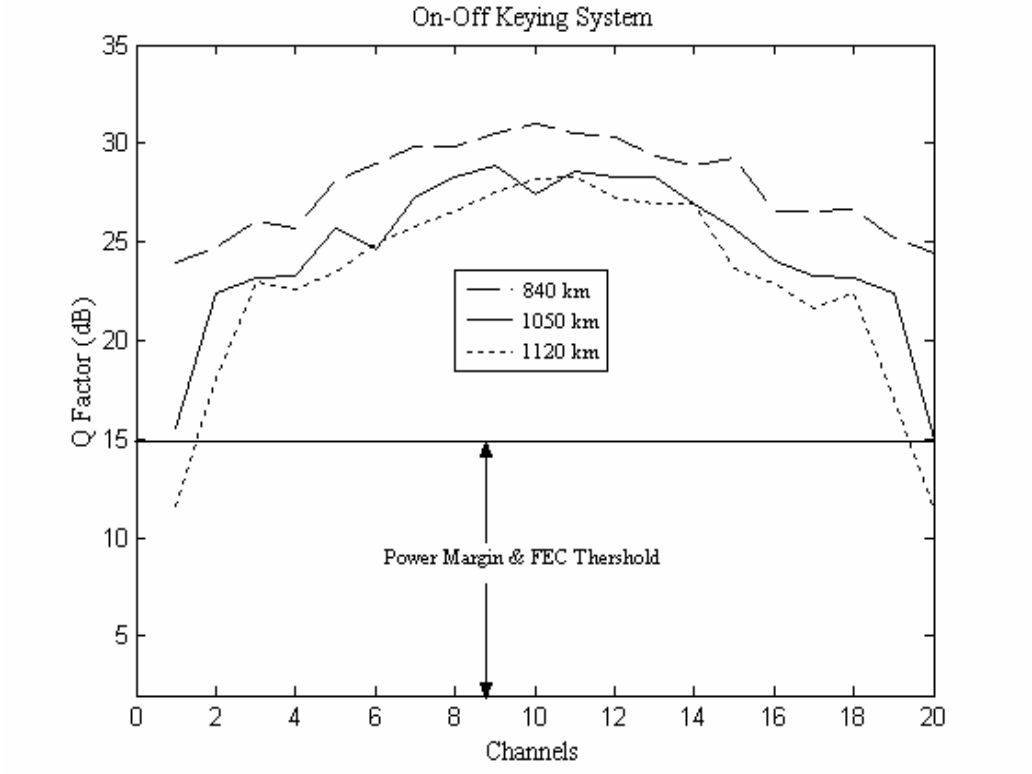

Figure 2.11: Q factor variations with channels for different transmission distances.

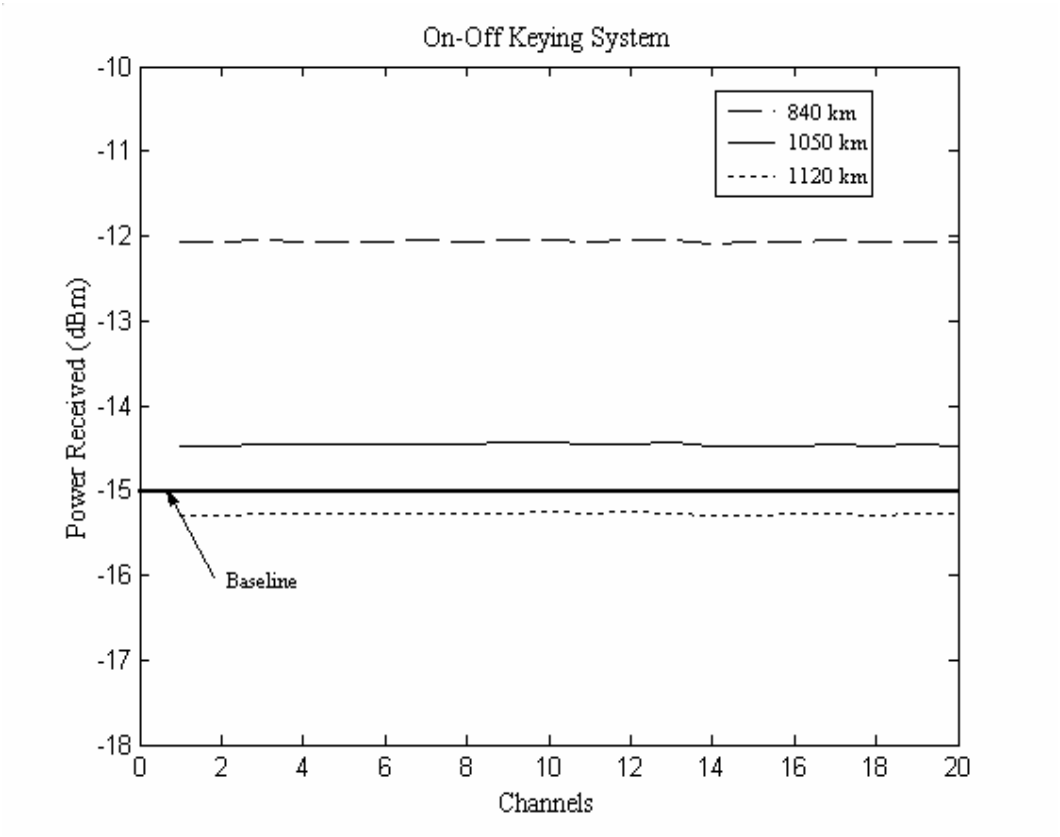

Figure 2.12: Optical power versus different channels for different transmission distances.

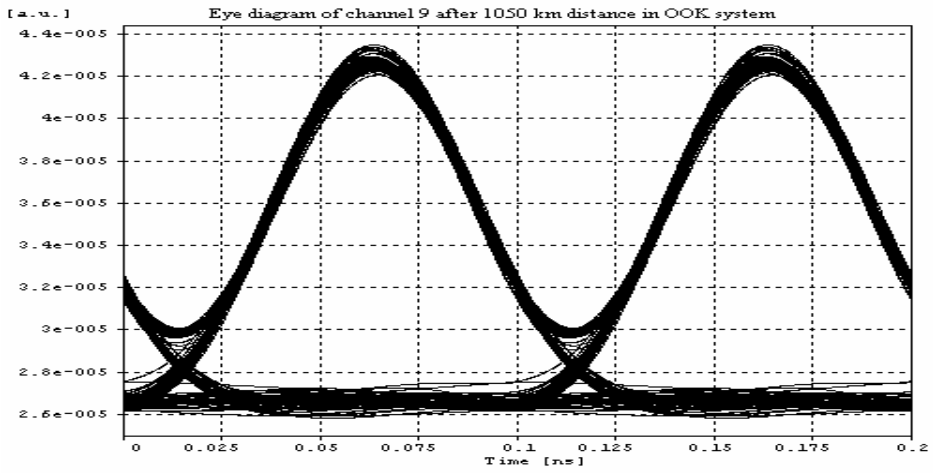

Figure 2.13a: Eye diagram after distance 1050 km of channel no. 9.

figure (2.11) with different transmission distances. It is observed that with the increase in transmission distance in the OOK system, the quality of extreme channels goes on decreasing. For transmission distance 1120 km, it is observed that Q factor of two extreme channels is less than 15 dB. Also power received is not same for all these transmission distance as in figure (2.12). For transmission distance 840 km, approximately -12.05 dBm power is observed for all channels. Also power improvement is observed in the case of 1050 km transmission distance. But for transmission distance 1120 km, there is power penalty approximately of 0.27 dB observed for all channels. For 1050 km distance, the power received for all channels is more than input power by 0.5 dB round off.

The eye diagram for distance 1050 km with P_{out} = -14.459 dBm for channel no. 5 is shown in figure (2.13a) having good quality as compared to eye diagram in figure (2.9a). This is due to lesser transmission distance in the OOK case. The optical spectrum of twenty channels for input and output signal power after transmission distance 1050 km is shown in figure (2.13b).

2.2.5 Comparison of DPSK and OOK Systems using SOA

The investigation is also made for the variation of bit error rate versus input signal power for the transmission distance 1050 km for the OOK system and 1190 km for the DPSK system. The figure (2.14) and (2.10) show the variation of bit error rate for different channels with increase in input signal power. With the increase in signal input power, the quality of signal goes on decreasing due to gain saturation. This tendency is almost same as in the case [Xu *et al.*, 2003]. All channels show (BER) bit error rate less than 10^{-10} up to the saturation power in DPSK.

For transmission distance 1050 km, the middle channels no. 10 and 15 has bit error rate less than 10^{-10} up to saturation power for both the OOK and the DPSK systems as shown in figure (2.14). It is observed that on-off keying system shows good performance for middle channels as compared to differential phase shift keying system for the same transmission distance. The DPSK system shows degradation earlier as compared to the OOK system if the launched input power is increased. From here, it is clear that when the SOA is in unsaturated mode the OOK system shows good performance.

For extreme channels, the OOK system degraded more as compared to DPSK system for same transmission distance which is shown in figure (2.15).

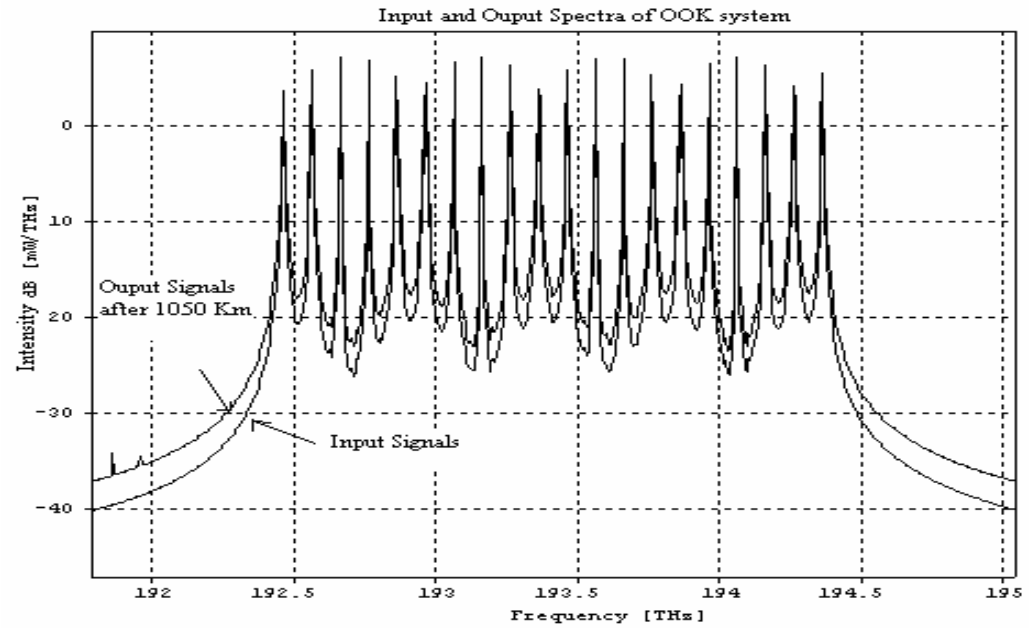

Figure 2.13b: Optical spectrum for twenty channels at different frequency before and after transmission distance 1050 km.

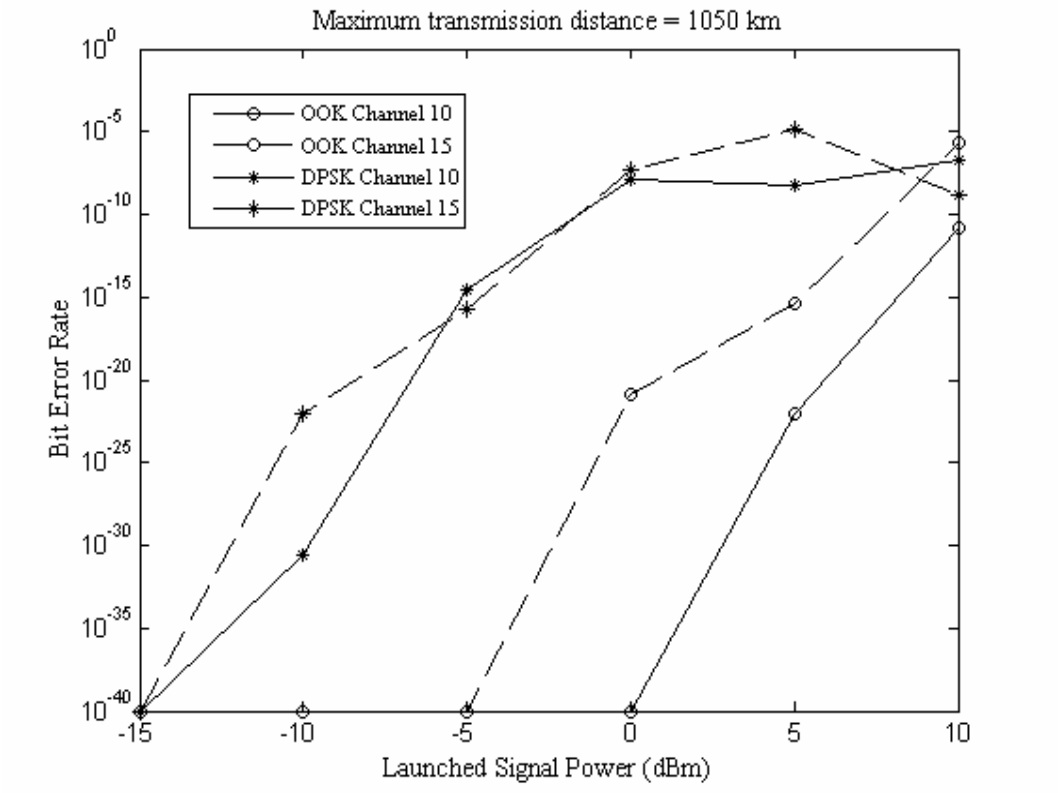

Figure 2.14: BER versus launched power of middle channels for OOK and DPSK systems.

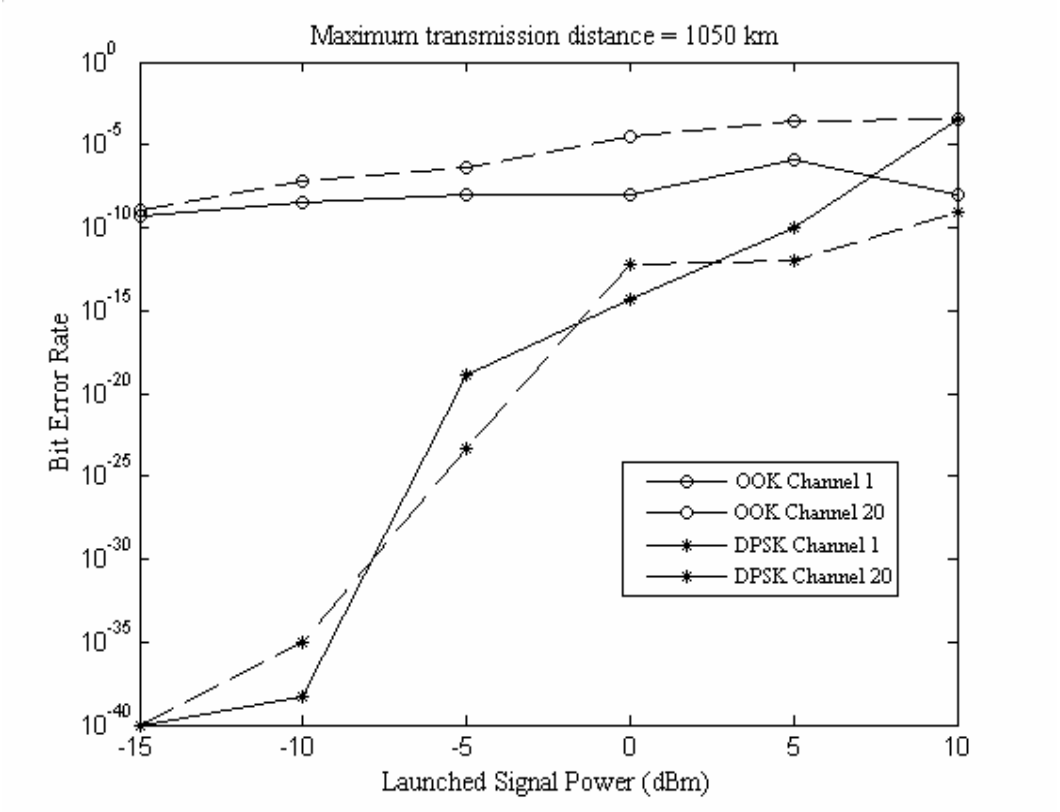

Figure 2.15: BER versus launched power of extreme channels for OOK and DPSK systems.

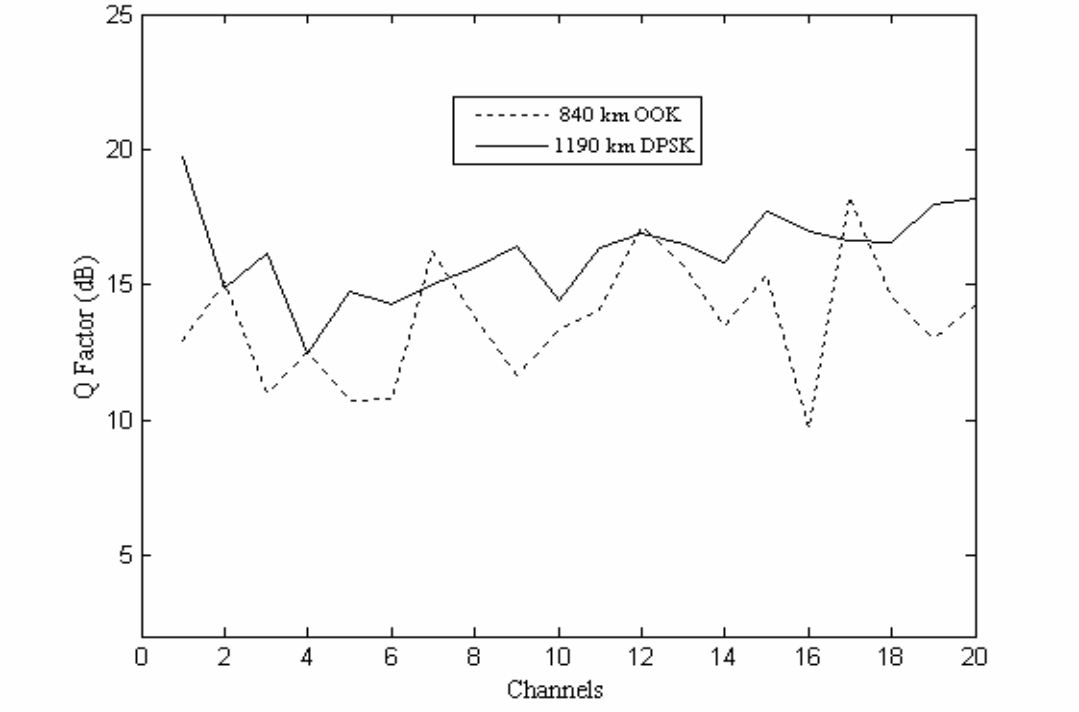

Figure 2.16: Q factor versus channels for OOK and DPSK systems at 20 GHz.

In the OOK system, with the increase in input power the BER increases more than 10^{-9} for the extreme channel numbers 1 and 20. But the DPSK system shows best performance for these extreme channels with the BER less than 10^{-10} up to saturation power. In the case of OOK system, both side extreme channels are degraded due to distortion. This distortion is due to amplitude modulation. Thus, it can be concluded that the OOK system has limited capacity as compared to the DPSK system.

Further investigation is made for the system with the same SOA in-line amplifier model for 20 GHz channel spacing in the same setup as shown in figure (2.6) and (2.10). With decreasing channel spacing from 100 GHz to 20 GHz, there is pronounced the cross gain modulation in SOA structure. Therefore, the Q factor is observed at sufficient power received for the distance 1050 km at 20 GHz. So, the transmission distance decrease by decreasing the channel spacing. This also meets with results observed in [Choi *et al.*, 2002; Spiekman *et al.*, 2000]. But the DPSK system has better quality as shown in figure (2.16) as compared to the OOK system.

2.3 Conclusions

In this chapter, the SOA model is proposed for minimum gain fluctuations and nil power penalty for the WDM multichannel transmission. The twenty channels at 10 Gb/s WDM has been transmitted over a transmission distance of 1190 km by using optimized SOAs as in-line and pre-amplifier with the DPSK modulation format at 100 GHz channel spacing. Also for the OOK system, the transmission distance is possible up to 1050 km for the first time. For this, the SOA bias current is optimized for reduction of crosstalk with sufficient amplification. The low crosstalk -10.314 dB, high optical gain 36.5 dB are achieved with reasonable ASE noise power. It is also observed that with the decrease in channel spacing, the quality of signal falls due to the increase in cross gain modulation. The DPSK system performs best for 1190 km transmission distance with bit error rate than 10^{-10} for all channels up to saturation power of the SOA. So by structural optimization of the SOA, the capacity and transmission distance has been increased for the DPSK system. But the OOK system is best for small number of channels up to saturation of the SOA. It is concluded that the DPSK system has large capacity as compared to the OOK system.

Chapter 3

Simulative Optimization of Semiconductor Optical Amplifier Structural Parameters for Multichannel WDM Transmission

This chapter is based on the optimization of SOA structural parameter for multichannel WDM transmission with DPSK systems, which is also related to the first objective of this research work. This can be achieved by reducing the cross gain modulation (XGM) and cross phase modulation (XPM) and optimizing the confinement factor of the SOA for improving the capacity and transmission distance. The optimization of the cross gain modulation (XGM) is done by using the analysis of the SOA for multichannel in pervious Chapter 2. The maximum transmission distance of 5220 km is evaluated for 400 Gb/s soliton RZ-DPSK WDM signals by using cascaded optimized SOA.

3.1 Optimization of Confinement Factor of SOA

For multichannel WDM optical communication system, channel interference is due to pulse broadening. This can be avoided only if channel spectrum retains its shape even when they pass through any optical components or devices. When multichannel signals pass through the SOA medium, the channel interfere exists but this can be avoided by confining the each channel spectrum. The confinement factor of the SOA reflects the faithful optical confinement of the applied input signal. The confinement factor is the structure parameter of the SOA. If confinement factor is high then output optical signal become quite sharp. The gain saturation is achieved at fast rate for high confinement factor.

The RZ differential phase-shift keying (DPSK) modulation format has attracted intense research interests [Xu. C. *et al.*, Apr. 2003] as the signal power is constant for this format, so this format when applied to SOA-based WDM transmission link reduces the cross gain modulation (XGM) effect accordingly. Also RZ-DPSK could provide 3 dB reductions in required received OSNR for given bit error rate (BER) [Xu. C. *et al.*, Apr. 2003]. We have investigated that 20 × 10 Gb/s transmission over 1190 km by using cascaded SOA with DPSK modulation format with channel spacing 100 GHz as reported in Chapter 2. We have reported that the 400 mA bias current is optimum with low crosstalk and ASE noise power.

Till the date, the maximum transmission distance was reported up to 1190 km with capacity of 20 × 10 Gb/s by using differential phase shift keying (DPSK) modulation format. Using the OOK system, the maximum transmission distance is 1050 km with 200 Gb/s bit rate as reported in previous Chapter 2. There is no previous literature found to optimize the confinement factor of the SOA for WDM transmission. In this part, the work reported in [Xu *et al.*, 2003 Li *et al.*, 2004] is further extended to optimize the SOA for increasing the transmission distance at 10 Gb/s.

3.1.1 Optimization of SOA Model

To optimize the SOA model, the simulation has been carried out for the setup given in figure (2.1) of Chapter 2 for our SOA in-line amplifier parameter as in section 2.2.2. The DPSK signal formed by encoding a continuous wave (CW) Lorentzian light source with different power and data in terms of RZ-DPSK format is launched into optical phase modulation. The RZ data was pseudorandom binary sequence (PBRS) with word length 2^{27}-1 at 10 Gb/s. The full wave half maxima (FWHM) line_width of CW light source is 1 MHz. The low pass Bessel filter has 3 dB bandwidth of 5 GHz for the generation of data source in terms of RZ format. Then DPSK signal is launched into the SOA as in section 2.2.2 of the Chapter 2. At the output, a raised cosine optical filter with bandwidth 50 GHz is used. The output of filter is fed into the DPSK receiver for detection of the signal. The time domain simulations are carried out with simulation bandwidth 0.466 THz with centre wavelength 1550.38 nm.

The simulations are carried out for different confinement factors of an SOA in-line amplifier model which is used for the transmission. The results in figure (3.1) show the variation of amplification factor with increase in input signal power for different confinement factors. It is observed that, for 0.35 confinement factor the amplification factor is low. But for confinement factor 0.45, good amplification factor is obtained, which is more than 18 dB for -15 dBm input signal power.

It is observed that amplification factor goes on increasing with the increase in the confinement factor. It is also observed that amplification factor goes on decreasing with the increase in input power. The noise power generated in the SOA due to spontaneous emission is also measured as shown in figure (3.2). The amplified spontaneous emission (ASE) noise power for confinement factor 0.45 is 227.24 μW is observed for input -20 dBm, which is very near as reported in case [Yamatoya *et al.*, 2004].

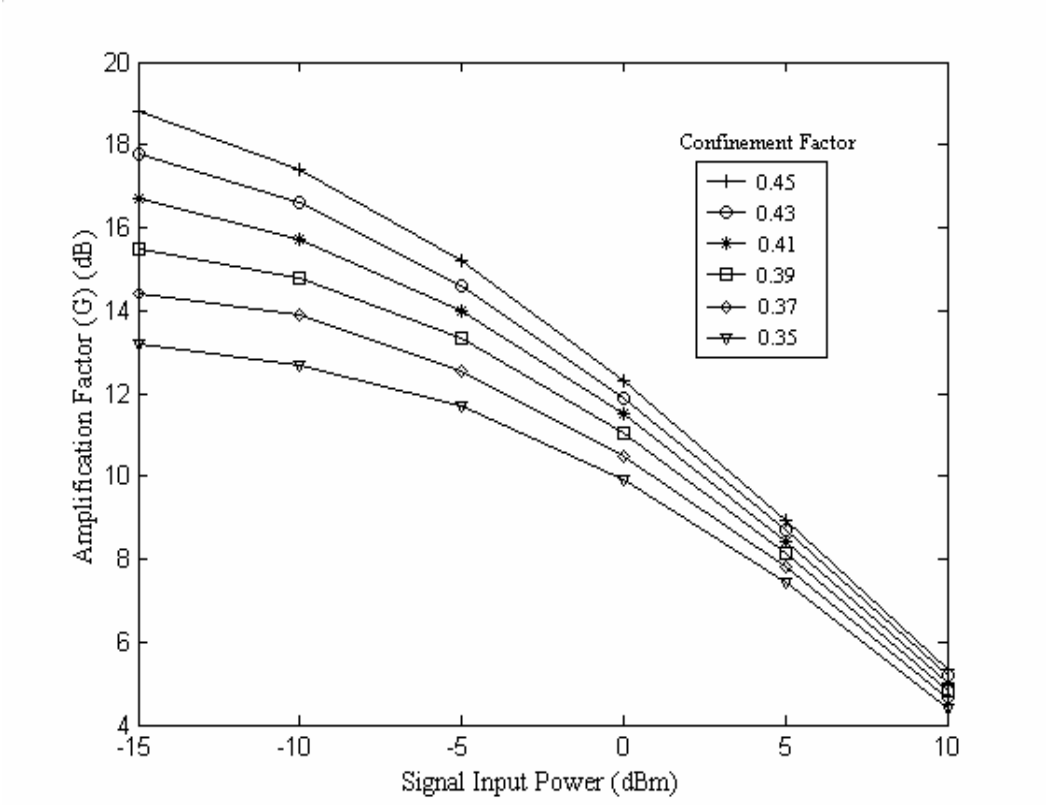

Figure 3.1: Amplification factor varies with signal input power at different confinement factors.

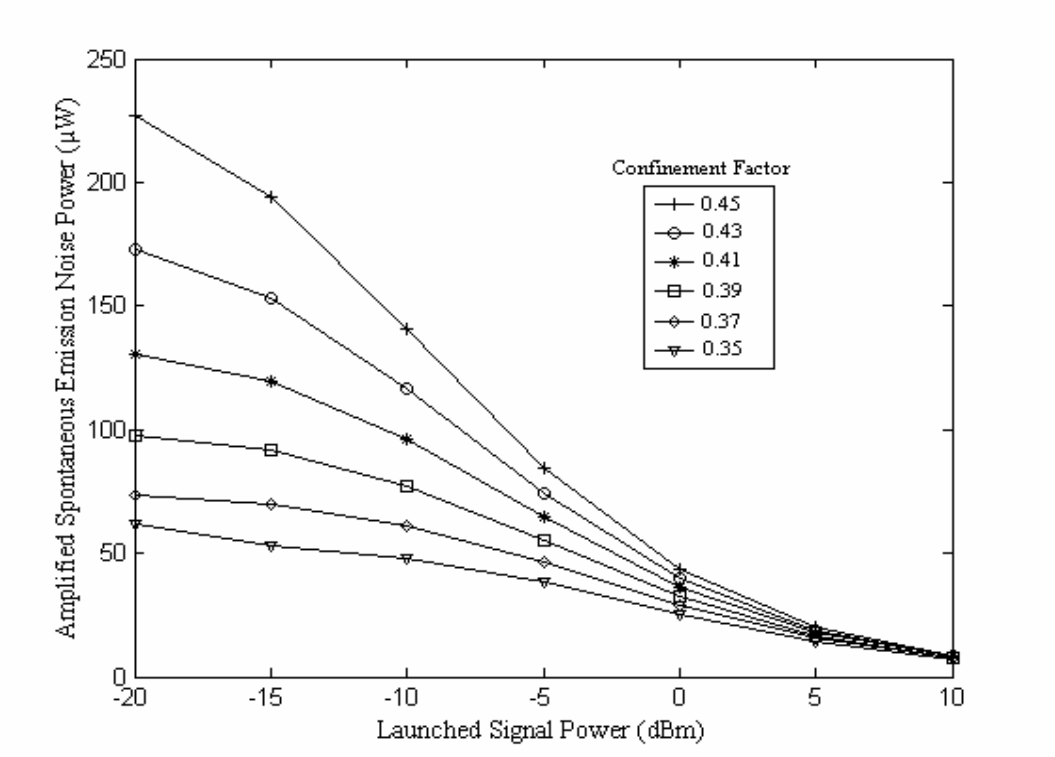

Figure 3.2: Amplified spontaneous power versus signal input power for different confinement factors.

For 0.35 confinement factor, the ASE noise power is very low as compared to confinement factor 0.45, but at 0.35, the amplification factor is very low which is not suitable. For confinement factor less than 0.43, ASE noise power is less than as compared to the ASE at confinement factor of 0.45 and reported as 227 μW at -20 dBm for current 400 mA [Yamatoya and Koyama, 2004]. Further, it is also observed that as there is increase in the input signal the ASE noise goes on decreasing in the SOA due to gain saturation and the amplification stops with the increase in the power.

We also found the SOA-induced crosstalk for the SOA model for two or more channels. Therefore, simulations are carried out for the setup as shown in the figure (3.5) with two channel DPSK signals without single mode and dispersion shifted fiber. The crosstalks of these channels are measured by varying the input signal power for different confinement factors as shown in figure (3.3).

It is also observed that with the increase in confinement factor, the crosstalk increases, which show good agreement with the above analysis. It is noted that at confinement factor 0.41 the crosstalk observed is -9.63 dB with input power -15 dBm at 100 GHz channel spacing and this shows an improvement in the result reported in [Choi *et al.*, 2002]. Further more it is observed that with the increase in launched power for different confinement factors, leads to an increase in the channel crosstalk.

The power penalty in the presence of impairment is defined as the increase in signal power required (in dB) to maintain the same bit error rate as that in the absence of that impairment. It also found the same power penalty for the SOA model. So simulations are carried out for the setup as shown in figure (3.5) with 60 km standard single mode fiber (SMF), one or more DCF (dispersion compensating fiber) as per [Agrawal, 2002] and a SOA in-line amplifier at the end. The length of DCF is chosen in accordance with [Agrawal, 2002] for complete compensation ($\overline{D} = 0$),

$$L_2 = \frac{-D_1 L_1}{D_2} \tag{3.1}$$

Where L_1 , L_2 are the lengths of SMF and DCF and D_1 , D_2 are the dispersion parameters for SMF and DCF. For SMF, the value of dispersion parameter D at the operating wavelength is 17 ps/km/nm. The corresponding value for DCF is six times greater with an opposite sign. The loss of SMF is 0.2 dB/km and loss of DCF is 0.55 dB/km. For fully compensating system, the dispersion parameters D_2 = -112 ps/km/nm.

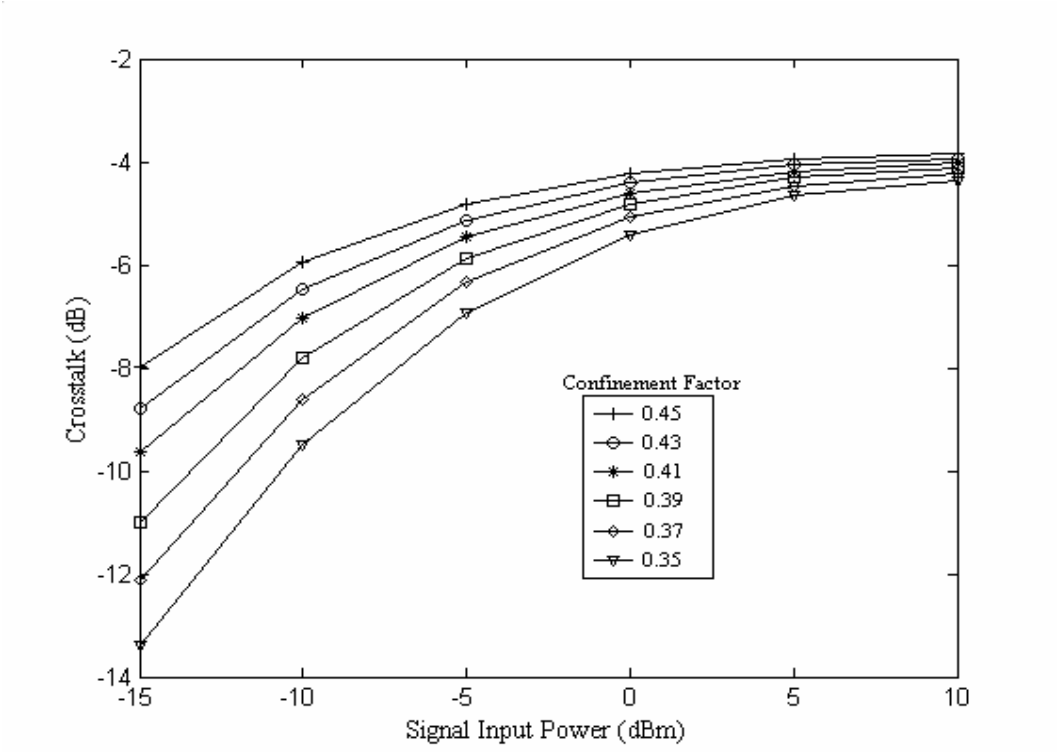

Figure 3.3: Crosstalk variation with launched power of the SOA for different confinement factors.

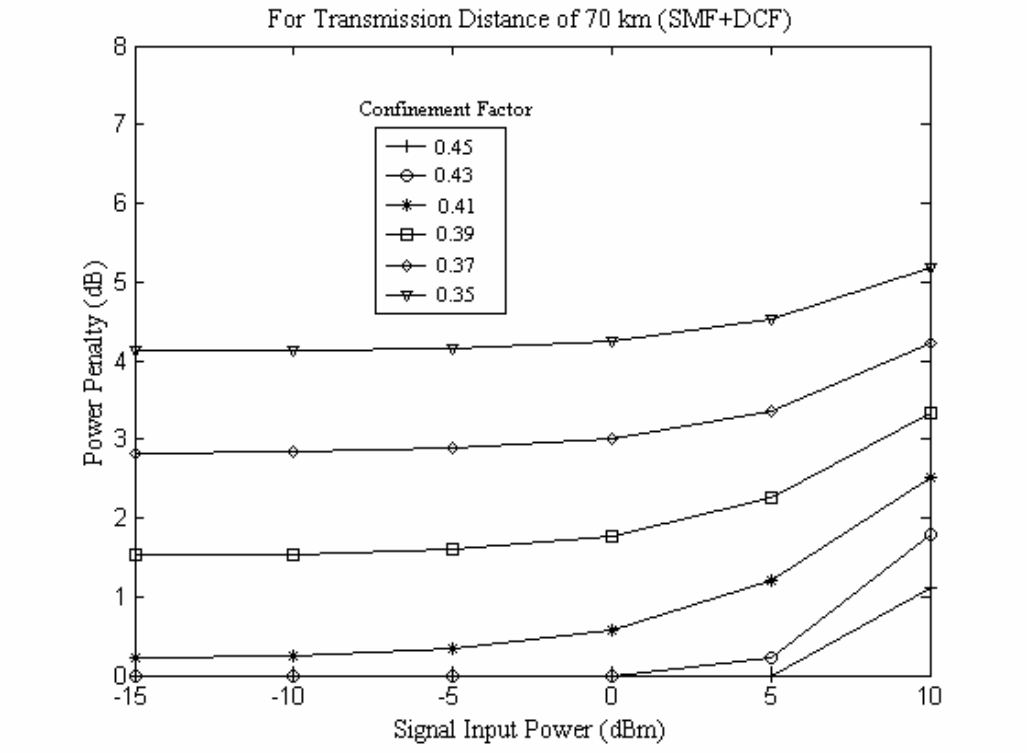

Figure 3.4: Power penalty variation with signal input power for different confinement factors of SOA.

Also second order dispersion parameters for SMF and DCF are $\partial D_1/\partial\lambda$ =0.08 ps/nm^2/km and $\partial D_2/\partial\lambda$ = - 0.48 ps/nm^2/km. The power penalty is calculated as per [Agrawal, 2002]. For good quality of output more than 15 dB at receiver, the penalty is given in equation (2.26) of Chapter 2.

The simulation result is shown in figure (3.4) for different confinement factors of the SOA. It is observed that by decreasing the confinement factor the power penalty goes on increasing which shows good agreement with power penalty analysis.

We observed that for the confinement factor of 0.41, almost negligible penalty is observed with -15 dBm input signal power. For confinement factor higher than 0.41, zero penalty is observed for single channel. But in multichannel there is SOA-induced crosstalk among different channels. Therefore, we can say that there may be a large bit error rate (BER). From the results, it is concluded that the confinement factor should lie in between 0.43 and 0.39, where the average amplification, ASE noise and crosstalk are observed.

3.1.2 Amplifier Model

The standard InGaAlAs traveling wave SOA with negligible residual facet reflectivity is taken as the amplifier model in our simulation. After solving the rate equations in Chapter 2, the relevant parameters are as follow: the length is 750 μm, the width of active layer is 2 μm, its thickness is 0.2 μm and optimized confinement factor is 0.41. The transparency of carrier density in the SOA is taken as 1.5×10^{18} cm^{-3} and the differential gain is 2×10^{-16} cm^2. The carrier recombination time τ at this density is estimated to be 300 picoseconds at the given the saturation power P_s = 20.84 mW. The unsaturated gain is ranging from 39.14 dB to 37.44 dB for the input signal ranging from -20 dBm to +10 dBm. The optimum injection current is evaluated to be 400 mA. This shows good agreements with result reported in [Yamatoya *et al.*, 2004]. Also the faster response was obtained at higher bias currents. The optical bandwidth of the SOA is 40 nm and the spontaneous emission factor considered here is 2. The input and output coupling losses of the SOAs are taken as 3 dB.

3.1.3 20 × 10 Gb/s RZ-DPSK WDM Signal Transmission

The transmission performance of WDM signals with DPSK modulation format is analyzed by using cascaded SOA. Figure (3.5) shows a schematic setup of 20 × 10 Gb/s

DPSK WDM system. Twenty Lorentzian laser sources in the wavelength ranging from 1550.38 nm to 1557.63 nm (100 GHz channel spacing) are modulated by each optical $LiNbO_3$ phase modulator with return to zero (RZ) format. The input of each transmission channel is -15 dBm. So, the design carries 200 Gb/s WDM RZ signals over different transmission distances with 70 km SOA spacing. Each span consists of a 60 km standard single mode fiber (SMF), one or more DCF (dispersion compensating fiber) as per [Agrawal, 2002] and a SOA at the end. For SMF, the value of dispersion parameter *D* at the operating wavelength is 17 ps/km-nm. The corresponding value for DCF is six times greater with the opposite sign. The loss of SMF is 0.2 dB/km and loss of DCF is 0.55 dB/km. The same fully compensating system is used here as in section 3.1.1. The time domain simulations have been carried out for this setup as shown in figure (3.5) with bandwidth 3.25 THz and centre frequency 193.417 THz.

In order to find the behaviour of the SOA with different confinement factors, the crosstalk and power penalty are observed simultaneously for long haul WDM transmission. The simulations are carried out for different transmission distances and confinement factors as shown in figure (3.5). The figure (3.6) shows the power penalty versus transmission distance for different confinement factors. For the confinement factor of 0.39, the power penalty goes on increasing up to 2.9 dB for distance 840 km with BER less than 10^{-10} as shown in figure (3.6) and (3.7). With further decrease the confinement factor to 0.37 power penalty goes to 19.4 dB, which is higher as compared to observed in 0.39 with same BER. For confinement factor of 0.45, the power penalty observed is nil but the BER goes on increasing with increase in the transmission distance. The increase in the BER is more at higher confinement factors even at zero power penalties. So the maximum transmission distance is possible with confinement factor just lower to the higher confinement factor with negligible power penalty and BER less than 10^{-9}.

If the confinement factor is more than 0.43, a high output is observed. But cross gain modulation (XGM) increases with the increase in confinement factor which causes degradation in the quality of the output signals. For confinement factors 0.43 and more, almost the same quality is observed up to saturation of the SOA. For limited transmission distance up to 700 km, quality of the signal is reasonable. But for transmission distance more than 700 km, the SOA structure with confinement factor 0.45 goes to deep saturation as compared to SOA structure with confinement factor 0.43. For transmission distance beyond 1700 km, poor bit error rate of more than 10^{-5} is observed. The BER meter is limited to measure the minimum BER of 22.75×10^{-3}.

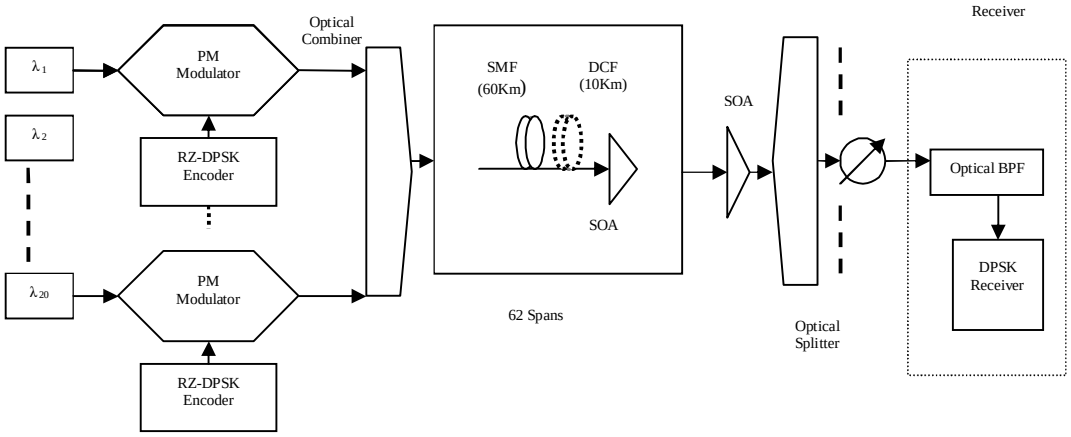

Figure 3.5: Schematic setup of transmission system of 20 × 10 Gb/s RZ-DPSK WDM signals.

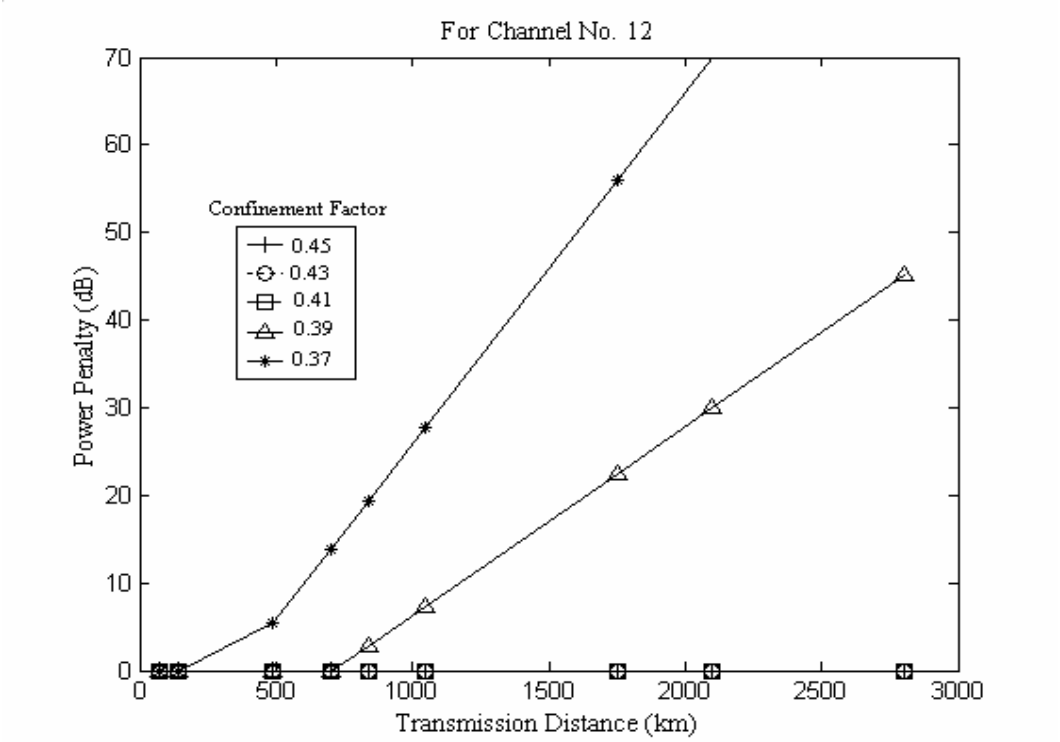

Figure 3.6: Power penalty as the function of transmission distance for varying confinement factors.

Table 3.1

Confinement factor versus maximum transmission distance.

Confinement Factor (Γ)	0.37	0.39	0.41	0.43	0.49
Maximum Transmission Distance	140 km	700 km	more than 2800 km	840 km	700 km

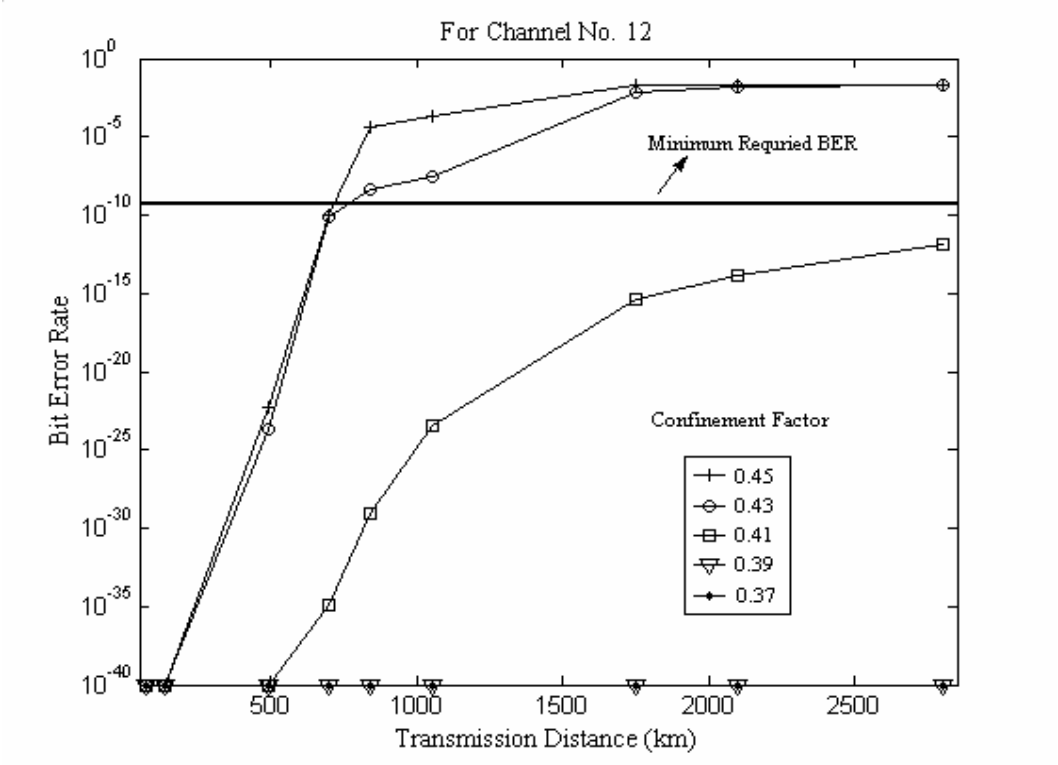

Figure 3.7: Bit error rate as the function of transmission distance for varying confinement factors.

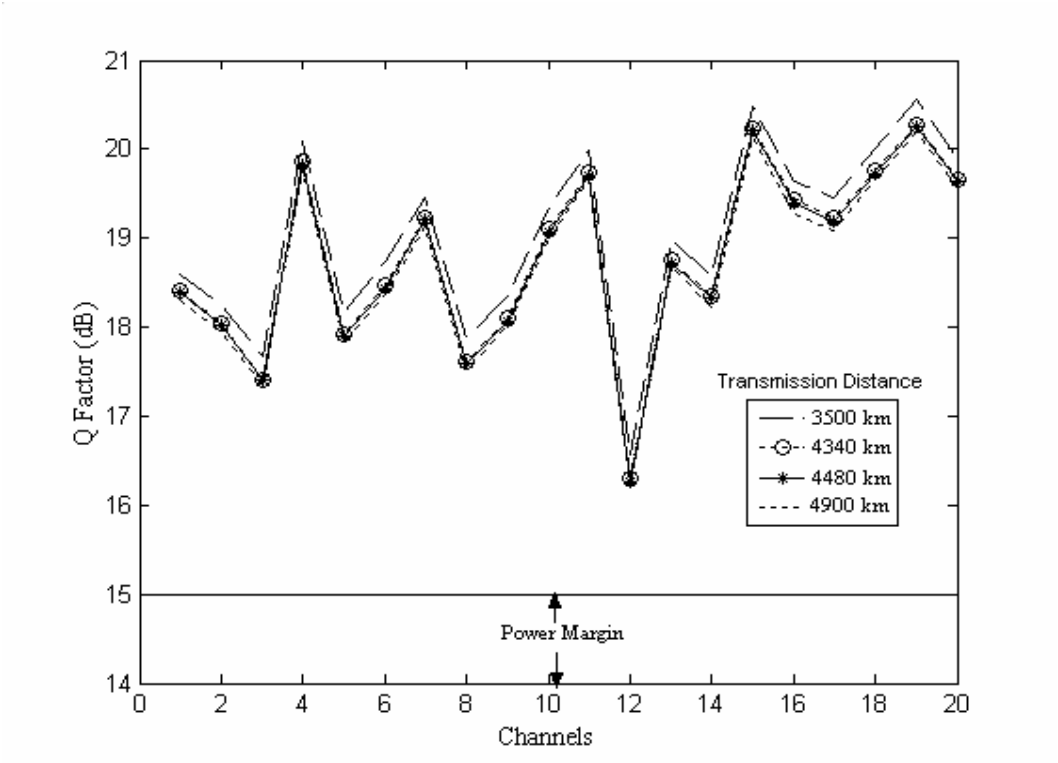

Figure 3.8: Q factor variations with channels for different transmission distances.

So, almost the same response is observed for both confinement factors 0.45 and 0.43 for transmission distance more than 1700 km. Table (3.1), shows that in the presence of crosstalk and power penalty, the maximum transmission distance is observed at confinement factor 0.41. Hence 0.41 confinement factor shows low power penalty and crosstalk for long haul WDM transmission distance. So at low crosstalk, low ASE noise power and low power penalty with good agreement of amplification factor is obtained at 0.41 confinement factor of the SOA in-line amplifier and pre-amplifier.

The transmission distance is further increased in order to find out the longest possible transmission distance. The Q factor is measure for the different channels with different transmission distances as shown in figure (3.8). The quality is measured for transmission distance 3500 km, 4340 km, 4480 km and 4900 km is shown in figure (3.8), which is same for all channels and more than 15 dB. The quality of signal for all channels goes on decreasing at low rate with the increase in transmission distance. But power received is not same for all these transmission distances as in figure (3.9).

At transmission distance of 3500 km, it shows approximately -11.9 dBm power received for all channels. Also at transmission distance 4340 km, it shows approximately -14.2 dBm power received for all channels. But for transmission distance 4480 km, there is power penalty of approximately 0.29 dB observed for channel no. 12. The transmissions of 200 Gb/s DPSK WDM signals are possible up to a distance of 4900 km with the power penalty approximately 1 dB for all channels. For 4340 km distance, power received is improved over input power by factor 0.2 dB for most distorted channel no. 12 with quality more than 15 dB.

The bit error rate variation with the increase in launched power for all the channels is shown in figure (3.10) for the maximum transmission distance of 4340 km. As we increase the input power, the BER goes on increasing. As we increase the signal input power, the quality of signal goes on decreasing which is due to the cross gain saturation.

The eye diagram observed for 4340 km with power output -14.56 dBm, -14.41 dBm, -14.84 dBm and -14.25 dBm for channel no. 5, 10, 11 and 20 is shown in figure (3.11).

The optical spectrum of twenty channels for input and output signal power after the transmission distance of 4340 km is shown in figure (3.12).

As we are increased the confinement factor, the XGM occurs in WDM system. Hence this is degraded the quality of output signals for WDM multichannel system. If we decrease the confinement factor, then power penalty is observed in the channels of WDM systems.

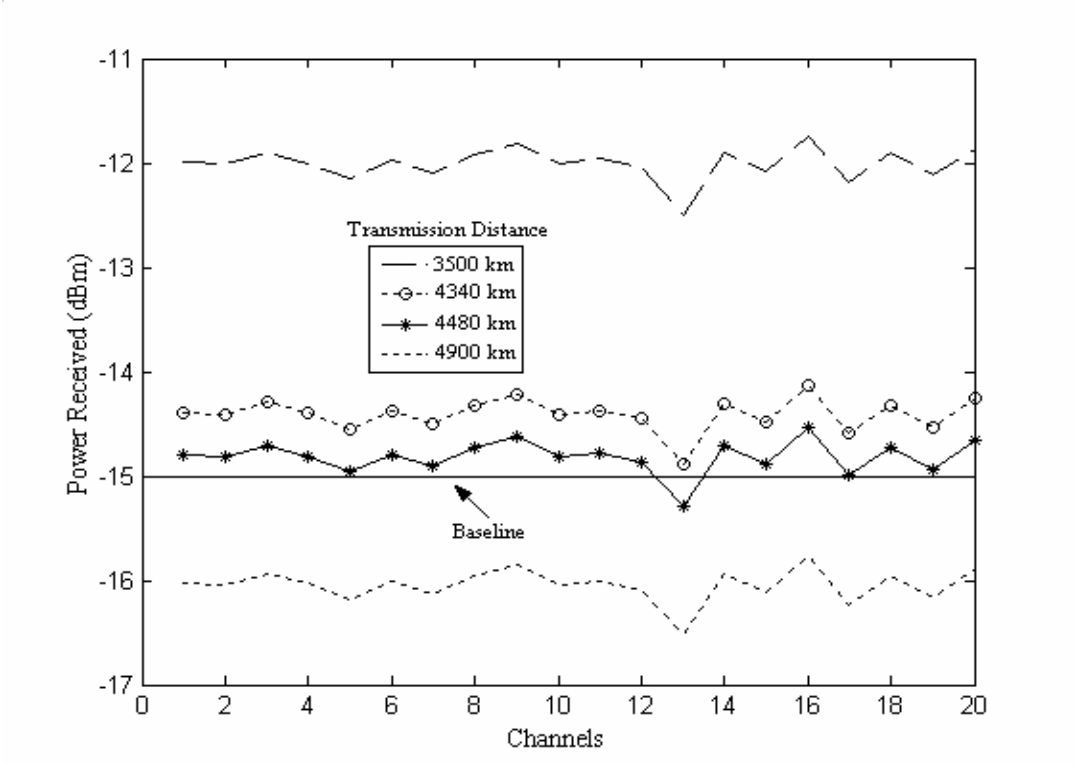

Figure 3.9: Optical power versus different channels for different transmission distances.

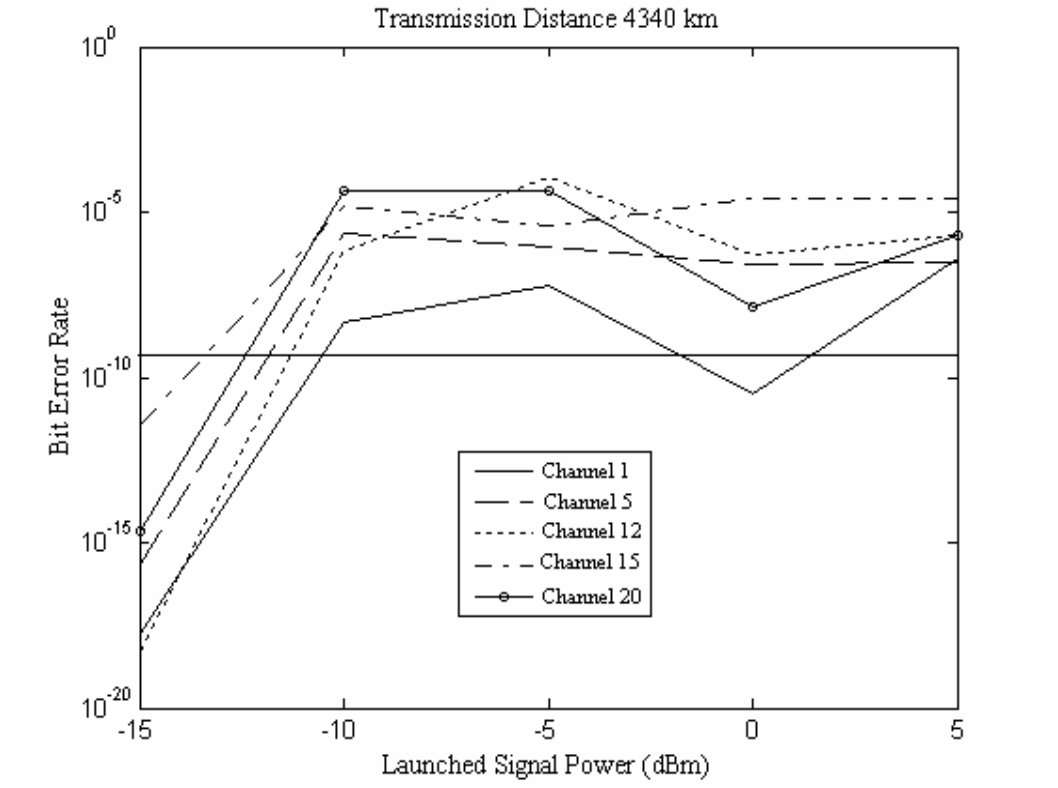

Figure 3.10: Bit error rate as the function of launched signal power for all channels for 4340 km.

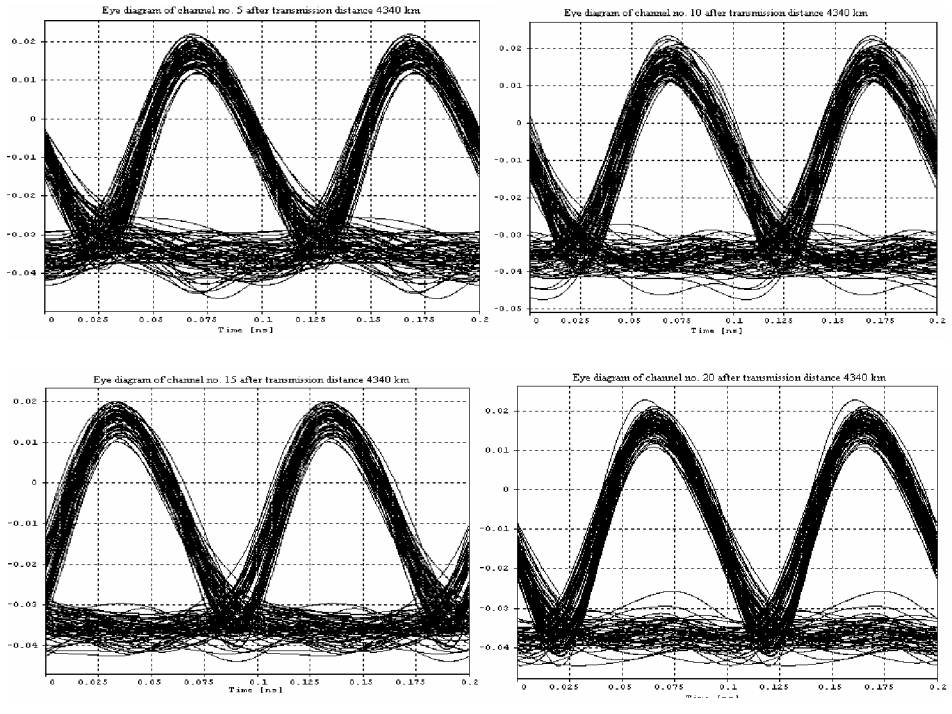

Figure 3.11: Eye diagram after distance 4340 km of channel no. 5, 10, 15 and 20.

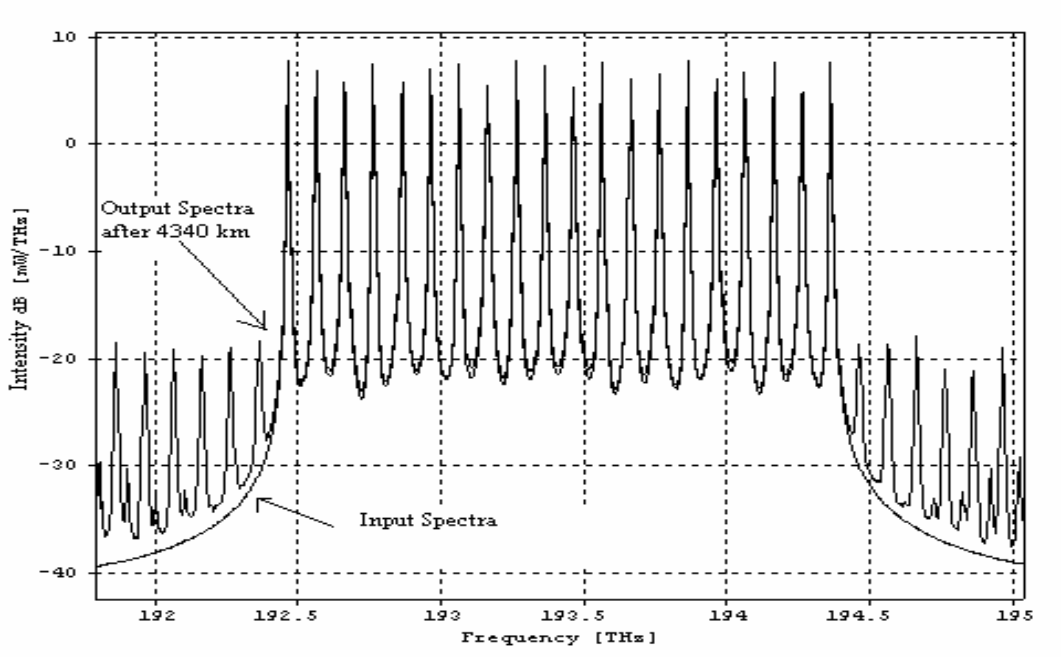

Figure 3.12: Optical spectrum for twenty channels at different frequency before and after transmission distance 4340 km.

It is also observed that with the increase in differential gain of the SOA structure, the cross gain modulation is enhanced. As we increase the confinement factor or differential gain of SOA structure, the saturation power of the SOA structure goes on decreasing.

3.2 Minimization of Cross Gain Saturation in SOA for WDM Transmission

Today's telecommunications networks compete to provide large and cheap bandwidth and integrated services using different technologies over the same physical infrastructure. The dense wavelength division multiplexed systems (DWDM) has emerged as an optical technology to achieve these objectives. Transmission systems based on the optical fiber (DWDM) technology provide the maximum transmission bandwidth. The optical fiber is capable of transmitting multichannel over long distances. The revolutionary growth in internet traffic is forcing network operators to deploy ever-higher transmission capacities in their terrestrial fiber backbone networks. It will be necessary to offer multi-terabit capacities over a single fiber, based on the use of this DWDM technology. To cope with this demand, it is likely that the next generation of wavelength division multiplexing (WDM) systems will use a 40 Gb/s or more bit rate [Nielsen *et al.*, 2000; Bonati *et al.*, 1999]. But the cross gain modulation of the SOA is restricted to use it for long haul transmission distance.

Spiekman *et al.* [2000] reported 8 × 20 Gb/s transmission over 160 km with SOAs span of 47.9 km and optimize the transmission system design_parameters. Spiekman *et al.* [2003] reported 8 × 40 Gb/s transmission over 160 km by gain clamping to operate SOA in linear region. Settembre *et al.* [2004] reported the soliton propagation is preferred for long transmission distance. The transmission distance is further improved by using in-line sliding filters.

Till date, maximum transmission distance is reported up to 1190 km with capacity 20 × 10 Gb/s using differential phase shift keying (DPSK) modulation format. Also the maximum transmission distance reported is 160 km with 40 Gb/s bit rate for eight channels. There is no previous literature found to optimize the differential gain of SOA in terms of power penalty for WDM transmission. In this work, the optimization of differential gain of SOA is reported for improvement in the transmission distance at 40 Gb/s.

3.2.1 Optimization of Differential Gain in SOA Model

To optimize the SOA model, the block diagram of simulation setup is shown in figure (2.1) of Chapter 2 for SOA in-line amplifier parameters as in section 3.1.2. In the figure, data source is soliton return to zero format at 40 Gb/s bit rate. The electrical driver converts the logical inputs signal (a binary sequence of zero and one) into electrical signal. A continuous wave (CW) Lorentzian light source with different power and data is launched into optical phase modulator in terms of electrical signal with RZ-DPSK format. The soliton RZ data was pseudorandom binary sequence (PBRS) with word length 2^9-1 at 40 Gb/s. The full wave half maxima (FWHM) line_width of CW light source is 1 MHz. The low pass Bessel filter having 3 dB bandwidth of 40 GHz for generation of data source in terms of RZ format. Then the DPSK signal is launched into the SOA as in section 3.1.2 with variation in differential gain. At the output, a raised cosine optical filter with bandwidth 60 GHz is used. The output of filter is fed into the DPSK receiver for detection of the signal.

The DPSK receiver is composed of the tunable Mach-Zehnder interferometer having two optical output ports. In the interferometer, optical paths are differing by a delay that must be set equal to one bit time duration. Each optical output is detected by an ideal PIN photo detector and the output electrical signal is the difference between the detected currents. The time domain simulations are carried out with simulation bandwidth 2.14 THz with centre wavelength 1550.04 nm.

Simulations are carried out for different differential gains of an SOA in-line amplifier, which is used for wavelength division multiplexing system. The graph between the amplification factor and input signal power for different differential gains is shown in figure (3.13). It is observed that amplification factor goes on decreasing with increase in input signal power. This is due to the power saturation that occurs with increase in the power. For 1×10^{-16} cm^2 (100 atto cm^2) differential gain, the amplification factor is quite low and remains constant with the variation of input power. But for 2×10^{-16} cm^2 differential gain, good amplification factor more than 17 dB is obtained at -25 dBm input signal power. It is observed that amplification factor goes on increasing with increase in differential gain.

The noise power generated in SOA due to spontaneous emission is observed in figure (3.14). It is observed that as with the increase in input signal the ASE noise goes on decreasing in SOA due to gain saturation.

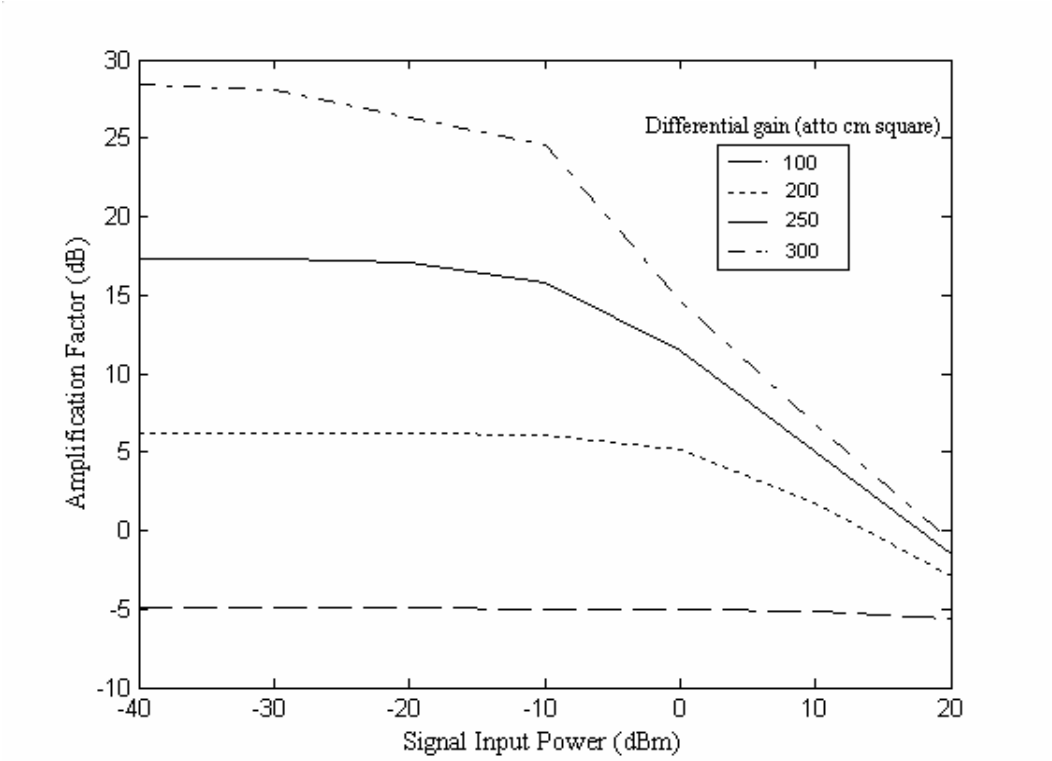

Figure 3.13: Amplification factor varies with signal input power at different differential gains.

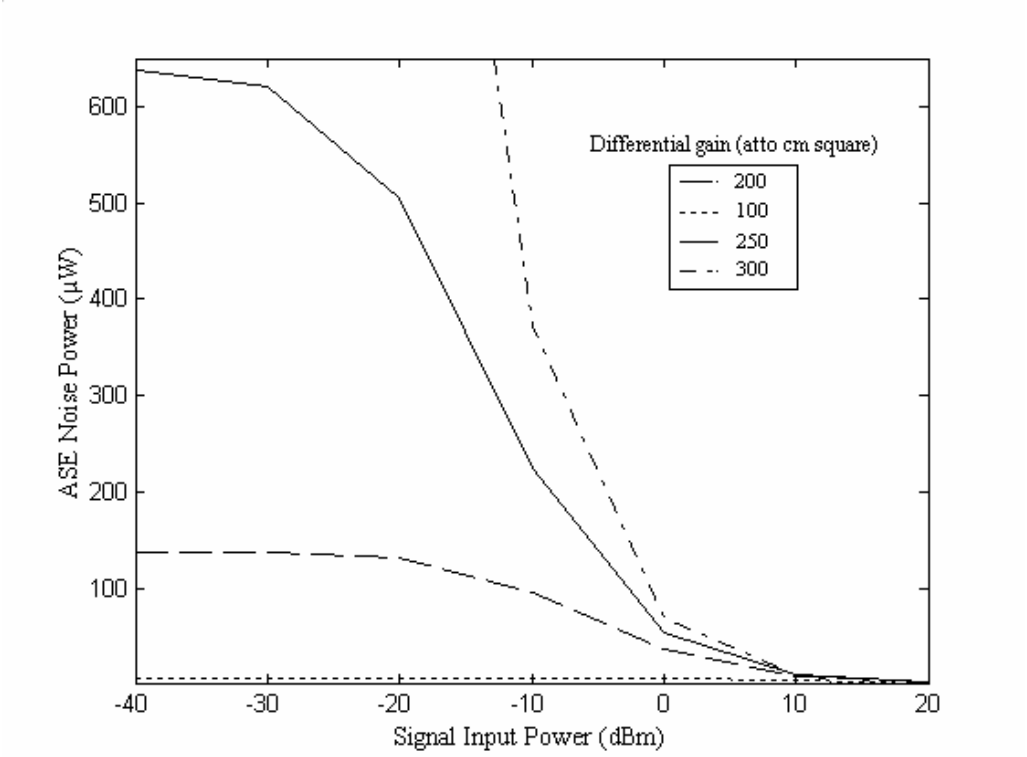

Figure 3.14: Amplified spontaneous power versus signal input power for different differential gains.

After saturation, the amplification stops with further increase in input power. The amplified spontaneous emission (ASE) noise power is 130.66 μW for differential gain up to 2×10^{-16} cm^2 at input signal -20 dBm, which is less than as reported in case [Yamatoya *et al.*, 2004]. For differential gain 3×10^{-16} cm^2, the ASE noise power is very high as compared to reported in [Yamatoya *et al.*, 2004]. So the observed ASE noise power for differential gain 2×10^{-16} cm^2 is less with sufficient amplification factor.

In order to see the influence of SOA-induced crosstalk, simulation is carried out for two or more channels. The simulation setup is similar to figure (3.6), which consists of only two channels having soliton RZ-DPSK format and a SOA without single mode and dispersion compensating fiber. The crosstalk is reported [Oberg and Olsson, 1998] as

$$crosstalk = \frac{P_{1,out}\left(P_{2,in=off}\right) - P_{1,out}\left(P_{2,in=on}\right)}{P_{1,out}\left(P_{2,in=off}\right)} \tag{3.2}$$

Where $P_{2,in}$ is input power, $P_{1,out}$ is amplified output power and index 1 and 2 are two signal wavelengths. The crosstalk of these two channels is observed by varying the input signal power for different differential gains as shown in figure (3.15). It is observed that with the increase in differential gain, the crosstalk increase, which shows a good agreement with above multichannel crosstalk analysis.

It is found that at differential gain 2×10^{-16} cm^2, the crosstalk is -7.21 dB with input power -25 dBm at 200 GHz channel spacing, which shows an agreement with the result reported in [Choi *et al.*, 2002]. It is also observed that with the increase in launched power for different differential gains, there is increase in the channel crosstalk. It is concluded that low crosstalk and ASE noise power with good agreement of amplification factor is obtained at 2×10^{-16} cm^2 (200 atto cm^2) differential gain of SOA.

3.2.2 SOA Parameters

The InGaAlAs traveling wave SOA with negligible residual facet reflectivity is taken as the amplifier model in our simulation. After solving the rate equations above, the relevant parameters are as follows: the length is 750 μm, the width of active layer is 2 μm, its thickness is 0.2 μm and optimized confinement factor is 0.41. The transparency carrier density in the SOA is taken 1.5×10^{18} cm^{-3} and the differential gain is estimated to be 210 atto cm^2. The carrier recombination time τ at this density is 0.3 ns with the saturation power P_s = 19.85 mW. The optical gain of SOA is ranging from 37.99 dB to 36.22 dB for input signal -40 dBm to +10 dBm.

The optimum injection current is evaluated to be 400 mA, which is same as reported in result [Yamatoya and Koyama, 2004], as faster response was obtained at higher bias currents. The optical bandwidth of SOA is 40 nm and considered spontaneous emission factor is 2. The input and output coupling losses of SOAs are taken as 3 dB.

3.2.3 Simulation of WDM Transmission at 10 × 40 Gb/s Soliton RZ-DPSK Signals

The analysis is also made for the transmission performance of WDM signals with RZ-DPSK modulation format using cascaded SOA in-line amplifiers. Figure (3.16) shows a schematic setup of 10 × 40 Gb/s DPSK WDM system. In this figure, each transmitter section consists of data source, laser source, electrical driver and optical phase modulator. The data source is soliton return to zero format at 40 Gb/s. The electrical driver converts binary sequence into electrical signal. Ten Lorentzian laser sources in the wavelength range 1546.4 nm to 1553.63 nm (100 GHz channel spacing) are modulated by each optical $LiNbO_3$ phase modulator with return to zero (RZ) soliton format.

The input of each transmission channel is -14 dBm. So, the design carries 400 Gb/s RZ-DPSK WDM signals over different transmission distances with 70 km SOA spacing. Each span consists of a 60 km standard single mode fiber (SMF), one or more DCF (dispersion compensating fiber) and an SOA at the end. The length of dispersion compensating fiber (DCF) is chosen in accordance with [Agrawal, 2002] for complete compensation ($\overline{D} = 0$). The length and dispersion parameter of SMF and DCF is same as in section 3.1.4. After the number of repeated spans, the same SOA is used as pre-amplifier. The time domain simulations have been carried out for this setup as shown in figure (3.16) with bandwidth 2.29 THz and centre frequency 193.415 THz. In order to find the behaviour of SOA with different differential gains, the Q factor and power received is observed simultaneously up to 15 × 70 km (15 spans) WDM transmission with channel spacing 200 GHz. The simulations are carried out for the setup as shown in figure (3.16) for different differential gains by varying the transmission distance.

Figure (3.17) shows the plot of power received versus transmission distance for different differential gains of the SOA. For the distance of 350 km, all differential gain from 190 atto cm^2 to 210 atto cm^2 show good amplification with sufficient quality for all channels. For the differential gain 2×10^{-16} cm^2 (200 atto cm^2), the power received goes on decreasing slowly after 350 km distance. But for differential gain 1.9×10^{-16} cm^2 (190 atto cm^2), the power received goes on decreasing rapidly.

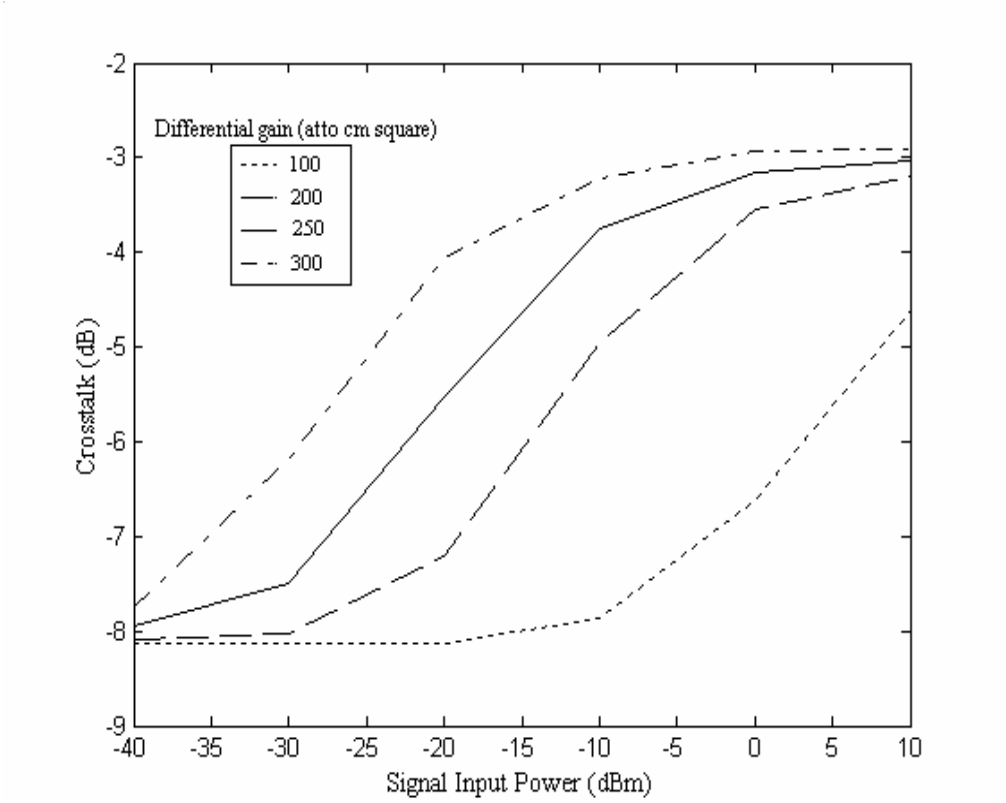

Figure 3.15: Crosstalk variations with launched power of SOA for different differential gains.

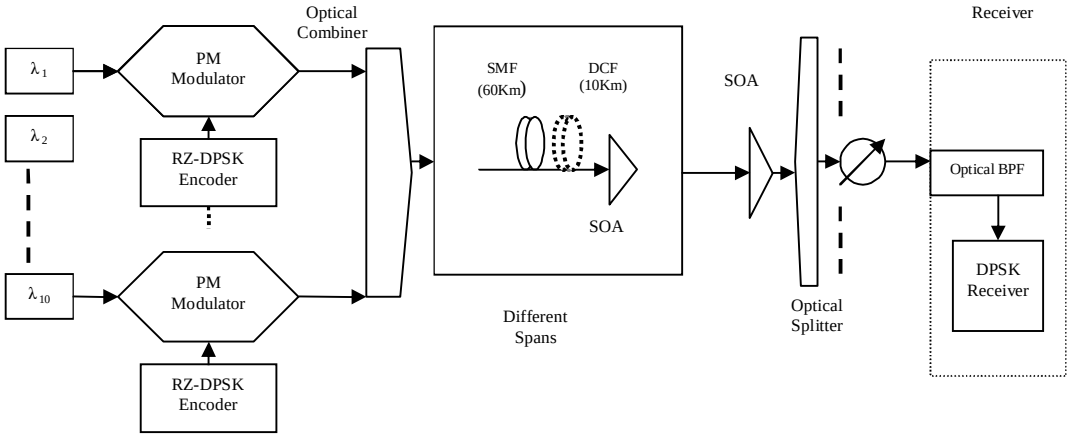

Figure 3.16: Schematic setup of transmission system for 10 × 40 Gb/s RZ-DPSK WDM signals.

The large drop of power received occurs after 1050 km transmission distance, even good quality is observed as shown in figure (3.18). With the increase in differential gain 2×10^{-16} cm^2, the power penalty decreases. For the transmission distance of 1050 km, amplified power is received for the differential gain 2×10^{-16} cm^2, but the quality of the signal falls as shown in figure (3.18).

The graph between bit error (BER) rate and received power is shown in figure (3.19) for transmission distance of 1050 km. It is seen that as the differential gain is increased, the BER increases. For differential gain of 1.9×10^{-16} cm^2, the power penalty is observed to be around 8 dB with good BER up to saturation power. The increase in BER is more than 10^{-6} at higher differential gain *i.e.* 2.5×10^{-16} cm^2, even nil power penalty is observed. When the differential gain is 2×10^{-16} cm^2, the maximum transmission distance is achieved with nil power penalty and BER less than 10^{-25} up to saturation power. But with differential gain of 2.1×10^{-16} cm^2 for transmission distance of 1050 km, it shows the received power per channel more than 1.98 dBm by applying -20 dBm input power per channel only. This shows an improvement over transmission distance and capacity as reported in [Spiekman *et al.*, 2003].

The further increase in the transmission distance in simulations setup finds the maximum possible transmission distance. Simulations are performed with channel spacing 100 GHz for both differential gain 200 atto cm^2 and 210 atto cm^2 of the SOA. The applied input power is -14 dBm per channel. The Q factor is observed for ten channels with different transmission distances as shown in figure (3.20). The observed quality is more than 15 dB for transmission distance 700 km, 1050 km, 4550 km as in figure (3.20). The maximum transmission distance observed for differential gain 210 atto cm^2 is 1050 km with quality more than 15 dB of received signal for all channels and received power is more than 2.3 dBm per channel. This shows an improvement over the results reported [Li. *et al.*, 2004; Spiekman *et al.*, 2003]. As we increase the distance 1120 km, there is drop in quality of some channel as shown in figure (3.20). This is due to the cross gain saturation which occurs in SOA, this means high value of differential gain of the SOA.

But as differential gain is decreased to 200 atto cm^2, the transmission distance observed is more than 4550 km with received power -13.75 dBm per channel. Hence, nil power penalty is observed. The received power is more than -13.75 dBm for all channels at transmission distance 4550 km with differential gain 200 atto cm^2 of the SOA in-line amplifiers as shown in figure (3.21).

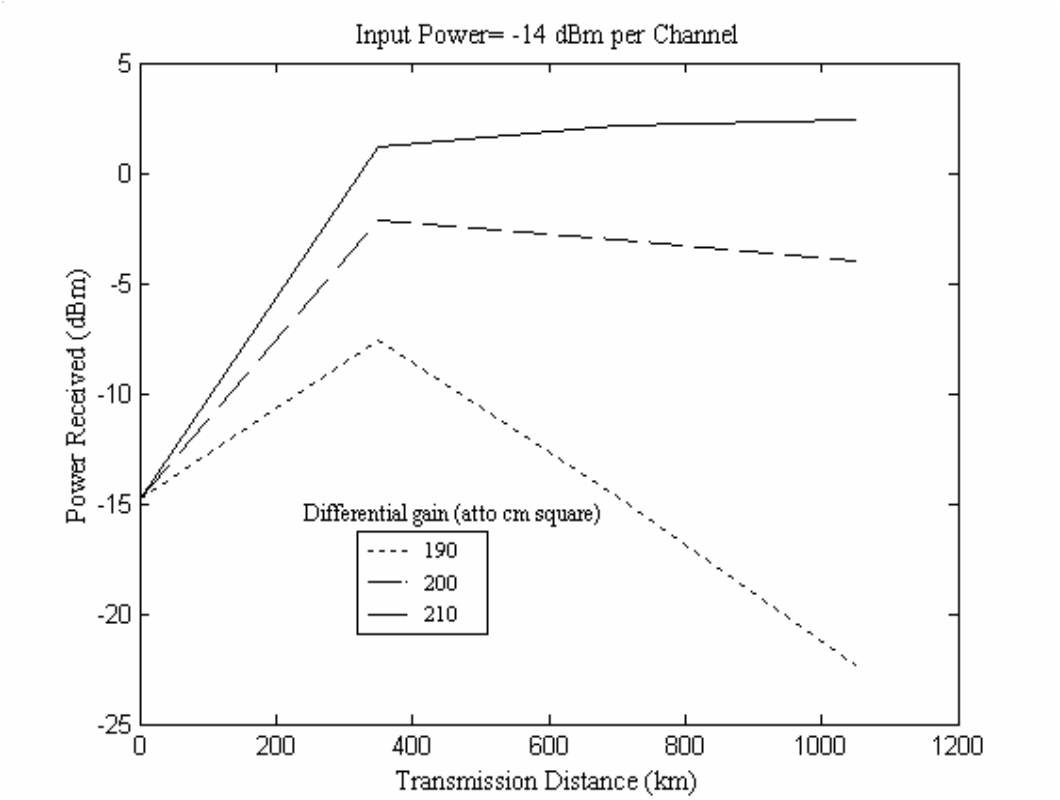

Figure 3.17: Power received as function of transmission distance for varying differential gains.

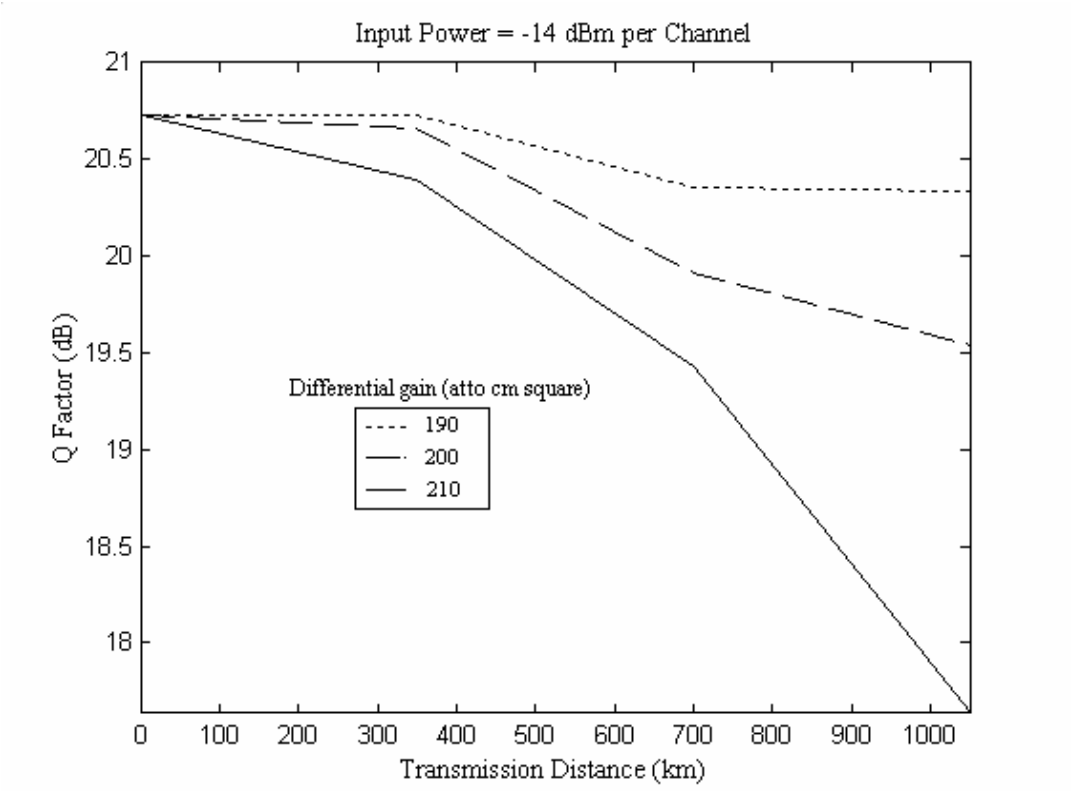

Figure 3.18: Q factor as function of transmission distance for different differential gains.

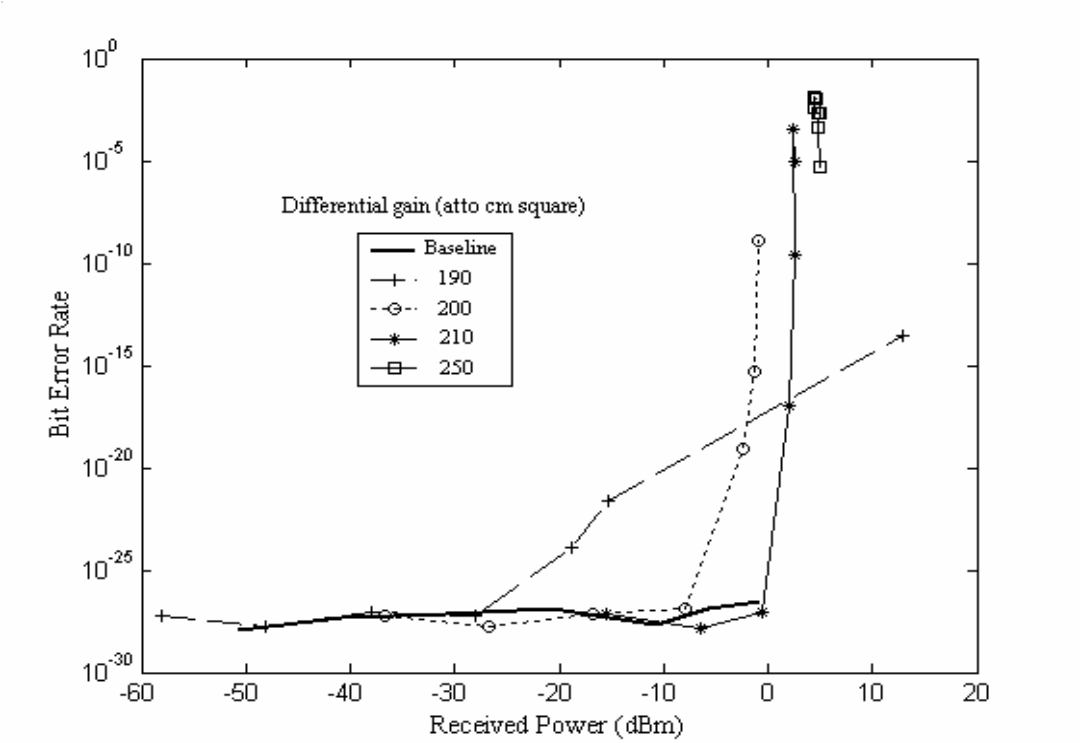

Figure 3.19: Bit error rate as function of received power for varying differential gains for transmission distance 1050 km with channel spacing 200 GHz.

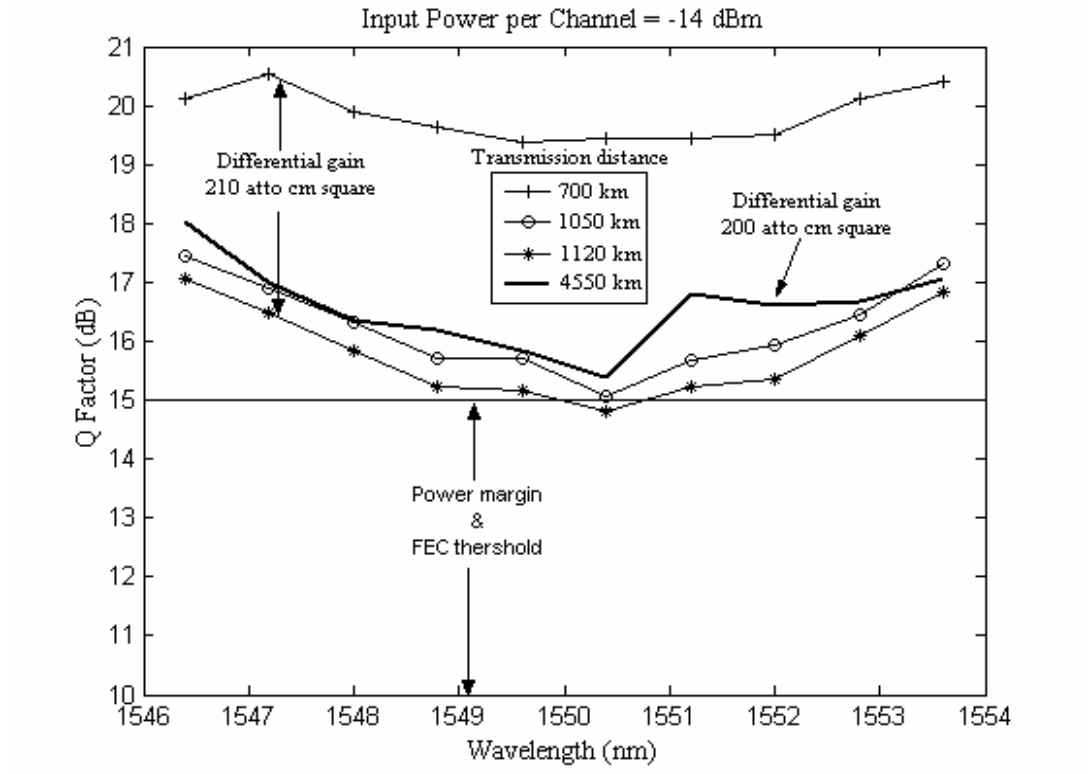

Figure 3.20: Q factor variations with channels for different transmission distances.

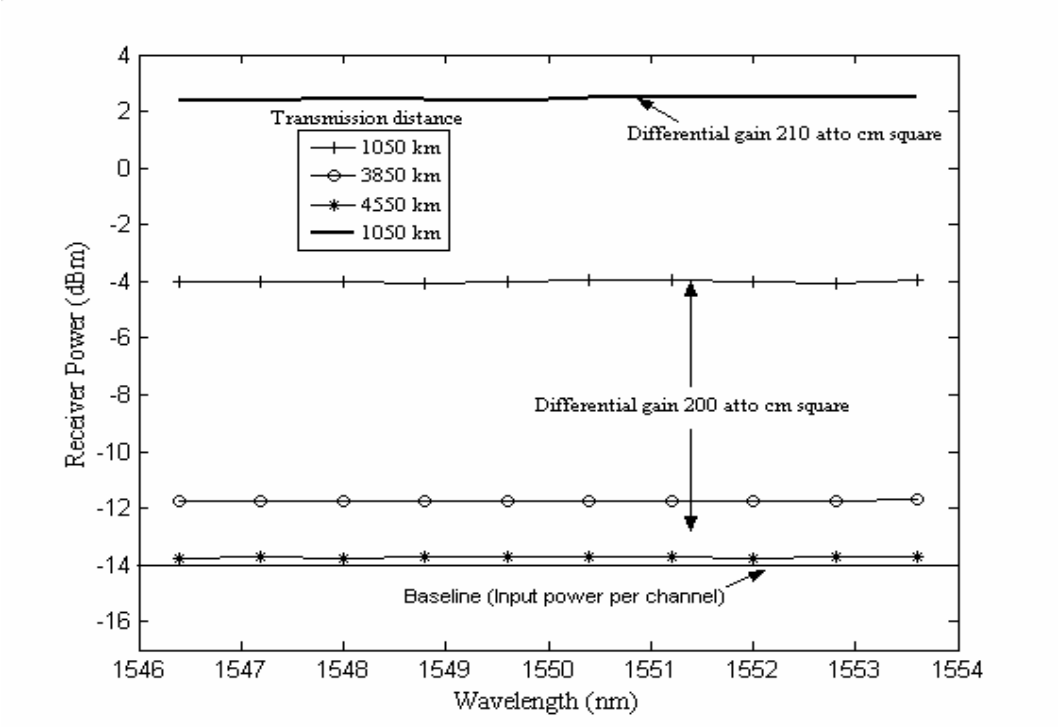

Figure 3.21: Optical power versus different channels for different transmission distances.

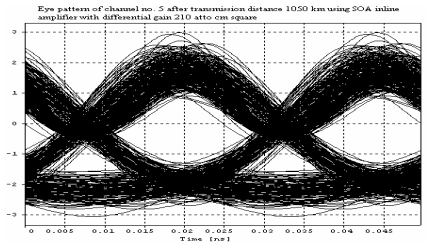

Figure 3.22a: Eye diagram after distance1050 km of channel no. 5.

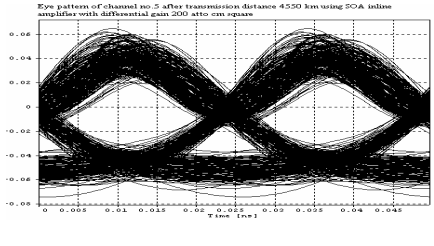

Figure 3.22b: Eye diagram after distance 4340 km of channel no. 5.

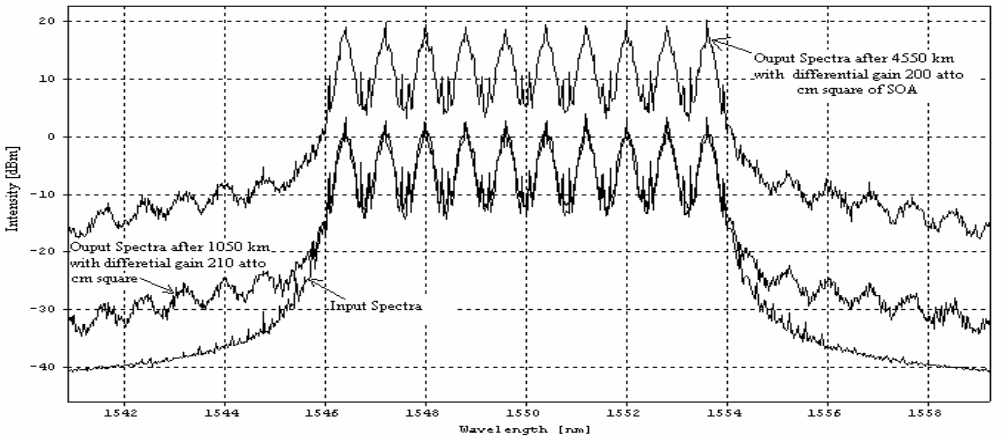

Figure 3.23: Optical spectrum for twenty channels at different frequency before and after transmission distance 4340 km.

But, for higher transmission distance of more than 4550 km, there is possibility of power penalty occurring at some channels. Therefore transmission of 400 Gb/s soliton RZ-DPSK WDM signals is possible up to distance of 4550 km without any power penalty which is a large improvement over [Spiekman *et al.*, 2003; Singh and Kaler, Dec. 2005].

The eye diagram for transmission distance 1050 km at differential gain 210 atto cm^2 is shown in figure (3.22a), with received power 2.4 dBm for channel no. 5. Similar eye diagram is observed that has been shown in figure (3.22b) for transmission distance 4550 km with differential gain 200 atto cm^2. For this, received power is -13.74 dBm. The optical power spectrum of ten channels for input signal and output spectra, after transmission distance 1050 km and 4550 km, for differential gain 210 atto cm^2 and differential gain 200 atto cm^2 is shown in figure (3.23).

With increase in transmission distance, the quality of signal per channel goes on decreases using SOA in-line amplifiers. The experimental results reported in [Li. *et al.*, 2004] validate our simulation results.

3.3 SOA for 10 × 80 Gb/s WDM Transmission by Using Soliton RZ-DPSK Format

Next generation of wavelength division multiplexing (WDM) systems would use a 40 Gb/s or more bit rate [Nielsen *et al.*, 2000; Bonati *et al.*, 1999] To cope with this demand, there is need of research at 80 Gb/s by using optimized SOA for multichannel WDM communication system.

Spiekman *et al.* [2003] reported 8 × 40 Gb/s transmission over 160 km by gain clamping to operate SOA in linear region. Till date, maximum bit rate reported is 40 Gb/s. For this, maximum WDM transmission distance is 160 km for eight channels [Spiekman *et al.*,2003]. There is no previous literature found at high bit rate 80 Gb/s and more by using SOAs. Also, further optimization of structural parameters of SOA is needed in order to decrease the SOA induced crosstalk with nil power penalty for WDM transmission.

3.3.1 Simulation and Results

The standard InGaAlAs traveling wave SOA with negligible residual facet reflectivity is taken as the amplifier model in our simulation. The relevant parameters are same as in section 2.2.2 of the Chapter 2. Figure (3.16) shows a schematic setup of 10 × 80 Gb/s WDM system.

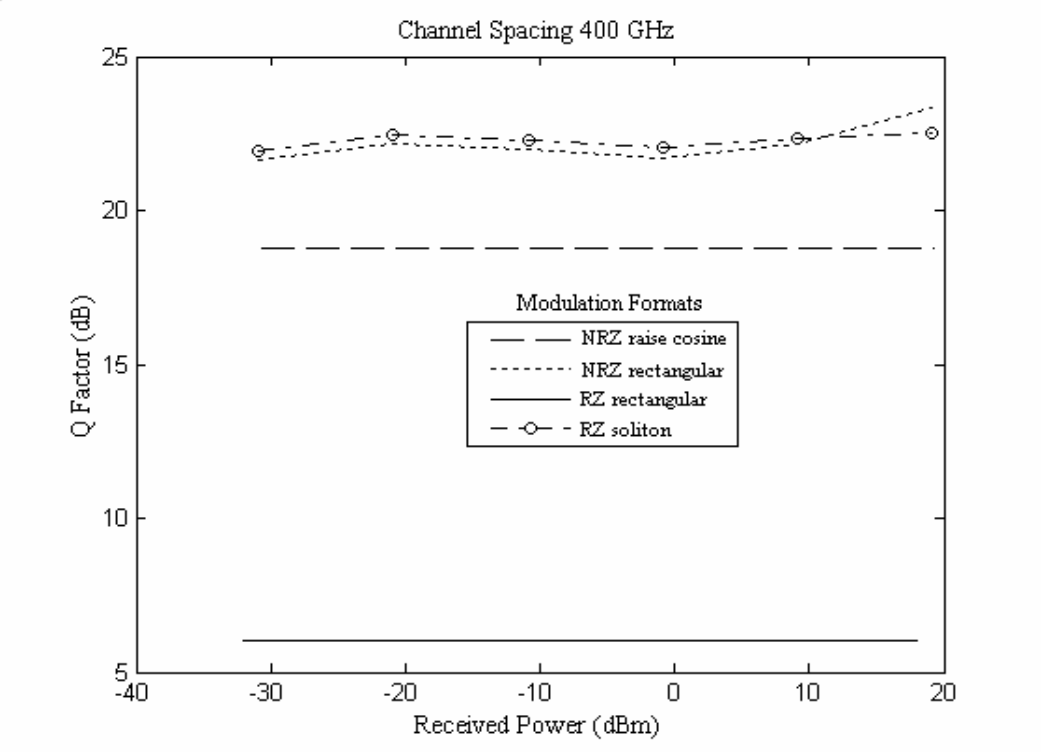

Figure 3.24: Q factor varies with received signal power for different modulation formats.

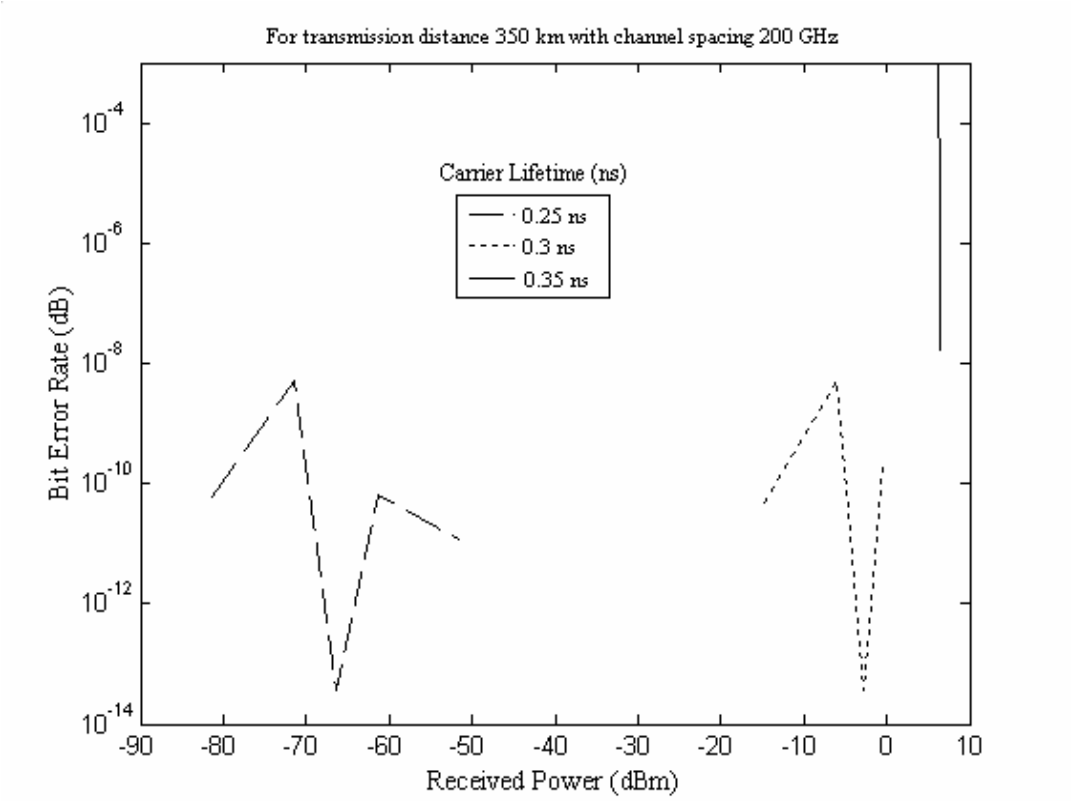

Figure 3.25: Bit error rate as the function of received signal power for different carrier lifetimes.

Ten lorentzian laser sources in the wavelength ranging from 1528.42 nm to 1572.19 nm (200 GHz channel spacing) are modulated by each optical $LiNbO_3$ phase modulator with different modulation formats.

The different modulation formats are analyzed without any transmission distance and SOA. The results shown in figure (3.24) represent that soliton return to zero format shows highest quality with variation of average received power per channel. Also from the previous results reported [Xu C. *et al.,* 2003] show RZ-DPSK could provide 3 dB reduction in required received OSNR for given bit error rate (BER). If we use soliton RZ format, this shows highest Q factor as shown in figure (3.24). So this format is used for transmission of signals over long distance.

The transmission performance of WDM signals is analyzed using cascaded SOA. Therefore, the design carries 800 Gb/s soliton RZ WDM signals over 350 km with 70 km SOA spacing. Each of span consists of same standard single mode fiber (SMF) and DCF as in section 3.1.2. In order to measure the performance of SOA in multichannel, the time domain simulations have been carried out for the setup as shown in figure (3.16) at 80 Gb/s with bandwidth of 5.46 THz and centre frequency of 193.415 THz.

The bit error rate is the function of received power for the transmission distance of 350 km is shown in figure (3.25). If large carrier lifetime of 0.3 ns is taken, then zero power penalty is observed with bit error rate (BER) less than 10^{-13}. By increasing the carrier lifetime to 0.35 ns, the power saturation occurs. Hence, the received signals have BER more than 10^{-8}. But if the carrier lifetime 0.25 ns is decreased, then large power penalty is observed for received signals with the BER same as that when the carrier lifetime is 0.3 ns. Hence cross gain saturation is decreased with increase in carrier lifetime which is same as that reported in [Xu S. *et al.,* 2003].

Figure (3.26) shows the plot of power received versus transmission distance for different differential gains of the SOA. For the distance 350 km, all differential gain from 190 atto cm^2 to 210 atto cm^2 show good amplification with sufficient quality for all channels. For the differential gain of 1.5×10^{-16} cm^2, large power penalty is observed with good quality of signal. But for differential gain of 2.5×10^{-16} cm^2, the power received goes on increasing rapidly while the quality of signal goes on decreasing. As the differential gain is slightly increased to 2×10^{-16} cm^2, the power penalty decreases at good quality of signal.

The graph between Q factor and received power for different length of SOA is shown in figure (3.27) for transmission distance 350 km.

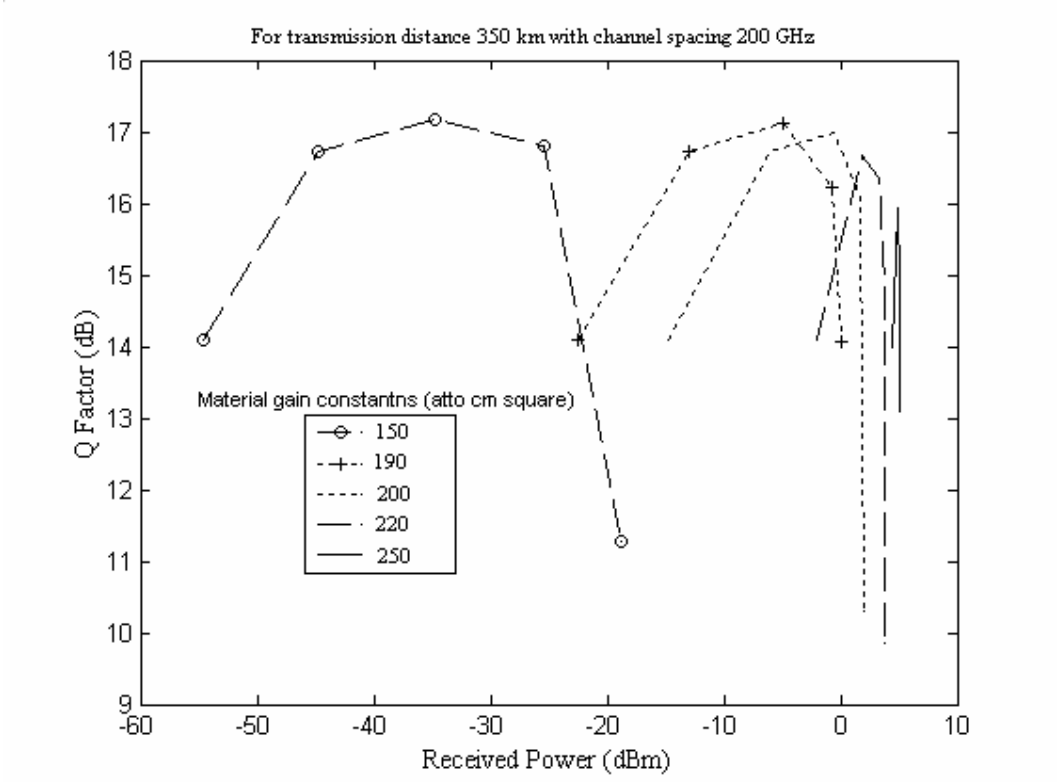

Figure 3.26: Q factor as the function of received signal power for different differential gains.

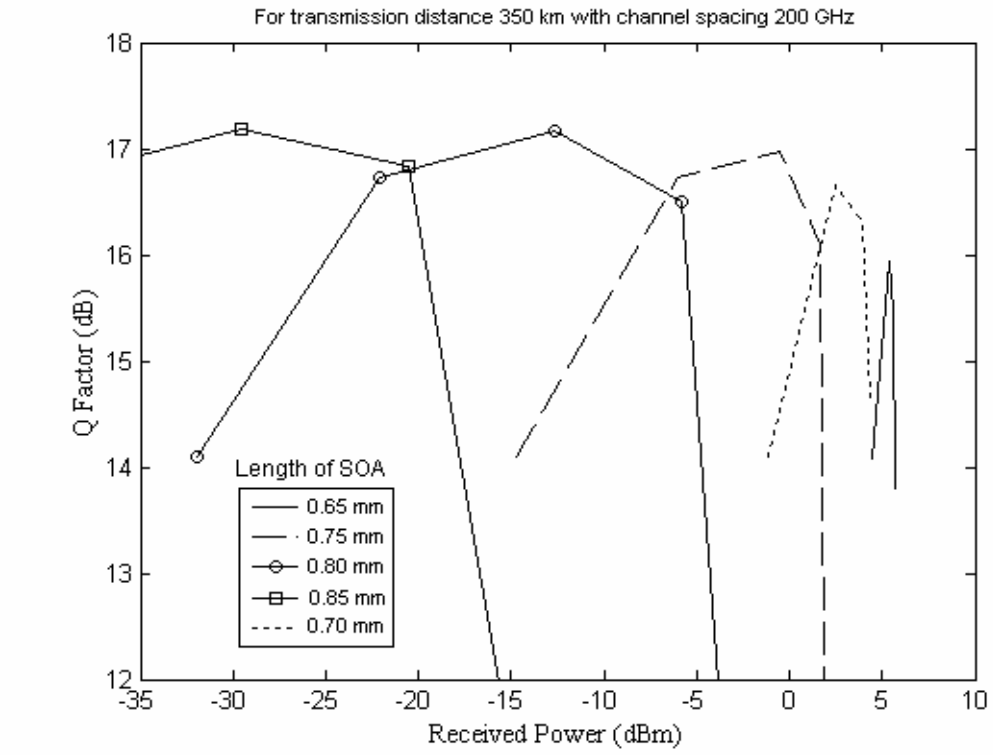

Figure 3.27: Q factor as the function of received signal power for different active region lengths.

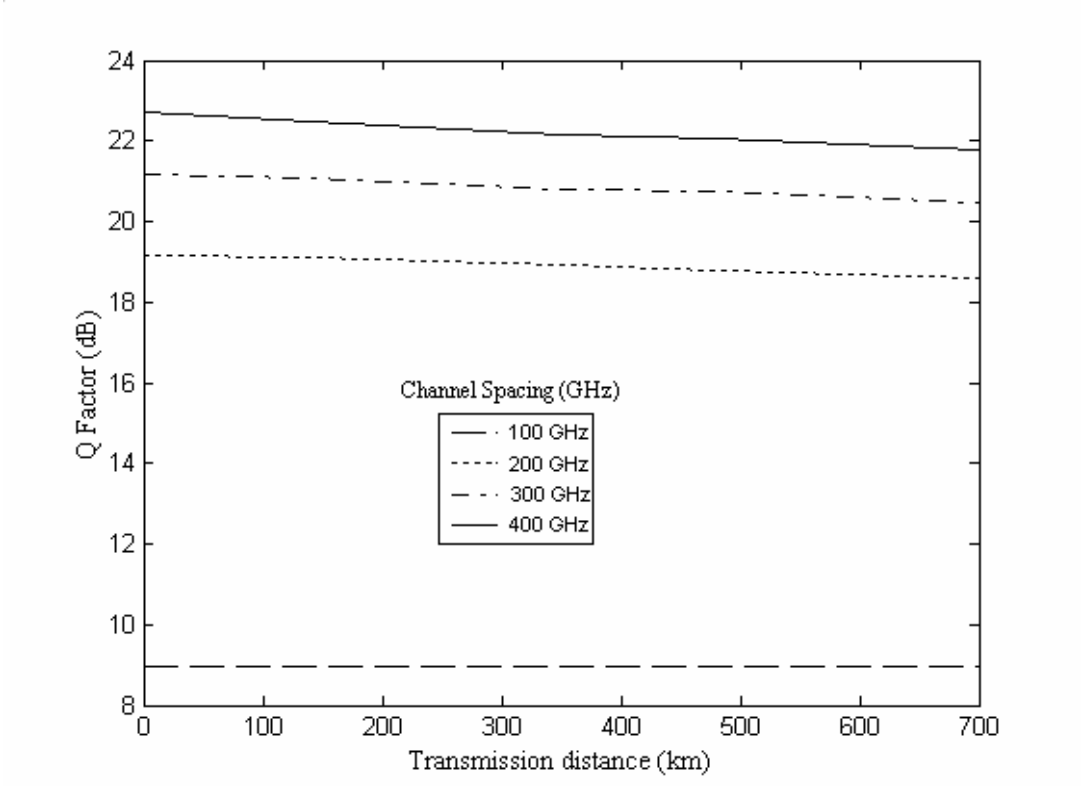

Figure 3.28: Q factor against transmission distance for different channel spacing with launched power -14 dBm.

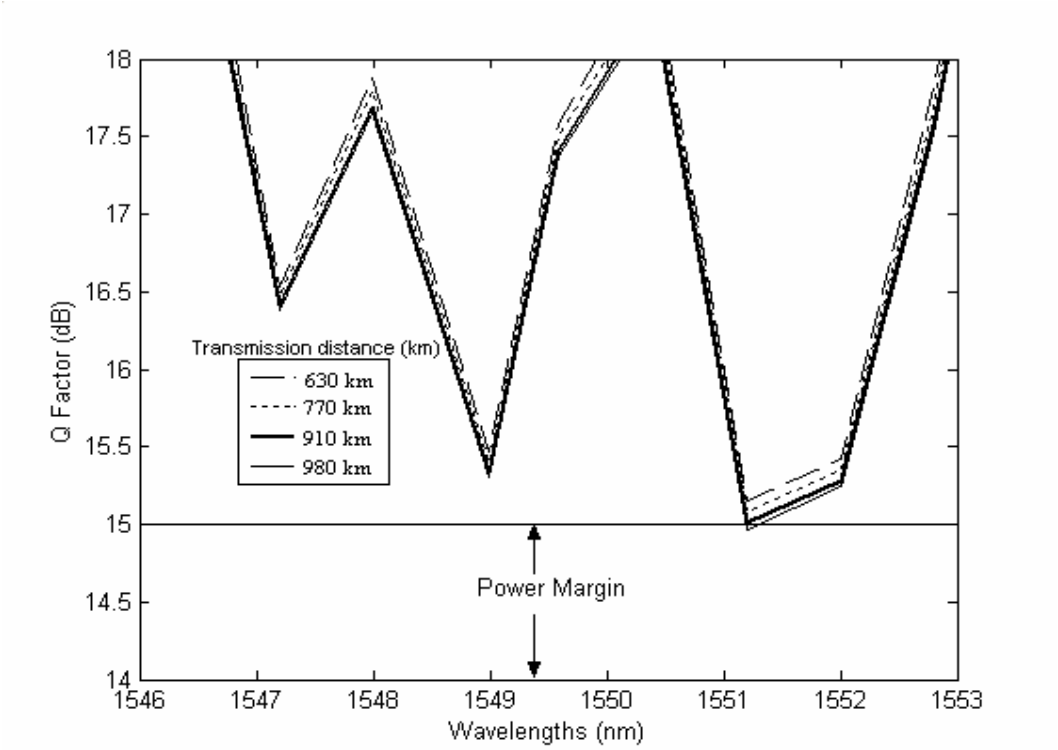

Figure 3.29: Q factor variations with channels for different transmission distances.

It is seen that as the length of active region of SOA is increased, the quality of signal increases. For length of 0.65 mm, the quality of signal goes on decreasing with increase in input signal. This is due to power saturation. For length of 0.85 mm, the power penalty observed is around 9 dB with good Q factor up to saturation power. At active region length of 0.75 mm, the maximum transmission distance is achieved with nil power penalty and Q factor more than 16 dB up to saturation power. Hence optimum carrier lifetime, differential gain and length of active region are obtained.

The simulation is also carried out for different channel spacing for 10 × 80 Gb/s soliton RZ WDM signals over 350 km single mode fiber with the SOA spacing 70 km. Keeping all parameters in the simulation setup same as that in section 3.2.3 and taking input of each transmission channel to be -14 dBm with channel spacing 400 GHz, the dependence of average Q factor on the transmission distance is shown in the figure (3.28). It is observed that the Q factor decreases as the transmission distance is increased. Again, if the wavelength spacing is decreased, the Q factor decreases. This is because of the nonlinear effects induced by SOA amplifier. If the power over the length is kept constant and at low level, then signal to noise ratio will improve over distances.

The dependence of Q factor for different channels is measured as shown in figure (3.29) by taking input signal power -14 dBm per channel with channel spacing 200 GHz. The measured quality for transmission of 630 km, 770 km and 910 km as in figure (3.29) is more than 15 dB. The power received is more than -3 dBm per channel for all these transmission distances. For transmission distance 910 km, the observed quality is 15 dB at distorted channel. But for transmission distance 980 km, there is Q penalty of 0.03 dB approximately for one channel.

3.4 Analysis and Minimization of Cross Phase Modulation in SOA for WDM Optical Communication Systems

When the SOA is working in saturation regime, it has high nonlinearity which restrains it from being used in long distance WDM transmission system. The nonlinear effects of SOA are cross gain modulation (XGM), cross phase modulation (XPM) and four wave mixing (FWM) which produce cross talk among WDM channels and limits the transmission distance.

The gain saturation of the SOA produces phase noise, which will affect the performance of DPSK signals. Wei *et al.* [2004] reported the penalty more than 7 dB, when a return to

zero DPSK signal with finite optical signal to noise ratio was amplified by a saturated SOA. They reported that the SOA alters the noise characteristics and introduces extra phase noise to optical signal.

Kikuchi *et al.* [1991] reported that phase noise is induced by carrier density fluctuation associated with intensity noise and spontaneous carrier recombination. They demonstrated that phase noise limits to the numbers of repeater amplifiers for single channel. Wei *et al.* [2005] reported that phase noise impact is less at higher bit rates. They suggested that saturated induced phase noise can be significantly reduced by increasing the bit rate and carrier lifetime of SOA for single channel DPSK signal amplification. Different solutions by researchers are reported in section 2.2.1 of the Chapter 2 to minimize these nonlinearities for long distance transmission in WDM system. We investigated 10 × 40 Gb/s solution for RZ-DPSK WDM signal transmission over 4550 km by changing the structure according to cross gain saturation analysis.

Till date, no work has been reported for the evaluation of XPM noise in multichannel WDM system. Also, the maximum transmission distance of 4450 km is reported by using cascaded SOA for 10 × 40 Gb/s soliton DPSK signals [Singh and Kaler, 2006].

In this chapter, the cross phase noise induced by the SOA gain saturation is analyzed. The analysis for differential phase errors provides the relations with the SOA parameters. This relation analyzes that the impact of saturated induce cross phase noise on the BER performance can be reduced in SOAs by reducing the differential gain and by increasing carrier lifetimes. Xu *et al.* [2003] is reported that for type-II quantum well SOAs with increased carrier lifetime and reduced differential gain have been proposed to reduce the crosstalk and distortion in WDM system with the OOK modulation. A similar result of SOAs with longer carrier lifetimes is suitable for single channel DPSK signal [Wei *et al*., 2005]. There are also other parameters like confinement factor, width and bias current which are optimized by using the XPM analysis. If this SOA is successfully fabricated, then it can be utilized for WDM DPSK applications.

3.4.1 XPM Analysis in the SOA

The phase noise is generated in the SOA by direct phase noise from amplified spontaneous emission (ASE) and carrier density fluctuation due to intensity noise spontaneous emission and non carrier recombination [Xu C. *et al.*, 2003]. It is observed that the ASE noise generated by the SOA is negligible for low bias current. The large penalty and noise occurs when noise is loaded at the input of the SOA [Wei *et al.*, 2004].

Wei *et al.* [2004] demonstrated that the performance of RZ-DPSK signal was not affected when the noise loaded after the SOA. They also reported that the carrier recombination process is stochastic. The gain coefficient of the SOA is recalled from section 2.1.2 of the Chapter 2 as

$$g(t,z) = [N(t,z) - N_t]a\Gamma L \tag{3.3}$$

Where L is the length of active region of SOA. The crosstalk can be suppressed by keeping the gain coefficient constant.

The phase noise generation through carrier density fluctuation is due to the intensity noise. The carrier density fluctuation in SOA induces a phase shift to light wave [Agrawal and Olsson, 1989]. The SOA cross phase modulation closely relate with cross gain modulation. The phase shift induced by the presence of signal in the SOA is related to gain coefficient $g(t,z)$. Also the phase shift induced by presence of signal in SOA is [Agrawal and Olsson, 1989]

$$\Phi(t) = \frac{g(t,z)\beta L}{2} = \frac{\beta}{2}\log_e G(t) \tag{3.4}$$

Where β is the line_width enhancement factor. $G(t)$ is the saturated amplifier gain of the SOA. This phase shift depends upon the total output intensity of previous SOA in cascade.

In order to optimize the semiconductor optical amplifiers in multichannel WDM, taking the rate equation that governs the carrier density in the SOA gain region [Xu *et al.*, 2003]

$$\frac{\partial N(t,z)}{\partial t} = \frac{J}{qt_a} - \frac{N(t,z)}{\tau} - a\,(N(t,z) - N_t)\frac{\sum_{i=1}^{M} P_i(t,z)}{hvwt_{eff}} \tag{3.5}$$

Where t is the time, z is the position along the propagation direction of light, J is the injection current density, $N(t,z)$ is the carrier density, t_a is the thickness of active region, τ is the carrier recombination time, a is the differential gain, N_t is the transparency carrier density, M is the total number of channels, $P_i(t,z)$ is the power in the ith channel, hf is the energy of photon, w is the width of waveguide, t_{eff} is the effective thickness of the waveguide and $\Gamma = t_a/t_{eff}$ is the confinement factor.

As with the variation in time, the distance moved by the photon varies as $t_1 = t/\tau$ and $z_1 = z/L$ considered here. The solution of gain for variable condition as in Chapter 2 is given by

$$g(t_1,z_1)=\frac{a\Gamma}{\tau P_L}\left[\begin{array}{l}\dfrac{I\tau}{wqt_a}\exp\left(\dfrac{\Delta P_1}{\tau}\right)\\ +\sum_{n=1}^{M}\dfrac{(-1)^n}{P_L^{n-1}}L\,\overline{N}^n(t_n,z_n)\exp\left(\dfrac{\Delta P}{\tau}\right)\end{array}\right] \tag{3.6}$$

Where ΔP_1 and $N(t_1,z_1)$ are the time variation of power and carrier density. Also derivative power coefficient is taken as $P_L=\partial P(t_1,z_1)/\partial t_1$ and the derivative carrier density, $\overline{N}=\partial N(t_1,z_1)/\partial t_1$ for reducing the complexity of the system.

The phase shift induced by the presence of signal in the *i*th SOA with variation in time is

$$\Phi(t_1)=\frac{g(t_1,z_1)\beta L}{2}=\frac{\beta}{2}\log_e G_i(t) \tag{3.7}$$

The differential phase error as [Wei *et al.*, 2005] given by

$$\Delta\Phi(t)=\Phi(t)-\Phi(t_1)$$

$$\Delta\Phi(t)=\sum_{i=1}^{k}\Delta\Phi_i \tag{3.8}$$

Where, k is the number of SOAs in multichannel optical communication system. When variations in time phase shift occur, there is position of phase also varies with time. So we can write differential phase error as the function of time and position of photon.

$$\Delta\Phi(t,z)=\sum_{i=1}^{k}\beta L\Delta g_i(t_{1i},z_{1i}) \tag{3.9}$$

$$\Delta\Phi(t,z)=\sum_{i=1}^{k}\beta L\Delta\log_e G_i(t_{1i},z_{1i}) \tag{3.10}$$

The variation in gain is

$$g(t_1,z_1)=g(t,z)+\Delta g \tag{3.11}$$

Where Δg is the small dynamic variation of $g(t_1,z_1)$around $g(t,z)$. Its solution as

$$\begin{aligned}\Delta g(t_1,z_1)=&\frac{a\Gamma I}{wqt_aP_L}\exp\left(\frac{\Delta P_1}{\tau}\right)+\frac{1}{\tau}\sum_{n=1}^{M}\frac{(-1)^n}{P_L^n}\times\exp\left(\frac{\Delta P_n}{\tau}\right)\\ &\times\left[a\Gamma L\,\overline{N}^n(t_n,z_n)-g\,\overline{P}^{n-1}(t_{n-1},z_{n-1})\right]\end{aligned} \tag{3.12}$$

Also differential phase error is

$$\Delta\Phi(t,z)=\sum_{i=1}^{k}\beta L\left[\begin{array}{l}\dfrac{a\Gamma I}{wqt_aP_L}\exp\left(\dfrac{\Delta P_{1i}}{\tau}\right)\\ +\dfrac{1}{\tau}\sum_{n=1}^{M}\dfrac{(-1)^n}{P_L^n}\exp\left(\dfrac{\Delta P_{ni}}{\tau}\right)\left[a\Gamma L\,\overline{N}_i^{\,n}(t_{ni},z_{ni})-g_i\,\overline{P}_i^{n-1}(t_{(n-1)i},z_{(n-1)i})\right]\end{array}\right] \tag{3.13}$$

Equation (3.13) shows that the differential phase variation depends on the variation of bias current, carrier lifetime, confinement factor and power of the signals. If the carrier lifetime is longer, then smaller will be the phase shift which produces interchannel crosstalk which is same as reported in [Wei *et al.*, 2005; Xu *et al.*, 2003]. Similarly, by decreasing the differential gain, it results in reduction of phase fluctuation *i.e.* less crosstalk. By increasing the bias current, the SOA-induced crosstalk increases, which leads to increase the cross phase saturation in the SOA. Also equation (3.13) shows that increase in launched power leads to increase in the cross phase modulation (XPM).

3.4.2 Power Penalty due to XPM in SOA

The power penalty occurs as

$$P_{penalty} = \frac{V L P_{io}}{\Gamma \alpha (I \tau / q - N_t)} - L^2 P_{io} \tag{3.14}$$

Where power variation is represented as $\partial P_i(t,z)/\partial z = P_{io}$. Equation (3.14) shows that the differential gain and the carrier lifetime are inversely proportional to power penalty. As we increase the differential gain, the power penalty goes on decreasing but the quality of signal should be recognizable for power margin and forward error check should be maximum up to 15 dB. It is also shown from equation (3.14), as with the increase in input power the power penalty goes on increasing. It is summarized that if the cross phase modulation is (XPM) reduced below a level then, there is improvement in power penalty result.

3.4.3 Bit Error Rate Estimation due to XPM in SOA

Differential phase error as the function of time and position of photon

$$\Delta\Phi(t,z) = \Delta\Phi_1(t,z) + \Delta\Phi_2(t,z) \ldots\ldots\ldots + \Delta\Phi_i(t,z) \ldots\ldots + \Delta\Phi_I(t,z) \tag{3.15}$$

The variance of differential phase error is

$$\sigma^2_{\Delta\Phi(t,z)} = \sum_{i=1}^{k} \frac{(\Delta\Phi_i(t,z) - \Delta\Phi_m(t,z))^2}{k} \tag{3.16}$$

Where $\Delta\Phi_m(t,z)$ is the mean value of differential phase shift.

$$\sigma^2_{\Delta\Phi(t,z)} = \sum_{i=1}^{k} \frac{\beta L}{k} \left[\begin{array}{l} \dfrac{a\Gamma I}{wqt_a P_L} \exp\left(\dfrac{\Delta P_{1i} - \Delta\Delta_{1m}}{\tau} \right) + \dfrac{1}{\tau} \sum_{n=1}^{M} \dfrac{(-1)^n}{P_L^n} \exp\left(\dfrac{\Delta P_{ni} - \Delta\Delta_{nm}}{\tau} \right) \\ \times \left[\begin{array}{l} a\Gamma L \left\{ \overline{N}_i^n(t_{ni}, z_{ni}) - \overline{N}_m^n(t_{nm}, z_{nm}) \right\} - (g_i - g_m) \\ \times \left\{ \overline{P}_i^{n-1}(t_{(n-1)i}, z_{(n-1)i}) - \overline{P}_m^{n-1}(t_{(n-1)m}, z_{(n-1)m}) \right\} \end{array} \right] \end{array} \right]^2 \tag{3.17}$$

Where subscript *m* is denoted as the mean value. By using Gaussian approximation and estimate the BER through the differential phase Q factor [Wei *et al.*, 2005].

$$Q_{\Delta\Phi} = \frac{\Pi}{2\sqrt{\sigma^2_{\Delta\Phi(t,z)} + \frac{N_o}{E_b}}} \tag{3.18}$$

When power penalty occurs

$$Q_{\Delta\Phi} = \frac{\Pi}{2\sqrt{\frac{N_o}{E_b} - \sigma^2_{\Delta\Phi(t,z)}}} \tag{3.19}$$

The bit error is estimated as

$$BER \approx erfc\left(\frac{Q_{\Delta\Phi}}{2}\right) \approx \exp\left[-\frac{\Pi}{8\left(\sigma^2_{\Delta\Phi(t,z)} + \frac{N_o}{E_b}\right)}\right] \tag{3.20}$$

When there is no cross phase noise, then the BER for DPSK is

$$BER = \frac{1}{2}\exp\left[-\frac{E_b}{N_o}\right] \tag{3.21}$$

So from equation (3.20) and (3.21), we conclude that bit error rate degradation occurs due to cross phase noise among the WDM channels.

3.4.4 SOA Structure Parameters

The InGaAlAs traveling wave SOA with negligible residual facet reflectivity is taken as the amplifier model in our simulation. After solving the rate equations above, the relevant parameters are as follows, almost similar to that used in XGM: the length is 750 μm, the width of active layer is 2 μm, its thickness is 0.2 μm and optimized confinement factor is 0.41. The transparency carrier density in the SOA is taken as 1.5×10^{18} cm^{-3} and the differential gain is estimated to be 200.002 atto cm^2. The carrier recombination time τ at this density is 0.3 ns with the saturation power P_s = 20.82 mW.

The gain of SOA is ranging from 39.13 dB to 34.10 dB for the input signal ranging from -30 dBm to +15 dBm. The optimum injection current is evaluated to be 400 mA, which is same as reported in result [Yamatoya and Koyama, 2004], and faster response has been obtained at higher bias currents. The input and output coupling losses of SOAs are taken as 3 dB.

3.4.5 Model Validation

In order to optimize the structure of the SOA, there is a need to reduce the SOA induced XPM which occurs due to multichannel system. The block diagram of simulation setup is shown in figure (3.16) for the SOA parameters in section 3.4.4. But here, this consists of only two channels and a single SOA without single mode fiber (SMF) and dispersion compensating fiber (DCF). The data sources are soliton return to zero formats at 40 Gb/s bit rate. Each channel consists of electrical driver that is used to convert the logical input signal into electrical signal. A continuous wave lorentzian light source with power -14 dBm and signal source are launched into optical phase modulator. The soliton return zero (RZ) data was pseudorandom binary sequence with word length 2^{10}-1 at 40Gb/s. The full wave half maxima line_width of continuous wave (CW) light sources is 10 MHz each. For each channel, the low pass Bessel filter have 3 dB bandwidth of 20 GHz for the generation of data source in terms of RZ format. Therefore, these two channels combined and launch into the SOA as in section 3.4.4 with variation of different parameters. At the output a raised cosine optical filter with bandwidth 50 GHz is used for both the channels. The time domain simulations are carried out with simulation bandwidth 2.29 THz which can be of wavelength 1550 nm.

The simulations are carried out for different bias currents of the SOA, which are further used for WDM system. The graph between phase and time is shown in figure (3.31a) for a channel in presence of other channels. It is observed that phase is increased with increase in bias currents, which shows good agreement with the above analysis in equation (3.7). It is also observed from figure (3.31b) that with increase in the bias currents the output also increases in this channel.

It is observed that if the bias current is decreased from 400 mA, huge power penalty is observed. Similar results are observed in [Yamatoya and Koyama, 2004]. From figure (3.31a), it is noticed that for a bias current of 500 mA and more, the positive phase shift is received. Hence, with the increase in the bias current above 500 mA power would also increase from saturation power by lot of amount.

When these SOAs are cascaded for injection current of 500 mA or more then, gain saturation occurs in the SOA due to large improvement in the amplified spontaneous emission noise. Therefore, cross phase noise is increased. The optimum injection current is 400 mA, which is same as reported in result [Yamatoya and Koyama, 2004] and also faster response has been obtained at higher bias current.

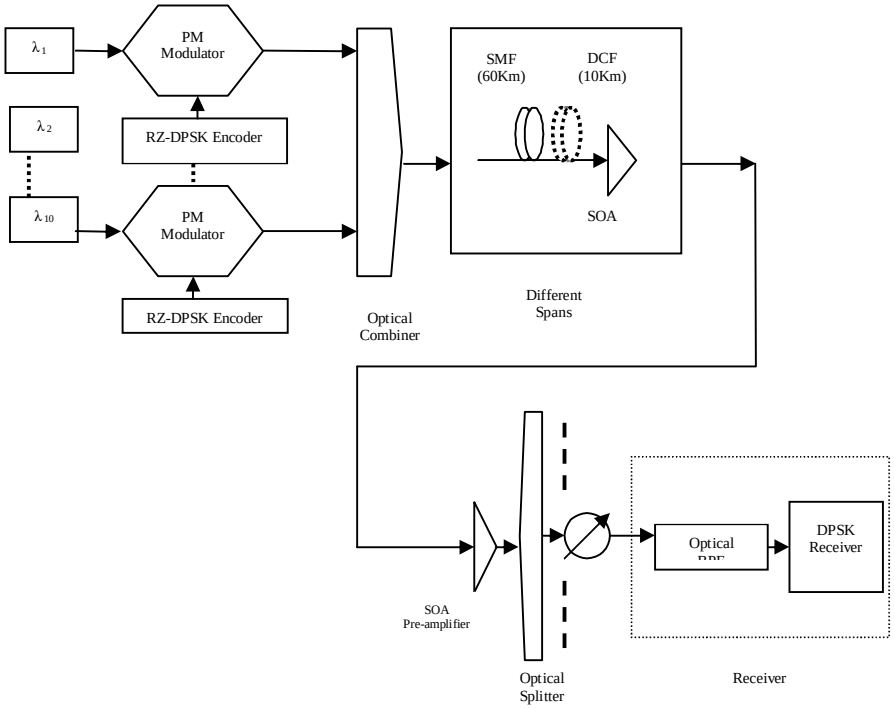

Figure 3.30: Schematic setup of transmission system for 10 × 40 Gb/s RZ-DPSK WDM signals.

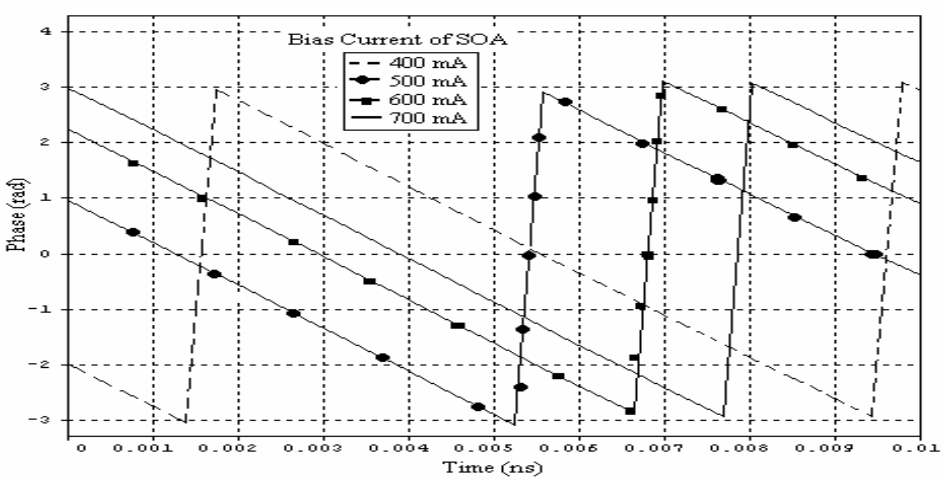

Figure 3.31a: Plot between phase noise and time for different bias currents.

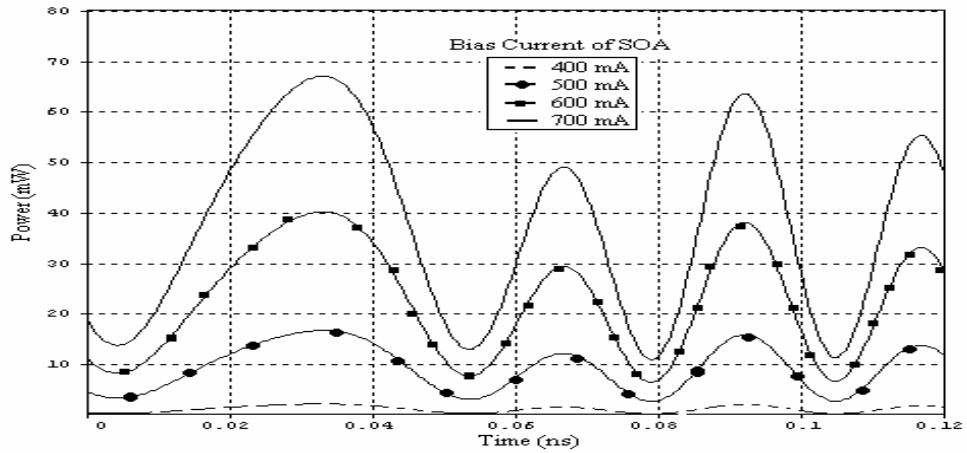

Figure 3.31b: Plot between received power and time for different bias currents.

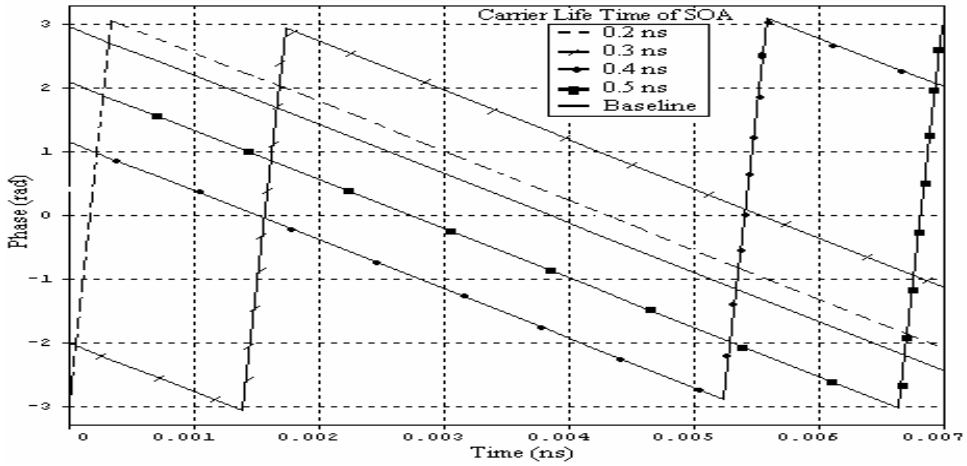

Figure 3.32a: Plot between phase noise and time for different carrier lifetimes.

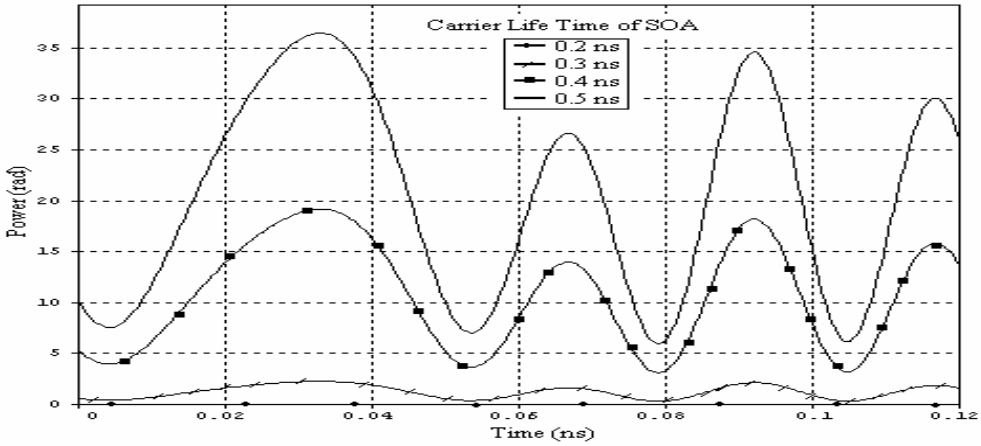

Figure 3.32b: Plot between phase noise and time for carrier lifetimes.

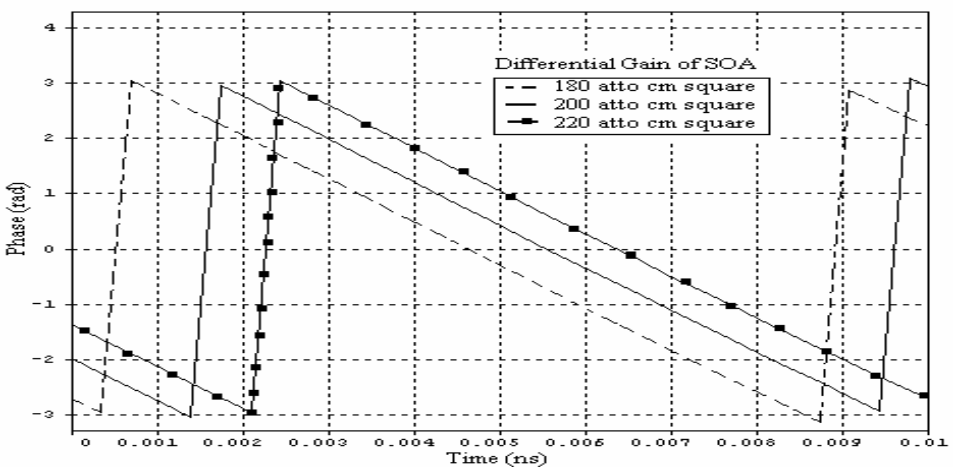

Figure 3.33a: Plot between phase noise and time for different differential gains.

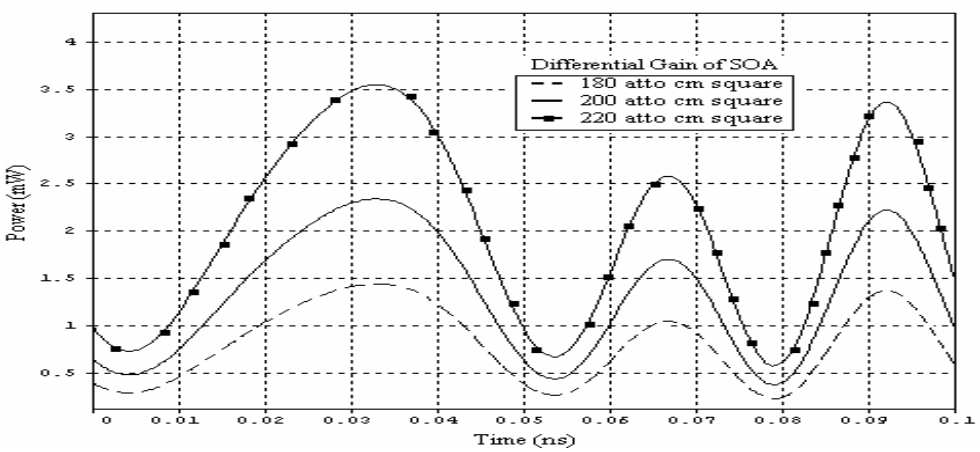

Figure 3.33b: Plot between phase noise and time for differential gains.

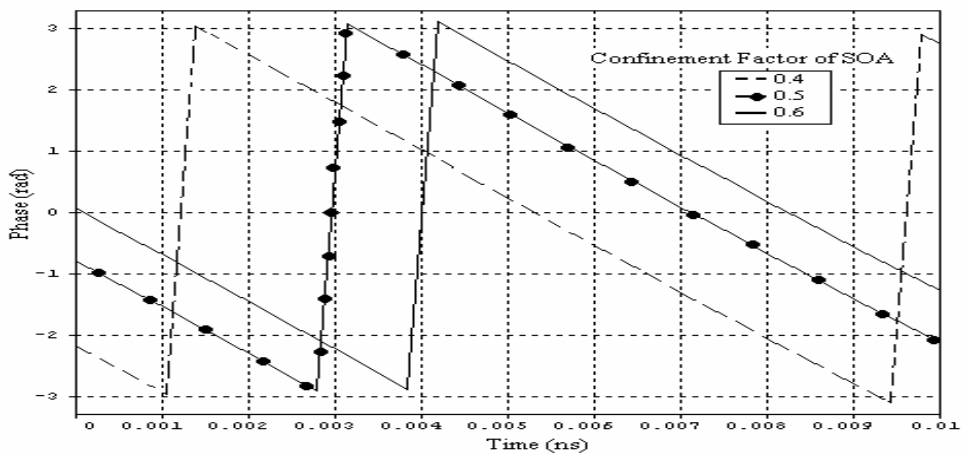

Figure 3.34a: Plot between phase noise and time for different confinement factors.

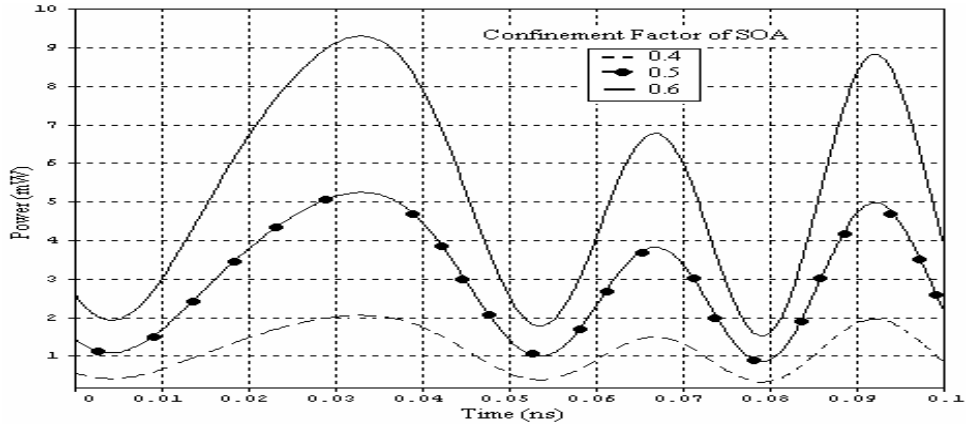

Figure 3.34b: Plot between received power and time for different confinement factors.

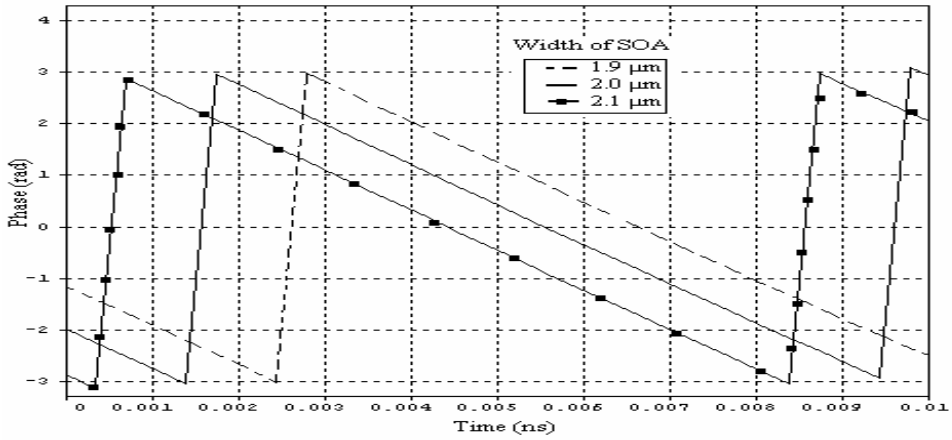

Figure 3.35a: Plot between phase noise and time for different widths of SOA.

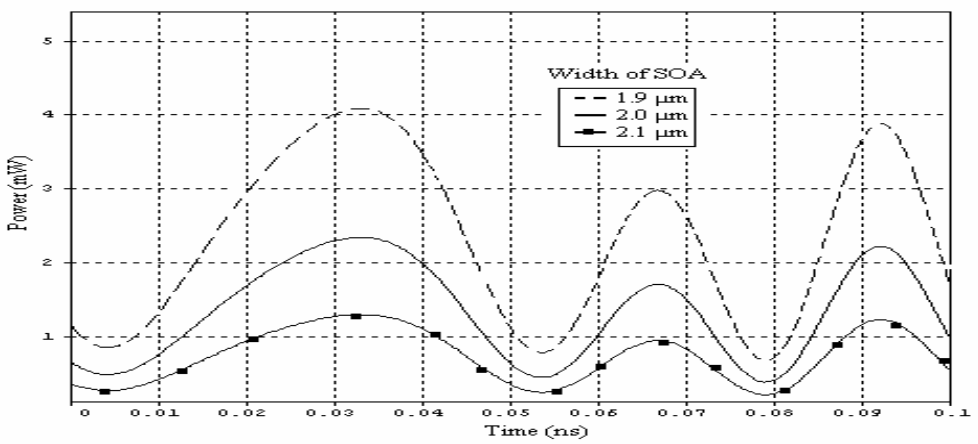

Figure 3.35b: Plot between phase noise and time for differential widths of SOA.

Figure 3.31– 3.35: Cross phase modulation in two channels at 40 Gb/s with transmitter bandwidth 20 GHz and receiver bandwidth 50 GHz for channel spacing 200 GHz. Also laser bandwidth is 10 GHz.

The phase noise variation due to carrier lifetime is shown in the figure (3.32a). It is observed that difference phase error reduces with the increase in carrier lifetime. This result shows good agreement with [Wei *et al.*, 2005; Xu *et al.*, 2003] and analysis equation (3.7). From figure (3.32a), we observed that at 0.2 ns carrier lifetime has large differential phase error and large power drop for the same channel. If carrier lifetime is more than 0.3 ns, then large drop in phase shift is observed as shown in figure (3.32a). But with drop in phase for large life time, there is increase in received power as shown in figure (3.32b). This large power forces the SOAs in power to deep saturation in cascaded transmission. Figure (3.33a) shows the variation of phase with differential gain of the SOA. The differential gain variation has little effect on cross phase noise. But if the differential gain drops from 180 atto cm^2 then, large power penalty is observed as shown in figure (3.33b). The phase noise and power increase with improvement in differential gain. This shows good agreement with XPM of the SOA equations (3.13), (3.14) and in [Xu *et al.*, 2003].

Similarly, the phase shift variation of the confinement factor and width of the SOA is shown in figures (3.34a) and (3.35a). With improvement in confinement factor, there is improvement in the phase shift and power of same channel which are shown in figures (3.34a) and (3.34b). Also with increase in the width of the SOA, the phase shift and power drops as shown in figures (3.35a) and (3.35b). From figures (3.31) to (3.35), the variation of phase shift is estimated. Further optimization of structural parameters of the SOA can be obtained only, when SOA is used for long haul wavelength division multiplexing (WDM) transmission system.

3.4.6 Optimization of the SOA Model for Long Haul WDM Transmission Links

If the SOA is used as an in-line amplifier in wide area network, fiber dispersion effect must be taken into account. So, in long haul transmission links, the total input power is redistributed after each span and different output powers are obtained after each span of fiber and SOA. Figure (3.16) shows a schematic setup of 10 × 40 Gb/s RZ-DPSK soliton WDM link. In this, ten channels are transmitted at a bit rate of 40 Gb/s over a distance of 70 km in single mode, dispersion compensating fiber, an SOA at end and another similar SOA is used as the pre-amplifier. The XPM behaviour is measured here for channel number 8 only.

The XPM effects on the SOA with different confinement factors and bias currents for 70 km transmission links as shown in figures (3.36a) and (3.36b).

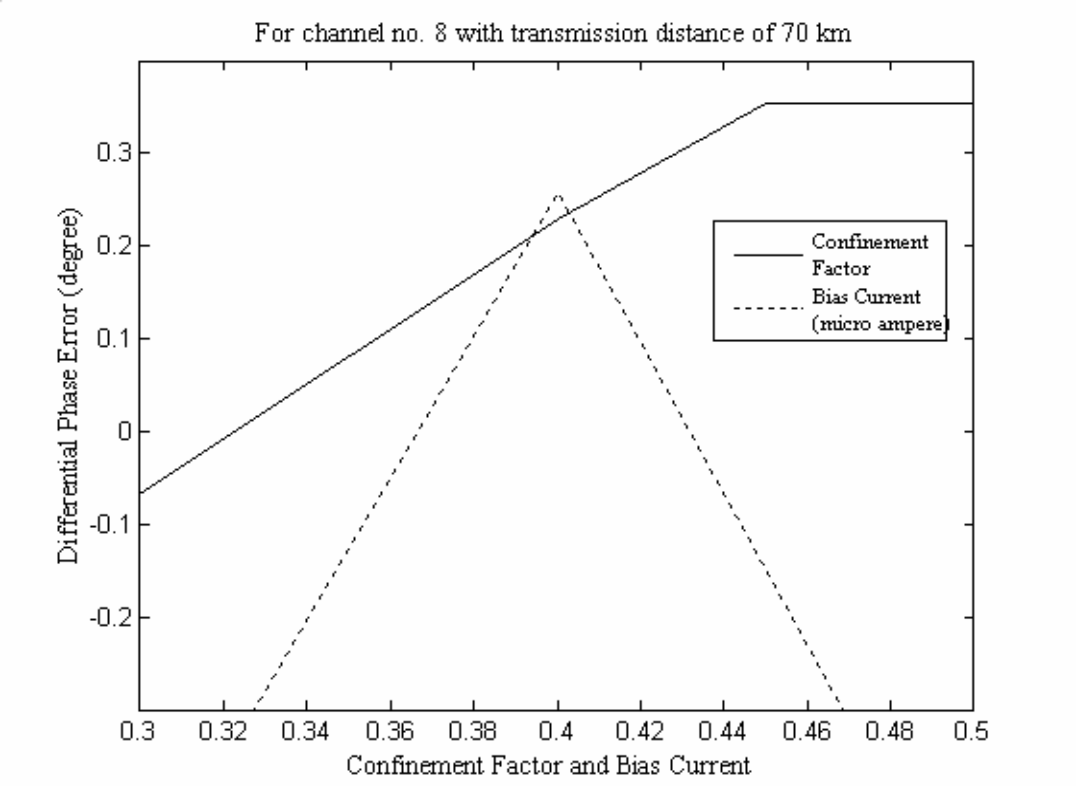

Figure 3.36a: Plot between differential phase error with confinement factors and bias currents.

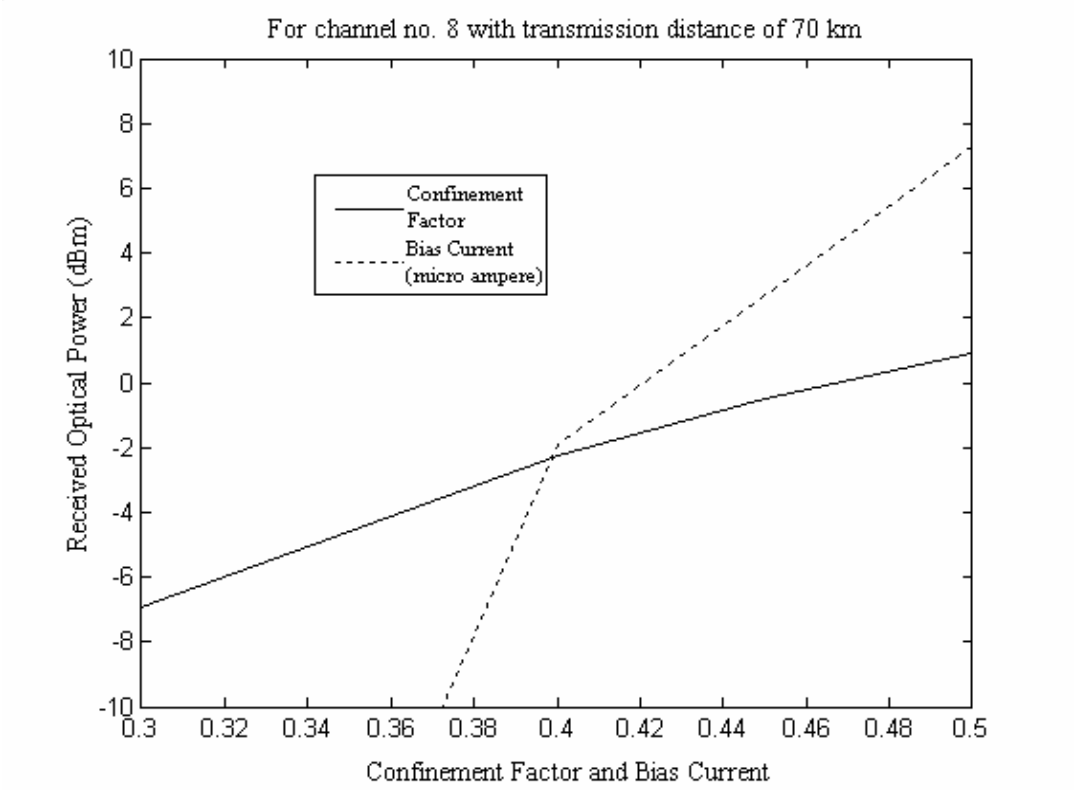

Figure 3.36b: Plot between received power with confinement factors and bias currents.

With the drop in the confinement factor, the differential phase error goes on decreasing and received power goes on increasing. The confinement factor around 0.4 shows the minimum differential phase error with sufficient output power. The differential phase error goes on increasing with increase in the bias current, similarly optical power received is also increased. At 300 mA, minimum differential phase error is observed with power penalty more than 17 dBm. Then differential phase error starts increasing. At 400 mA bias current, 0.26 degree differential phase error is obtained with sufficient output optical power. For bias current more than 400 mA, the differential phase noise drops. This bias current is not considered for long transmission link because bias current above 400 mA has large improvement in output optical power. The SOA with bias current larger than 400 mA will saturate the SOAs for cascaded long haul transmission. Also, the bias current more than 400 mA produces large amplified spontaneous emission noise. Therefore 400 mA bias current is found to be optimum and best [Yamatoya and Koyama, 2004].

The carrier lifetime and width of the SOA is also analyzed for channel number 8 with transmission distance 70 km shown in figures (3.37a) and (3.37b). As with increase in the carrier lifetime of the SOA, the differential phase error goes on decreasing. This result shows good agreement with results reported in [Wei *et al.*, 2005]. The power penalty is observed up to the carrier lifetime of 0.25 ns. But, for carrier lifetime of 0.35 ns and more, the high optical output signal is observed which will saturate the SOAs for cascaded transmission links. Similarly, as the width of the SOA is increased, the differential phase error approaches the negative value. But, the width of the SOA beyond 2 μm leads to large power penalty as shown in figure (3.37b).

Now the maximum transmission distance of 4550 km is considered. Therefore, 65 spans (70 × 65 km) have to be used. For this transmission distance, the confinement factor and differential gain of the SOA are optimized for decreasing the complexity.

In previous analysis, it is found that for confinement factor less than 0.4 shows power penalty in cascade transmission system. Also with slight decrease in differential gain from 199 atto cm^2, power penalty is observed. At 210 atto cm^2 large cross phase modulation (XPM) is observed. The table (3.2) represents the differential phase shift for different confinement factor of the SOA for channel number 8 with transmission distance 4550 km. It is observed that for the confinement factor 0.4 there is large power drop but quality of signal is the best. Hence, it shows agreement with equation (3.19).

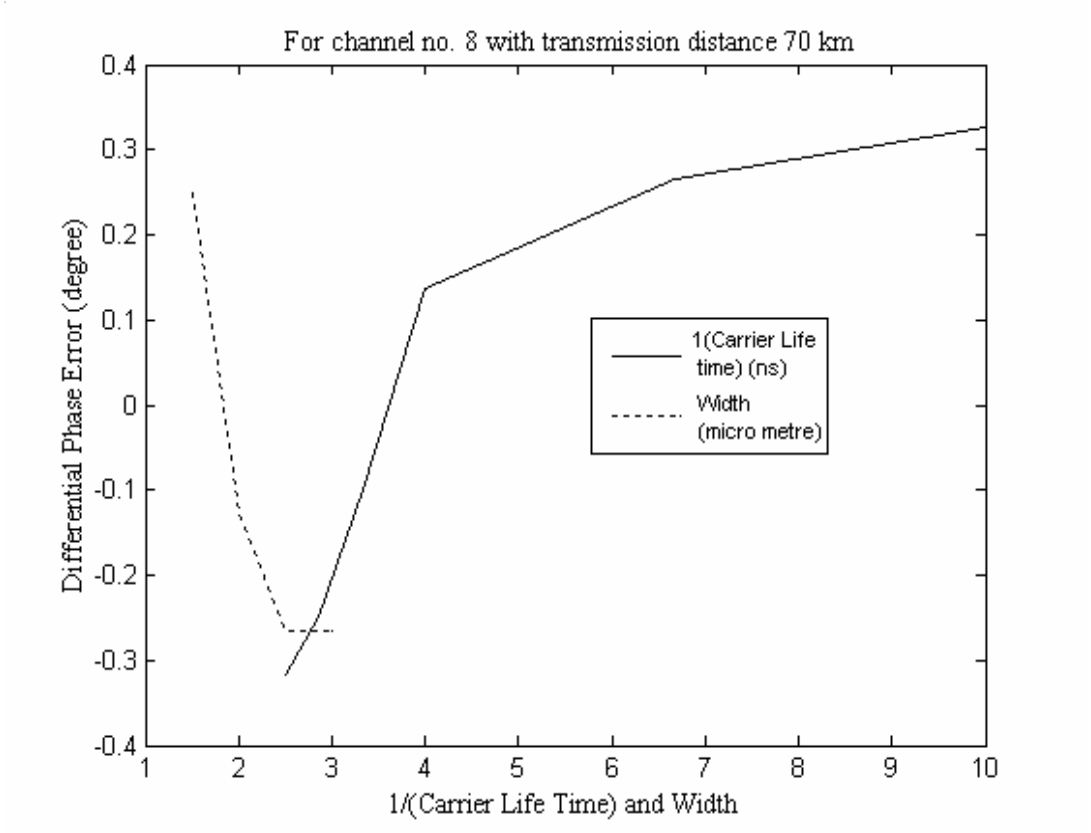

Figure 3.37a: Plot between differential phase error with inverse of carrier life tines and widths.

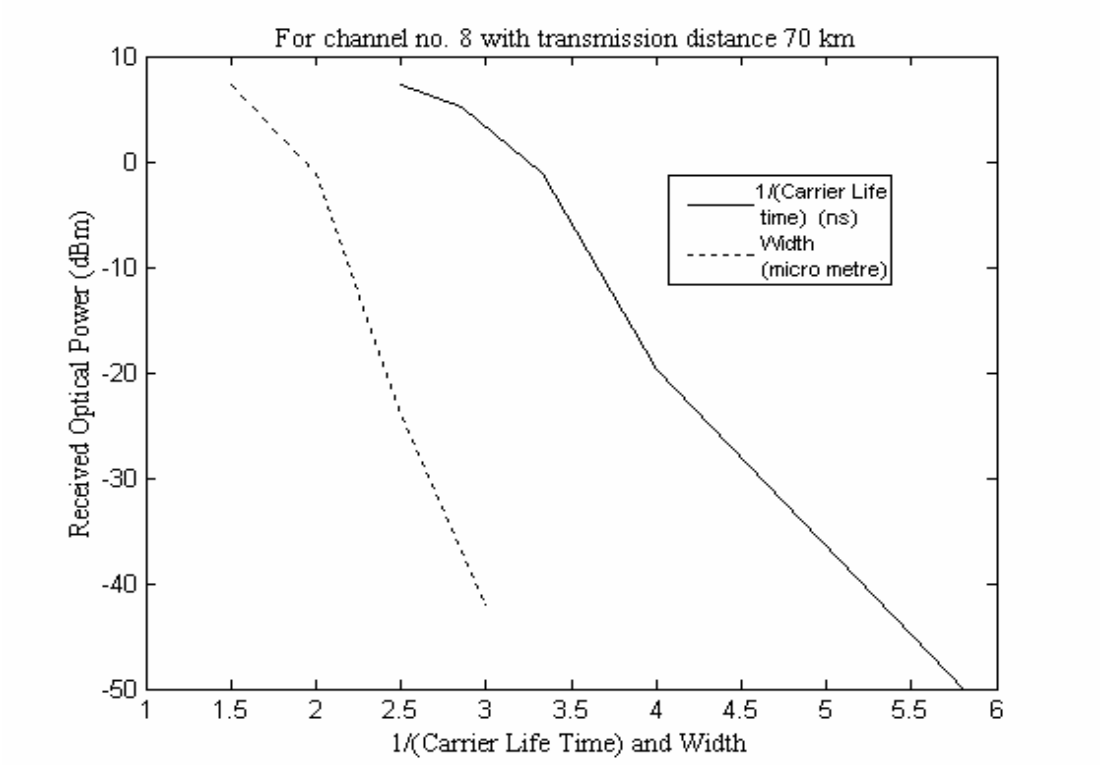

Figure 3.37b: Plot between received output power with inverse of carrier lifetimes and widths.

Table 3.2

Differential phase shift with different confinement factor for a channels number 8 with bit rate of 40 Gb/s for transmission distance 4550 km.

Confinement Factor (Γ)	0.400	0.410	0.415	0.420	0.500
Differential Phase Error (ΔΦ) (degree)	-0.874	-0.628	-0.626	-0.385	-0.386
Optical Received Power (dBm)	-54.70	-13.75	-1.84	0.45	1.15
Quality Factor (dB)	20.89	17.39	10.88	9.41	Below 6

Table 3.3

Differential phase shift with different differential gains for a channels number 8 with bit rate of 40 Gb/s for transmission distance 4550 km.

Differential gain (atto cm^2)	199	200	200.1	200.5	201	202
Differential Phase Error (ΔΦ) (degree)	-0.87	-0.63	-0.64	-0.38	-0.26	0.020
Optical Received Power (dBm)	-21.6	-13.8	-13.1	-10.68	-7.21	-3.8
Quality Factor (dB)	18.3	17.4	17.3	17.20	15.42	12.09

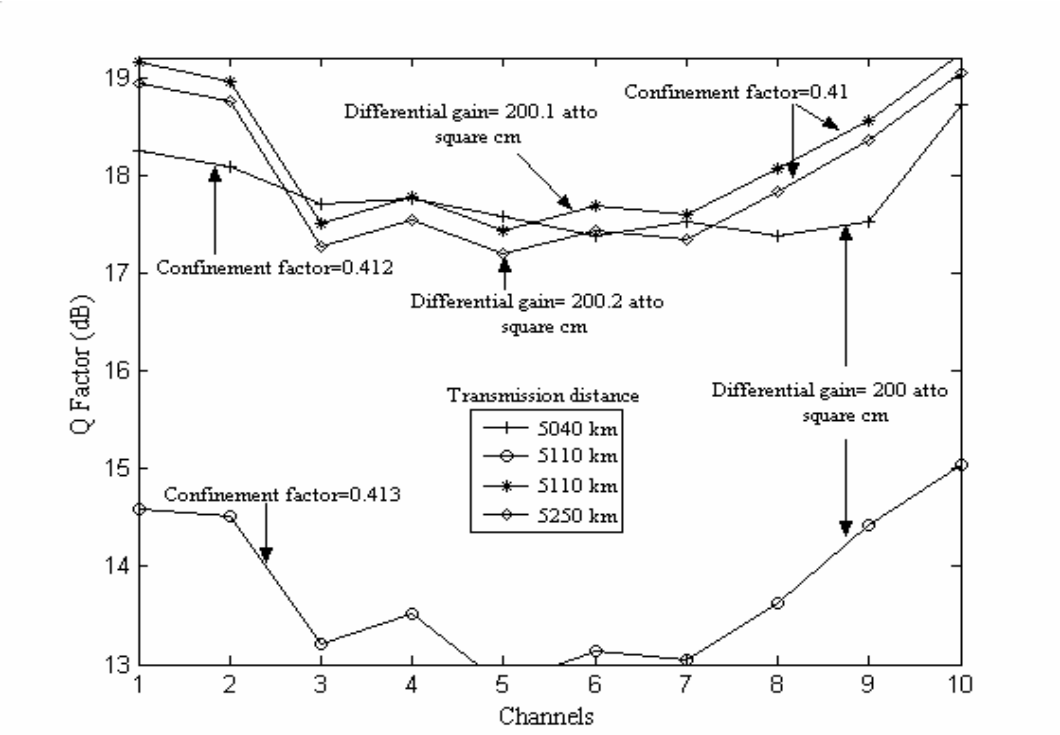

Figure 3.38: Plot between Q factor and channels for different differential gains and confinement factors.

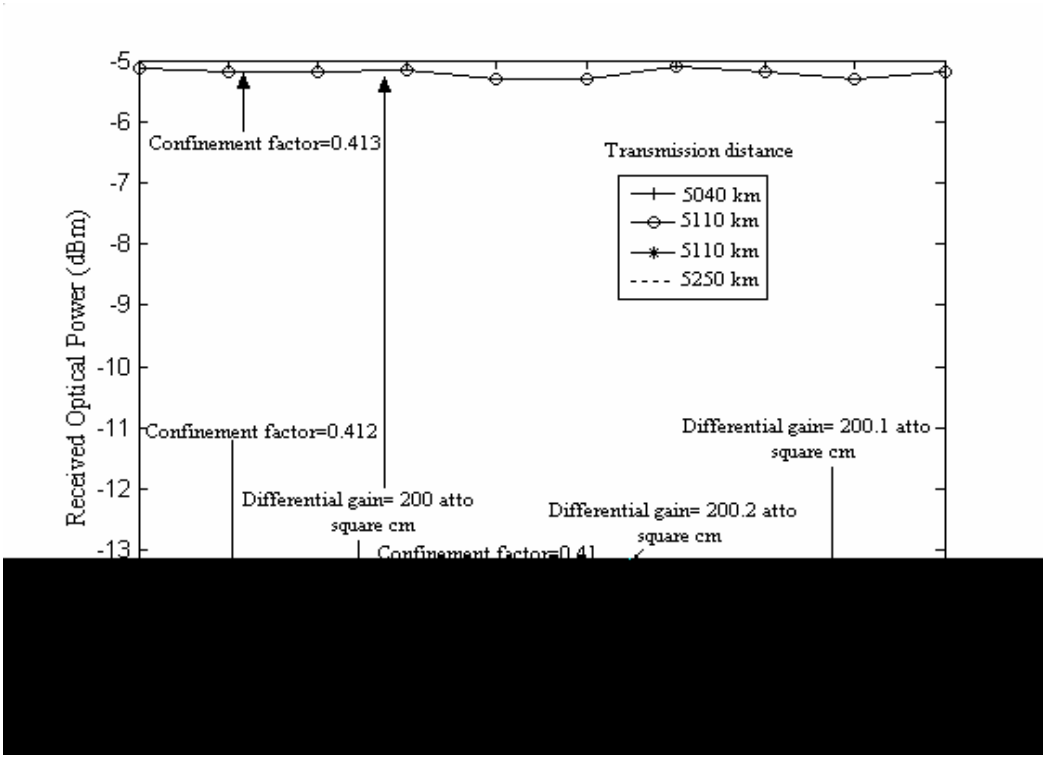

Figure 3.39: Plot between received optical power and channels for different differential gains and confinement factors.

Also for the confinement factor of 0.415 onwards, there is drop in the quality of channel number 8 due to increase in XPM. This shows that variance of XPM is large, so as from equation (3.18), the Q factor drops and also bit error rate (BER) increases from 10^{-9}. The table (3.3) shows the observed differential phase shift with different differential gains for channel number of 8 for the transmission distance of 4550 km. As for differential gain 199 atto cm^2, large power penalty of 6.56 dBm is observed. This meets with above analysis as in equation (3.19). It is also observed that quality factor goes on decreasing with the increase in differential phase error. For differential gain 201 atto cm^2 and beyond, there is drop in quality due to increase in the differential phase error.

It is summarized that confinement factor of 0.41 and different gain of 200.1 atto cm^2 are best for further transmission. For the larger transmission distance, the differential spans used are 72, 73 and 75 spans. First of all we change the confinement factor 0.412 and 0.413 for differential gain 200 atto cm^2.

For confinement factor 0.413, there is drop in the quality of all channels. Even power received is more than -5 dBm for 5110 km transmission distance as shown in figure (3.38) and (3.39). This is due to increase in XPM and XGM in SOAs. For confinement factor 0.412, we have observed that quality factor is more than 17.5 dB for each channel for transmission distance 5040 km as shown in figures (3.38) and (3.39). For this, nil power penalty is observed. This shows a large improvement of transmission distance over the results reported in [Li *et al.*, 2004].

Now the differential gain of 200.1 atto com^2 and 200.2 atto cm^2 are chosen with confinement factor 0.41. For the differential gain of 200.1 atto cm^2, the maximum power penalty of 0.46 dBm is observed for some channels, even quality of all channels are sufficient for transmission distance 5110 km. From equation (3.14), with slight increase in differential gain of 200.2 atto cm^2 nil power penalty is noted for transmission distance 5250 km, as shown in figure (3.39). As shown figure (3.38), the observed quality for all channels is more than 15 dB.

3.5 Conclusions

In this Chapter, it is investigated that the twenty channels at 10 Gb/s WDM is transmitted over a distance of 4340 km by using the SOA as in-line and pre-amplifier with the DPSK modulation format at 100 GHz channel spacing. For this, the confinement factor of the SOA is optimized for reducing the SOA-induced crosstalk and power penalty at sufficient amplification. The low crosstalk -9.63 dB, high optical gain 39.13 dB with the low ASE

noise power 119.2 μW are achieved for the input of -15 dBm for the SOA. Therefore, the cross gain saturation of the SOA depends upon the confinement factor and the bias current. The DPSK system performs best for the transmission distance of 4900 km with bit error rate observed less than 10^{-10} for all channels with power penalty of 1 dB.

The optimization of the differential gain of the semiconductor optical amplifier at 40 Gb/s is also done. The soliton RZ-DPSK WDM signals with high capacity up to 0.4 Tb/s is transmitted up to a transmission distance of 1050 km successfully by using the optimized semiconductor optical amplifiers. The spectral efficiency approaches to 0.4 bit/s/Hz for the transmission system. The transmission distance of 1050 km is observed with the differential gain of 210 atto cm^2 of the SOA with improvement in the power more than 1.55 mW. To achieve this goal, the SOA differential gain is optimized for reducing the cross gain saturation which occurs due to the SOA-induced crosstalk and also reduction in power penalty with sufficient amplification. The cross gain saturation is further reduced by using the SOA with differential gain 200 atto cm^2. Therefore maximum transmission distance observed is 4550 km with good quality and nil power penalty per channel. These results of low cost semiconductor optical amplifiers can be used for connecting the metro networks at 40 Gb/s.

The simulation of ten-channel 80 Gb/s WDM transmission 910 km using the SOAs as in-line and pre-amplifier with soliton RZ-DPSK modulation format at 200 GHz channel spacing has been done. The spectral efficiency is approaching to 0.4 bit/s/Hz for this transmission distance by using the SOA.

In another part of the Chapter, the theoretical study of the SOA cross phase noise is proposed due to the gain saturation in WDM links. The crosstalk is found to be dependent on the SOA structure parameters. The nonlinear cross phase noise is expected to be suppressed by increasing the carrier lifetime, width while reducing differential gain, confinement factor in WDM links. This SOA model may be attractive, when used as pre-amplifiers and in-line amplifiers for long haul links up to 5250 km for 10 × 40 Gb/s soliton DPSK WDM signals. This SOA model can offer a cost effective solution for WDM links.

These results provide useful information for the designing of long WDM transmission links by using low cost semiconductor optical amplifiers.

Chapter 4

Optimum Placement of Optimized SOAs for Long Haul WDM Transmission of RZ-DPSK Signals

This chapter deals with the placement of the SOA in a single mode and dispersion compensated fiber link for 10 Gb/s non return to zero format, which is part of third objective of the research work. Another part of the chapter investigates the power budget improvement for long haul WDM and DWDM transmission of RZ-DPSK signals by using optimum placement of the optimized SOAs. This is the second objective of the research work.

4.1 Placement of Optimized SOA in Fiber Optical Communication System

The optical amplifier increases the link distance which is limited by fiber loss in optical communication system. However, the amplifiers also introduce nonlinear effects which not only limit the bit rate but also the propagation distance in an optical fiber link.

Optical amplifiers can serve several purpose in the design of fiber optic communication system *i.e.* in-line, booster and pre-amplifiers. Mecozzi *et al.* [1995] demonstrated the feasibility of 10 Gb/s transmission over a 500 km optical link consisting of single mode fiber and in-line SOAs. Settembre *et al.* [1997] investigated that transmission distance can be increased by using sliding filters for both intensity modulated direct detection (IM DD) soliton and non return to zero (NRZ) systems. For IM DD NRZ system, the maximum transmission is limited up to 900 to 1000 km. Kim *et al.* [2003] demonstrated the transmission of 10 Gb/s optical signal over 80 km through standard single mode fiber with the transmitter by using SOA as booster-amplifiers. That can be achieved by utilizing the negative chirp converted in the SOAs and self phase modulation induced by the high optical power.

The use of power compensation by the SOA is an important method for power improvement without degrading the optical signal in single mode fiber link. The SOA can be placed before or after single mode fiber link for power compensation of propagating signals. Spans are made up of fiber link and SOAs for the long distance transmission. The signal degradation due to gain fluctuation of the SOA depends upon the length of the

fiber link. Another parameter of the SOA is amplified spontaneous emission (ASE) noise power which affects the signal performance. The power compensation is done by three methods post-, pre- and symmetrical-power compensation. In first method, the placement of the SOA is done at the end of fully dispersion compensating link. In the second method the optical signal in optical communication system is pre-power compensated by placing the SOA at the start of the fully dispersion compensating fiber link. In the third method, the power compensation is done by symmetrical way. This can be achieved by placing one SOA at the start and another at the end.

Due to the non linear nature of the propagation, the system performance depends upon power levels [Nuyts *et al.*, 1996] and position of the dispersion compensating fibers [Rothnie *et al.*, 1996]. The sufficient power levels depend upon the placement of optical amplifier in optical communication system. Earlier in literature [Mecozzi *et al.*, 1995; Settembre *et al.*, 1997; Kim *et al*., 2003], SOA is used as in-line and pre-amplifier. Singh *et al*.[1997] also evaluated that the post-amplifier placement is better in broadcast network topologies. Here the results of post-, pre- and symmetrical-power compensation by using optimized SOA is compared on the basis of bit error rate, eye diagram and eye closure, for different transmission distances and signal input powers.

4.1.1 Simulation

The block diagram for the simulations of post-, pre- and symmetrical-power compensation methods using SMF and DCF are shown in figure (4.1). Each transmitter section consists of data source, electrical driver, laser source and amplitude modulator. The data source is non return to zero format at 10 Gb/s bit rate and is indicated by Data source, 10 shown in figure (4.1). The electrical driver converts the logical input signal into electrical signal. It is represented by the NRZ blocks for the post-, pre- and symmetrical-power compensations respectively. The continuous wave laser source (CW_lorentzian, 1550 for three configurations) generates laser beam at 1550 nm. The input data source is modulated at laser beam by using amplitude modulator (Sin_mz for all configurations). The output of the modulator is fed to the optical link with the SOA through optical splitter. The optical splitters (b137, b136, b134) are used for the measurement of optical input power for transmission link. The post- and pre-power compensations represent two spans. We assume two spans such that there are two SOAs at end of the single mode and dispersion fibers. For a span, the length of single mode

fiber is 96 km with 16 ps/nm/km dispersion and the length of dispersion compensation fiber is 16 km with -96 ps/nm/km dispersion and a SOA at the end.

The two spans for the post- and pre-power compensation is indicated by b156 and b153. The connectors are used in these spans indicated as b40, b33, b64, b60. There are two SOAs used in each power compensation methods. The symmetrical power compensation is represented as the combination of the pre- and post-power compensations. In symmetrical power compensation, there are two fiber links of SMF and DCF used having length 102 km. The connectors are indicated by b170, b166, b105, b107, b106 which are used for the connection of SMF and DCF link. In all the three power compensation method, there is 204 km optical fiber link. The output power for all compensation methods is measured by optical power meter (indicated by out-power for all configurations). The output signal of the fiber link is connected to the optical splitter to detect the quality and power level of signal. The output optical splitters are indicated by b10, b72, b110 for all configurations. The output optical signal is detected at the receiver by PIN detector (b6, b69 and b115 for these configurations) and is passed through the electrical filter (Bessel) and the output is observed on electroscope. The eye diagram, eye closure, Q factor and bit error are measured from the electroscope.

The CW Lorentzian laser is used here with centre emission wavelength 1550 nm (193. 4145 THz frequency). The amplitude modulator is sine square with excess loss of 3 dB. The simulated bit rate is 10 Gb/s with pseudorandom binary sequence (PBRS) with word length of 2^7-1. The electrical filter is Bessel type with 3 dB bandwidth equal to 8 GHZ. The responsivity of PIN detector is 0.875. All fiber nonlinearities and dispersion effects are considered in the simulation. The attenuation and nonlinear coefficients for single mode fiber is 0.29 dB/km and 1.27 $W^{-1}km^{-1}$ and that of dispersion compensating fiber is 0.55 dB/km and 5.07 $W^{-1}km^{-1}$. The PMD coefficient of both SMF and DCF is 0.1 ps $km^{-1/2}$. The time domain simulations are performed at the centre wavelength of 1550 nm with bandwidth of 0.1 THz.

The optimized SOA used as in Chapter 2 which having negligible residual facet reflectivity is taken as the amplifier model in our simulation. The parameters are as follows: the length is 750 μm, the width of active layer is 2 μm, its thickness is 0.2 μm and the confinement factor is 0.4. The transparency carrier density in the SOA is taken to be 1.5×10^{18} cm^{-3} and the differential gain of 2×10^{-16} cm^2. The carrier recombination time τ at this density is estimated to be 300 ps given the saturation power P_s = 21.36 mW.

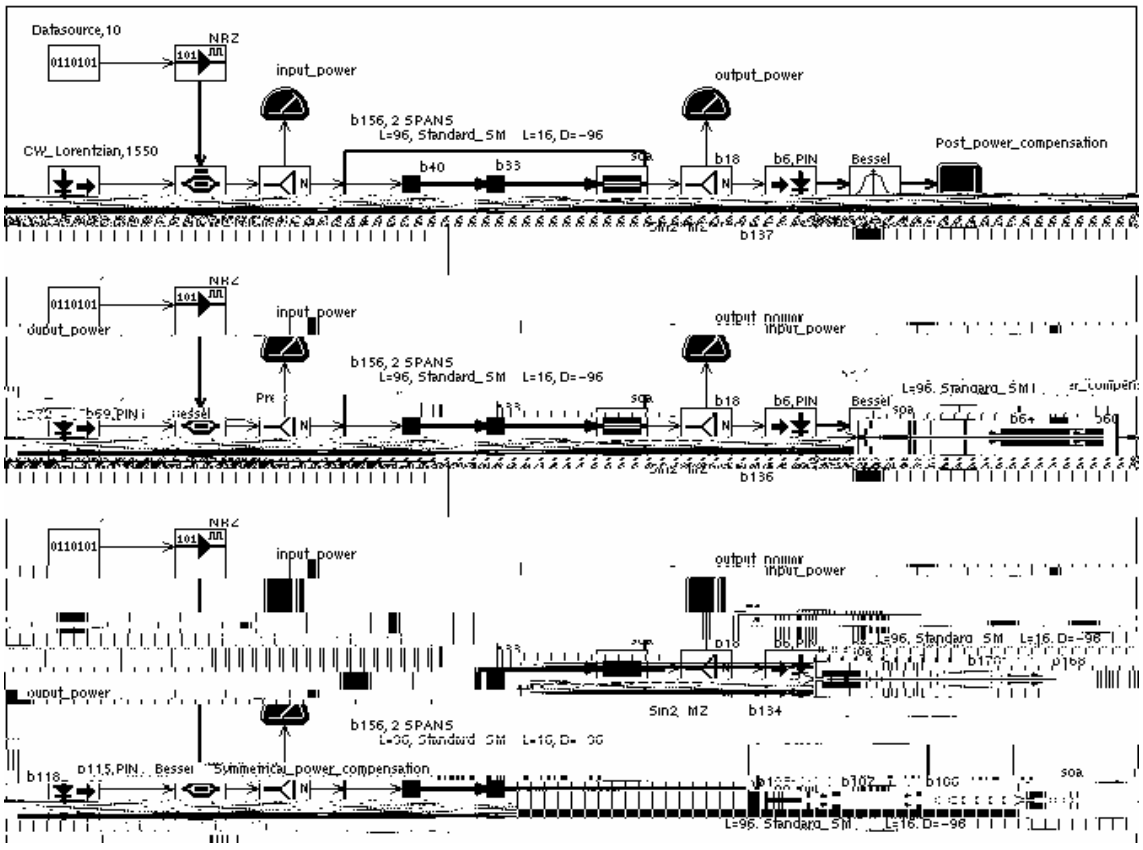

Figure 4.1: Simulation setup for post-, pre- and symmetrical-power compensation using semiconductor optical amplifiers.

Table 4.1

Variation of signal input power at fiber link with variation of power at laser.

Signal input power at laser (dBm)	-25	-15	-10	-5	0	5	10	15
Signal input power to fiber link (dBm)	-31.35	-21.35	-16.35	-11.35	-6.35	-1.35	3.65	8.65

The optimum injection current evaluated is 400 mA. The input and output coupling losses of SOAs are taken as 3 dB.

4.1.2 Results and Discussions

In order to observe the performance of three power compensation methods, the applied signal CW laser is given in table (4.1) and the corresponding input power applied to the fiber link is also indicated. The input power applied to the optical fiber link drops from actual value due to losses in the amplitude modulator etc. The total length of the optical communication link is 204 km and two SOAs are used in each power compensation method.

The graph between bit error rate and signal input power at fiber link is shown in figure (4.2). For post-power compensation, the bit error rate is low which indicates the best performance. It is also observed that the bit error rate increases with the increase in signal input power at optical fiber link. This is due to gain saturation of the SOA. The gain of the SOA increases with the increase in signal input power. When input power to fiber link increases from -1.35 to 1.65 dBm, it increases the bit error rate up to 10^{-20} for post-power compensation method, which is acceptable for the high data rate optical transmission. The clear eye diagram for post power compensation is shown in figure (4.3).

For pre-power compensation at low signal input power of -31.35 dBm, the bit error rate is good. This shows that SOA can be placed as pre-amplifier for low signal input power. This pre-amplifier shows good bit rate and output power for transmission distance of 204 km. For single span, placing the SOA for transmission distance of 102 km, gives good performance. This result shows improvement over the results reported in [Kim *et al.*, 2003]. The performance of pre-power compensation method is deteriorating for high signal input -21.35 dBm onwards.

The bit error rate goes on increasing with the increase in signal input power. The applied signal higher than the saturation power of the SOA will move the SOA towards saturation. Hence, the output signal is degraded. This degraded output signal is propagated through optical fiber links. The optical link degrades the power of the signal further, but the quality is almost remains the same as from the SOA. Hence, with the increase in spans, the quality of signal goes on decreasing as shown in eye diagram (4.4). From figure (4.4) to (4.5), it is observed that the symmetrical-power compensation shows improved performance as compared to the pre-power compensation method.

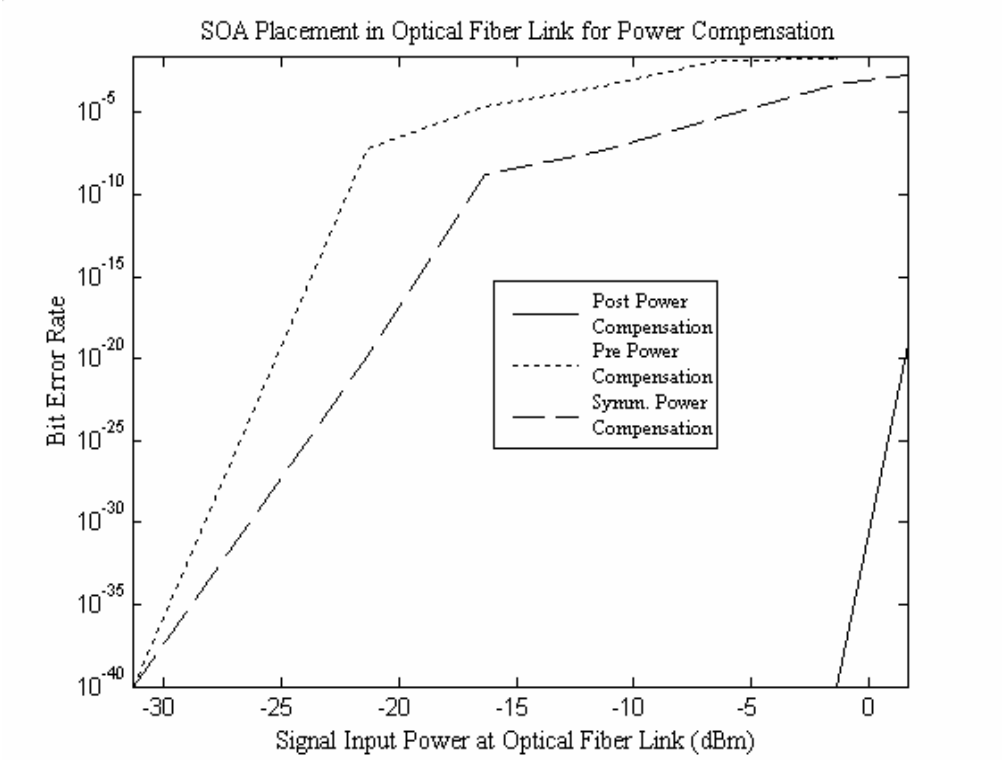

Figure 4.2: Bit error rate as the function of signal input power for post-, pre- and symmetrical-power compensation methods.

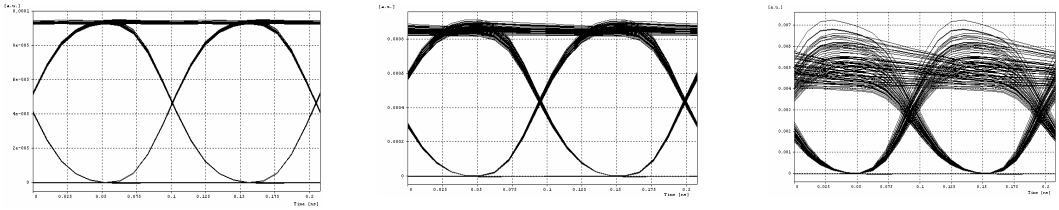

(a) -10 dBm. (b) 0 dBm. (c) +10 dBm.

Figure 4.3: Eye diagrams for post-power compensation for various values of signal input power: (a) -10 dBm (b) 0 dBm (c) +10 dBm.

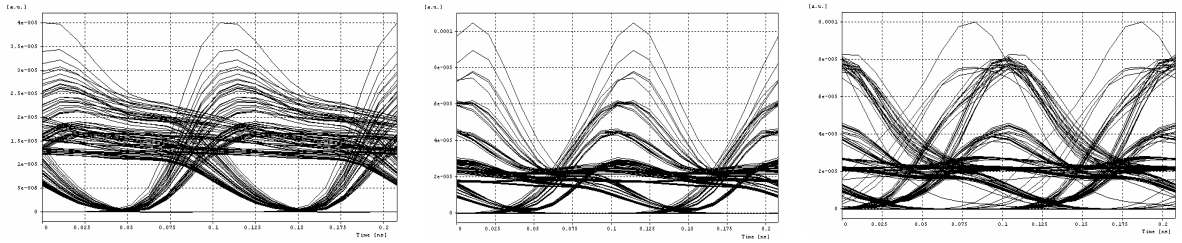

(a) -10 dBm. (b) 0 dBm. (c) +10 dBm.

Figure 4.4: Eye diagrams for pre-power compensation for various values of signal input power: (a) -10 dBm (b) 0 dBm (c) +10 dBm.

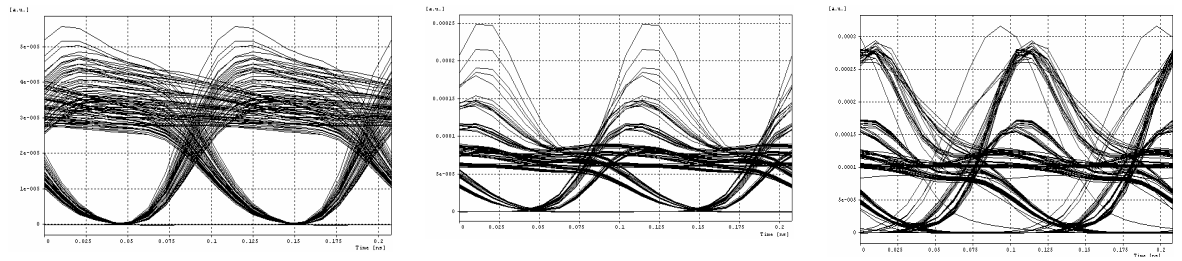

(a) -10 dBm. (b) 0 dBm. (c) +10 dBm.

Figure 4.5: Eye diagrams for Symmetrical-power compensation for various values of signal input power: (a) -10 dBm (b) 0 dBm (c) +10 dBm.

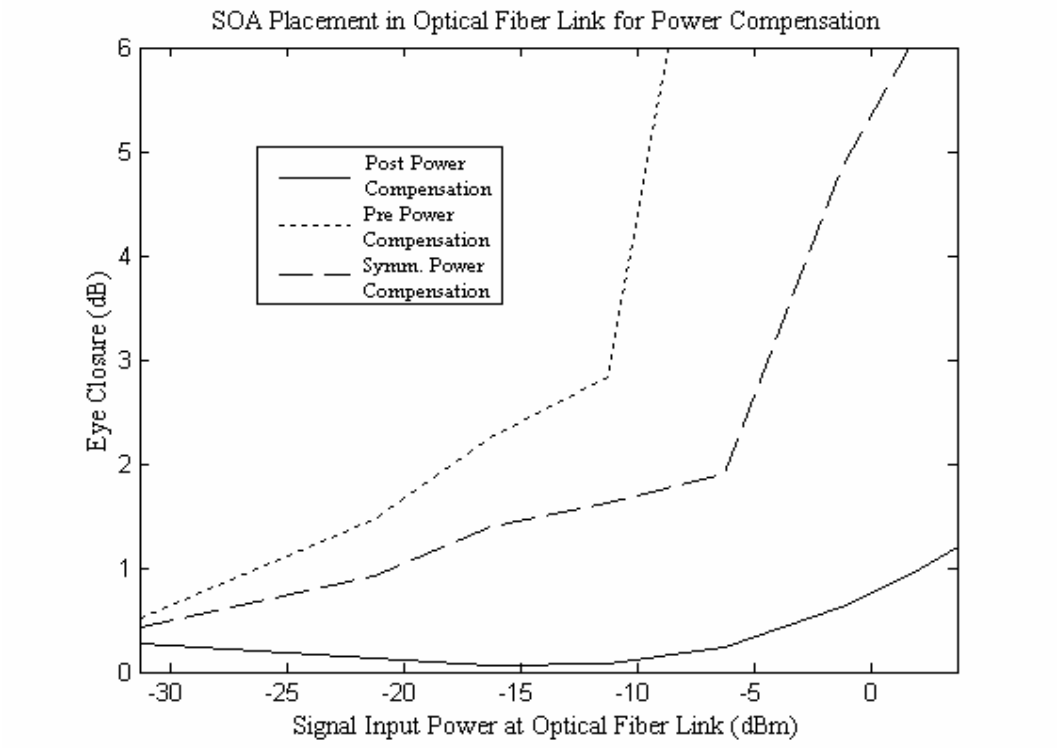

Figure 4.6: Eye closure penalty as the function of signal input power for post-, pre- and symmetrical-power compensation methods.

The symmetrical-power compensation method combines the performance of pre- and post-power compensation methods.

Therefore, the gain saturation of first SOA will degrade the quality of signal propagating in the transmission link. The eye diagram for symmetrical-power compensation is shown in figure (4.5). The comparison for -16.35, -4.35, 3.65 dBm signal input power for fiber link in terms of eye diagrams for the three configuration is shown in figure (4.3) to (4.5). The ratio of the average eye opening and the eye opening is expressed in dB, which is a measure of eye closure penalty. The graph of this penalty is shown in figure (4.6) for the three SOA placement methods.

The eye closure penalty is large for the low signal input at optical fiber link of -31.35 dBm as compared to -6.35 dB signal input power as shown in figure (4.6). This is due to the amplified spontaneous emission noise power. This shows good agreement with [Yamatoya and Koyama, 2004] for low signal input power, the high ASE noise power is observed. It is observed that the post-power compensation methods has eye closure penalty less than 1 for signal input power of 1.65 dBm.

For other pre- and symmetrical-power compensation, there is large eye closure penalty more than 1 at the same input power. The eye closure penalty goes on increasing with the increase in signal input power. This means that the quality goes on decreasing with the increase in the signal input power. This shows good agreement with the result [Jennen *et al.*, 2001]. Figure (4.7) reported for received signal input power and the applied signal input power. The post-power compensation method gives sufficient output power up to large signal input power of 1.65 dBm. Another placement of the SOA as pre- and symmetrical-power compensation gives power penalty for signal input around -16 dBm only. The length of dispersion compensated fibers and single mode fiber are increased simultaneously for the setup of post-, pre- and symmetrical-power compensation methods for five different cases as shown in table (4.2). For all placement methods, the signal input power for link is -16.35 dBm. The graph between bit error rate and cases in table (4.2) is shown in figure (4.8). It is observed that the bit error rate decreases up to the length of 105 km and good bit error rate is noted for higher distance. For the transmission distance of more than 140 km, the bit error rate is increased for all power compensation methods. For small transmission distance (30 km) with two spans, the SOA gets saturated in the 2^{nd} span due to the high input at the SOA for post-, pre- and symmetrical-placement of SOA for power compensation.

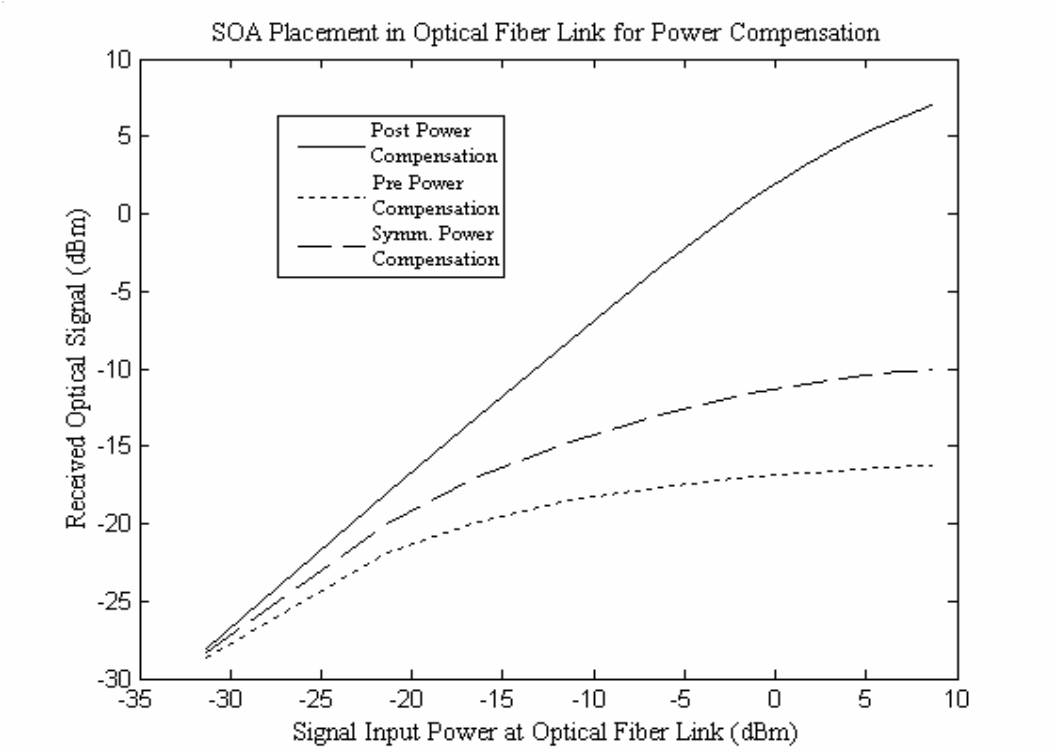

Figure 4.7: Received optical signal power as the function of signal input power for post-, pre- and symmetrical-power compensation methods.

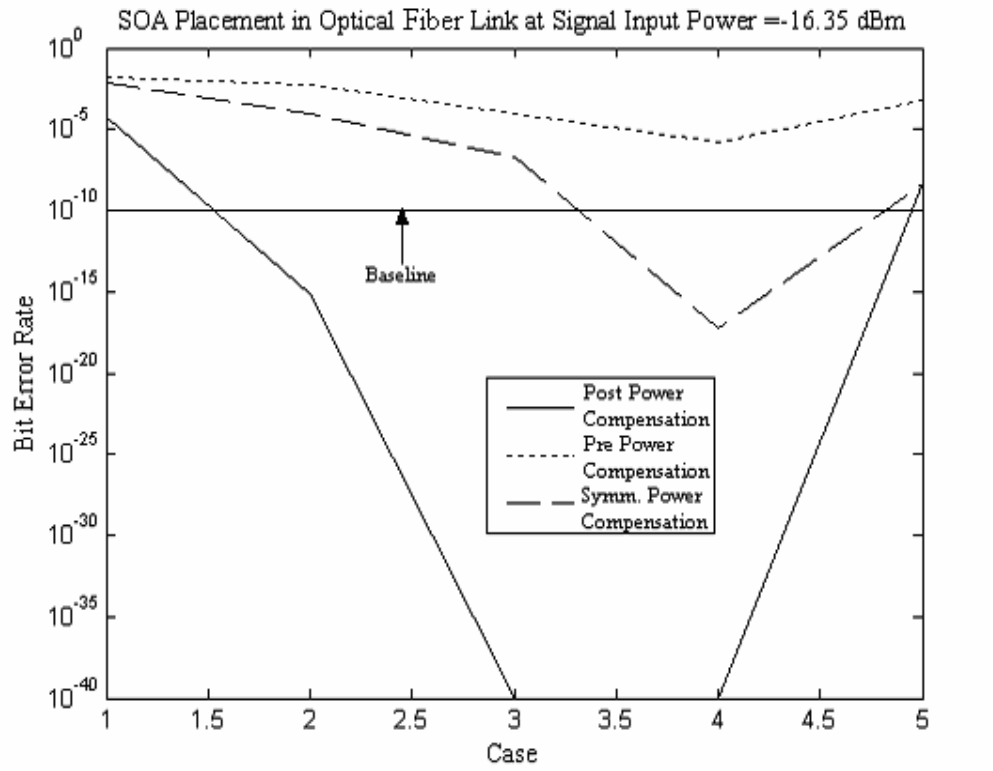

Figure 4.8: Bit error rate for post-, pre- and symmetrical power compensation for different cases indicated in table (4.2).

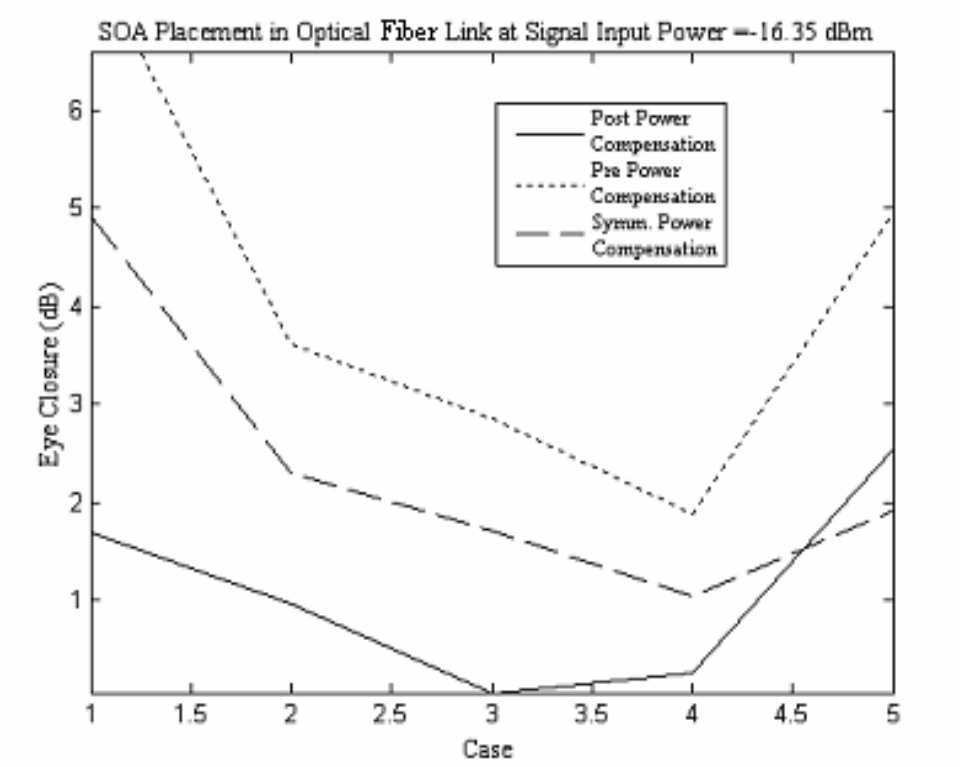

Figure 4.9: Eye closure penalty for post-, pre- and symmetrical power compensation for different cases indicated in table (4.2).

Table 4.2

Different cases for variation of single mode and dispersion compensation fiber for different power compensation methods.

Case	DCF (km)	SMF (km)	Output Power Received in Different Power Compensation Methods (dBm)		
			Post	Pre	Symm.
1	5	30	13.77	6.41	6.96
2	10	60	5.99	-4.59	-3.53
3	15	90	-9.59	-17.09	-15.26
4	20	120	-27.02	-31.88	-28.90
5	25	150	-44.52	-48.62	-44.88

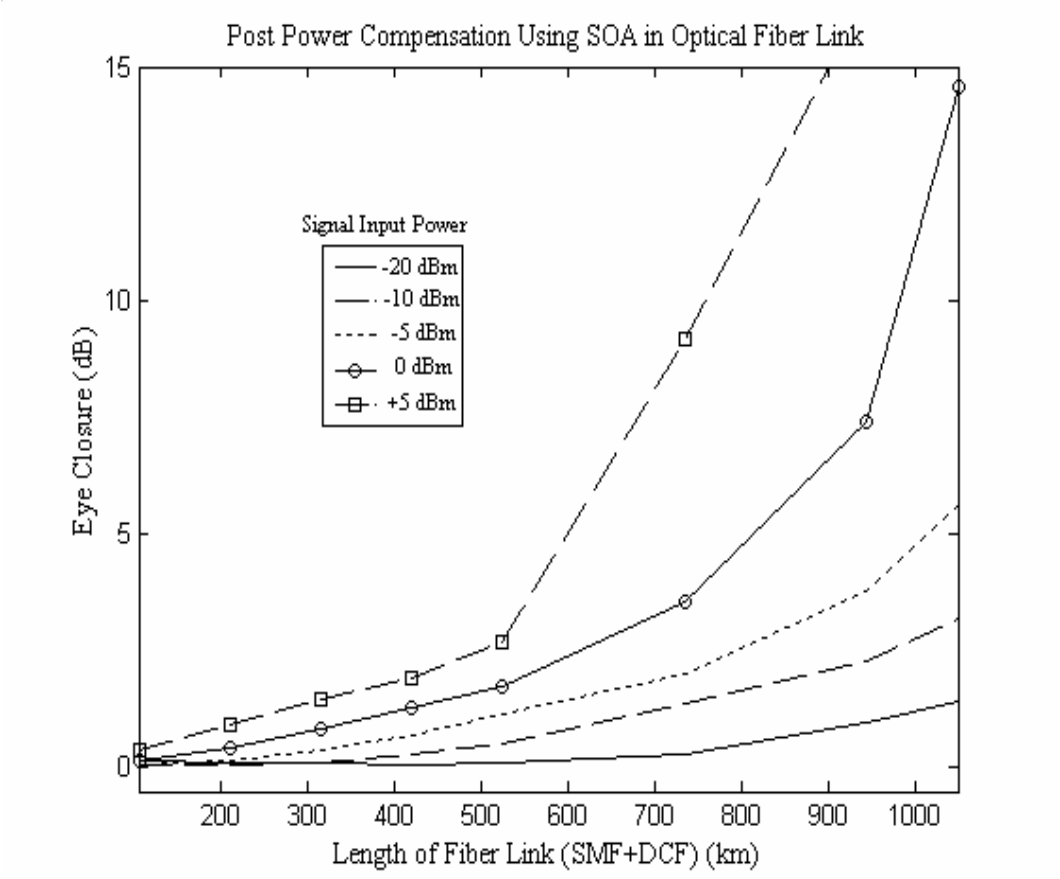

\Figure 4.10: Eye closure penalty as the function of length of fiber link for post power compensation at different signal input powers.

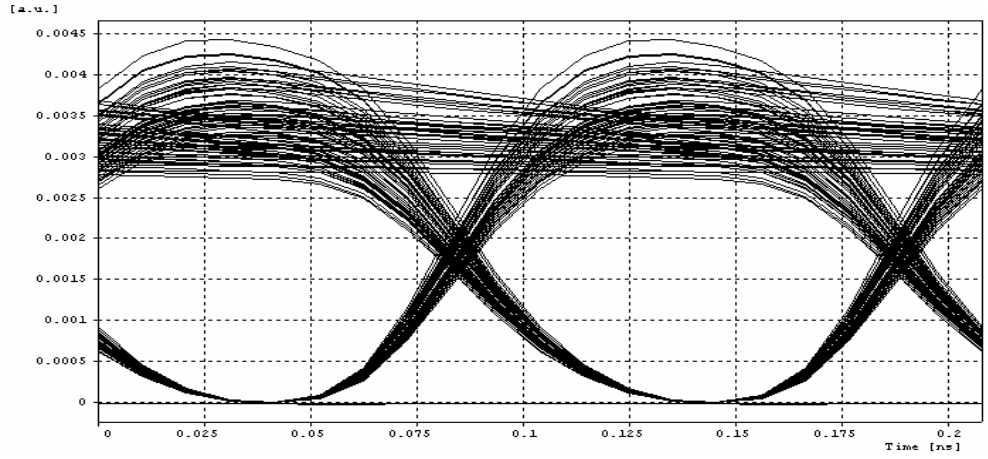

Figure 4.11: Eye diagram for maximum transmission distance of 945 km at -20 dBm signal input power.

For large transmission distance (150 km), the effect of ASE noise power on the SOA degrades the output signal in the 2nd span for post-, pre- and symmetrical-power compensation methods. The same trends are observed in figure (4.9) for the eye closure penalty measurement. It is also observed from table (4.2) that for the post-power compensation method with length of SMF 90 km and the length of DCF 15 km has sufficient power at minimum eye closure penalty.

So this transmission length of SMF and DCF is taken to observe the performance of the post SOA placement for power compensation in the large distance transmission link. For post-power compensation methods, the eye closure penalty is observed for transmission distance at different signal input power applied to laser. As shown in figure (4.10), as the transmission distance and signal input power are increased, the eye closure penalty goes on increasing. Therefore, the placement of the SOA for different transmission distances also depends upon the signal input power. For lower signal input power (< -20 dBm), the effect of ASE noise power will increase eye closure penalty little. But for high signal input power (> 0 dBm), the effect of gain saturation increases the eye closure penalty with increase in spans. At -20 dBm signal input power, the maximum transmission distance of 945 km is observed. This shows improvement over the results reported in [Settembre *et al.*, 1997]. The clear eye diagram is observed in figure (4.11). Hence, post-amplifier placement is best in optical communication system.

4.2 Power Budget Improvement for Long Haul WDM Transmission with Optimum Placement of SOAs

Current efforts of research and development are aimed at increasing the total capacity of medium and long haul optical transmission systems by the use of wavelength division multiplexing. The advances in the optical communications have been possible by the development of efficient and powerful optical amplifiers.

As discussed in section 2.2.1 of the Chapter 2, many researchers reported for longer and unrepeated transmission distances and ultra fast broadband transmission by using SOA. The cross gain saturation of SOA is minimized for WDM transmission links which achieved highest transmission distance up to 4550 km as presented in Chapter 3.

Rottwitt *et al.* [1993] reported the reduction in Q factor up to 4 dB in transmission lines of 9000 km length with signal wavelength 1534 and 1554 nm using EDFAs with bit rate distance product of 55 Gb/s Mm was illustrated. In 1991, experiment reported the

possibility of data transmission over 21000 km at 2.5 Gb/s and over 14300 km at 5 Gb/s [Bergano *et al.*, 1991]. Using EDFAs, the transmission of 10 Gb/s signal over a distance up to 10,000 km over standard fiber with periodic loss and dispersion management was demonstrated [Nakazawa *et al.*, 2000]**.** In 1994, solition was transmitted over 35000 km at 10 Gb/s and 24000 km at 15 Gb/s [Mollenauer, 1994]. Erwan *et al.* [2001] demonstrated 24000 km transmission of dispersion managed solition at 40 Gb/s. In 2001 experiment, broadband DCF, were used to transmit a 1 Tb/s WDM signal over 9000 km [Pincemin *et al.*, 2000]. Due to the large advantage of SOA, it is necessary to utilize the SOA in long haul WDM transmission system.

4.2.1 Characteristics of SOA Model

The behaviour of the SOA model is determined by simulating the SOA in-line amplifier parameter given in section 2.2.2 by using setup as shown in figure (2.1) of the Chapter 2.

The optical gain of the optical amplifier for different input signal powers is measured as shown in figure (4.12). It is found that the polarization sensitivity to the gain at saturation power is 0.108 dB at 1550 nm which is less than [Morito *et al.* 2003]. After saturation power, the polarization sensitivity increases. The variation of the gain is same as that in case [Jennen *et al.*, 2001].

It also determines the characteristics for the SOA in-line amplifier model for two or more channels. So simulations are carried out for the setup as shown in figure (4.13) with two channel DPSK signals without single mode and dispersion shift fiber. The cross talk is calculated as per [Oberg and Olsson, 1998]. The crosstalk of these channels is observed by varying bias current (mA) for different channel spacing as shown in figure (4.14). It is observed that with the increase in bias current the crosstalk increases, which shows good agreement with result reported in [Li *et al.*, 2004]. It is noted that at 400 mA the crosstalk is -7.734 at 100 GHz and -6.9 at 20 GHz, which shows an improvement in the result reported in [Choi *et al.*, 2002]. As this SOA model have longer length. Also higher speed operations can be expected by using the SOA with a longer device length and larger optical confinement factor [Joergensen et *al.*, 1997; Girardin *et al.*, 1998].

4.2.2 10 × 10 Gb/s WDM Signal Transmission over 420 km

The transmission performance of WDM signals is analyzed by using cascaded SOA reported in section 2.2.2 of the Chapter 2. Figure (4.13) shows a schematic setup of 10 × 10 Gb/s WDM system.

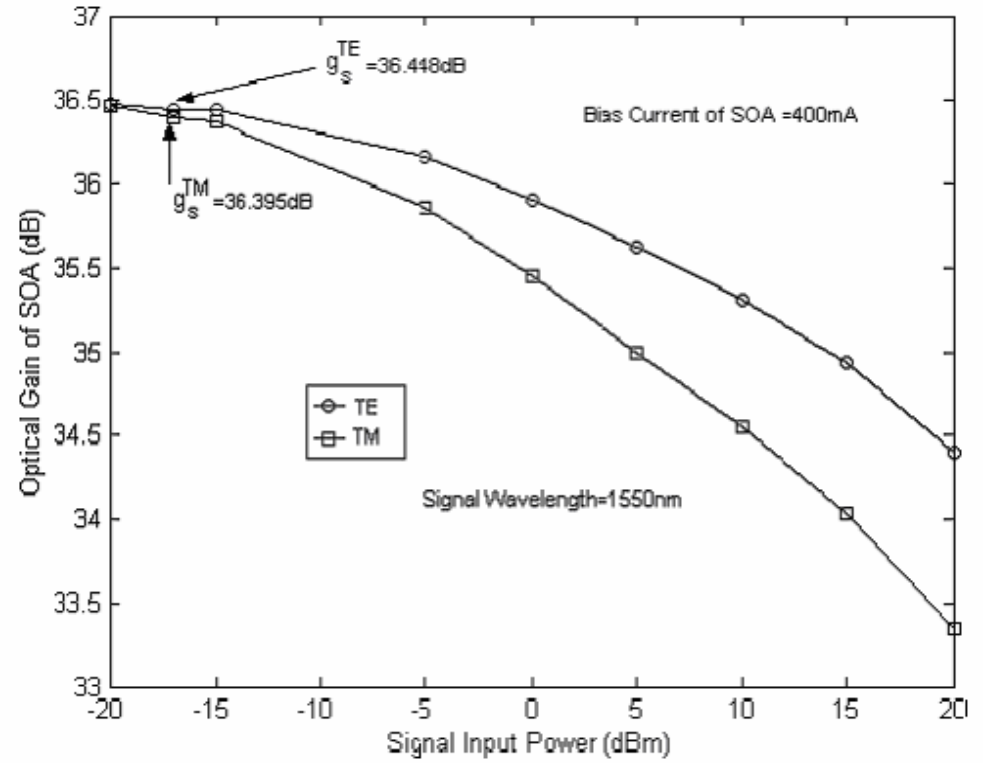

Figure 4.12: Gain of SOA varies with signal input power for 400 mA injection current.

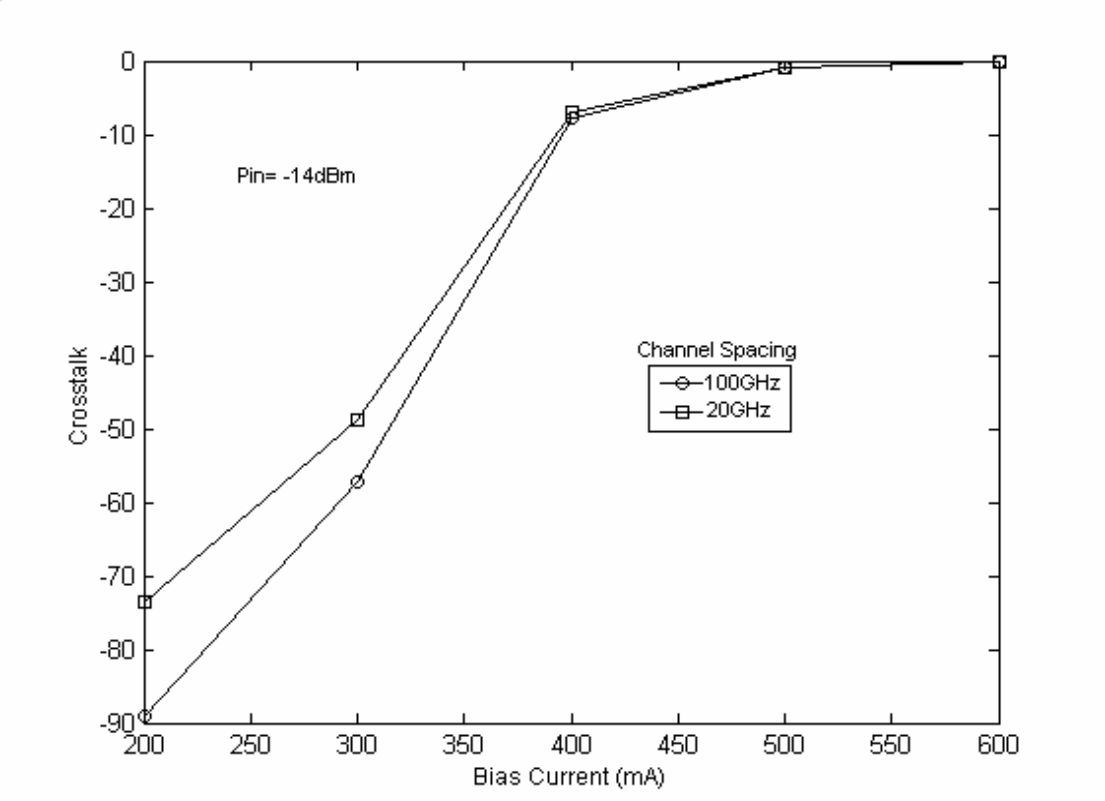

Figure 4.14: Crosstalk as the function of bias current for different channel spacing.

Ten Lorentzian laser sources in the wavelength range 1546 nm to 1554 nm (100 GHz channel spacing) are modulated by each optical $LiNbO_3$ phase modulator with bandwidth 10 GHz for return to zero (RZ) format. The input of each transmission channel is -14 dBm.

Therefore, design carries 100 Gb/s RZ-DPSK WDM signals over 420 km with 70 km SOA spacing. Each of six spans consists of a 60 km standard single mode fiber (SMF), one or more DCF (dispersion compensating fiber) as per [Agrawal, 2002] and a SOA at the end. The DPSK receiver is composed of tunable Mach-Zehnder interferometer having two optical output ports. The optical path difference of interferometer is set to one bit time duration. Each output of interferometer is detected by ideal PIN photodetector. The output electrical signal is the difference between detected currents. The simulations have been carried out for this setup as shown in figure (4.13) for 6 spans (420 km). the dependence of Q factor on signal input power is measured for different optical filters as shown in figure (4.15).

With the increase in signal input power, the quality of the signal goes on decreasing because of gain saturation as saturation power is -16.7 dBm for the SOA model. This tendency is almost same as in the case of NRZ signal format [Geraghty *et al*., 1997]. It is also observed that with the decrease in the optical filter bandwidth the Q factor goes on increasing up to 0.4 nm optical filter bandwidth and then goes on decreasing. The optimum 3 dB bandwidth for optical filter is observed as 0.4 nm and this bandwidth is used for higher transmission. Further, if the channel spacing is decreased from 100 GHz to 20 GHz as shown in the figure (4.16), the quality of channel no. 5 goes on decreasing. This is due to the increase in the crosstalk among the channels as result is already obtained in figure (4.16) This shows a good agreement with the results [Choi *et al.*, 2002; Li *et al*., 2004].

The results are shown in the figure (4.17) for on-off keying (OOK) system and DPSK system at 420 km transmission distance for channel no. 5. The bit error rate (BER) of DPSK receiver is given as

$$BER = \frac{1}{2}\exp\left(-\eta N_p\right) \tag{6.1}$$

Where η is the quantum efficiency of PIN photodetector and N_p is the number of photons per bit. For η =1, a BER of 10^{-9} or Q factor = 6 dB is obtained for N_p = 20. The BER goes on decreasing as we increase the input signal power.

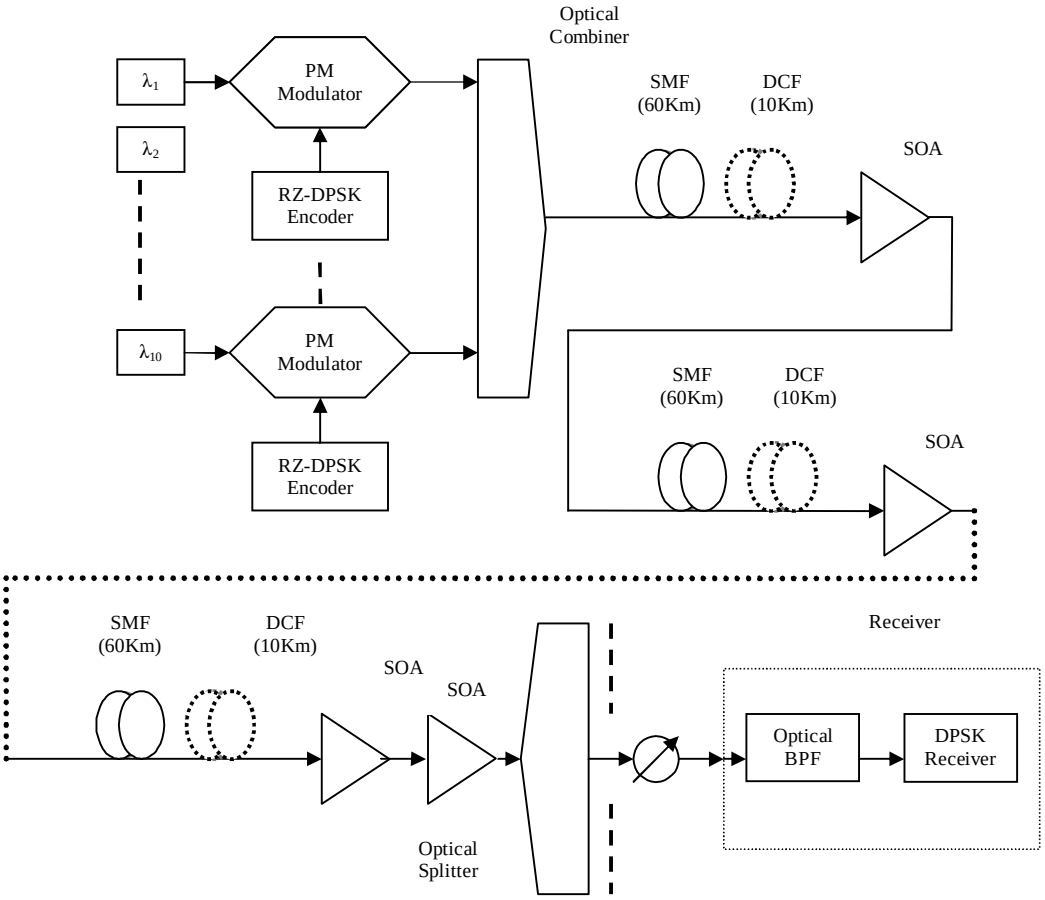

Figure 4.13: Schematic of transmission system of 10 × 10 Gb/s WDM signals.

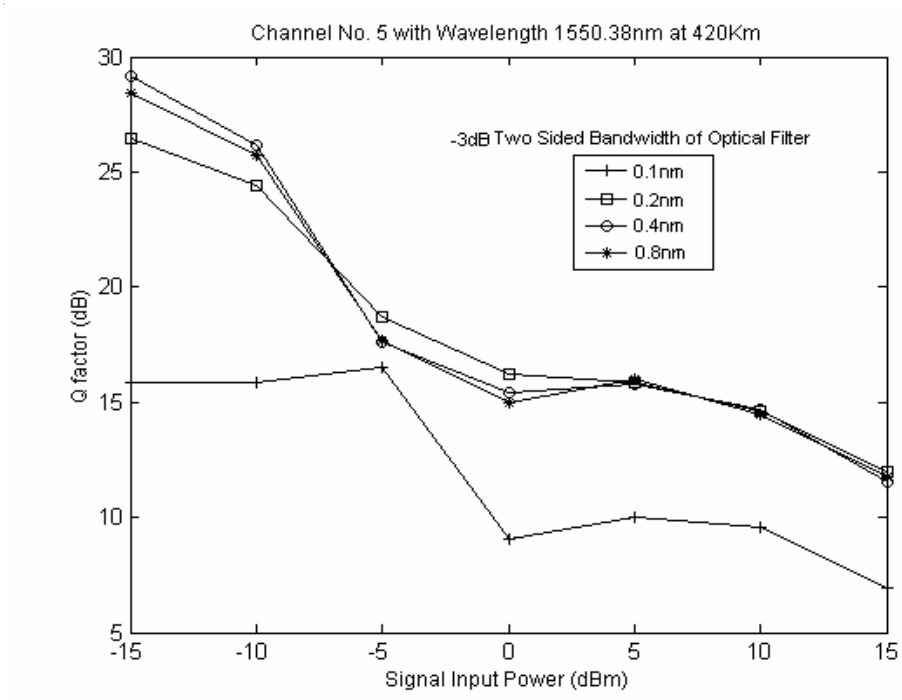

Figure 4.15: Q factor variations with signal input power for different bandwidth of optical filter.

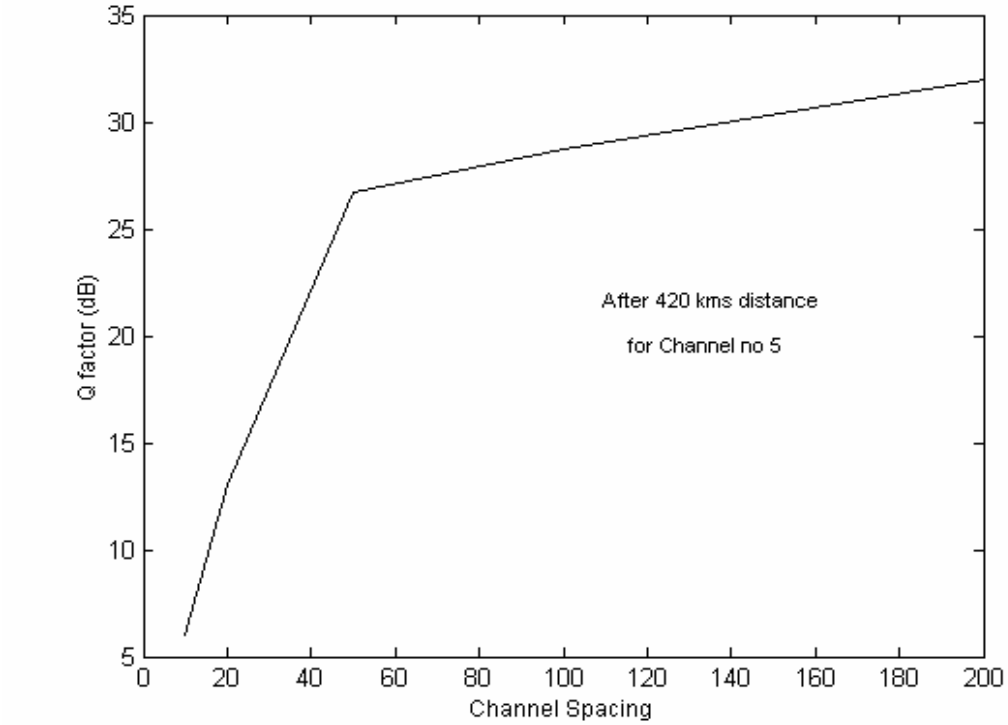

Figure 4.16: Quality factor varies with channel spacing.

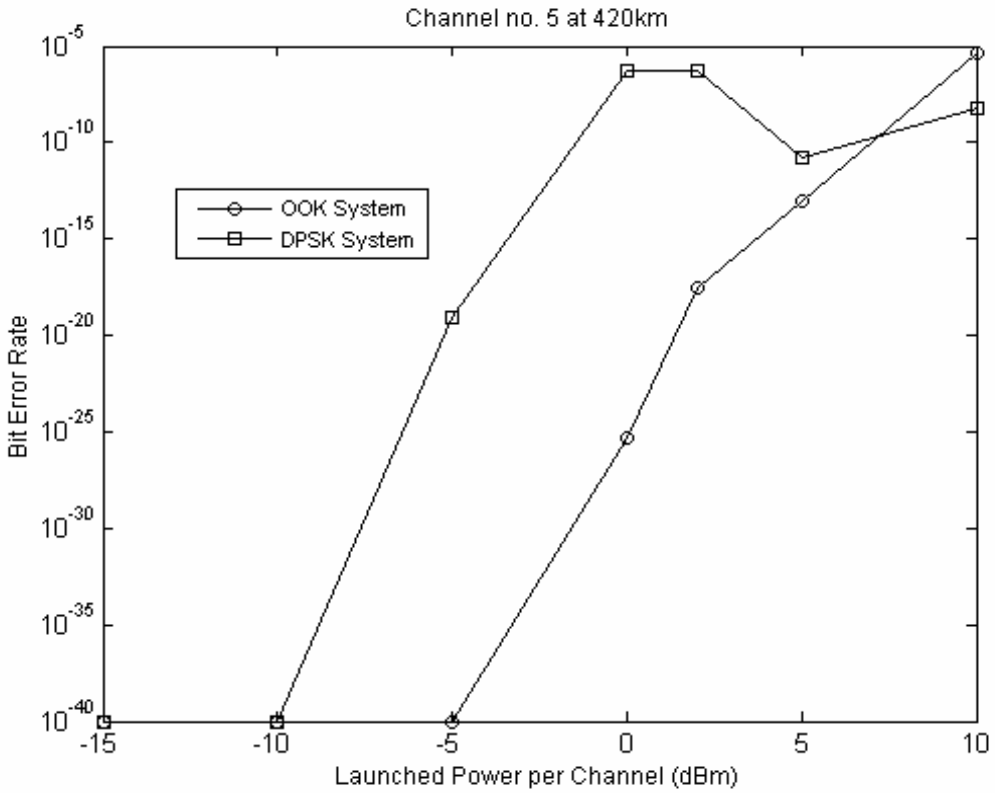

Figure 4.17: BER as the function of signal input power for different systems.

The launched power per channel is successfully received in the OOK system with the BER ground of 10^{-9}, but quality of signal in the DPSK system falls at 0 dBm and 2 dBm. So, by using our SOA in-line amplifier model, there is successful transmission of signal through SMF without using any dispersion management scheme [Xu *et al.*, 2004].

4.2.3 10 × 10 Gb/s WDM Signal Transmission over Higher Distance

For the long haul transmission distance, same setup is used as shown in the figure (4.13). There are different strategies used for long distance transmission for placement of the optimized SOAs. For the transmission distance 17227 km, there are 246 spans and additional fiber is used as shown in the figure (4.18) which is called conventional span scheme. Each of 246 spans consist of a same 60 km SMF, 10 km DCF and a SOA at the end.

Another better scheme is obtained for the same transmission distance called equal span scheme as shown in the figure (4.19). For this, an additional SOA is used to compensate the degradation after 20 spans with each span of 60 km SMF +10 km DCF+1 SOA.

The optimum span scheme is formed for power improvement at the output of 17227 km transmission link. In this, there is a SOA used after optimum spans. For this, the optimum spans are set 61, 50, 40, 31, 23, 16, 11, 7, 4, 2, and 1 and after every optimum span a, SOA is used again as shown in figure (4.20).

For every SOA used in different scheme, the gain is taken after reduction of ASE noise power as given [Mynbaev and Scheiner, 2004]:

$$g = \frac{P_{out} - P_{ASE}}{P_{in}} \tag{6.2}$$

If P_{in} varies from -15 dBm to +5 dBm then the ASE noise power P_{ASE} varies from 210 μW to 35 μW. So the actual gain 36.5 dB changes according to ASE noise power.

Due to power improvement in optimum span scheme, the quality of signal decreases. So an optimum span scheme-1 is described by showing figure (4.20). In this, the last SOA after 1 span is not used as in the optimum span scheme. In another optimum span scheme-2, where last SOA after 1 span and SOA pre-amplifier are not used. The simulations have been carried out for the different span schemes used between DPSK transmitter and receiver for 10 channels at 10 Gb/s at 100 GHz channel spacing.

The variation of optical power received with wavelength for different span schemes are investigated as shown in the figure (4.21). In first span, input is -14 dBm and amplification factor is 15 dB approximately.

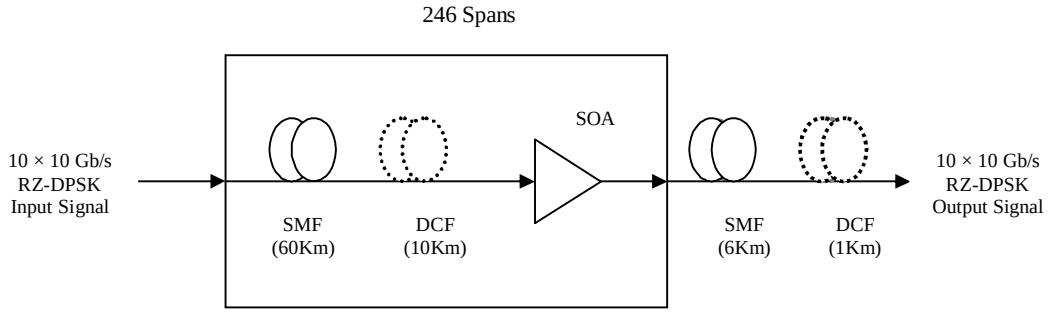

Figure 4.18: Schematic diagram of conventional span scheme for transmission distance 17227 km.

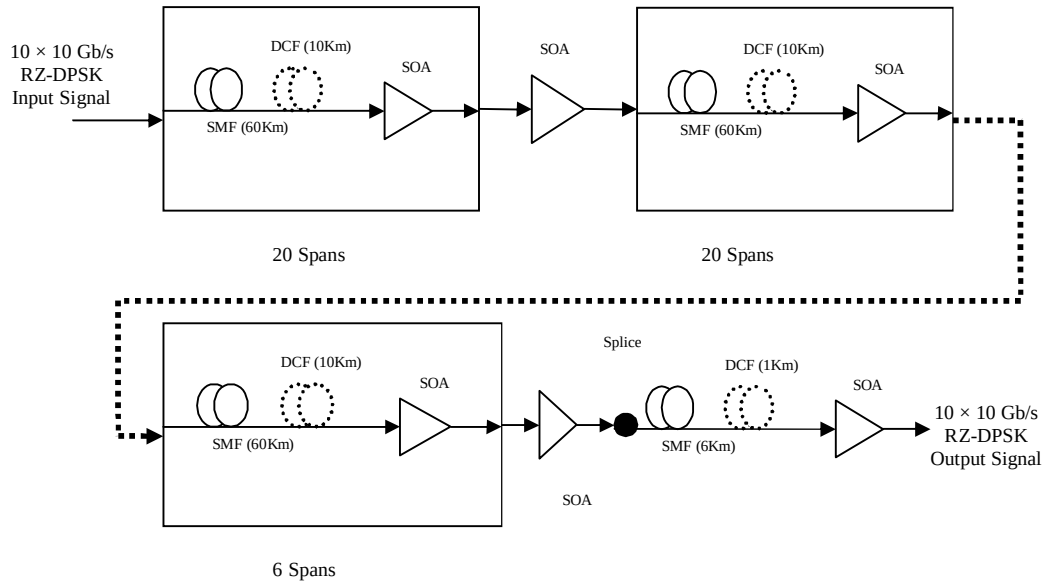

Figure 4.19: Schematic diagram of equal span scheme for transmission distance 17227 km.

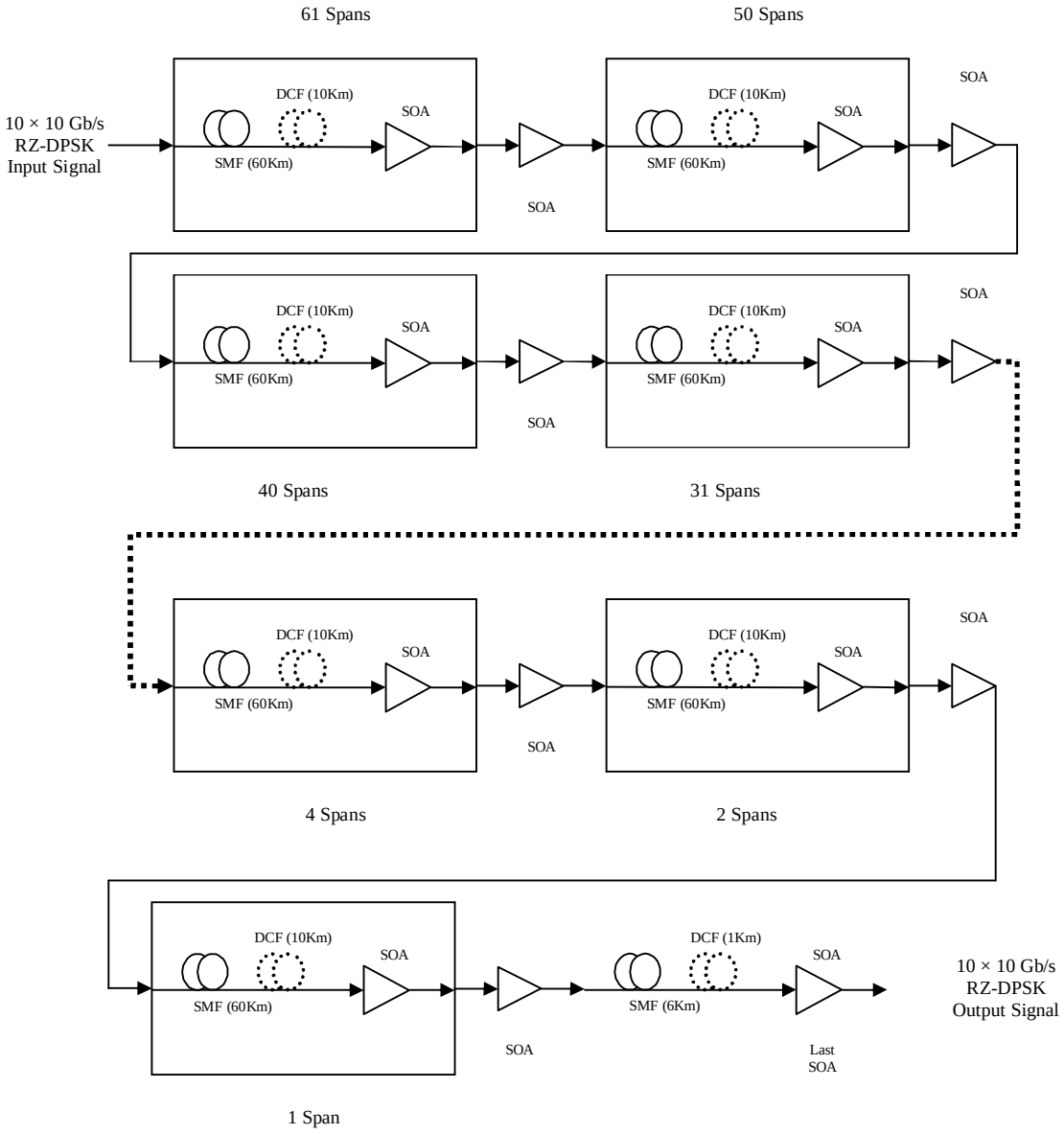

Figure 4.20: Schematic diagram of optimum span scheme for transmission distance 17227 km.

Also SMF and DCF loss is 19.5 dB. So output signal drops with small decrease in quality. In conventional span scheme for transmission distance 17227 km, the power observed is less than -100 dBm, even the quality of signal is good as shown in figure (4.22). For equal span scheme, we observe that good signal power is received at the output but the Q factor is less than 15 dB for most of the channels.

The investigation is also carried out for the optimum span scheme; the power observed at the output is high as compared to the input power. For 17227 km, this scheme shows good quality factor, even with large improvement in the power. Similarly, the optimum span scheme-1 shows less power improvement of 2 dB approximately with good quality. But optimum span scheme-2 has large power drop from baseline curve (input power) even at good Q factor. So a comparison is made as in table (4.3) showing improvement of transmission distance as compared to 8 × 10 Gb/s WDM signal transmission [Li *et al.*, 2004].

From above, it is observed that the optimum span scheme and optimum span scheme-1 are good for further transmission. For higher transmission distance, the same optimum span scheme is repeated 2, 3 and 4 times to achieve the transmission distance of 34454 km, 51681 km and 68908 km respectively. The optimum span scheme-1 is further repeated as shown in figure (4.23). As shown in figure (4.23), the optimum span scheme-1 is repeated for 3 spans and is applied to the SOA. The SOA output is fed to single span of optimum spam scheme-1 to achieve the transmission distance of 68908 km. The same idea is used for optimum span scheme, but there is decrease in quality of signal as simulation is carried out.

It is investigated that the Q penalty is increased with increase in transmission distance for optimum span scheme. It means quality of signal decreases due to increase in the power as illustrated in figure (4.24) and (4.25). As the power increases, the SOAs lead toward the saturation. At transmission distance of 68908 km, the quality of signal is less than 14 dB for a channel at power 0.87 dBm for optimum span scheme.

The eye diagram for optimum span scheme after 68908 km with P_{out} = 0.817 dBm for channel no. 5 is shown in figure (4.26). The optical spectrum of ten channels for input signal and output signal power after transmission distance 68908 km is shown in the figure (4.29).

It is also investigated that the optimum span scheme-1 has high quality factor of 25.8 dB but low output power of -38.5 dBm is obtained, which can be improved by putting one SOA after this scheme easily.

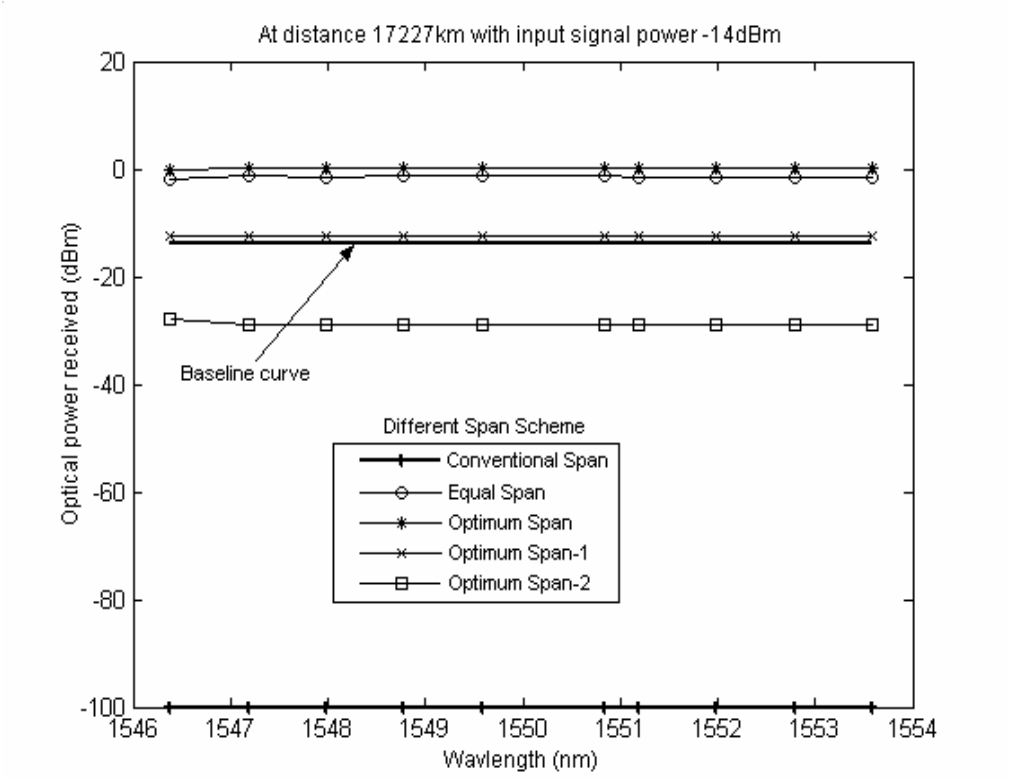

Figure 4.21: Optical power received versus different channels for different span schemes.

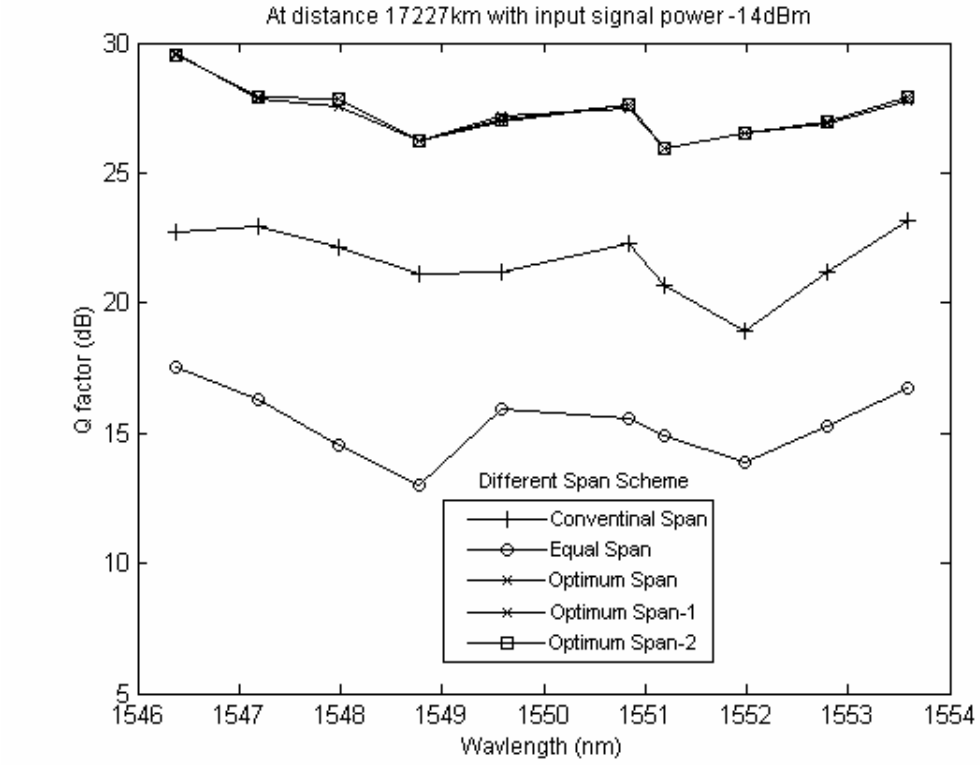

Figure 4.22: Q factor versus channels at different wavelength for different span schemes.

Table 4.3

At transmission distance 17227 km with input power P_{in}= -14 dBm.

Parameters	Conventional span scheme	Equal span scheme	Optimum span scheme	Optimum span scheme-1
No. of SOA used	246	260	258	257
Minimum Q factor	22.3 dB	15.6 dB	27.5 dB	27.6 dB
Power per channel	less than -100 dBm	-1.32 dBm	0.097 dBm	-12.5 dBm
Power Penalty	More than 86 dB	-12.68 dBm	-14.097 dBm	-1.5 dBm

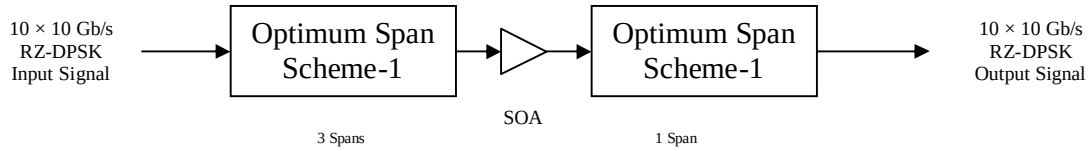

Figure 4.23: Schematic diagram of optimum span scheme-1 for transmission distance 68908 km.

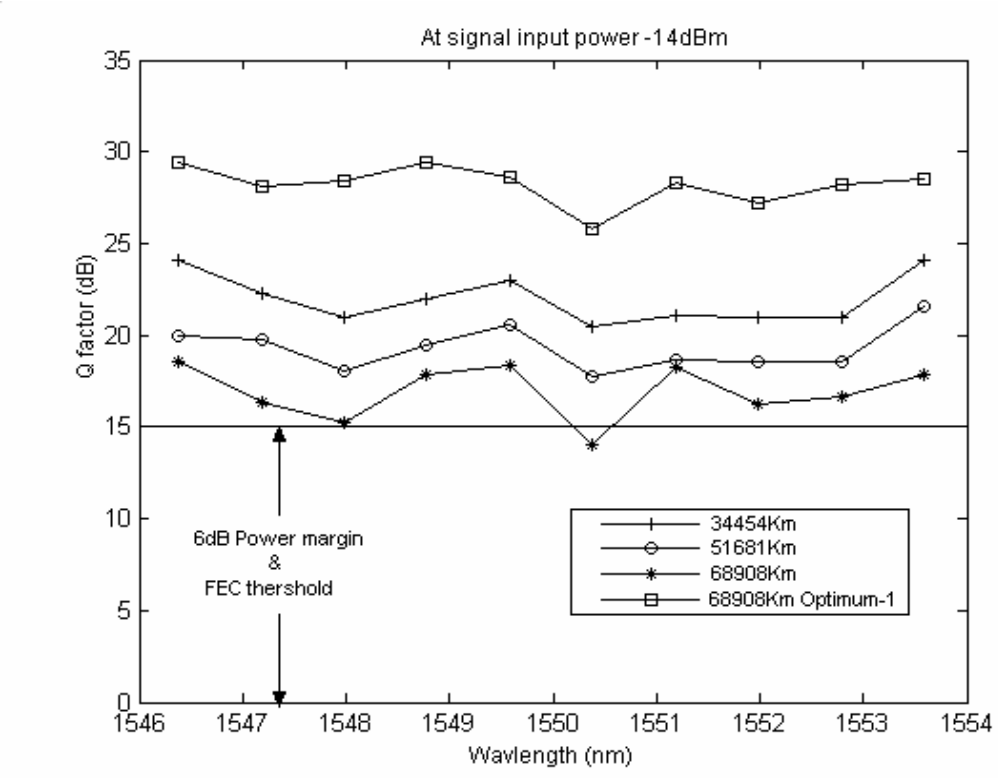

Figure 4.24: Q factor variations with channels for different transmission distances.

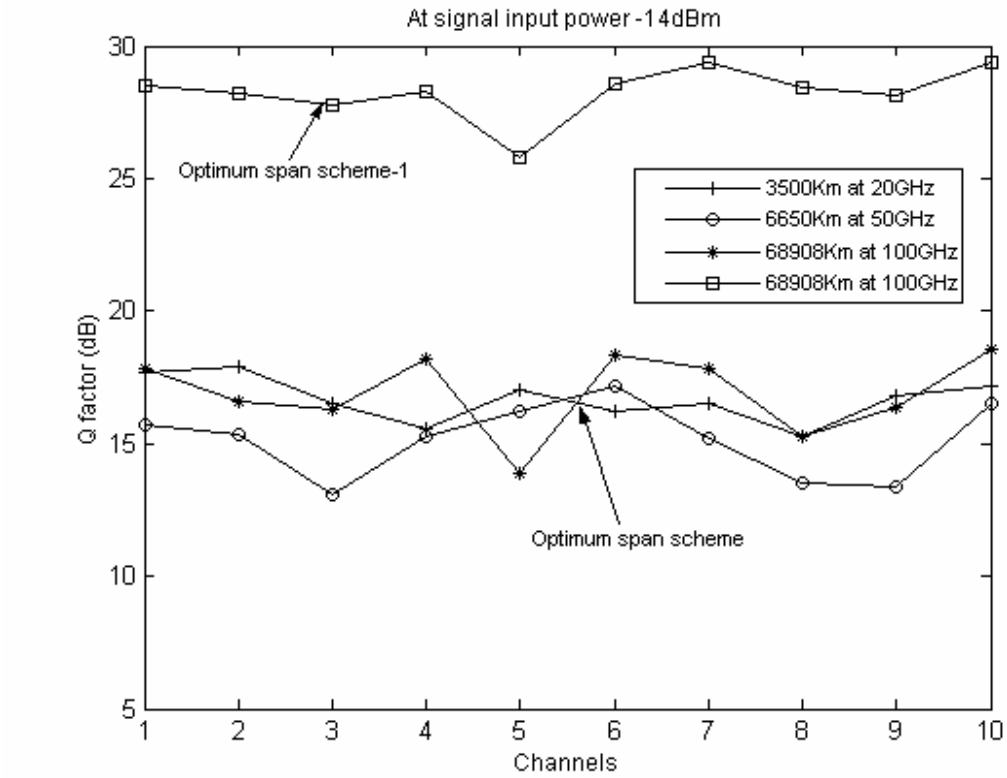

Figure 4.25: Q factor versus channels for different channel spacing.

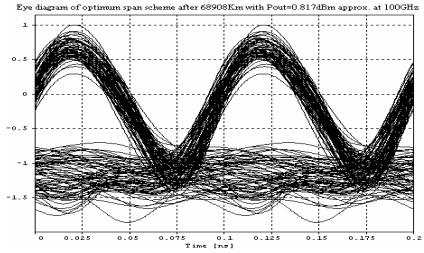

Figure 4.26: Eye diagram using optimum span scheme at 100 GHz.

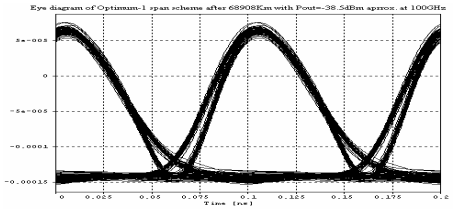

Figure 4.27: Eye diagram using optimum span scheme.

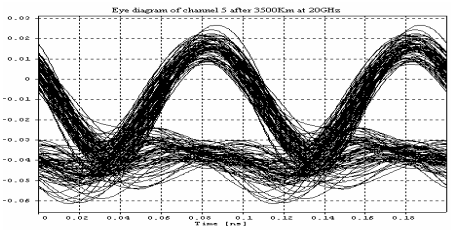

Figure 4.28: Eye diagram using optimum span scheme at 20 GHz.

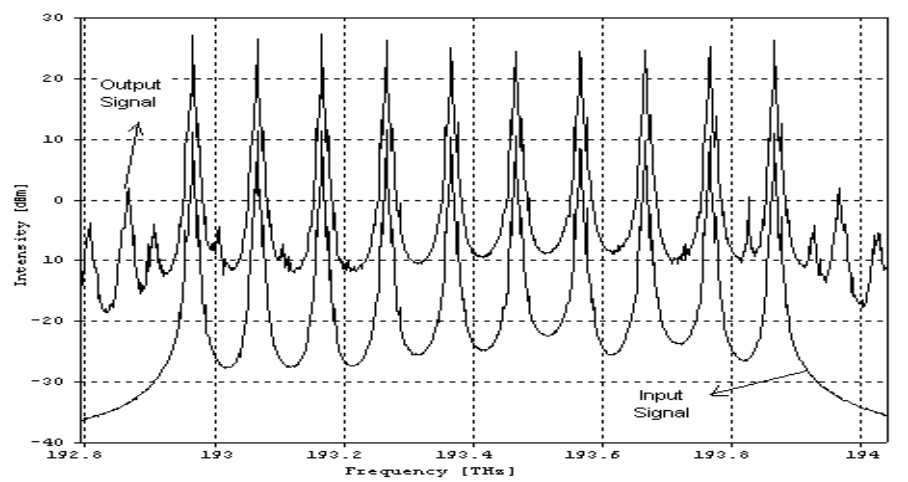

Figure 4.29: Optical spectrum for different channels before and after transmission distance 68908 km using optimum span scheme.

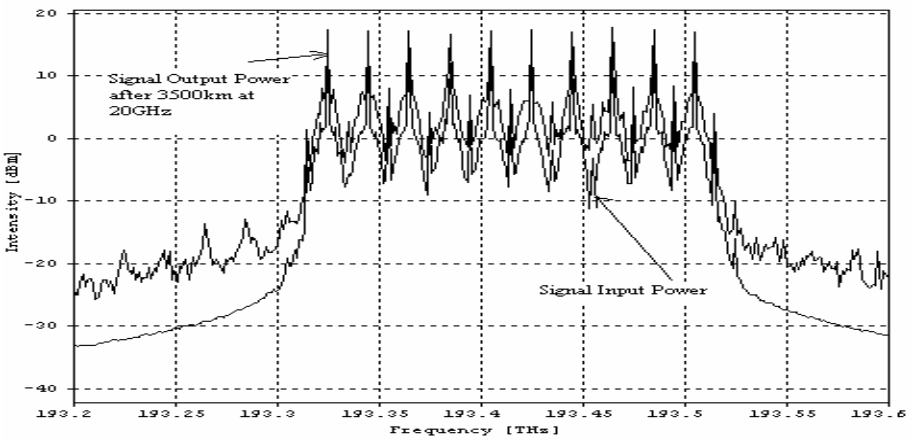

Figure 4.30: Optical spectrum for ten channels at different frequency before and after transmission distance 3500 km.

Table 4.4

Power budget for 68908 km transmission distance.

Parameters	**Optimum span scheme**	**Optimum span scheme-1**
Launched power	-14 dBm	-14 dBm
Fiber loss	17227 dB	17227 dB
Maximum Redundant Amplifier gain	37704.5 dB	37595 dB
Input and output insertion loss	6222 dB	6204 dB
Receiver sensitivity	0.87 dBm	-38.5 dBm
Power Penalty	-14.87 dB	24.5 dB
Margin	-14.87 dB	24.5 dB

The clear eye diagram is observed for the distance covering after 68908 km with P_{out} = -38.5 dBm as shown in figure (4.27). The bit rate-distance product is 6890.8 Tb/s km.

The system is further investigated for 20 GHz, 50 GHz channel spacing for the same SOA in-line amplifier model in the same setup as shown in the figure (4.13) for the optimum span scheme. The reasonable Q factor is obtained with large power improvement of 4.59 dBm per channel for transmission distance of 6650 km at 50 GHz. It is also observed that the reasonable quality of signal after covering distance 3500 km at 20 GHz with power improvement of 4.4 dBm, which is an improvement over [Spiekman *et al.*, 2000]. The eye diagram for channel no.5 after the distance 3500 km is shown in figure (4.28). Figure (4.30) shows optical spectrum of the ten channel signal before and after 3500 km transmission, which is same as in [Li *et al.*, 2004] even at lower channel spacing.

The comparison chart for power budget of 68908 km transmission distance for optimum span scheme and optimum span scheme-1 is given in table (4.4), which shows different power penalty and margin. The actual gain in different schemes is less than maximum redundant gain. As from [Mynbaev and Scheiner, 2004], the ASE noise is not redundant. The further optimization of SOA is possible for increasing the transmission distance.

4.3 Simulation of DWDM Signals Using Optimum Span Scheme with Cascaded Optimized SOAs

Dense wavelength division multiplexing utilizes a large aggregate bandwidth in a single fiber by taking the advantage of the advanced optical technology that is able to launch and multiplex many wavelength in one fiber, switch wavelength optically and at receiving end, demultiplex and read each wavelength separately [Kartalopoulos, 2000]. DWDM is a technology that depends mainly on optical components i.e. amplifiers, multiplexers, filters, transmitter and receiver array.

Cho *et al.* [2003] demonstrated the transmission of 25 Gb/s RZ-DQPSK signals over 1,000 km of SMF-28 fiber with channel spacing 25 GHz. Uptill now, many researchers provided solutions for increased transmission distance and capacity with utilization of SOAs reported in Chapter 2, 3, 4. which investigates that the twenty-channel at 10 Gb/s WDM transmission over 4340 km by using SOA as in-line and pre-amplifier with DPSK modulation format at 100 GHz channel spacing. But no previous research has been reported with channel spacing less than 25 GHz for optical transmission with SOA.

4.3.1 Minimization of Crosstalk in System with SOA Model

The InGaAlAs traveling wave SOA with negligible residual facet reflectivity as reported in the section 2.2.2 of the Chapter 2 is taken as the amplifier model in our simulations. The characteristic for our SOA in-line amplifier model has been determined for two or more channels at channel spacing 20 GHz. So the simulations are carried out for setup as shown in figure (4.13) with two channel DPSK signal without using single mode and dispersion shift fiber. The crosstalk of these channels is measured by varying bias current (mA) for different channel spacing and different optical phase modulator bandwidth as shown in figure (4.31). It is observed that with the increase in bias current the crosstalk increases, which shows good agreement with the above analysis and previous results [Choi *et al*., 2002]. It is noted that at 400 mA, the crosstalk is -14.1 dB at 20 GHz which shows an improvement over the result reported in [Choi *et al*., 2002].

The optical phase modulator bandwidth is also optimized as shown in figure (4.31). At optimum bias current, low crosstalk and optimum bandwidth is obtained for optical phase modulator *i.e*. 5.5 GHz as shown in figure (4.31).

4.3.2 10 × 10 Gb/s DWDM Signal Transmission

The transmission performance of DWDM signals is analyzed by using cascaded SOAs. Figure (4.13) shows a schematic diagram of 10 × 10 Gb/s DWDM system. Ten Lorentzian laser sources in the wavelength ranging from 1549.91nm to 1550.06 nm (20 GHz channel spacing) are modulated by each optical $LiNbO_3$ phase modulator with return to zero (RZ) format. The operating wavelength for transmission link had ITU standard wavelengths. The optimized bandwidth for optical phase modulator ($LiNbO_3$) is used. For SOA, 400 mA is the optimized current.

From simulation results shown in figure (4.31), the optimum bandwidth for phase modulator is 5.5 GHz at 400 mA bias current with crosstalk less than -14 dB between two channels. The input power of each transmission channel is -20 dBm. Therefore, design carries 100 Gb/s DWDM RZ signals over 70 km with SOA at the end. It consists of a 60 km standard single mode fiber (SMF), one or more DCF (dispersion compensating fiber) and a SOA at the end. The length of DCF is chosen in accordance to the [Agrawal, 2002] for complete compensation. The time domain simulations have been carried out for this setting as shown in figure (4.13).

The Q factor variation with all the channels has been measured for 70 km transmission with and without use of end SOA as shown in figure (4.32).

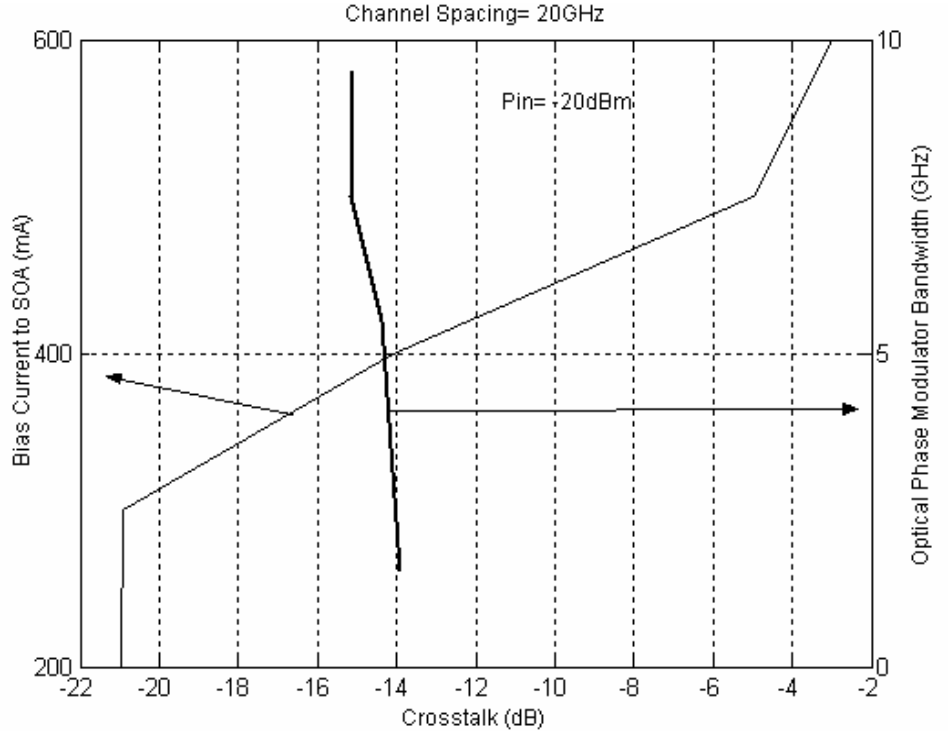

Figure 4.31: Crosstalk as function of bias current and optical phase modulator bandwidth.

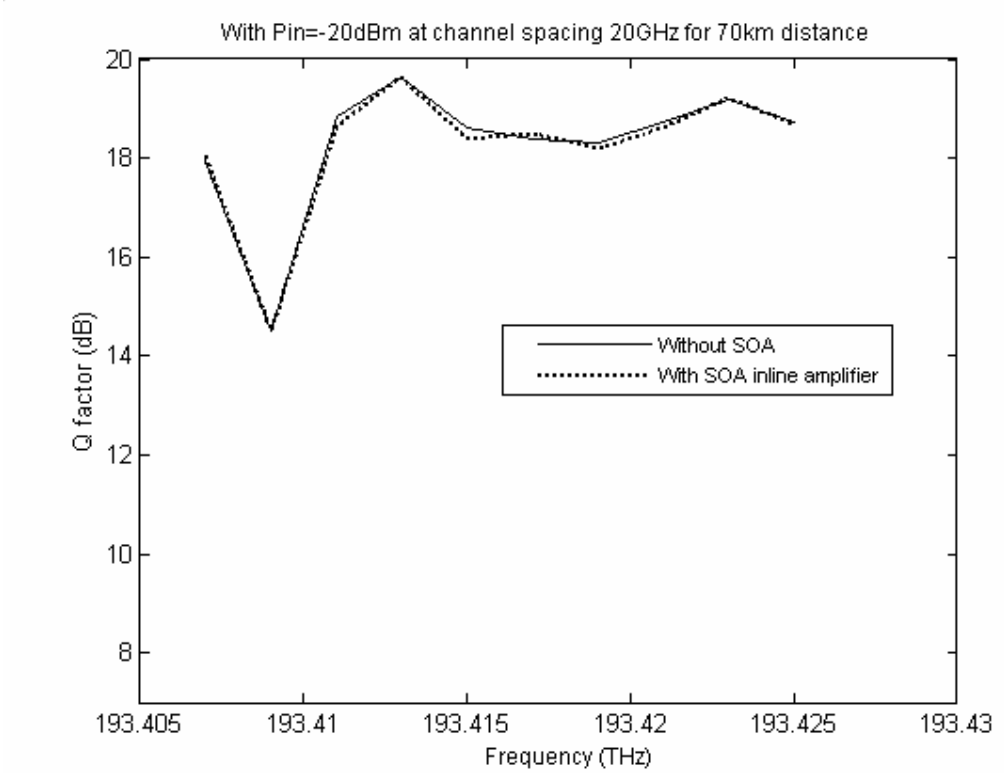

Figure 4.32: Received quality for different channel as a function of with and without SOA.

Figure (4.33) shows the optical power received, for different channels for 70 km transmission distance with and without using SOA. A large power drop occurs more than 15 dB without using any amplifier. When using SOA as in-line amplifier after 70 km fiber, there is improvement in power around 1dB from input power. While SOA used as in-line and pre-amplifier, shows large improvement of output power more than 15 dB at same quality.

4.3.3 10 × 10 Gb/s WDM Signal Transmission over Higher Distance

For the long haul transmission distance, the same setup is used as shown in figure (4.13). There are different transmission schemes used for long distance transmission. For the transmission distance 5670 km, there are 81 spans and additional fiber is used as shown in figure (4.34a) which is called conventional span scheme. Each of 81 spans consist of a same 60 km SMF, 10 km DCF and a SOA at the end.

There is another best scheme obtained for the same transmission distance called equal span scheme as shown in figure (4.34b). For this, an additional SOA is used to compensate the power degradation after 20 spans with each span 60 km SMF +10 km DCF+1 SOA.

The optimum span scheme has also been made for power improvement at the output of 5670 km. In this SOA is used after every optimum span. For transmission distance of 5670 km, the optimum spans are 31, 23, 16, and 11 as shown in figure (4.34c).

In conventional span scheme, the received power falls due to attenuation in the transmission path, even distortion can be managed. So, for long distance transmission, there is continuous fall in received power from the applied input, even in the path SOA can boost up the power after equal distance. As from figure (4.34d), for longer cascaded distance.

$$P_{in1} < P_{in} \tag{6.3}$$

$$P_{in} < P_s \tag{6.4}$$

$$P_{inN} < P_{ini} < P_{in2} < P_{in1} < P_{in} < P_s \tag{6.5}$$

As from above equations, amplifiers input goes on decreasing, this causes decrease in distortion due to nonlinearity and amplified spontaneous emission (ASE) noise, which is true as shown in figure (2.3) of Chapter 2. So, large power penalty occurs due to longer transmission distance. The equal span scheme is acceptable for larger distance transmission compared to conventional span scheme but there is OSNR (Optical signal to

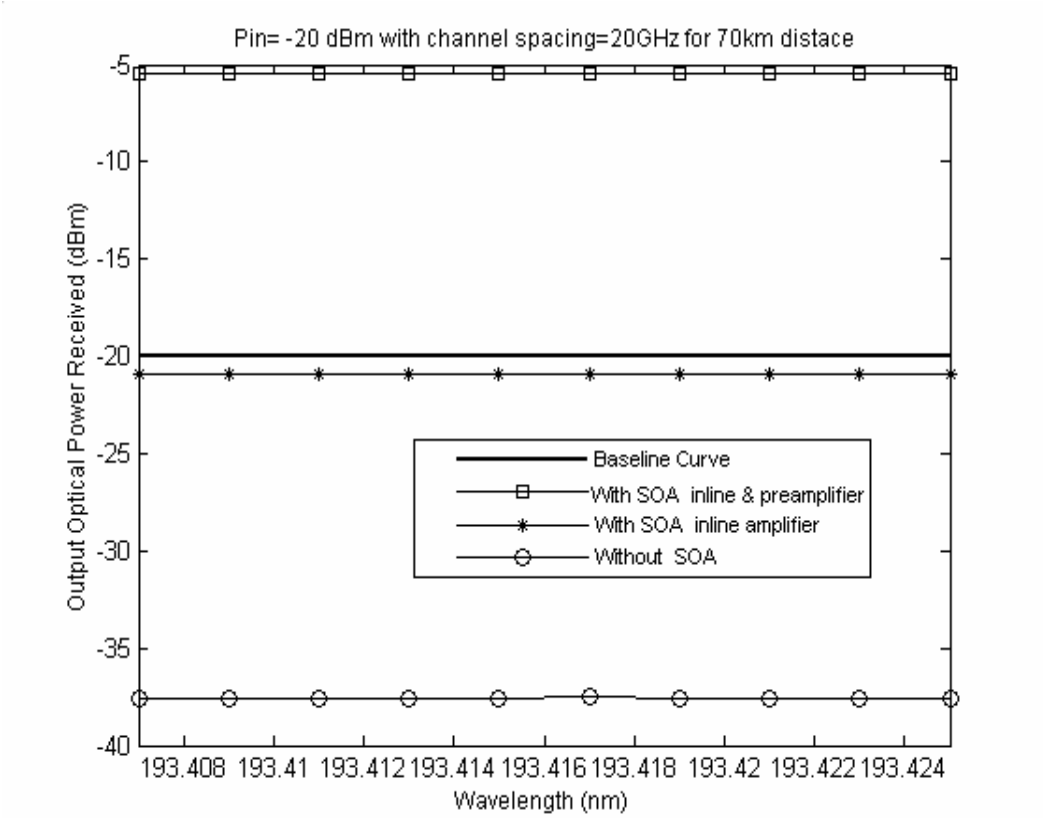

Figure 4.33: Received optical power for different channel as a function of with and without SOA.

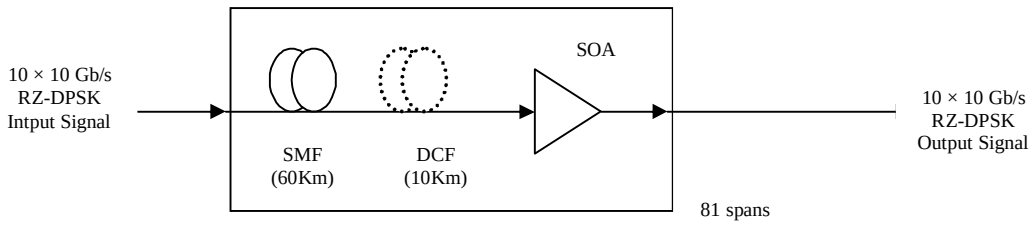

Figure 4.34a: Schematic of conventional span scheme for transmission distance 5670 km.

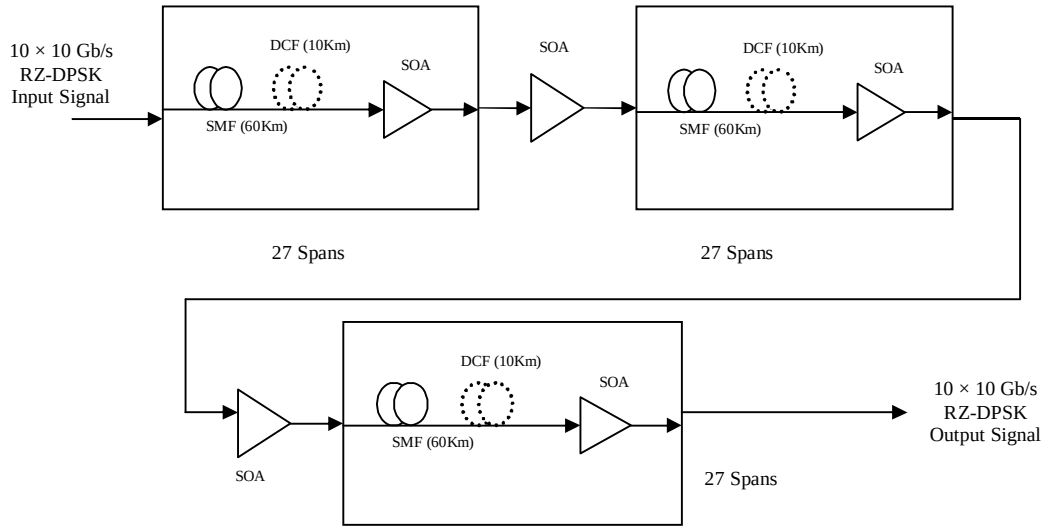

Figure 4.34b: Schematic of equal span scheme for transmission distance 5670 km.

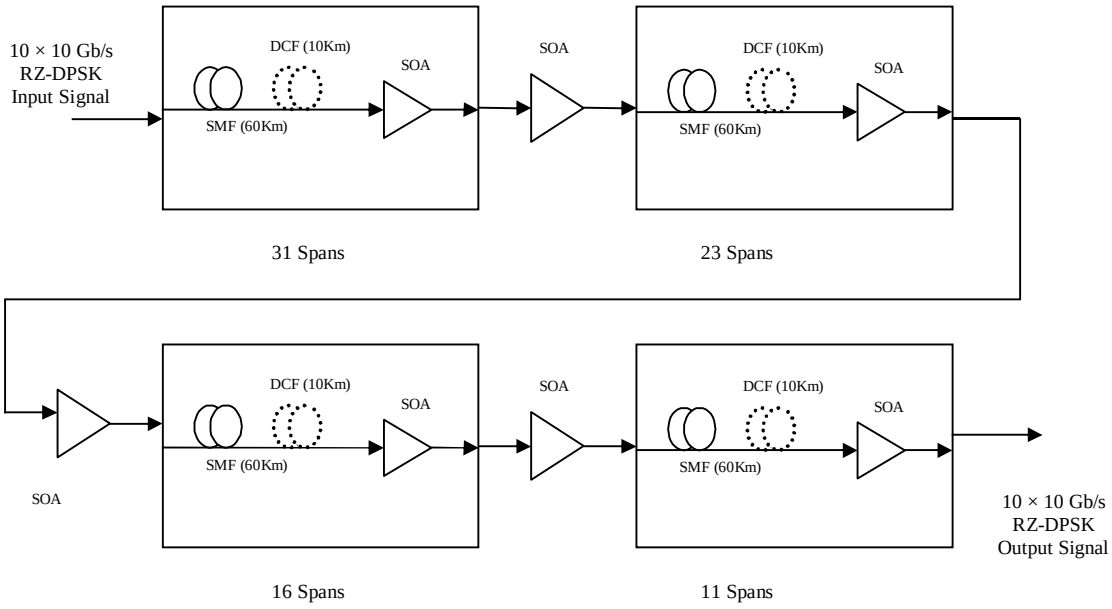

Figure 4.34c: Schematic of optimum span scheme for transmission distance 5670 km.

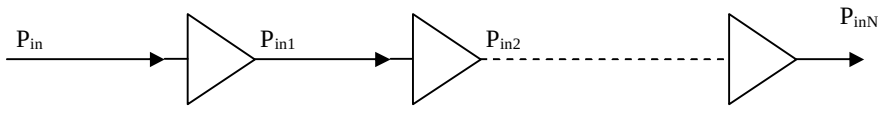

Figure 4.34d: Equivalent schematic of conventional span scheme.

noise ratio) penalty occurs. Degradation occurs due to continuous rise in ASE for equal span. For this scheme we obtain still obtain

$$P_{inN} < P_{in} < P_s \tag{6.6}$$

In optimum span scheme, large span is used in the start and then span decreases. This scheme is formed in such a manner so that each input of SOA is less than saturation power, so that good quality signal is obtained after SOA. Here

$$P_{inN} \geq P_s > P_{in} \tag{6.7}$$

It is also found from above, the ASE power at the output of different span scheme

$$P_{ASEconventional} < P_{ASEOptimum} < P_{ASEEqual}$$

Also found that power penalty varies for different scheme

$$P_{Optimum} < P_{Equal} < P_{Conventional}$$

Where $P_{ASEconventional}$, $P_{ASEEqual}$, $P_{ASEOptimum}$ are the ASE power of conventional, equal and optimum span scheme respectively. Also $P_{Optimum}$, P_{Equal}, $P_{Conventional}$ are the power penalty for optimum, equal and conventional span scheme.

The simulations have been carried out for the different span schemes used which is between DPSK transmitter and receiver for 10 channels at 10 Gb/s at 20 GHz channel spacing as shown in figure (4.13). The simulation results for 5670 km transmission distance for different scheme as shown in figure (4.35). The received power for optimum span is much higher than conventional and equal span after 5670 km distance.

It is observed from figure (4.36) that the OSNR for optimum and equal span scheme are almost the same. So in optimum span, power improvement and good OSNR is observed. The variation of optical power received with wavelength for different span schemes is also investigated as shown in figure (4.37). In conventional span scheme low power of -73 dBm is observed. The quality of signal for some channel is less than 15 dB as shown in figure (4.38). For equal span scheme, it is observed that around -40 dBm signal power is received at the output, but Q factor is less than 15 dB for some channels.

The investigation made for the optimum span scheme show that the power improvements observed at output by factor 1.8 dB approximately as compared to input power for transmission distance 5670 km with good quality more than 15 dB for all channels, which is an improvement over the transmission distance reported in [Cho *et al.*, 2003; Spiekman *et al.*, 2000]. From above 5670 km transmission system, as given in table (4.5), we have observed that optimum span scheme is good for further transmission.

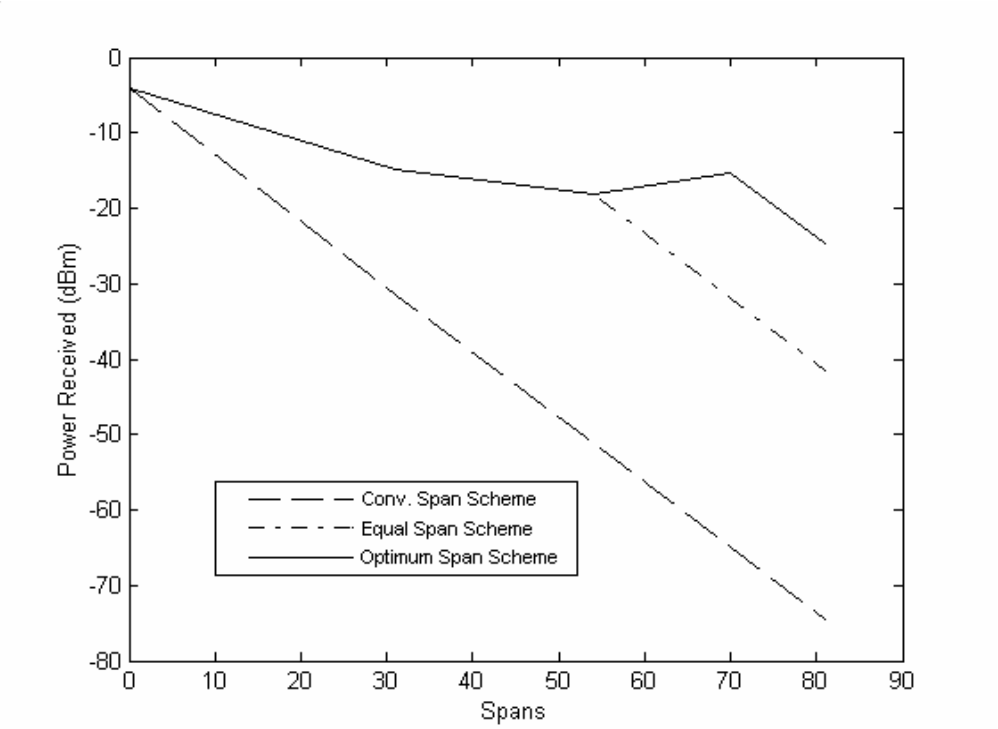

Figure 4.35: Power received versus spans for different span scheme for transmission distance 5670 km.

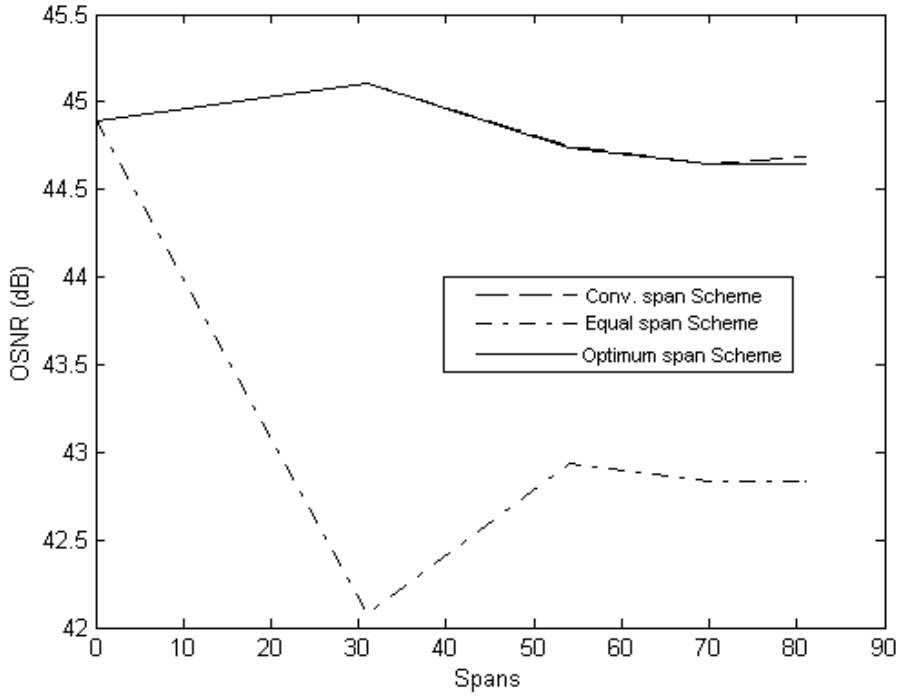

Figure 4.36: OSNR versus spans for different span scheme for transmission distance 5670 km.

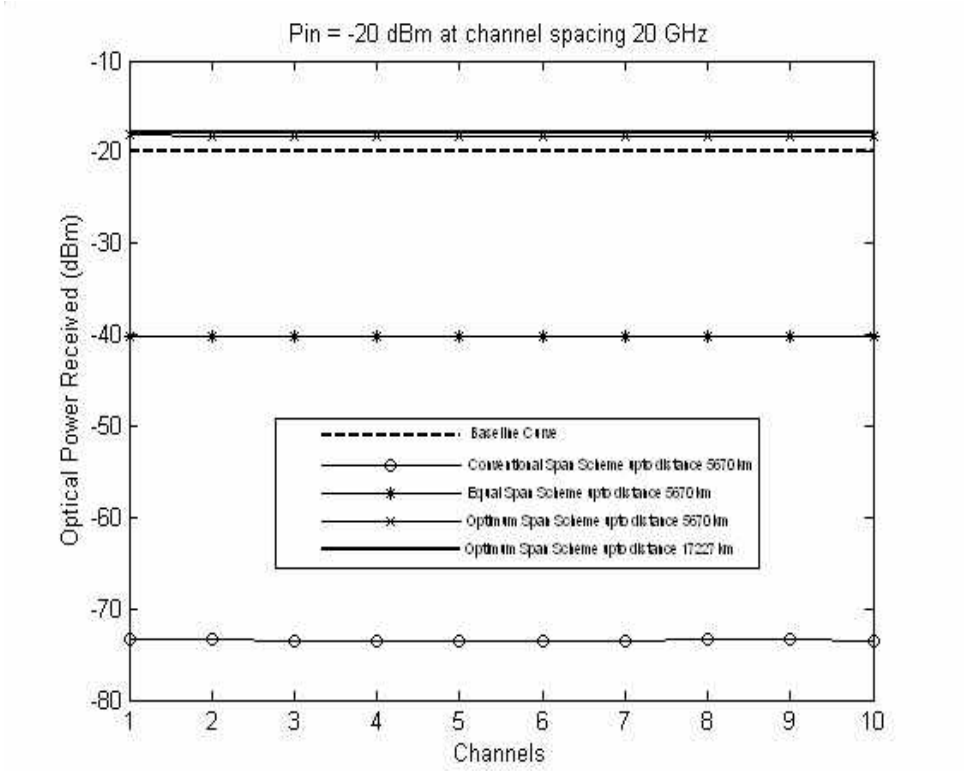

Figure 4.37: Optical power versus different channels for different span schemes and distances.

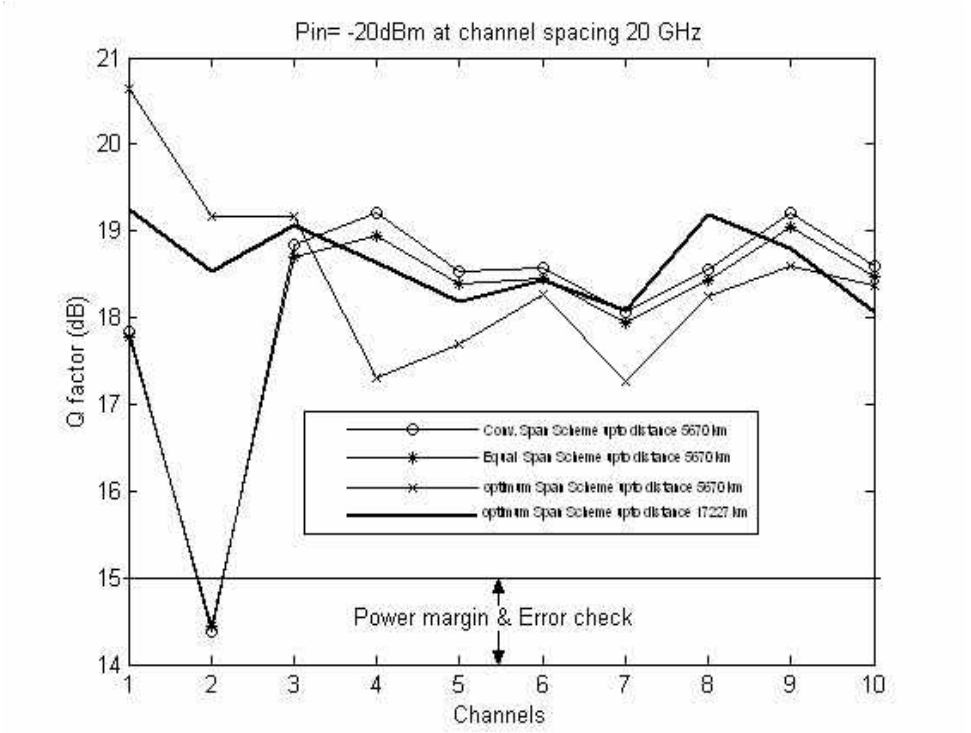

Figure 4.38: Q factor versus channels at different channels for different span schemes and distances.

Table 4.5

At transmission distance 5670 km with input power P_{in}= -20 dBm.

Parameters	Conventional span scheme	Equal span scheme	Optimum span scheme
No. of SOA used	81	85	84
Minimum Q factor (dB)	+14.38 dB	+14.45 dB	+17.28 dB
Minimum Power per channel	-73.40 dBm	-40.17 dBm	-18.18 dBm
Power Penalty	+53.60 dB	+20.68 dB	-01.82 dB

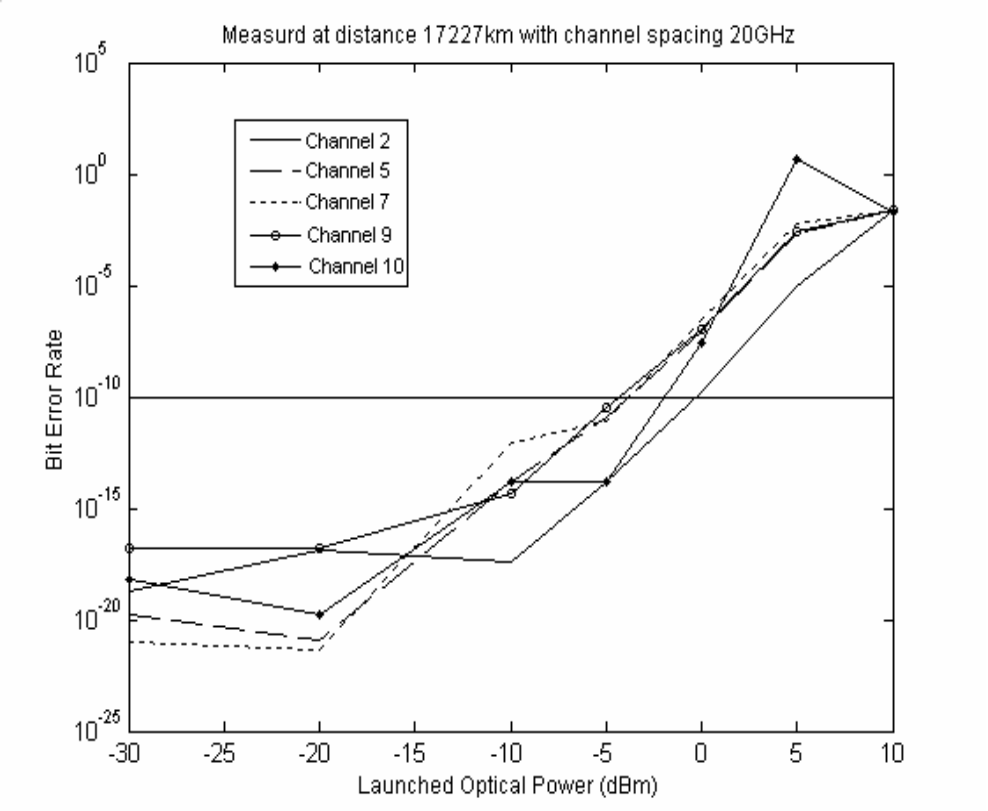

Figure 4.39: BER as the function of signal input power for different channels.

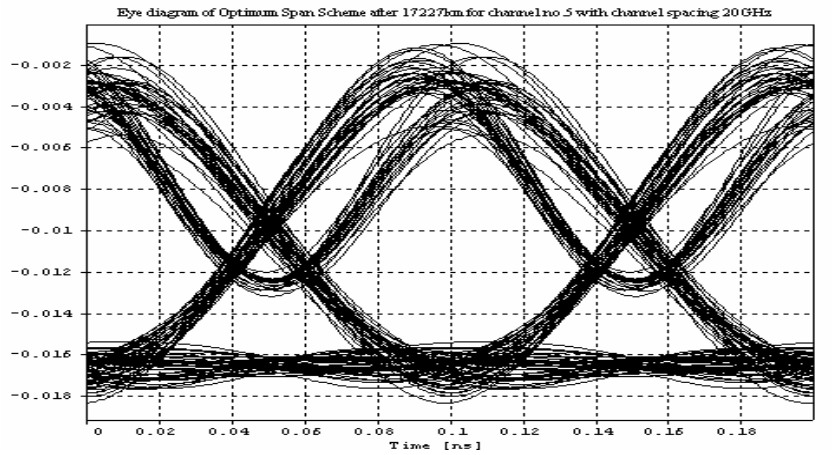

Figure 4.40a: Eye diagram using optimum span scheme at 20 GHz.

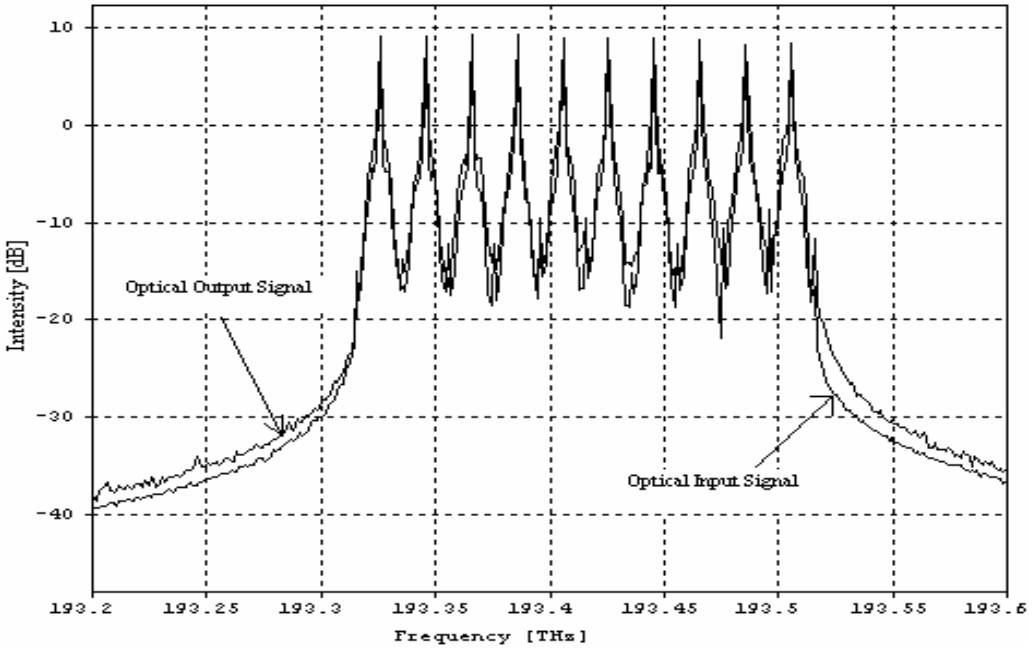

Figure 4.40b: Optical spectrum for different channel before and after transmission distance 17,227 km using optimum span scheme.

For transmission distance 17,227 km, the optimum spans are 61, 50, 40, 31, 23, 16, 11, 7, 4, 2, and 1 and after every optimum spans a SOA is used as shown in figure (4.20). For 17,227 km, this scheme shows good quality factor for all the channels as shown in figure (4.38), with power improvement of around -2.1 dB from figure (4.37). So comparison made as in table (4.5), shows improvement of transmission distance as compared to 8 × 10 Gb/s WDM signal transmission [Li *et al.*, 2004]. It is investigated that for optimum span scheme if the distance is increased the Q penalty also increases which means; quality of signal decreases due to increase in power as illustrated in figures (4.37) and (4.38).

At transmission distance 17,227 km with channel spacing 20 GHz, the good bit error rate at the floor of 10^{-10} is observed as shown in figure (4.39), which shows that power launch up to -5 dBm *i.e.* before the gain saturation power. The bit error rate obtained for received signal is less than 10^{-10} up to saturation power. The eye diagram for optimum span scheme after covering distance 17,227 km with P_{out} = -17.9 dBm for channel no.5 is shown in figure (4.40a). The optical spectrum of ten channels is observed for input signal and output signal power for transmission distance 17,227 km as shown in figure (4.40b).

4.4 Conclusions

It is concluded that the post-power compensation method shows good performance in terms of bit error rate, eye closure penalty and received power as compared to pre- and symmetrical-power compensation methods. The bit error rate and eye closure penalty increases with the increase in signal input power. The effect of ASE noise power is observed for three power compensation methods at low value of signal input power (below -30 dBm) and also gain saturation effect for high signal input power (above 0 dBm). It is found that the pre-power compensated method in single span is best for pre-amplification of very low signal input power. The maximum transmission distance observed for post power compensation method is 945 km.

We also investigated the ten-channels at 10 Gb/s WDM transmission distance of 68908 km by using SOAs as in-line and pre-amplifier with DPSK modulation format at 100 GHz channel spacing for the first time. In order to achieve this long haul transmission distance, the optimum span scheme is evaluated with power margin more than 24 dB. For this, the optimized SOA model is used with lower saturation power 21.36 mW to achieve low crosstalk -7.7342, high optical gain 36.5 dB with reasonable ASE noise power. It has been shown that optical filter with 0.4 nm bandwidth is optimum for higher transmission distance. It is also observed that with the decrease in channel spacing, the quality of

signal falls due to the increase in the crosstalk. For the transmission distance 17227 km, the optimum span scheme has performed well as received quality signal is more than 27.5 dB with signal output power 0.097 dBm for channel no. 5. But for 68908 km transmission distance, the optimum span scheme shows degradation in the quality up to 14 dB with increase in the signal output power 0.87 dBm. It has been shown that for the optimum span scheme-1, quality of the signal is 25.8 dB with signal power -38.5 dBm for channel no.5. This result generates the power penalty of 24.5 dB for 68908 km transmission distance. It is also observed that for 50 GHz channel spacing, maximum transmission distance is 6650 km and for 20 GHz, the maximum transmission distance of 3500 km is observed by using cascaded SOAs with 10 × 10 Gb/s RZ-DPSK format.

The simulations of ten channel at 10 Gb/s DWDM using cascaded SOAs with the DPSK modulation format at 20 GHz channel spacing has been performed. For this, the optimized SOA model is used. At optimum bias current, low crosstalk and optimum bandwidth is obtained for optical phase modulator *i.e*. 5.5 GHz. Using optimum span scheme it is possible to transmit 100 Gb/s RZ-DPSK signal at 17,227 km with power improvement of 2.1 dB at good quality of the signal. Finally, it has been shown that for 100 Gb/s RZ-DPSK, all channels are faithfully transmitted up to 17,227 km with maximum optical signal power up to gain saturation with BER floor less than 10^{-10}.

These conclusions give significant information for design of long haul optical fiber communication system by using low cost SOAs.

Chapter 5

Receiver Sensitivity Improvement using Polarization Insensitive Semiconductor Optical Amplifier

5.1 Introduction

This chapter focuses on the improvement of the receiver sensitivity and bandwidth for greater transmission capabilities, which is related to first and third objectives of this research work. The optical networking elements such as switches, splitters and multiplexers are being developed for the improvement of optical fiber telecommunication networks. These elements introduce an insertion loss, which must be accommodated within the power budget of transmission systems. Therefore, it requires the improved receivers sensitivity and bandwidth for greater transmission capabilities. Many researchers have worked to improve the receiver sensitivity as already discussed in the section 1.5.4 of Chapter 1

In this Chapter, the work [Dreyer *et al.*, 2002; Mason *et al.*, 2002; Yamatoya and Koyama, 2004] is extended to further optimize the SOA pre-amplifier model for higher receiver sensitivity for PIN and DPSK receivers at different bit rates.

5.2 Theoretical Analysis

The total recombination rate can be expressed as [Storkfelt *et al.*, 1991]

$$R(N) = AN + BN^2 + CN^3 \tag{5.1}$$

A, B and C being the nonradiative recombination, the spontaneous emission and the Auger recombination terms, respectively. Taking the derivative of equation (5.1),

$$R'(N) = A + 2BN + 3CN^2 \tag{5.2}$$

At room temperature A is negligible, so it is neglected from equation (5.2). Therefore, spontaneous emission term is

$$B = \frac{R'(N) - 3CN^2}{2N} \tag{5.3}$$

As from [Mynbaev and Scheiner, 2003], amplified spontaneous noise power P_{ASE} is

$$P_{ASE} = 2N_{sp}hfG\Delta f \tag{5.4}$$

$$P_{ASE} = 2N_{sp}hfGc\frac{\Delta\lambda}{\lambda}$$

Where N_{sp} is spontaneous emission factor ranges from 1.4 to more than 4 depending on both the pumping rate and the operating wavelength, hf is photon energy, G is amplifier gain, Δf is the optical bandwidth of the amplifier.

As noise figure F_n of SOA is given by [Dreyer *et al.*, 2002]

$$F_n = \frac{2P_{ASE}}{GhfB_o} \tag{5.5}$$

Where B_o is the optical filter bandwidth after SOA pre-amplifier. As in our case we are using SOA pre-amplifier without using any optical receiver filter for detection of signal. Therefore, amplified spontaneous power P_{ASE} from equation (5.5) can be written as

$$P_{ASE} = \frac{F_n Ghf}{2} \tag{5.6}$$

Also from Olsson *et al.* [1989], the spontaneous emitted power at the output of semiconductor optical amplifier is given by

$$P_{sp} = N_{sp}(G-1)hfB_o$$

By using the SOA as a pre-amplifier in our system, setup is exempted from the optical filter, the amplified spontaneous emission power is

$$P_{ASE} = P_{sp} = N_{sp}(G-1)hf \tag{5.7}$$

Therefore, photocurrent equivalent of spontaneous emission power [Olsson *et al.*, 1989] becomes

$$i_{sp} = \frac{P_{sp}q}{hf} = N_{sp}(G-1)q \tag{5.8}$$

So photocurrent equivalent of spontaneous emission power is decreased. Recalling the equation (2.9) of Chapter 2 for total noise

$$N_{tot} = N_{shot} + N_{s-sp} + N_{sp-sp} + N_{th} \tag{5.9}$$

The total noise N_{tot} from equation (5.8), is decreased due to absence of optical receiver filter B_o. The noise figure related to optical gain [Agrawal, 2002] is given by

$$F_n = 2\left(\frac{N}{N-N_o}\right)\left(\frac{g}{g-\alpha_{\text{int}}}\right) \tag{5.10}$$

As bias current I is increased, P_s is also increased to keep optical gain g high. Therefore, from equation (5.9), the noise figure is decreased, which in turn decreases the amplified spontaneous emission noise power from equation (5.5). To obtain faster

response, high bias current is used. Also, higher speed operations can be expected by using an SOA with a longer device length and larger optical confinement factor [Joergensen *et al.*, 1997; Girardin *et al.*, 1998]. The receiver sensitivity [Olsson *et al.*, 1989] is given by

$$P_{sen} = P_{in} G L_l \tag{5.11}$$

Where L_l is the loss between the last amplifier and the receiver. Our proposed SOA pre-amplifier model as in table (5.1), N_{tot} total noise is less because there is no need of optical filter and P_{ASE} amplified spontaneous emission noise power is quite low, so better sensitivity is obtained.

5.3 Results and Discussions

The simulations were carried out for the system setup as shown in figure (5.1) with SOA as pre-amplifier with parameters given in above table (5.1) model of SOA. For PIN-receiver, the EDFA noise figure is 8 dB with large gain 37.5 dB, and for DPSK receiver, noise figure is 4.5 dB with 1 dB gain only.

The transmitter bandwidth for 10 Gb/s and 15 Gb/s is selected to be 15 GHz, while for 40 Gb/s, it is 25 GHz. As shown in figure (5.2), the optical gain of SOA pre-amplifier is measured for both PIN and DPSK receiver at 1550 nm. It is found that for both TE (transverse electric) and TM (transverse magnetic) modes for the PIN receiver and the DPSK receiver are polarization insensitive to gain as compared to that reported in [Dreyer *et al.*, 2002]. The gain remains constant, *i.e.*, 30.06 dB up to gain saturation for both receivers.

The relationship between an input light and output ASE power of the SOA pre-amplifier is measured as shown in figure (5.3). As we increase the input light power the ASE power increases in same way ad occurs in [Yamatoya and Koyama, 2004], but the ASE power in our case was lower as compared to that reported in [Yamatoya and Koyama, 2004]. It is observed that for a PIN receiver ASE power is 22.3 μW with input power 0.1 mW for 10 Gb/s. It is observed that for a DPSK receiver ASE noise power is 4.1 μW only at 10 Gb/s, which is quite lower than the PIN receiver with an SOA pre-amplifier. It is also observed that as we increase the bit rate, the ASE power continues to decrease for this SOA pre-amplifier with same transmitter bandwidth.

The optical gain bandwidth for input wavelength is an important factor for optical pre-amplifier.

Table 5.1

Material and device parameter for the SOA model.

Symbol	Parameter	Value
A	Nonradiative recombination	Negligible (at room temperature)
I	Bias current	400 mA
L	Amplifier length	900 μm
w	Active layer width	2 μm
t	Active layer thickness	0.2 μm
Γ	Confinement factor	0.3
τ	Spontaneous carrier lifetime	0.18 ns
N_o	Transparency carrier density	1.08×10^{24} /m^3
a	Material gain constant	2×10^{-20}m^2
α	Line_width enhancement factor	300 /m
α_{int}	Input/Output insertion loss	3 dB
α_p	Material loss	2000 /m
P_s	Saturation power	47.47 mW
N_{sp}	Spontaneous emission factor	4

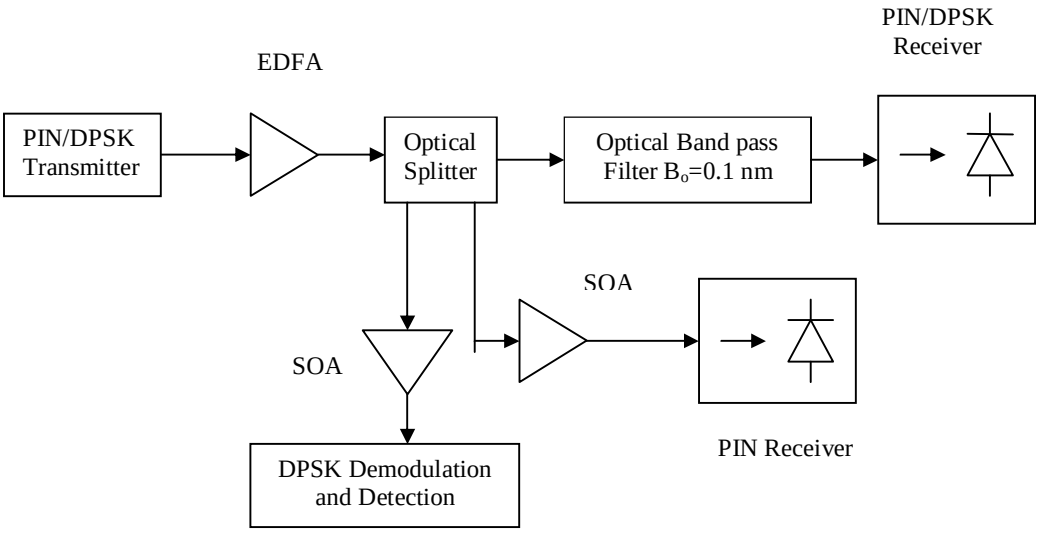

Figure 5.1: System setup used to evaluate the SOA in a pre-amplifier configuration.

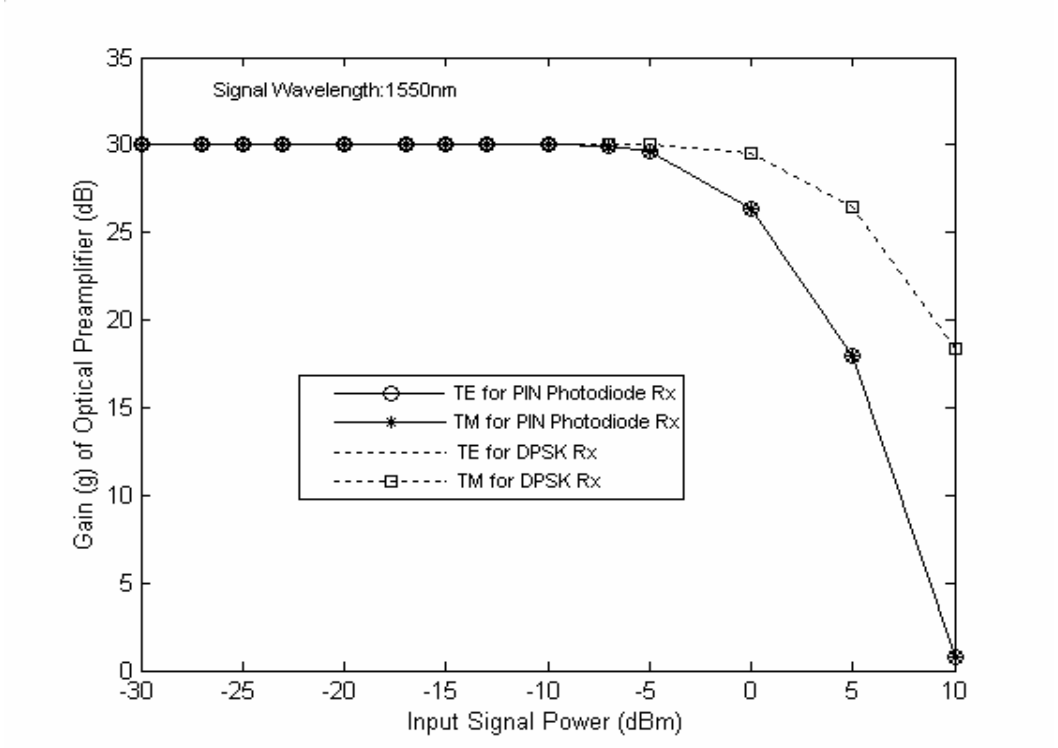

Figure 5.2: Optical gain of SOA pre-amplifier varies with input signal power for PIN and DPSK receivers with TE and TM modes.

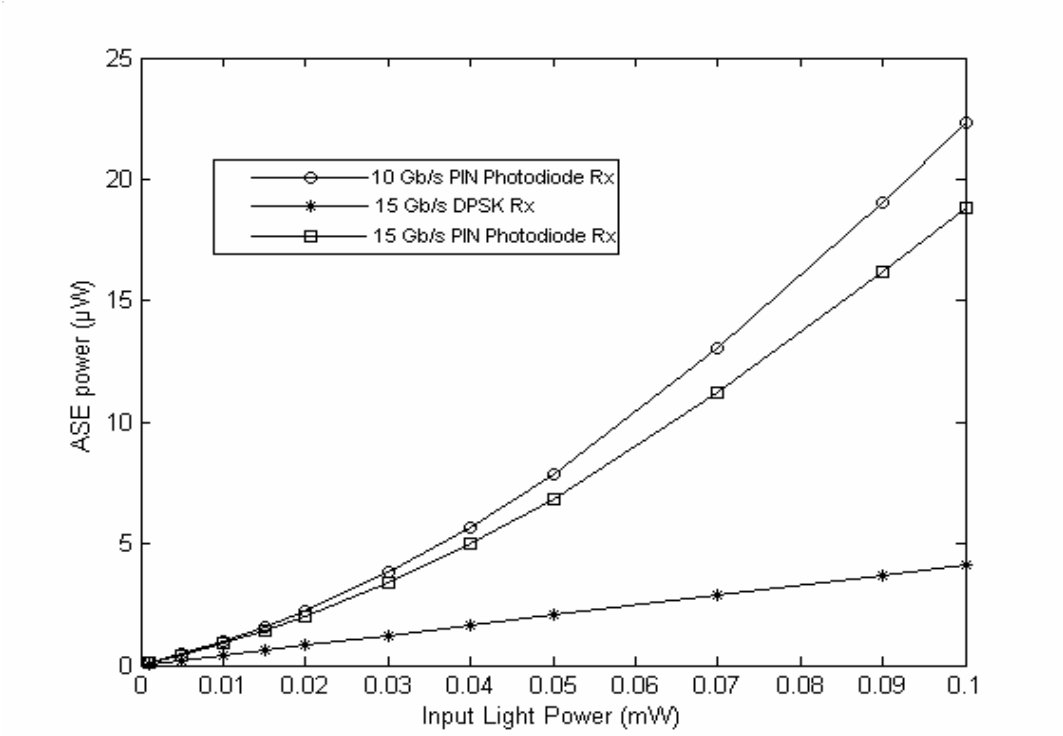

Figure 5.3: ASE noise power of SOA pre-amplifier variation with input light power for PIN and DPSK receiver at different bit rate.

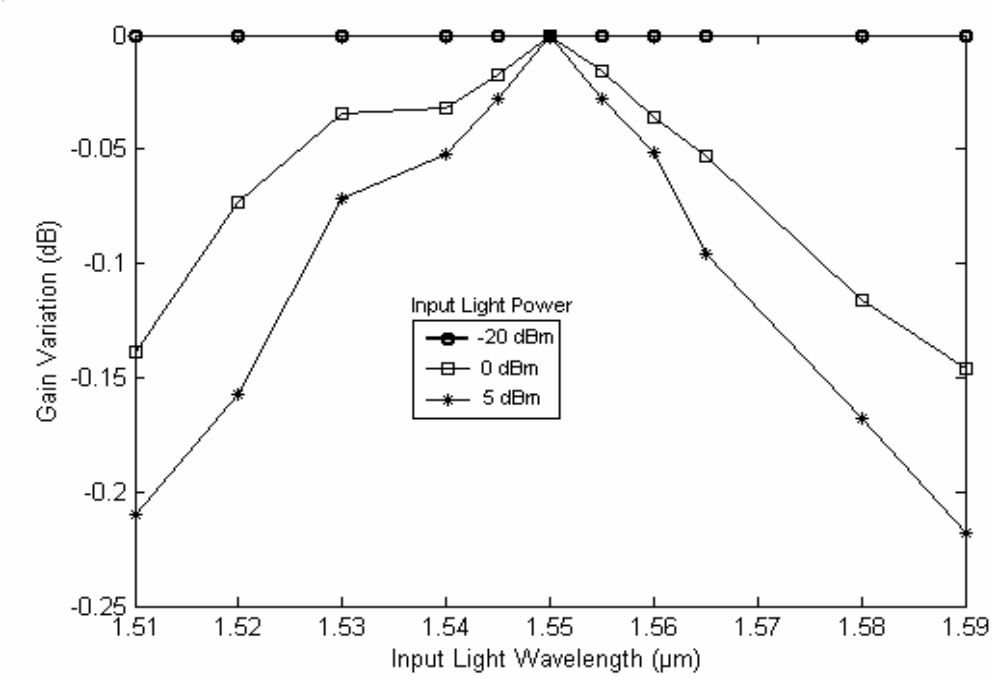

Figure 5.4: Gain variations versus input light wavelength for different input light power at 10 Gb/s with PIN receiver.

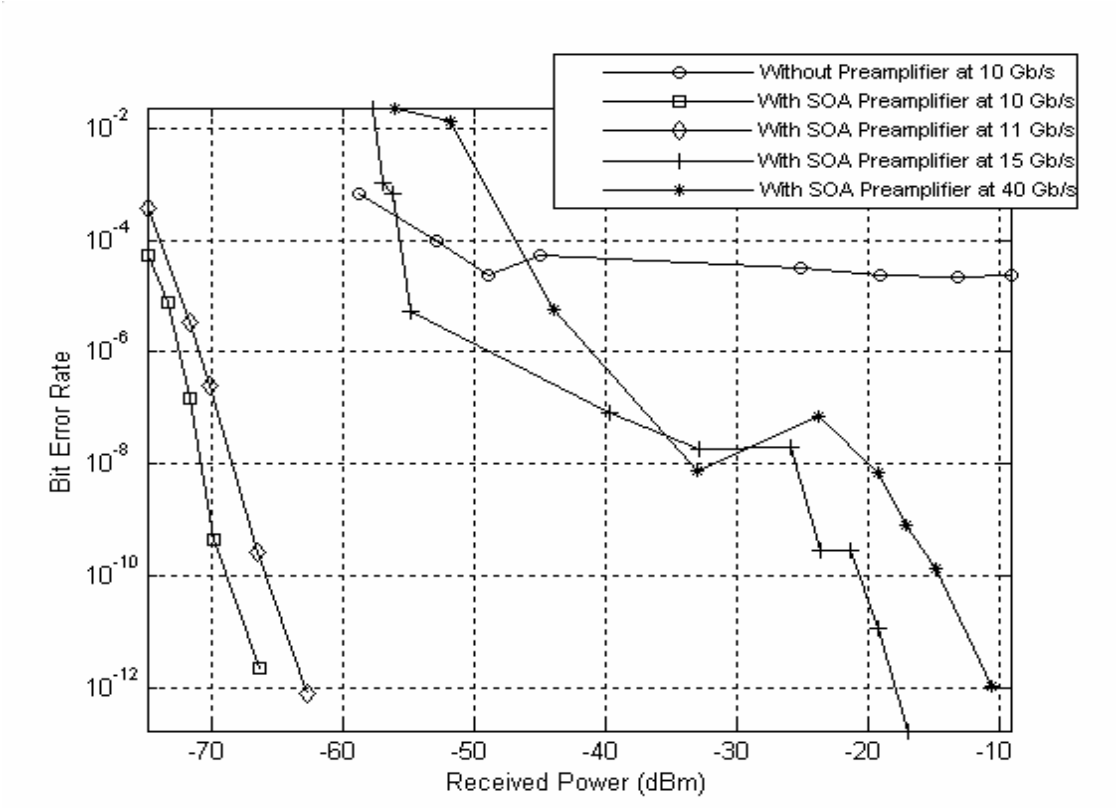

Figure 5.5: BER versus received power for different bit rate with SOA pre-amplifier PIN receiver.

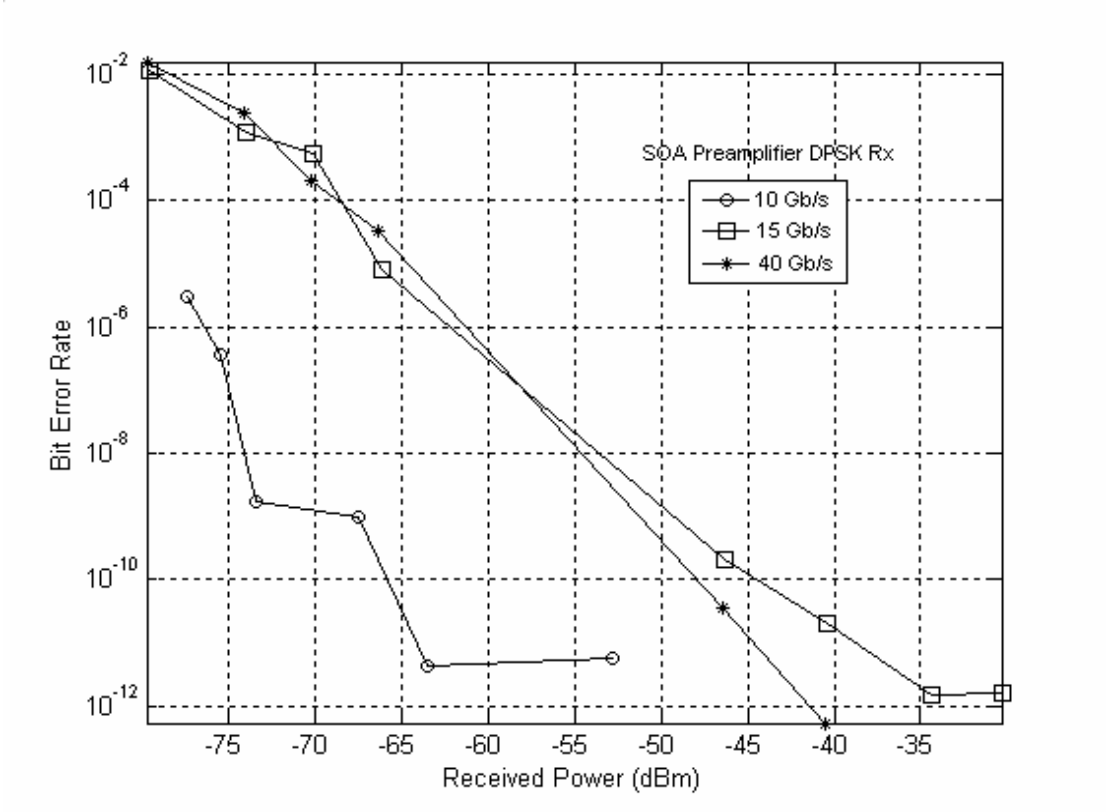

Figure 5.6: BER versus received power for different bit rate using SOA pre-amplifier DPSK receiver.

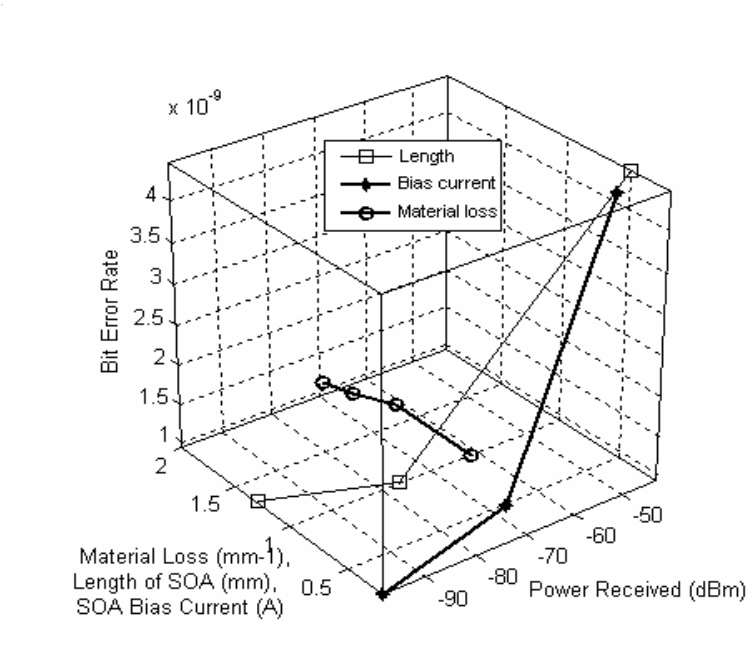

Figure 5.7: Material loss, Length, Bias current of SOA variation with power received and BER at input power = -27dBm.

The optical gain bandwidth was measured by changing the wavelength of the input light. Figure (5.4) shows the measured gain bandwidth for input light power of -20 dBm, 0 dBm and 5 dBm. The 3 dB bandwidth of the SOA pre-amplifier gain was more than 100 nm, which is too large as compared to [Yamatoya and Koyama, 2004]. It is observed that with an increase in the input light power, bandwidth of SOA pre-amplifier continues to decrease.

The receiver sensitivity is measured with above SOA model pre-amplifiers in the PIN receiver. We used same value of B_e = 7.5 GHz and B_o = 0.1 nm as reported in [Yamatoya and Koyama, 2004]. The signal is not detected without pre-amplifier at 10 Gb/s as shown in figure (5.5), and the BER is around 10^{-4} for our system setup. It shows that by using SOA pre-amplifier model without an optical filter the receiver sensitivity is -69.9 dBm with a BER floor at 4.6×10^{-10} for 10 Gb/s with extinction ratio 1 dB, while for 11 Gb/s the minimum receiver sensitivity observed is -66.5 dBm. For 15 Gb/s the receiver sensitivity observed is -23.6 dBm with same transmitter bandwidth. We also measured receiver sensitivity of -19.2 dBm at a BER floor of 10^{-9} for 40 Gb/s with a transmitter bandwidth of 25 GHz, which is an improvement over the result reported in [Mason *et al*., 2002].

For a DPSK receiver with SOA pre-amplifier, the results are shown in figure (5.6). We measured a sensitivity of -67.6 dBm at a BER floor of 9.6×10^{-10} for 10 Gb/s. The good improvement in receiver sensitivities of -45 dBm and -46.5 dBm at 15 Gb/s and 40 Gb/s is noted. Figure (5.8) shows the eye opening diagram at 40 Gb/s for both PIN and DPSK receiver with an SOA pre-amplifier.

We further optimize the SOA model for the improvement in the receiver performance at the input power -27 dBm. We observed that if material loss per millimeters is increased, the sensitivity also increases with same error floor 10^{-9} as shown in figure (5.7).

If we increase the length of the SOA, sensitivity increases along with improvement in quality of received signal. If we increase the bias current (mA), the sensitivity falls at a large value with same BER floor as shown in figure (5.7).

From this analysis, we therefore found that receiver sensitivity for our SOA pre-amplifiers model given by

$$P_{sen} = \frac{P_{in} G L_l L \alpha_p}{I} \tag{5.12}$$

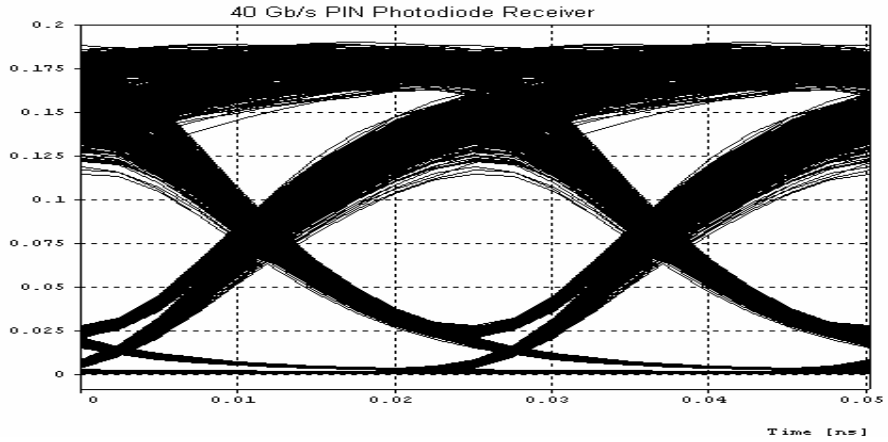

(a) For PIN Photodiode.

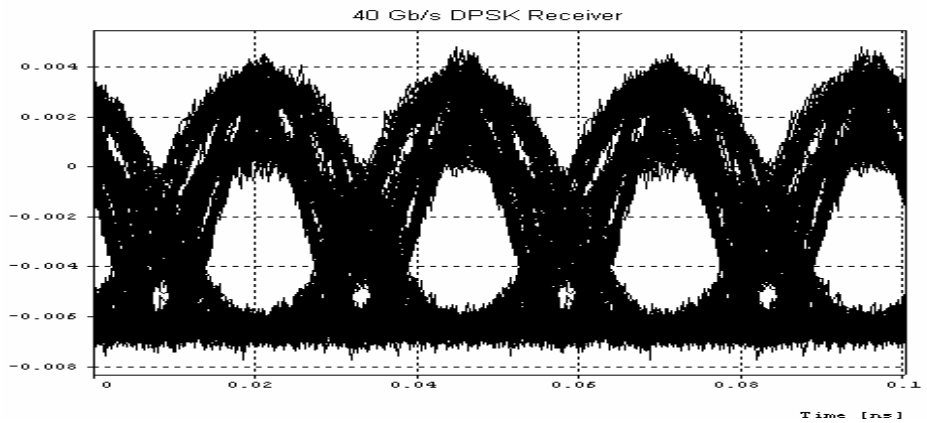

(b) For DPSK Receiver.

Figure 5.8: Eye diagram of received signal using SOA pre-amplifier for PIN and DPSK receivers at 40 Gb/s.

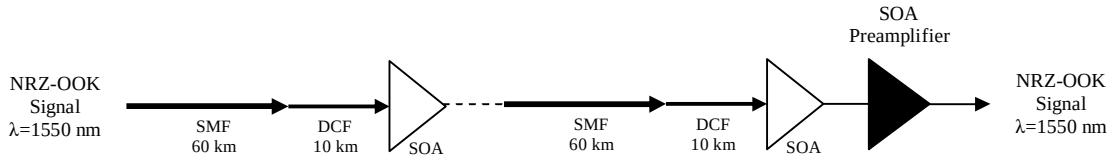

Figure 5.9: Block diagram of WDM system using SOA_1 as in-line amplifiers and SOA pre-amplifier at end.

5.4 Receiver Sensitivity for Multichannel WDM Transmission Links

When multichannel WDM system is used, there is need of receiver sensitivity improvement by using the SOA. For this, the XGM effect is taken into care. It is observed from above that the probability of power penalty occurs when above model is used for multichannel WDM transmission system.

This can be removed by using equation (2.30) in Chapter 2. So we take the carrier lifetime parameter for optimization of SOA. The optimized parameters are presented in section 5.4.1.

5.4.1 SOA Structure Parameters

The standard InGaAlAs traveling wave SOA with negligible residual facet reflectivity is taken as the amplifier model in our simulations. After solving the above equations and rate equations of chapter 2, the relevant parameters are as follows: the length is 900 μm, the width of active layer is 2 μm, its thickness is 0.2 μm and confinement factor is 0.3. The transparency carrier density in the SOA is taken to be 1.08×10^{18} cm^{-3} with the differential gain of 2×10^{-16} cm^2. The spontaneous carrier lifetime (carrier recombination time) τ at this density is evaluated 0.25 ns with saturation power P_s = 34.18 mW. The injection current is 400 mA. The optical bandwidth of SOA is 40 nm and spontaneous emission factor is considered 4. The input and output coupling losses of SOAs are taken as 3 dB. Nonradiative recombination is assumed to be negligible (at room temperature).

5.4.2 Multichannel WDM Transmission Links

Now, the above SOA pre-amplifier is considered for multichannel transmission system. Figure (5.9) shows a schematic of 20 × 10 Gb/s OOK WDM system.

Twenty Lorentzian laser sources in the wavelength range 1550.38 nm to 1557.63 nm (100 GHz channel spacing) are modulated by each optical $\sin^2$ Mach Zehnder amplitude modulator with return to zero (RZ) format. The input of each transmission channel is from -20 dBm to 0 dBm. Therefore, design carries 200 Gb/s WDM RZ-OOK signals over 350 km with 70 km SOA spacing. Each of the spans consists of a 60 km standard single mode fiber (SMF), one or more DCF and a SOA at the end. The length of DCF is chosen in accordance with [Agrawal, 2002] for complete compensation ($\overline{D} = 0$). The loss of SMF is 0.2 dB/km and loss of DCF is 0.55 dB/km. The time domain simulations have been carried out for the setup as shown in figure (5.10) for different carrier lifetimes with bandwidth 5.256 THz and centre wavelength 1550.3 nm.

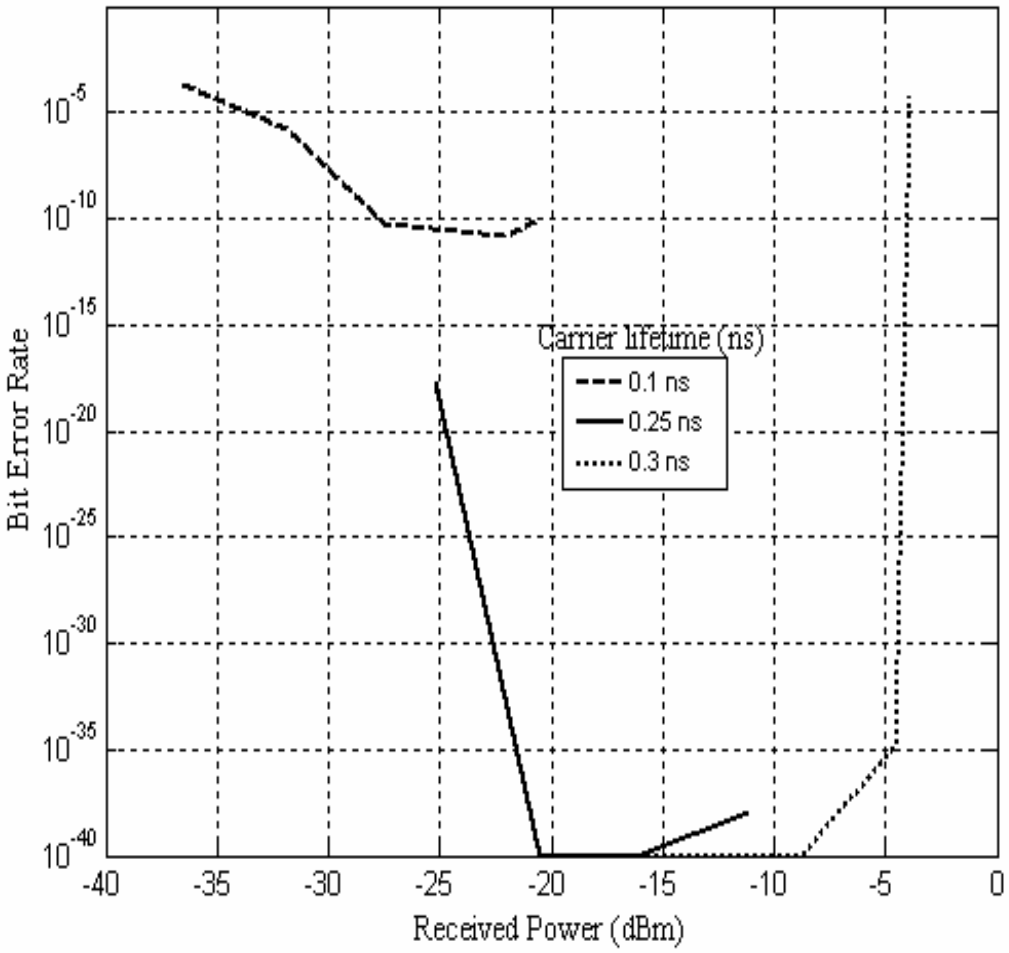

Figure 5.10: BER versus received power for different carrier lifetimes for SOA pre-amplifier in multichannel WDM transmission links.

The plot is shown in figure (5.10), the resulting BER versus the average detected power per channels. As from result, if lower value of spontaneous lifetime is taken, then detected power per channel is dropped by 15 dB with BER greater than 10^{-9}. The power drop occurs due to fall in gain of SOA. Also from equation (2.23) of Chapter 2, SOA-induced cross talk is generated at lower value of carrier lifetime. Therefore, variation of gain increases at 0.1 ns carrier lifetime. So this causes drop in quality of signals.

As shown from the results, if the carrier lifetime increases up to 0.25 ns, all channels are detected with sufficient power at BER less than 10^{-18}. Here gain fluctuations decrease due to the increase in carrier lifetime, so SOA-induced crosstalk is also less. In this case, average detected channels show BER less than 10^{-9} up to saturation of the SOA. Further, if the carrier lifetime increases up to 0.3 ns, the SOA-induced crosstalk is reduced. But as the input signal increases, SOA is saturated earlier as compared to lower value of carrier lifetimes. So result shows that good BER is observed at the receiver for input signal up to -5 dBm. So by using carrier lifetime 0.25 ns, good improvement in detected power per channel is observed with high input signal. These results show an improvement over results reported in [Xu *et al.*, 2003]. Further optimization of SOA structure is also possible for improvement of the receiver performance.

5.5 Conclusions

We have proposed an SOA model for an optical pre-amplifier for the PIN and the DPSK photoreceivers. The minimum receiver sensitivity of -69.9 dBm is observed at the BER floor of 4.6×10^{-10} for the PIN receiver at 10 Gb/s. Also improvement of receiver sensitivity of -19.2 dBm and -46.5 dBm for the PIN receiver and DPSK receiver at 40 Gb/s is observed. The impact of the ASE noise power, optical gain, gain variation for different input light wavelength for the PIN and the DPSK receiver are illustrated for different bit rates. It is observed that the ASE noise power for a PIN photo detector is 22.3 μW at -10 dBm, while for a DPSK receiver is 4.1 μW, which is quite low. It has been shown that gain variation increases with an increase in input light power and the tolerance of input wavelength power is more than 100 nm for large power. It is also observed that the optical gain is insensitive to polarization and remains constant at 30.06 dB.

Chapter 6

Gain Flattening Approach to Physical EDFA for 16 × 40 Gb/s NRZ-DPSK WDM Optical Communication Systems

6.1 Introduction

In this chapter, the investigation for gain flattening approach of EDFA in WDM transmission systems have been carried out, which is the part of first and second objectives of this research work. The major disadvantage of an EDFA is its non uniform gain spectrum and therefore the imbalance of power amongst different channels takes place at the receiver. The gain flattening of the EDFA for high capacity transmission link is also achieved by using gain flattening approach and optical super Gaussian notch filter at peak gain of the EDFA in transmission link.

The gain can be flattened by using a gain clamping erbium doped waveguide amplifier module with an optical feedback technique [Yeh *et al.*, 2005]. But this can reduce the gain and also requires additional components. There is competition in optical long-haul transmission to achieve high channel bit rates and large transmission capacity. Taga *et al.* [1994] demonstrated four channel transmission up to 459 km each at 2.4 Gb/s bit rate and also two channel transmission up to 4550 km each at 5 Gb/s.

Chung and Chung [2005] proposed a short period dispersion managed fiber which suppressed the dispersion and nonlinearities. The transmission distance of 320 km at 320 Gb/s bit rates with 100 GHz channel spacing was reported. Miyamoto *et al.* [1999] reported 8 channels transmission up to 367 km with bit rate of each channel 40 Gb/s. Pizzinat *et al.* [2003] reported that four channels at 40 Gb/s error free WDM (wavelength division multiplexing) transmission is possible for 750 to 800 km. Matsuda *et at.* [2004] demonstrated that 42.7 Gb/s WDM signals could be successfully transmitted in the L and U-band using hybrid amplifiers and hybrid optical amplifier consisting of Raman amplifier and L-EDFA transmitted up to the distance of 225 km.

Until now, the maximum transmission distance is up to 367 km using EDFAs for 8 channels at 40 Gb/s [Miyamoto *et al.*, 1999]. In this Chapter, a method is illustrated to increase the transmission distance and capacity of optical communication systems by using gain flattening approach of EDFAs at 40 Gb/s. A method of approximately gain

flattening the band from 1530 nm to 1560 nm is demonstrated here. In this approach, the fiber grating or any additional components are not used.

6.2 EDFA Parameters and Validation

In EDFA Physical Model [Giles and Desurvire, 1991], the saturation parameter χ is defined as:

$$\chi = \pi b_{eff}^2 \frac{n_t}{\tau_1} \tag{6.1}$$

Where b_{eff}^2 is the effective radius of the doped region (and consequently πb_{eff}^2 is the effective transversal area of the fiber doped region), n_t is the average ion density in [m^{-3}] and τ_1 is the so-called "metastable lifetime".

The gain $g(\lambda)$ and absorption $\alpha(\lambda)$ coefficients can be obtained from the emission $\sigma_{em}(\lambda)$ and absorption $\sigma_{abs}(\lambda)$ cross-sections as:

$$g(\lambda) = \sigma_{em}(\lambda) \Gamma(\lambda) n_t \tag{6.2}$$

$$\alpha(\lambda) = \sigma_{abs}(\lambda) \Gamma(\lambda) n_t \tag{6.3}$$

Where $\Gamma(\lambda)$ is the overlap integral between the optical mode inside the fiber and the erbium doping profile, while n_t is the average ion density in [m^{-3}].

In order to evaluate the response of $EDFA_1$, $EDFA_2$, pre-amplifier EDFA, the simulation has been performed as shown in figure (6.1) with single transmitter and receiver without any single mode fiber (SMF) and dispersion compensating fiber (DCF). For this, the DPSK signal is formed by encoding a continuous wave (CW) Lorentzian light source with different power and data in terms of NRZ-DPSK (non return to zero differential phase shift keying) format launched into optical phase modulator. The NRZ data was pseudorandom binary sequence (PBRS) with word length 2^{10}-1 at 40 Gb/s. The full wave half maxima (FWHM) line_width of continuous wave light source is 1 MHz. The low pass Bessel filter have 3 dB bandwidth of 40 GHz for generation of data source in terms of NRZ format. Then this DPSK signal is launched into different EDFAs for measuring the response. At the output, a raised Cosine optical filter with bandwidth 50 GHz is used. The output of the filter is fed into DPSK receiver for detection of signal. The time domain simulation is carried out with centre wavelength of 1550 nm.

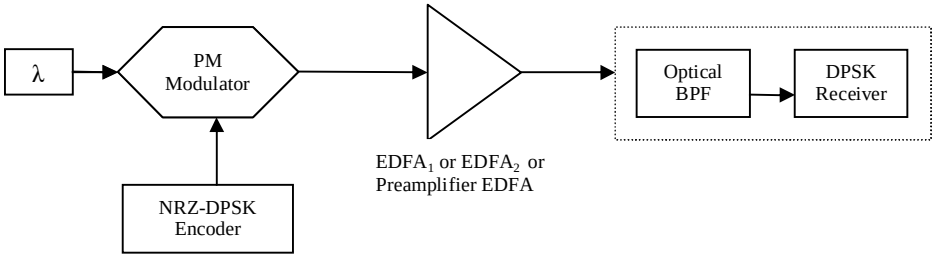

Figure 6.1: Schematic setup of measuring the response of EDFA1 or EDFA2 or Pre-amplifier EDFA.

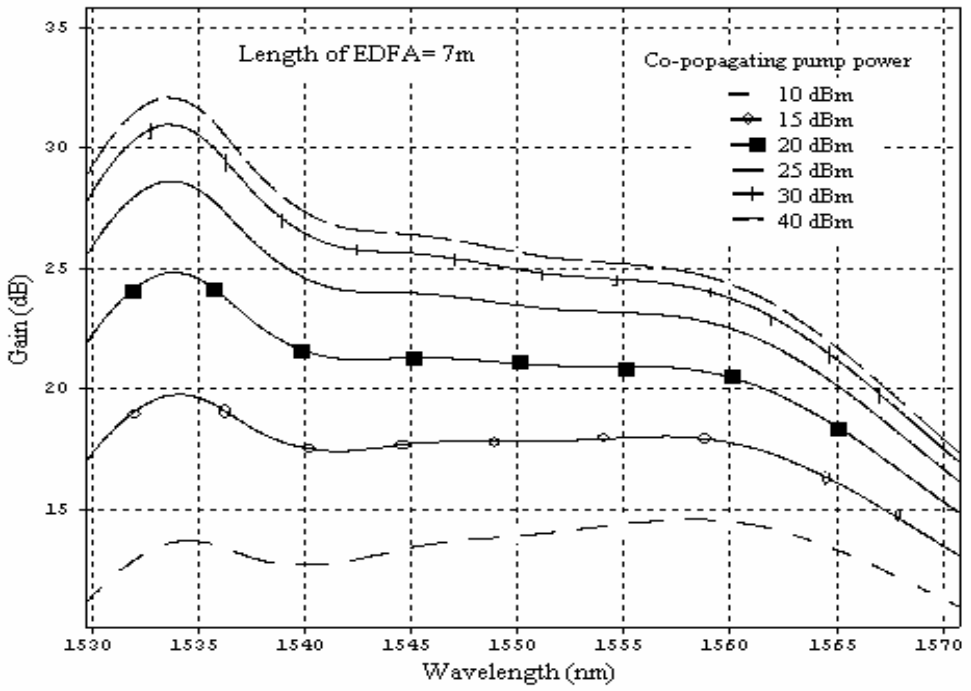

Figure 6.2: Gain as the function of wavelength for different pump powers of $EDFA_1$.

Table 6.1

EDFA parameters used in gain flattening approaches.

Parameters	**$EDFA_1$**	**$EDFA_2$**	**Pre-amplifier EDFA**
Doped Fiber Length	7 m	3 m	7 m
Input/Output Insertion Loss	0.5/0.3 dB	same	same
Co-propagating Pump Power	20 dBm	8 dBm	30 dBm
Pump Wavelength	1460 nm	same	same
Saturation Power	2.17×10^{13} /m/s	same	same
Absorption (dB/m)	0.26 – 7.54	same	same
Emission (dB/m)	1.61 – 7.44	same	same

Figure (6.2) shows the variation of gain with respect to wavelength for different values of co-propagating pump power for 1460 nm with length of 7 meters for the EDFA. The good gain is obtained for this length at sufficient pump. As the pump power increases, the gain increases. But variation of the gain with wavelength is non uniform. At 20 dBm pump power, a uniform gain for 20 nm bandwidth with gain excursion of ± 2 dB is achieved as shown in figure (6.2). The flatten gain is achieved by choosing suitable pump power and length of doped fiber. The parameters of $EDFA_1$ are optimum for approximately flat gain as presented in table (6.1). The physical EDFA model in the section 6.2 has been followed for evaluation of EDFA parameters as in table (6.1).

6.3 Simulation Setup for 16 × 40 Gb/s WDM Signals Transmission

6.3.1 Gain Flattening Approach-I

The transmission performance of WDM signals is analyzed using cascaded $EDFA_1$. This $EDFA_1$ has constant gain for large bandwidth. The centre frequency of simulation is shifted from 1550 nm to 1554 nm so that in both sides bandwidth can be used with the constant gain approach. If the centre frequency at 1550 nm, then some channels near to 1530 nm do not propagate for long transmission distances. This is due to the peak gain at 1530 nm. For long distance transmission, the channels near 1530 nm saturate quickly at small transmission lengths. The schematic setup of 16 × 40 Gb/s WDM system is shown in figure (6.3a). Sixteen Lorentzian shaped line_width laser sources in the wavelength range from 1534 nm to 1558 nm (200 GHz channel spacing) are each modulated by optical $LiNbO_3$ phase modulators with a non return to zero (NRZ) format. The input of each transmission channel is -10 dBm. The DPSK receiver is composed of tunable Mach-Zehnder interferometer having two optical output ports. The optical path difference of interferometer is set to the equivalent of one bit time duration. Each output of interferometer is detected by an ideal PIN photodetector. The output electrical signal is the difference between detected currents. The bit error rate (BER) of the DPSK receiver is given as

$$\text{BER} = \frac{1}{2}\exp\left(-\eta N_p\right)$$

Where η is the quantum efficiency of PIN photodetector and N_p is the number of photons per bit. For $\eta = 1$, a BER of 10^{-9} or Q factor = 6 dB is obtained for $N_p = 20$.

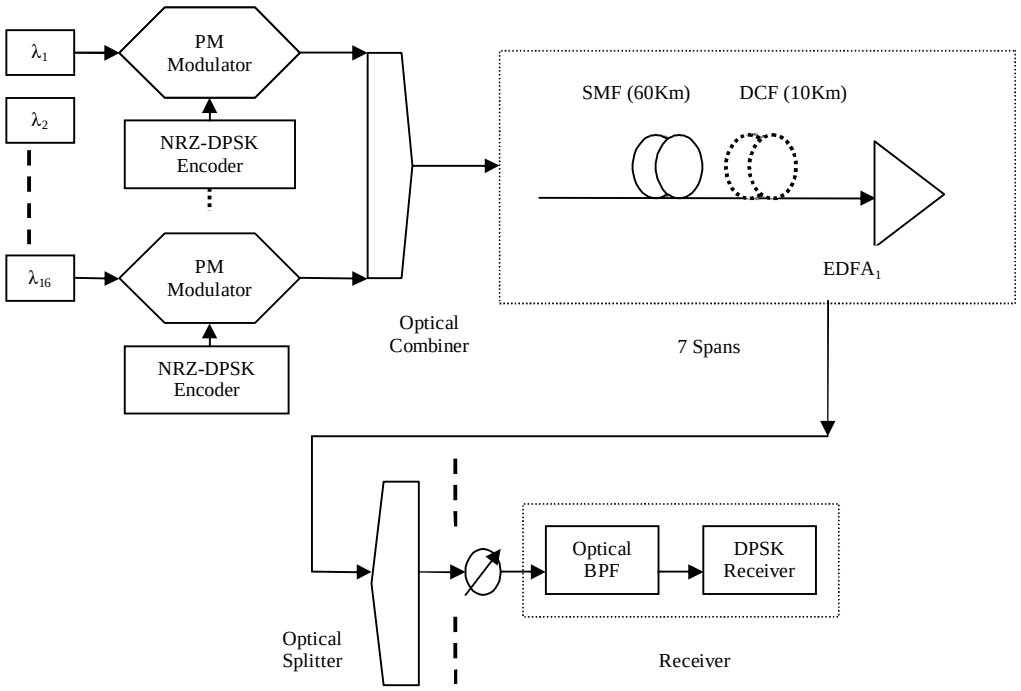

Figure 6.3a: Gain flattening approach-I for transmission system of 16 × 40 Gb/s WDM signals.

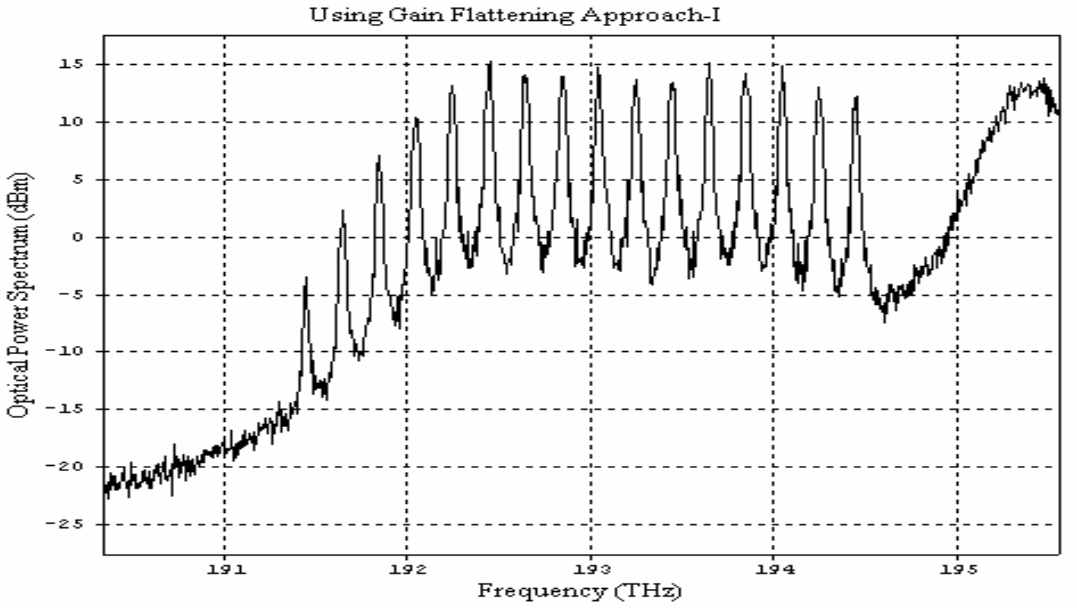

Figure 6.4a: Variation of optical power spectrum with frequency in gain flattening approach-I.

Therefore, the design carries 640 Gb/s WDM NRZ signals over 490 km with 70 km EDFA spacing. The arrangement for the gain flattening approach-I is shown in figure (6.3a). Each of the spans consists of a 60 km standard single mode fiber (SMF), one or more DCF (dispersion compensating fiber) and an $EDFA_1$ at the end. For SMF, the value of the dispersion parameter D is 17 ps/km-nm at the operating wavelength. The corresponding value for the DCF is six times greater with opposite sign. The loss of SMF is 0.2 dB/km and loss of DCF is 0.55 dB/km. The output power spectrum for 490 km is shown in figure (6.4a). There is large variation of power from -15 dBm to +15 dBm. As observed from figure (6.5), the last two channels have quality less than 15 dB. These channels have received power less than input power -10 dB as observed in figure (6.6). This occurs due to continuously large drop in power near 1560 nm. So this approach is not used for a 490 km transmission distance. It is suitable for a lower WDM transmission distance.

6.3.2 Gain Flattening Approach-II

The gain flattening approach-II is shown in figure (6.3b). In each of the spans, it consists of a 60 km standard single mode fiber (SMF), one or more segments of DCF, $EDFA_1$ and $EDFA_2$ as shown in figure (6.3b). For SMF, the value of the dispersion parameter D at the operating wavelength is the same as in the gain flattening approach-I. The corresponding value for the DCF is also six times greater with opposite sign. The loss in the SMF and the loss in the DCF are the same as in gain flattening approach-I. By connecting an $EDFA_1$ and $EDFA_2$ in series, the gain of the combination EDFAs becomes more flat and higher. The different parameters used in $EDFA_1$ and $EDFA_2$ are presented in table (6.1). The setup shown in figure (6.3a) is used for simulation. The simulation has been performed with a single transmitter and receiver without any single mode fiber (SMF) and dispersion compensating fiber (DCF) with variation of input power. The observed gain and noise figure is shown in figure (6.7). The gain of EDFA block (*i.e.* series combination of $EDFA_1$ and $EDFA_2$) is decreased with increase in input power. This shows good agreement with result reported in [Novak and Moesle, 2002; Takahashi *et al*., 1997]. The gain decreases due to the cross gain saturation [Novak and Moesle, 2002; Takahashi *et al.*, 1997] and the same effect is present in our results. At low value of signal input, the level of amplified spontaneous emission (ASE) noise is quite high. This ASE noise dominates the input signal. The noise figure of this EDFA block is also quite low as shown in figure (6.7).

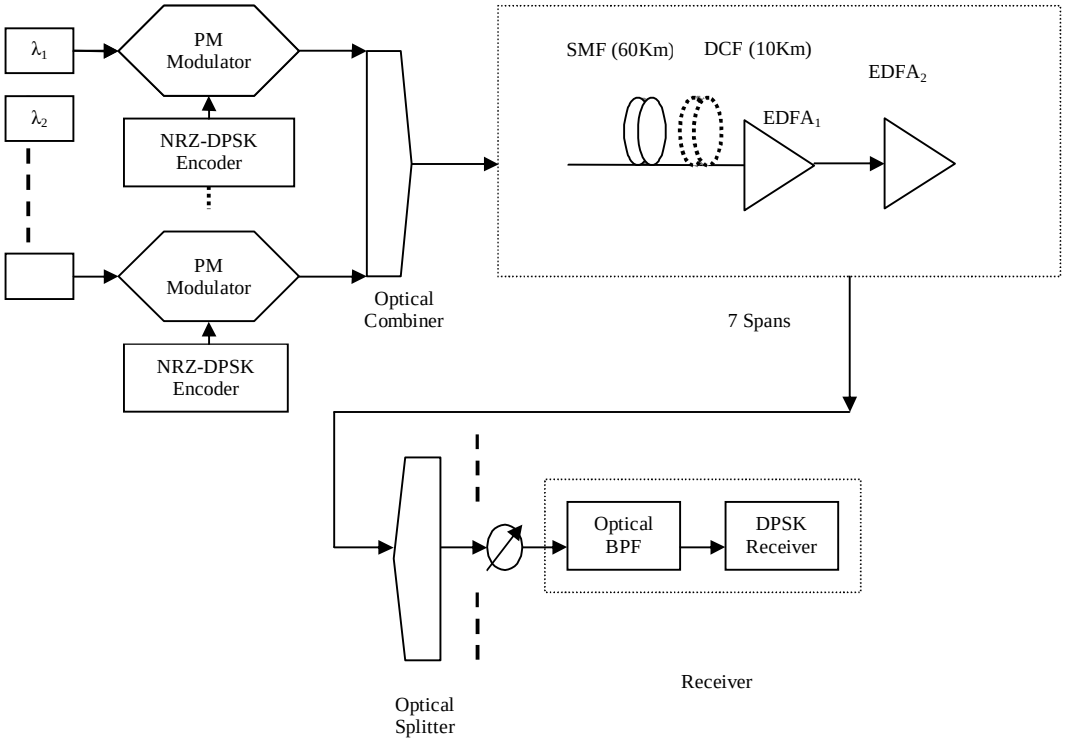

Figure 6.3b: Gain flattening approach-II for transmission system of 16 × 40 Gb/s WDM signals.

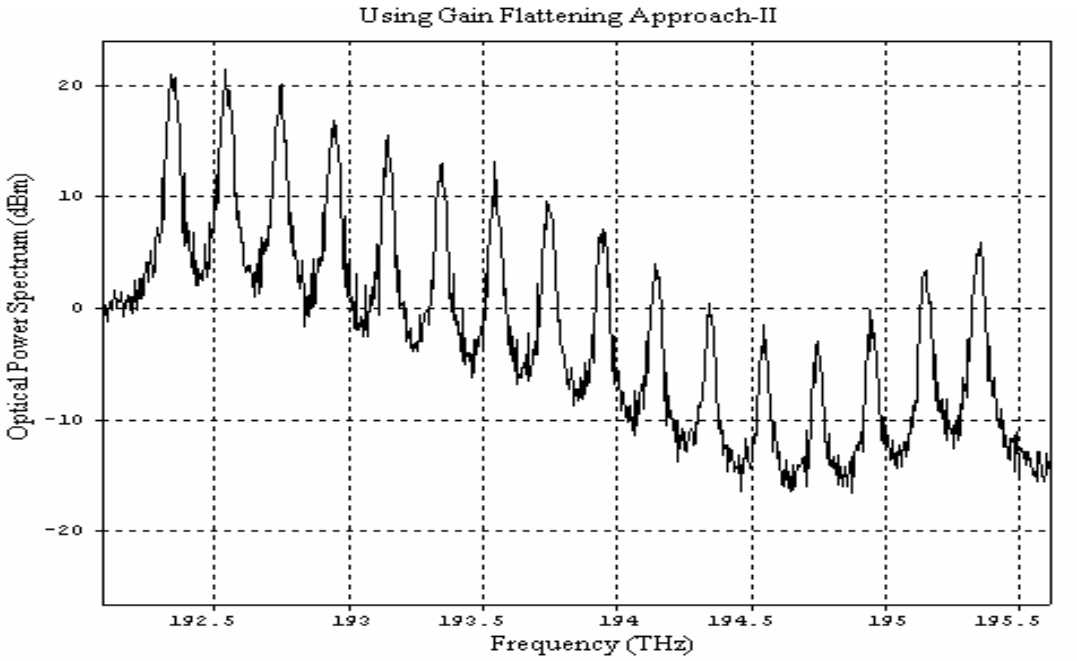

Figure 6.4b: Variation of optical power spectrum with frequency in gain flattening approach-II.

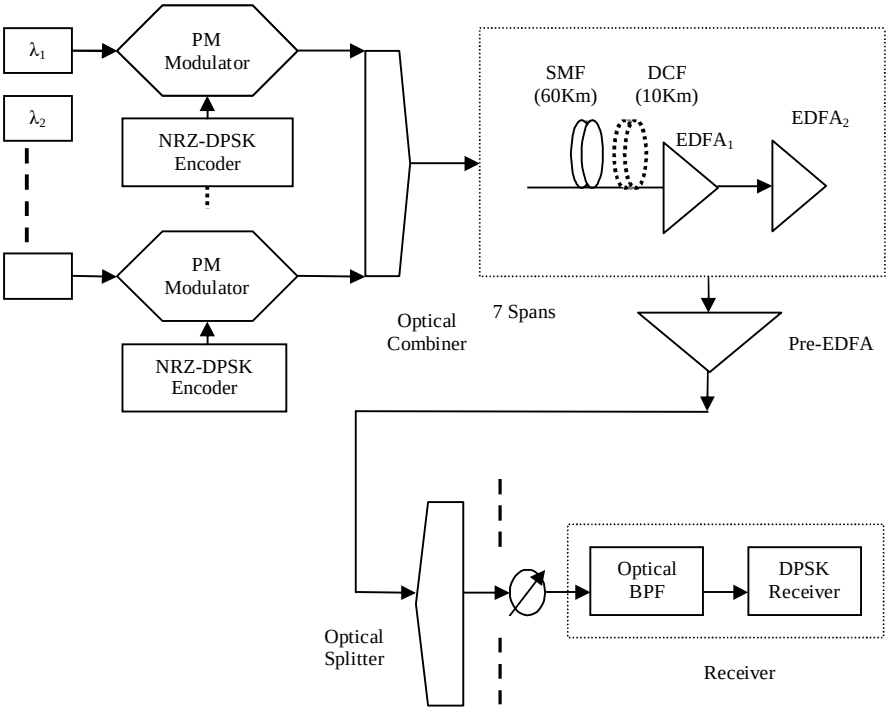

Figure 6.3c: Gain flattening approach-III for transmission system of 16 × 40 Gb/s WDM signals.

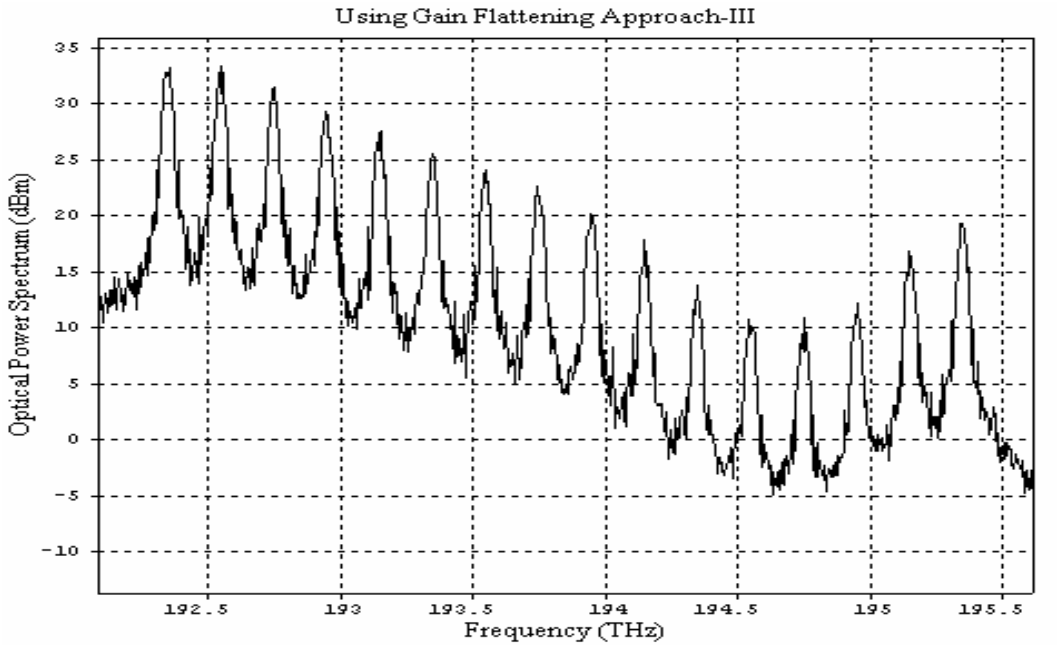

Figure 6.4c: Variation of optical power spectrum with frequency in gain flattening approach-III.

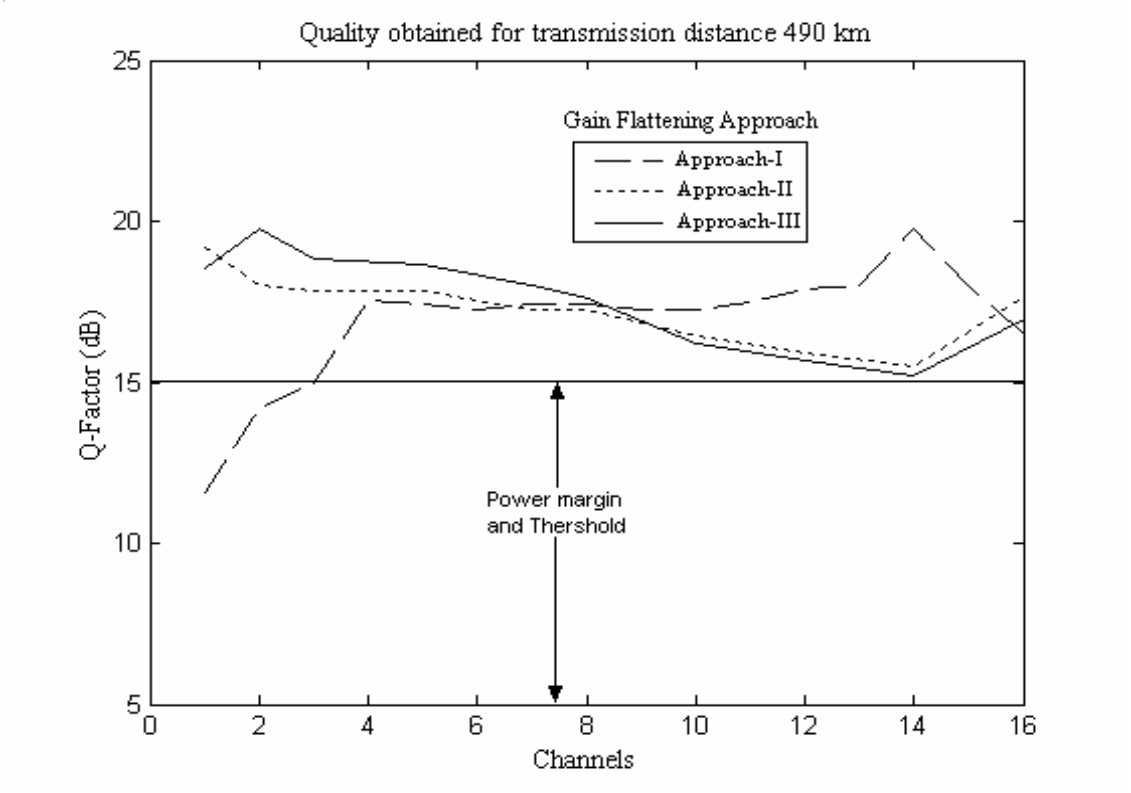

Figure 6.5: Q factor variations with wavelength for different gain flattening approaches.

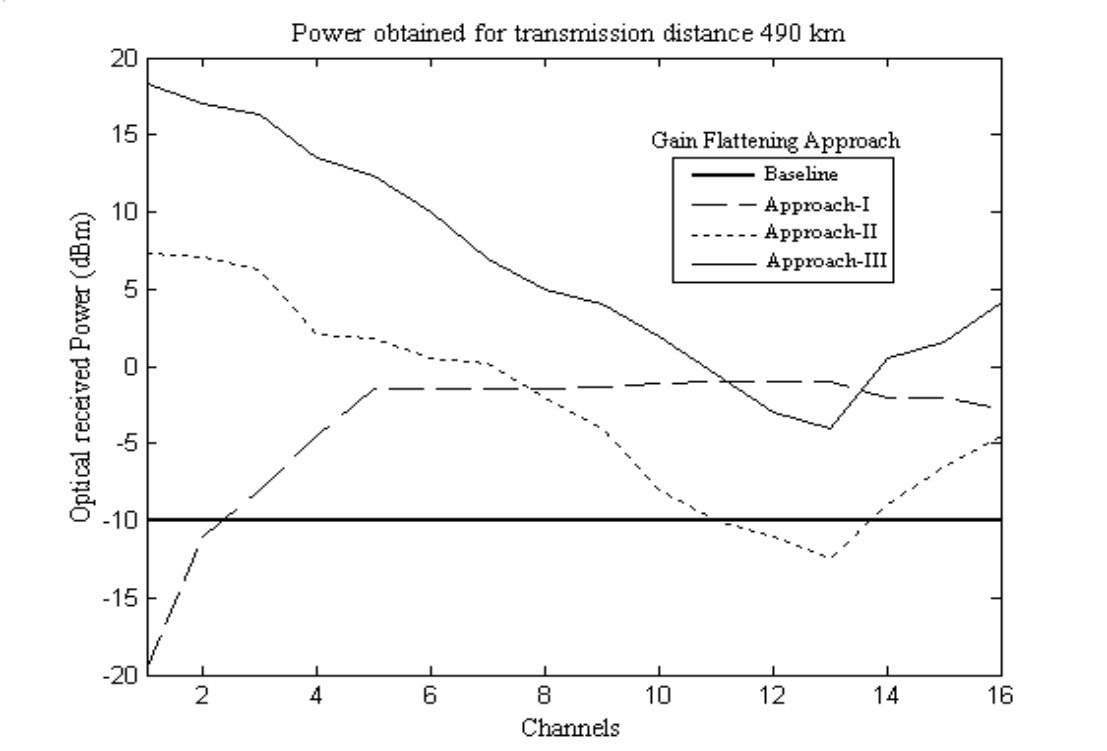

Figure 6.6: Variation of optical power received with wavelength for different gain flattening approaches.

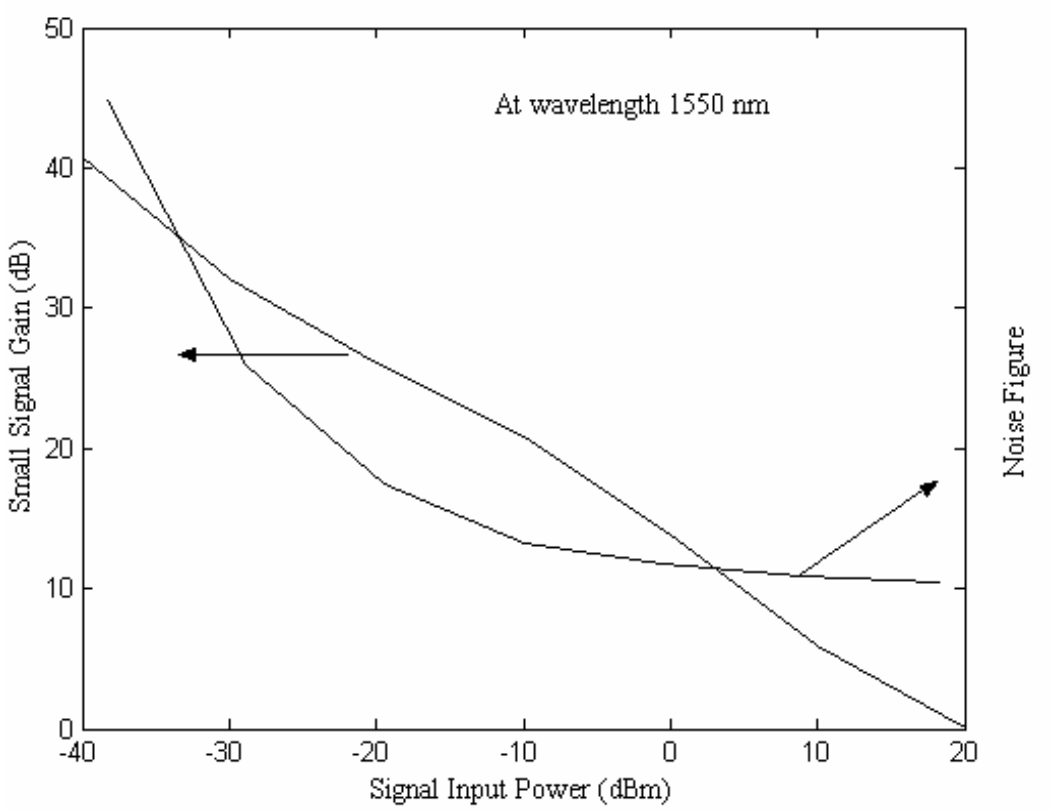

Figure 6.7: Gain and noise figure of $EDFA_1$ and $EDFA_2$ in series for gain flattening approach-II.

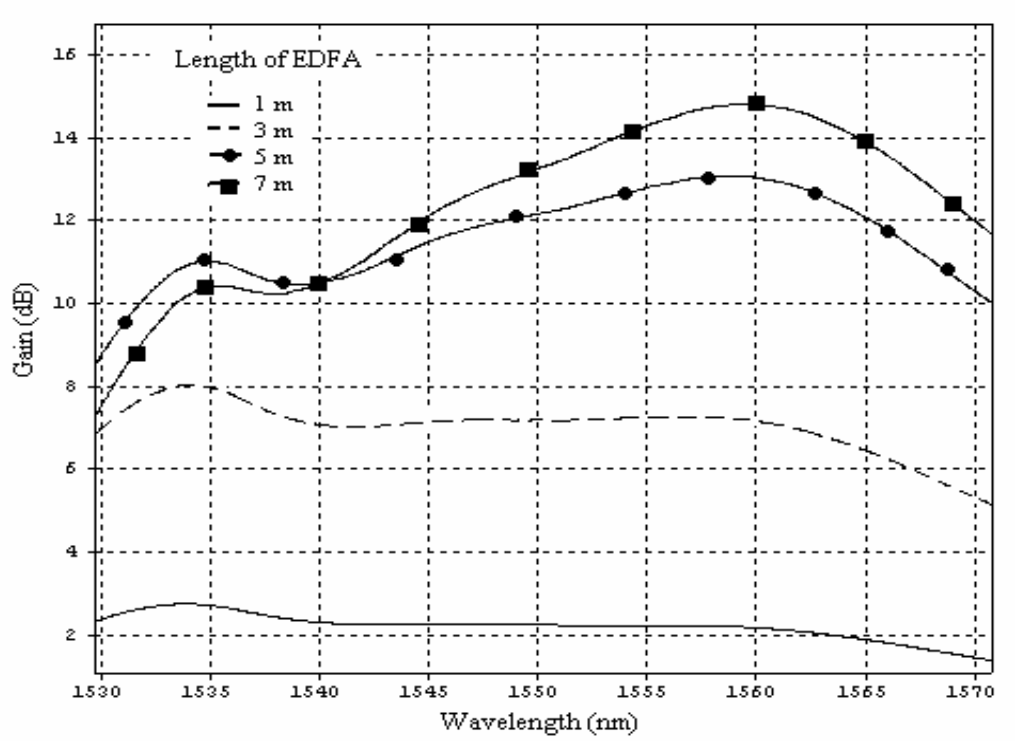

Figure 6.8: Gain as the function of wavelength of $EDFA_2$ for gain flattening approach-II.

In figure (6.2), there is a little valley in gain which is present before 1530 nm. This valley is decreased by $EDFA_2$. The gain variation of $EDFA_2$ as shown in figure (6.8) makes the gain of $EDFA_1$ more flat for suitable length.

This gain flattening approach-II is used in figure (6.1) for transmission of same sixteen channels at 40 Gb/s. This approach is also used for a transmission distance of 490 km. The centre wavelength for this approach is 1550 nm for minimum attenuations. As shown in figure (6.4b), the optical power spectrum is more uniform as compared to gain flattening approach-I. The quality factor of all channels is more than 15 dB as shown in figure (6.5). Also from figure (6.6), it is noted that for channel number 13, there is drop in power of -12.5 dBm. This shows that there is a power penalty of 2.5 dBm. This flattening approach is suitable up to the transmission distance of 420 km or less. This also shows improvement over [Taga *et al.*, 1994; Chung and Chung, 2005].

6.3.3 Gain Flattening Approach-III

The arrangement for gain flattening approach-III is shown in figure (6.3c). Each of the spans consists of a 60 km standard single mode fiber (SMF), one or more DCF. An $EDFA_1$ and $EDFA_2$ in series are at the end as shown in figure (6.3c).

In this an EDFA pre-amplifier is used to improve the received power. Here $EDFA_1$, $EDFA_2$ and EDFA pre-amplifier are used together, so that the gain of this approach is quite high. Therefore, we obtain a large output power. The parameters for the pre-amplifier are shown in table (6.1). The loss of SMF and the loss of DCF are the same as that in gain flattening approach-I. The gain of the EDFA block becomes more flat as compared to gain flattening approach-I.

The gain spectrum of the EDFA pre-amplifier is shown in figure (6.9). This pre-amplifier improves the received power. It also improves the gain flattening at wavelengths less than 1530 nm.

Figure (6.3c) illustrates the transmission of the same sixteen channels at 40 Gb/s with gain flattening approach-III with transmission distance of 490 km. Here the centre wavelength of 1550 nm is used for minimum attenuation in the communication path. As shown in figure (6.4c), the optical power spectrum is similar to that as observed in gain flattening approach-II. But a larger optical power spectrum is observed here. The variation of power for each channel improves with the increase in wavelength. It also shows good agreement with experiments [Taga *et al.*, 1994] for four channels at 591.2 Mb/s. The quality factors of all channels above 15 dB are shown in figure (6.5).

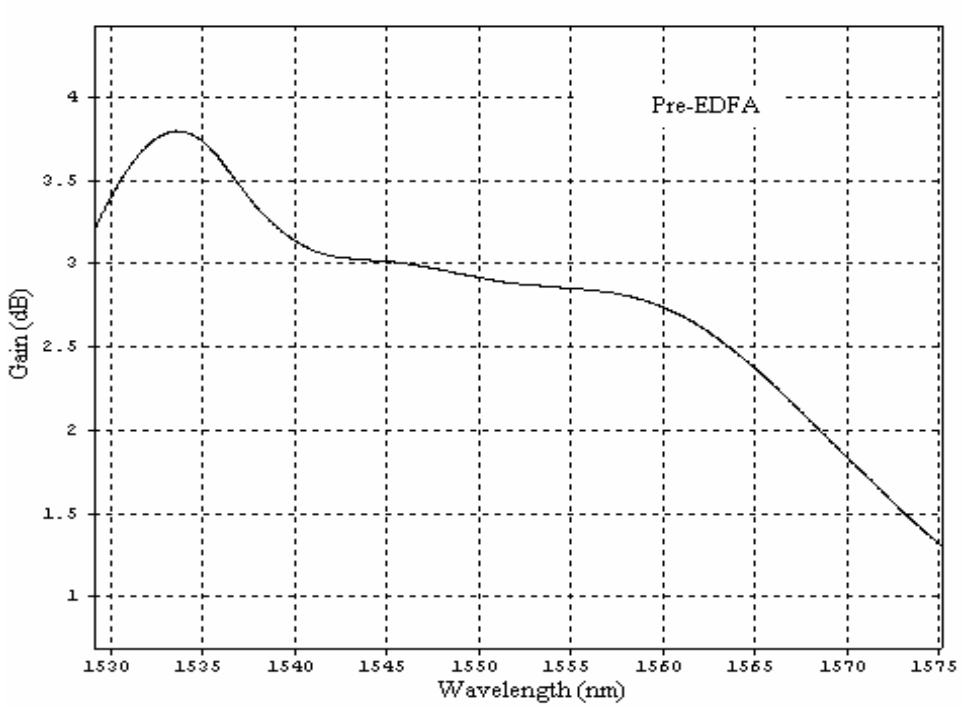

Figure 6.9: Gain as the function of wavelength of pre-EDFA for gain flattening approach-III.

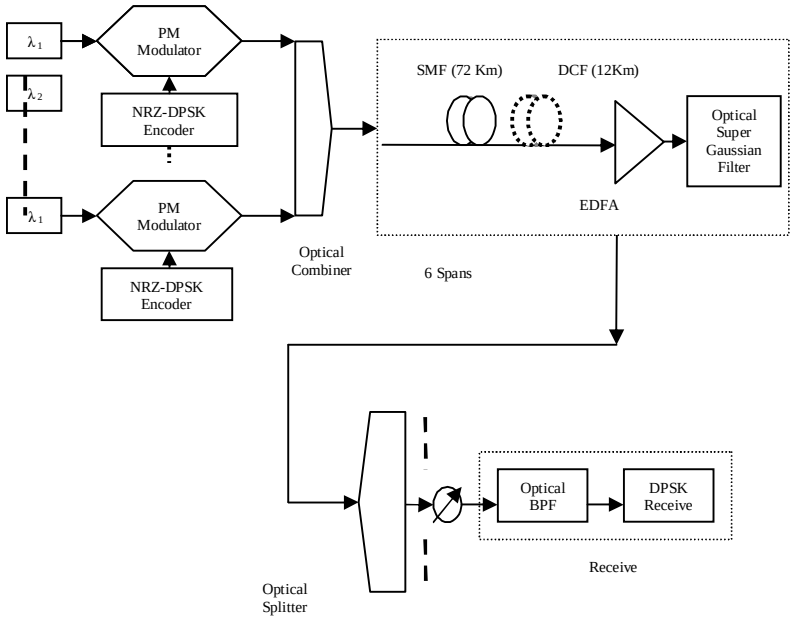

Figure 6.10: Schematic setup of transmission system of 16 × 40 Gb/s WDM signals.

It is also observed from figure (6.6); large power improvement is noted for transmission distance of 490 km. This shows an improvement over [Taga *et al.*, 1994; Chung and Chung, 2005; Miyamoto *et al.*, 1999; Pizzinat *et al.*, 2003]. Hence, the highest bit rate distance product of 313.6 Gb/s Mm is obtained for 40 Gb/s by using cascaded physical EDFAs. This bit rate distance product also shows an improvement over [Rottwitt *et al.*, 1993; Pizzinat *et al.*, 2003].

6.4 Gain Flattening of EDFA by Using Optical Super Gaussian Filter

In order to flatten the response of EDFA, the simulation has been performed as shown in figure (6.10). The time domain simulation is carried out with centre wavelength of 1550 nm. The value of all parameters is taken as reported in table (6.1). But optimum evaluated length is 10 meters for the EDFA. The length of EDFA is used to compensate the transmission link power drop. The peak gain of EDFA is notched by using optical super Gaussian notch filter with bandwidth 500 GHz at centre wavelength of 1532.5 nm. As we increase the pump power the gain increases. But variation of the gain with wavelength is non uniform. It is observed that at 20 dBm pump power with notch filter, we achieve a uniform gain for 20 nm bandwidth with gain excursion of ± 2 dB.

6.4.1 Simulation and Results of 16 × 40 Gb/s WDM Signals Transmission

The transmission performance of WDM signals using cascaded EDFA is analyzed. This EDFA parameter as in table (6.1) has constant gain for large bandwidth. The centre frequency of simulation is shifted to 1546 nm so that both sides bandwidth can be used with the constant gain approach. The notch filter is used so that for long distance transmission, the channels near 1530 nm does not saturate the EDFA quickly at small transmission lengths. The schematic setup of 16 × 40 Gb/s WDM system is shown in figure (6.10). For this, the DPSK signal is formed by encoding a continuous wave (CW) Lorentzian light source and data in terms of NRZ-DPSK (non return to zero differential phase shift keying) format launched into optical phase modulator. The NRZ data was pseudorandom binary sequence (PBRS) with word length 2^{10}-1 at 40 Gb/s. The full wave half maxima (FWHM) line_width of continuous wave light source is 1 MHz. The low pass Bessel filter have 3 dB bandwidth of 40 GHz for generation of data source in terms of NRZ format. Then this DPSK signal is launched into transmission link followed by EDFA for measuring the response.

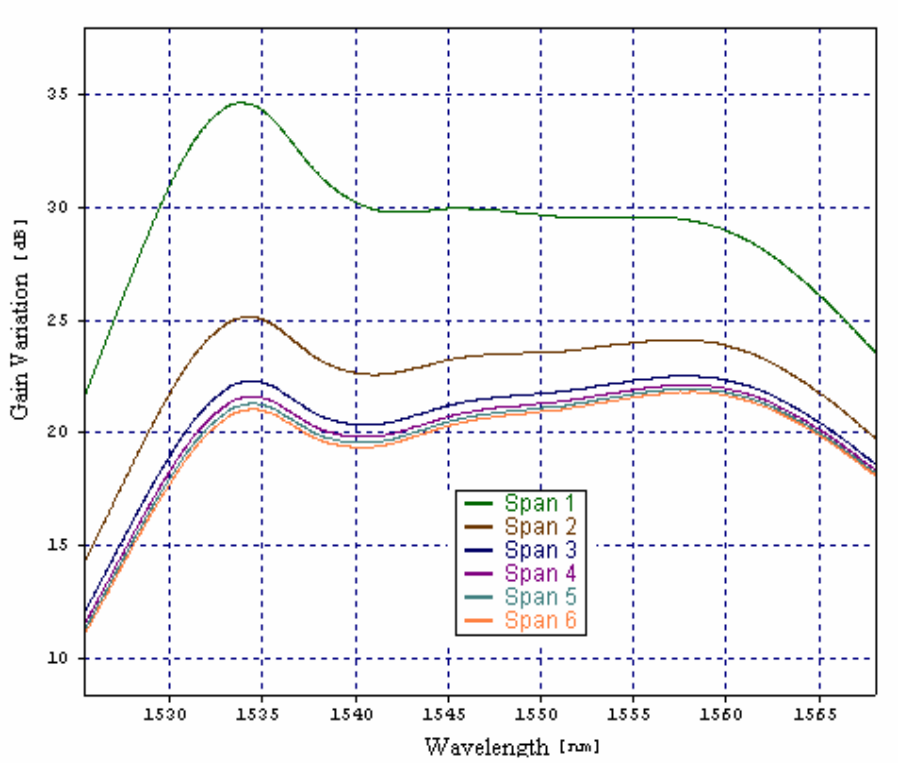

Figure 6.11: Gain variation with wavelength for different transmission spans.

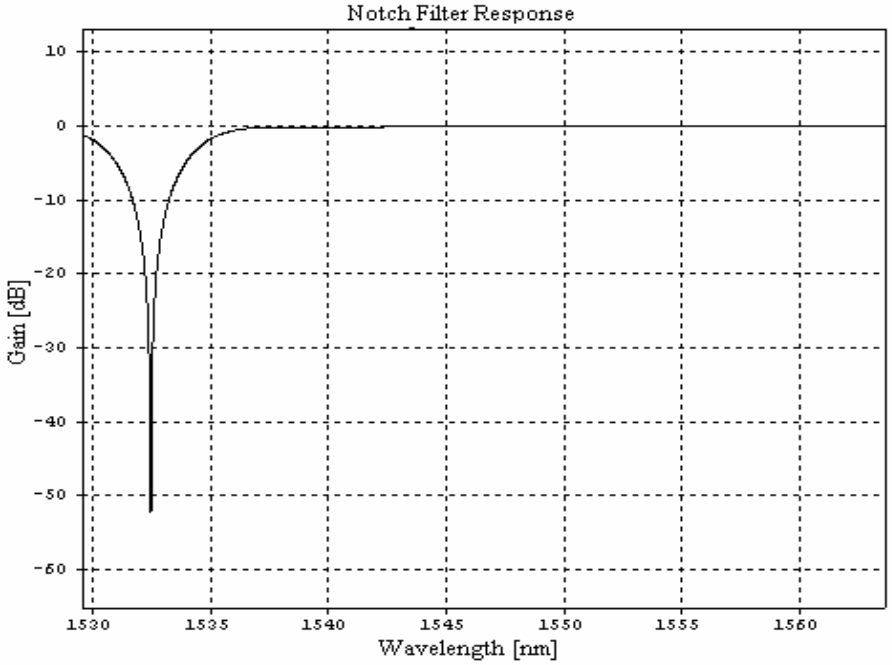

Figure 6.12: Optical super Gaussian notch filter response with wavelength.

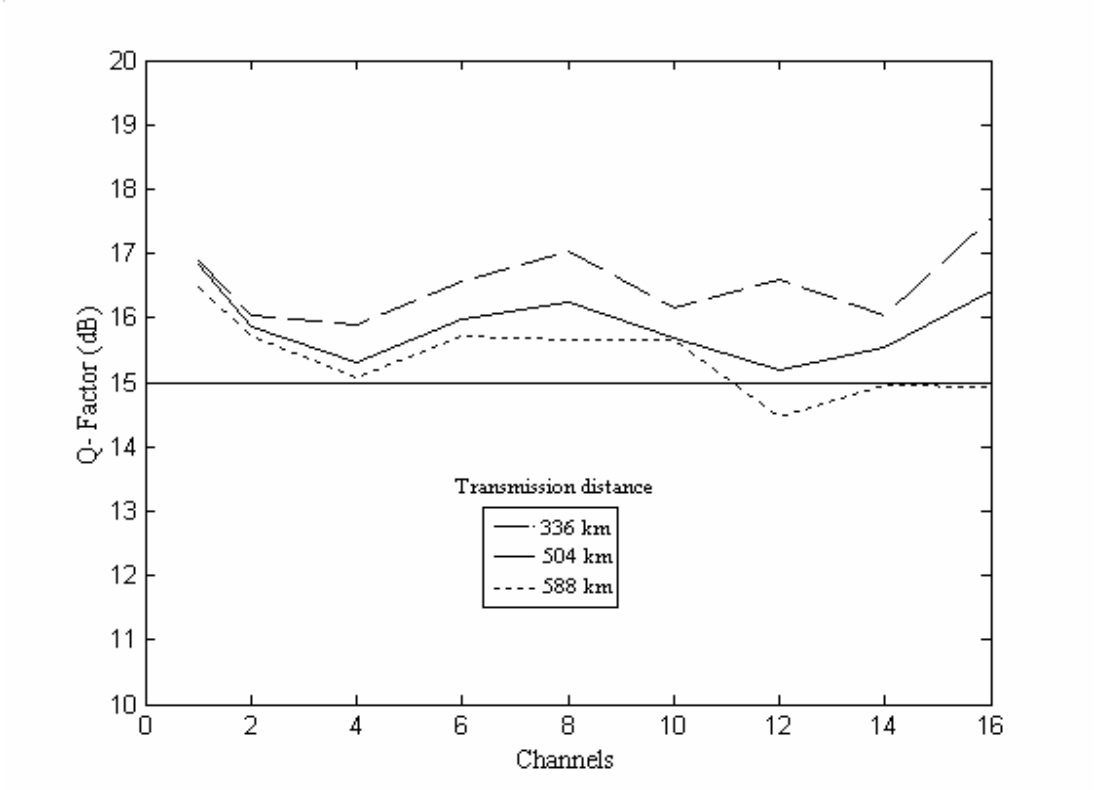

Figure 6.13: Quality variation with wavelength for different transmission distances.

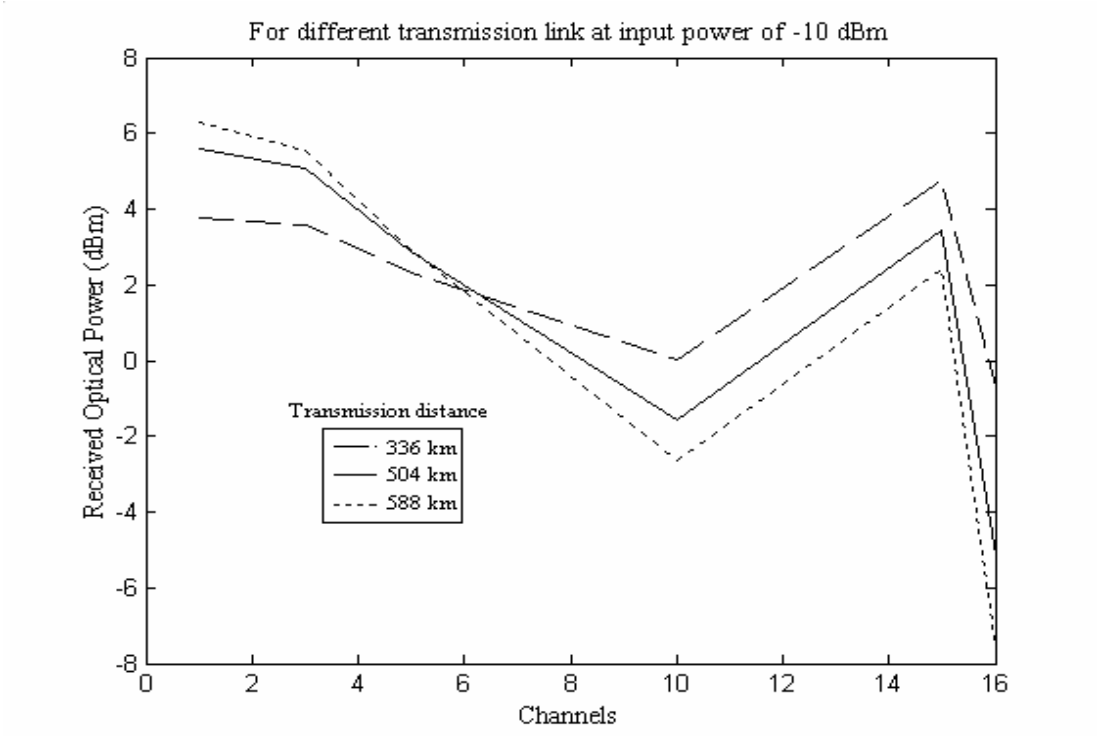

Figure 6.14: Received optical power variation with wavelength for different transmission distances.

At the output, a raised Cosine optical filter with bandwidth 50 GHz is used. The output of the filter is fed into DPSK receiver for detection of signal. Sixteen Lorentzian shaped line_width laser sources in the wavelength range from 1534 nm to 1558 nm (200 GHz channel spacing) are each modulated by optical $LiNbO_3$ phase modulators with a non return to zero (NRZ) format. The input of each transmission channel is -10 dBm. Therefore, the design carries 640 Gb/s WDM NRZ signals over different transmission distances with 84 km EDFA spacing.

Each of the spans consists of a 72 km standard single mode fiber (SMF), one or more DCF (dispersion compensating fiber) and an EDFA at the end. For SMF, the value of the dispersion parameter *D* is 17 ps/km-nm at the operating wavelength. The corresponding value for the DCF is six times greater with opposite sign. The loss of SMF is 0.2 dB/km and loss of DCF is 0.55 dB/km. The time domain simulation is performed for the setup shown in figure (1) with centre wavelength 1546.65 nm and 4.28 THz bandwidth.

The variation of gain with the wavelength for increase in spans is shown in figure (6.6). The response of optical super Gaussian notch filter is also shown in figure (6.12). It is observed that the gain of EDFA goes on flattening with increase in transmission distance as shown in figure (6.11). As from figure (6.10), the peak gain of EDFA is eliminated by notch filter in each span. Here notch filter is used in cascaded manner as EDFA. first order super Gaussian notch filter is used and EDFA for long distance transmission at high bit rate.

As shown in figure (6.13) as the transmission distance is increased, the quality of received signal goes on decreasing for all channels. This is due to the saturation of EDFA. As the gain of EDFA is not uniform, so some channels get saturated more as compared to near channels. Therefore, quality of received signal goes on decreasing. The power received for all transmission distance is more than applied input power of -10 dBm as shown in figure (6.14). As from figure (6.11), even the gain of EDFA moves toward flattening but due to continuous increase in input power after every span the EDFA reaches to saturation for some wavelengths. It is observed from figure (6.13) that all channels show good quality for transmission distance of 336 km. This shows improvement over the results reported in [Taga *et al.*, 1994; Chung and Chung, 2005]. For transmission distance of 504 km, the quality of signal reduces due to power saturation of EDFA. But all channels show quality more than 15 dB *i.e.* the power margin. This shows an improvement over [Taga *et al.*, 1994; Chung and Chung, 2005; Miyamoto *et al.*, 1999; Pizzinat *et al.*, 2003]. As the transmission distance increases up to 588 km, the quality of

Table 6.2

Power budget for transmission distance 504 km.

Parameters	336 km	504 km
Launched power	-10 dBm	-10 dBm
Fiber loss	84 dB	126 dB
Maximum Redundant Amplifier gain	~120 dB	~150 dB
Input and output insertion loss	3.2 dB	4.8 dB
Receiver sensitivity	-0.71 dBm	-5.15 dBm
Power Penalty	Nil	Nil
Margin	9.29 dB	4.85 dB

some received wavelengths near the peak gain of EDFA is lower. This is due to the saturation of EDFA.

The improved power budget calculated is reported in table (6.2). This shows good improvement in received power at reasonable quality for 504 km. Hence, the highest bit rate distance product of 322.56 Gb/s Mm is obtained for 40 Gb/s by using cascaded EDFAs. This bit rate distance product also shows an improvement over [Singh and Kaler, Sept. 2006].

6.5 Conclusions

The sixteen channels NRZ-DPSK signals transmission distance over 490 km at 40 Gb/s is simulated. This can be achieved by the gain flattening approach-III of the EDFA. The gain spectrum additions of these EDFAs make the gain nearly flat. Therefore, bit rate distance product of 313.6 Gb/s Mm is achieved.

The simulation of sixteen channels NRZ-DPSK signals transmission distance over 504 km at 40 Gb/s has been done for the first time. It is possible by placing optical super Gaussian notch filter after the EDFA in each span. The gain spectrum of the EDFA is moved towards flattening with increase in transmission distance. Hence, bit rate distance product of 322.56 Gb/s Mm can be achieved.

Chapter 7
Wavelength Converters for Optical Communication Networks Based On Semiconductor Optical Amplifiers

7.1 Introduction

This chapter deals with wavelength converters for optical communication networks based on the FWM and XPM in SOAs, which is the third objective of this research work.

Wavelength converters eliminate wavelength blocking in optical cross connects in wavelength division multiplexed (WDM) networks and also increase the flexibility and capacity of the network for a fixed set of wavelengths [Durhuus *et al.*, 1996]. The wavelength conversions based on semiconductor optical amplifiers (SOAs) and semiconductor lasers have been focused during the last few years [Kovacevic and Acampora, 1996; Durhuus *et al.*, 1996].

The wavelength converter is improved here by enhancing these nonlinearities of SOAs *i.e.* FWM and XPM. The structural optimization of SOAs is done for enhancing the FWM and XPM effects. We have successfully simulated 50 nm up and down wavelength conversion for non-return to zero differential phase shift keying (NRZ-DPSK) signal by using four wave mixing in a semiconductor optical amplifier (SOA) at 10 Gb/s. The chapter also provides the wavelength conversion using XPM in the SOA-MZI configuration with wide band more than 15 nm up and down conversions.

7.2 Wide Band Optical Wavelength Converter Based On Four Wave Mixing

Unlike wavelength converters based on cross gain modulation and cross phase modulation in SOAs, four wave mixing (FWM) based converters keep both amplitude and phase information and remain transparent to signal format [Durhuus *et al.*, 1996; Ludwig and Raybon, 1994]. It has also other capabilities including multi-wavelength conversion and fiber dispersion compensation [Ludwig and Raybon, 1994]. In a four wave mixing based converter [Agrawal, 2002], if v_1 and v_2 are the frequencies of input signal and the converted signal, the pump frequency chosen is such that

$$v_p = \frac{v_1 + v_2}{2}$$

At the SOA output, a replica of the input signal appears at centre frequency v_2. FWM requires the presence of both pump and input signal [Agrawal, 2002].

Wavelength conversion using four wave mixing effects in SOA generally has poor efficiency and narrow conversion range. FWM based wavelength conversion is limited when it is used in an ON-OFF keying (OOK) based transmission system. The signal power must be increased to maintain the OSNR (optical signal to noise ratio) resulting in variations of SOA gain and distortion in the converted signal. Lu *et al.* [2000] determined that a signal-to-pump ratio of -9 dB was required to achieve a trade off between OSNR and pattern distortion. It is noted that DPSK provides a 3 dB reduction in the received OSNR which is required for a given bit error rate [Xu C. *et al.*, 2003]. RZ-DPSK has a continuous pulse sequence and eliminates the pattern effect from the converted signal. This improves the OSNR (optical signal to noise ratio) of the converted signal.

Li *et al*. [2004] demonstrated single stage FWM wavelength conversion at 10 Gb/s for an RZ-DPSK signal with a signal-to-pump ratio of -3.8 dB and Q penalty of 1.5 dB to achieve better performance as compared to ON-OFF keying format. It has been reported that a ten stage cascade wavelength conversion is possible for 800 km transmission distance at 10 Gb/s using four wave mixing in SOA with narrow conversion range [Li *et al*., 2004].

Morgan *et al.* [1999] demonstrated all-optical wavelength translation over 80 nm at 2.5 Gb/s using two orthogonally polarized pumps. Hsu *et al.* [2004] demonstrated wavelength conversions with high efficiency of -10 dB over an 80 nm range at 10 Gb/s with the help of assisted beam and dual pump four wave mixing.

Earlier work on wavelength converters using FWM in SOA was limited to 80 nm wavelength conversion at 10 Gb/s. The Q factor penalty was found to be 1.5 dB at the narrow range of conversion, the work has been extended as reported in [Li *et al.*, 2004; Hsu *et al.*, 2004] for wide band conversion at 10 Gb/s by using numerical simulation. The structure of the semiconductor optical amplifier has been optimized to achieve minimum gain fluctuations with enhanced four wave mixing. Our simulated results show that the Q factor penalty can be reduced to -1.74 dB at 50 nm wavelength translation at 10 Gb/s.

The maximum transmission distance reported [Li *et al.*, 2004] for cascaded wavelength converter is less than 800 km for narrow conversion at a bit rate of 10 Gb/s. We have increased the maximum cascaded wavelength conversion distance to more than 1300 km by using an optimized SOA for wide band conversion.

7.2.1 Theoretical Analysis

The input signal applied to the SOA, P_{in}, is equal to $P(0)$. The output power, P_{out}, is equal to $P(L)$ or GP_{in}, where L is the length of semiconductor optical amplifier. The amplification factor, G, is given by:

$$G = \frac{P_{out}}{P_{in}} \tag{7.1}$$

In gain saturation [Agrawal. 2002], the optical gain per unit length, g, is reduced when P_{in} becomes comparable to saturation power P_s. Also the amplification factor G decreases with an increase in the signal power. The optical gain is found to saturate as:

$$g = \frac{g_o}{1 + P_{in}/P_s} \tag{7.2}$$

Where the small signal gain g_o is given by

$$g_o = \Gamma a\left(\frac{I\tau}{qV} - N_t\right) \tag{7.3}$$

Where Γ is the confinement factor, a is the differential gain, V is the active region volume, I is the bias current, τ is the carrier lifetime, q is the charge of electron and N_t is the transparency carrier density of the SOA.

Using the initial condition $P(0) = P_{in}$ together with $P(L) = P_{out} = GP_{in}$, the relation for large signal amplification gain is obtained:

$$G = G_o \exp\left(-\frac{(G-1)P_{out}}{G \quad P_s}\right) \tag{7.4}$$

This equation shows that the amplification factor G decreases from its unsaturated value G_o when P_{out} becomes comparable to P_s. The output saturation power P_{out}^s is defined as the output power for which the amplifier gain G is reduced by 3 dB from its unsaturated value G_o.

$$P_{out}^s = \frac{G_o \log_e 2}{G_o - 2} P_s \tag{7.5}$$

Here, P_{out}^s is smaller than P_s by about 30%, so we need $G_o >> 2$ in practice. P_{out}^s becomes nearly independent of G_o for $G_o > 20$ dB. The unsaturated gain is

$$G_o = g_o L \tag{7.6}$$

The gain variation, Δg , from Chapter 2

$$\Delta g(t_1,z_1)=\frac{a\Gamma}{\tau P_L}\left[\frac{I\tau}{wqt_a}\exp\left(\frac{\Delta P_1}{\tau}\right)+\sum_{n=1}^{M}\frac{(-1)^n}{P_L^{n-1}}L\exp\left(\frac{\Delta P_n}{\tau}\right)\times \left[\overline{N}^n(t_n,z_n)-(N(t,z)-N_t)\overline{P}^{n-1}(t_{n-1},z_{n-1})\right]\right] \tag{7.7}$$

If the carrier lifetime is increased, the gain variation is reduced as reported in [Xu *et al*., 2003]. Similarly, if the bias current is decreased, then the gain fluctuations and crosstalk are reduced. But by reducing the injection current from equations (7.3) and (7.6), the amplification factor is reduced. The injection current can be optimized for minimum gain fluctuation at sufficient amplification. Increasing the confinement factor produces gain saturation and increases crosstalk. Increasing launched power also leads to an increase in the induced crosstalk.

7.2.2 SOA Parameters

The standard InGaAlAs traveling wave SOA with negligible residual facet reflectivity is taken as the amplifier model in our simulations. After solving the rate equation (7.7) mentioned above and optimizing for the enhancement of FWM effect, the relevant parameters are as follows: the length is 500 μm, the width of the active layer is 2 μm, its thickness is 0.15 μm and the optimized confinement factor is 0.3. The transparency carrier density in the SOA is taken to be 1×10^{18} cm^{-3} and the differential gain is 3×10^{-16} cm^2. The carrier recombination time τ at this density is estimated to be 300 ps, which gives the saturation power P_s = 14.24 mW. The small signal gain ranges from 35.56 dB to 33.25 dB for input signal ranging from -40 dBm to +10 dBm. The optimum bias current is evaluated to be 400 mA which is in agreement with the results reported in [Yamatoya and Koyama, 2004], as faster response was obtained at higher bias currents. The input and output coupling losses of SOAs are taken as 3 dB.

7.2.3 SOA Validation

The various parameters of SOA are taken to optimize four wave mixing in SOA and improve the efficiency of the wavelength converter. The simulation setup is shown in figure (7.1). The DPSK signal is formed by sending a continuous wave (CW) Lorentzian light source into an optical phase modulator. The NRZ data was a pseudorandom binary sequence (PBRS) with word length 2^{10}-1 at 10 Gb/s. The full wave half maxima (FWHM) line_width of the CW light source is 5 MHz. A low pass Bessel filter with 3 dB

bandwidth of 5 GHz is used for NRZ format data generation. The DPSK signal is launched into a 3 dB optical coupler with pump power applied to another port of the coupler. After this, the coupler output is fed to the SOA with different parameters for measuring the response. The output of SOA (dark black) is measured using a raised cosine optical filter with bandwidth 20 GHz and centre wavelength of 1530 nm. The filter output is fed into DPSK receiver for detection of received signal at 1530 nm. We are using variable bandwidth simulation (VBS) technique for all setups in this paper. The simulation accuracy is statistical. The overall amplitude error is 0.3 dB and the overall group delay error is 1.2 ps. The variable bandwidth simulation is carried out with simulation bandwidth of 6.11 THz and centre wavelength of 1550.39 nm.

The OSNR is calculated with resolution of 0.01 THz. The results are shown in figures (7.2), (7.3) and (7.4). The results are shown in figure (7.2) for optical power versus wavelength. It is observed that with the increase in the confinement factor, the four wave mixing effect is pronounced due to gain variations in the SOA, as seen in the equation (7.7). It is further observed that if the confinement factor increase to 0.4, the SOA-induced crosstalk increases which produces gain saturation. Hence, gain saturation increases in FWM signals and poor eye quality is observed at the output. When confinement factor is 0.2 or less, the FWM is low and the detected signal is poor as shown in the eye diagram in figure (7.2).

But when confinement factor is 0.3, the high quality is observed in the eye pattern at the receiver. As shown in table (7.1), the highest Q factor (19.7 dB) and lowest jitter (0.006 ns) are observed for FWM signals at confinement factor 0.3.

The current is also optimized as shown in figure (7.3). The results show that as there is increase in current, the power level of the FWM signals goes on increasing rapidly, which shows an agreement with the above analysis. At a lower value of 300 mA, the FWM effect is less, so a poor eye pattern is observed at the output.

But for a high current of 500 A or more, there are more fluctuations in gain. Therefore, gain saturation occurs in the SOA and a poor eye pattern is observed for this current. At a bias current of 400 mA, a clear eye pattern is observed with sufficient FWM signals. For the bias current of 400 mA, the highest Q-factor of 16.55 dB and lowest jitter of 0.008 ns are observed for the FWM signal as shown in table (7.2).

The optimization of the active region width is also presented in figure (7.4). As the width of the active region of SOA increases, the gain fluctuations decrease. The FWM effect is reduced for a high width of 0.2 μm and the quality of the detected signal is good.

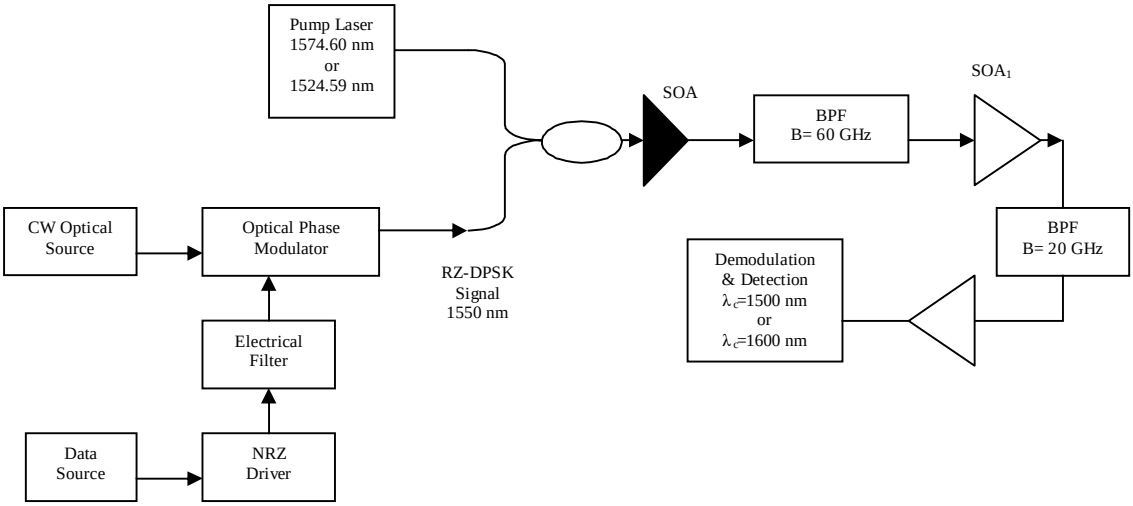

Figure 7.1: Schematic diagram of single stage up and down wavelength converter based on FWM in optimized SOA (dark black).

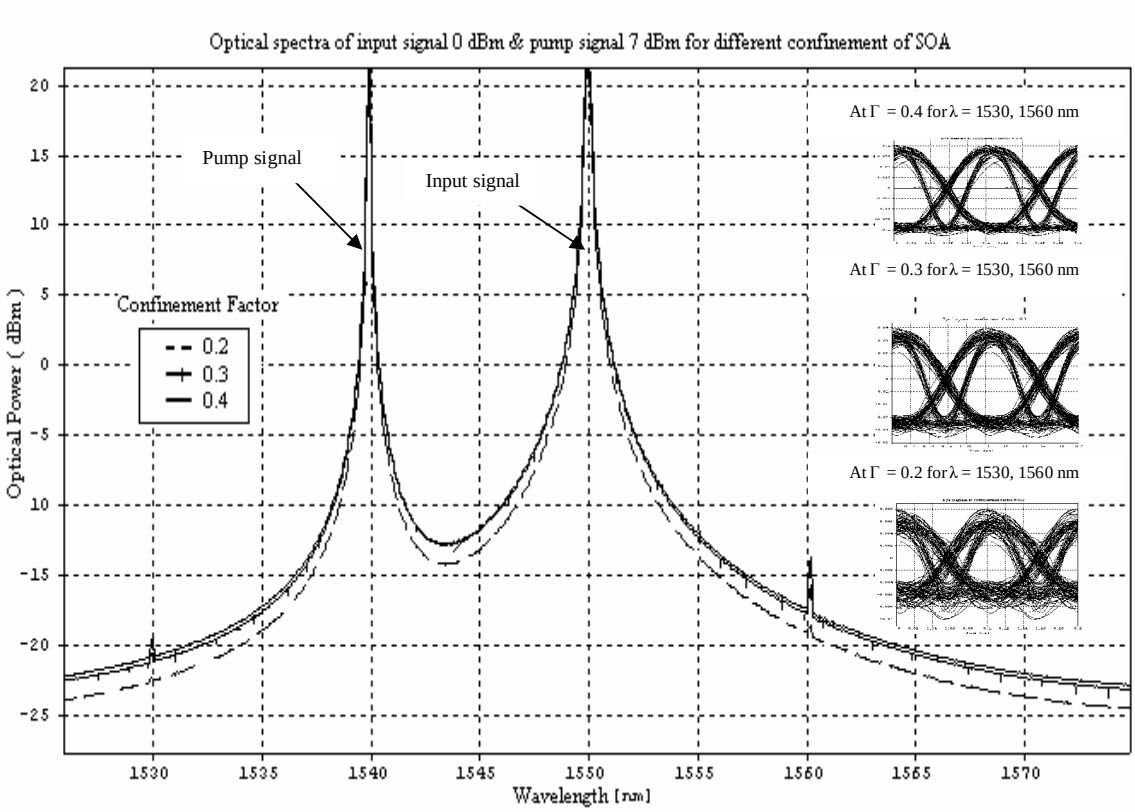

Figure 7.2: Optical power spectrum variations with wavelength of input, pump and FWM signals for different confinement factors of semiconductor optical amplifier with bias current and width of 400 mA and 0.15 μm respectively.

Table 7.1

Variation of quality and jitter for FWM signals with different confinement factors of SOA.

Confinement Factor	0.2	0.3	0.4
Q factor (dB)	14.1 dB	19.7 dB	12.9 dB
Jitter (ns)	0.01 ns	0.006 ns	0.015 ns

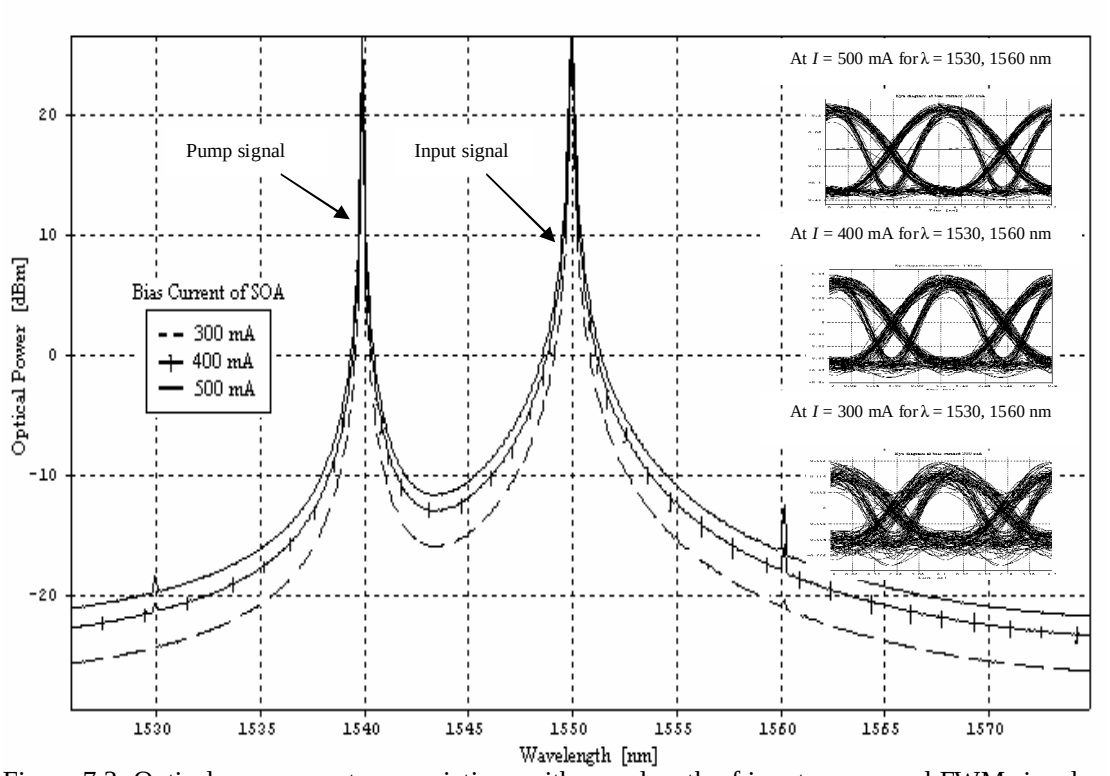

Figure 7.3: Optical power spectrum variations with wavelength of input, pump and FWM signals for different bias currents of semiconductor optical amplifier with confinement factor and width of 0.3 and 0.15 μm respectively.

Table 7.2

Variation of quality and jitter for FWM signals with different bias currents of the SOA.

Bias Current (mA)	300 mA	400 mA	500 mA
Q factor (dB)	10.69 dB	16.55 dB	12 dB
Jitter (ns)	0.012 ns	0.008 ns	0.013 ns

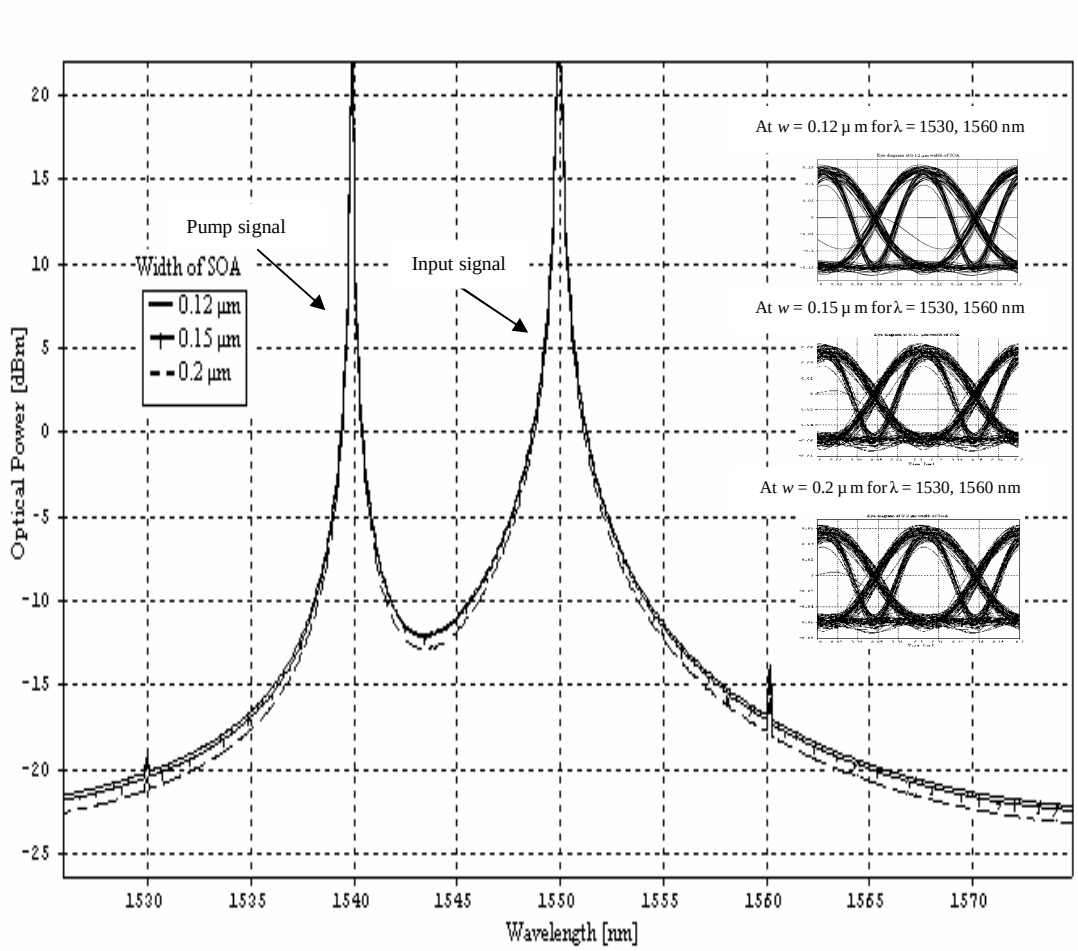

Figure 7.4: Optical power spectrum variations with wavelength of input, pump and FWM signals for different active region widths of semiconductor optical amplifier with optimized confinement factor and bias current of 0.3 and 400 mA respectively.

Table 7.3

Variation of quality and jitter for FWM signals with different active region widths of the SOA.

Width (µm)	0.12 µm	0.15 µm	0.2 µm
Q factor (dB)	11.3 dB	19.37 dB	16.44 dB
Jitter (ns)	0.016 ns	0.006 ns	0.008 ns

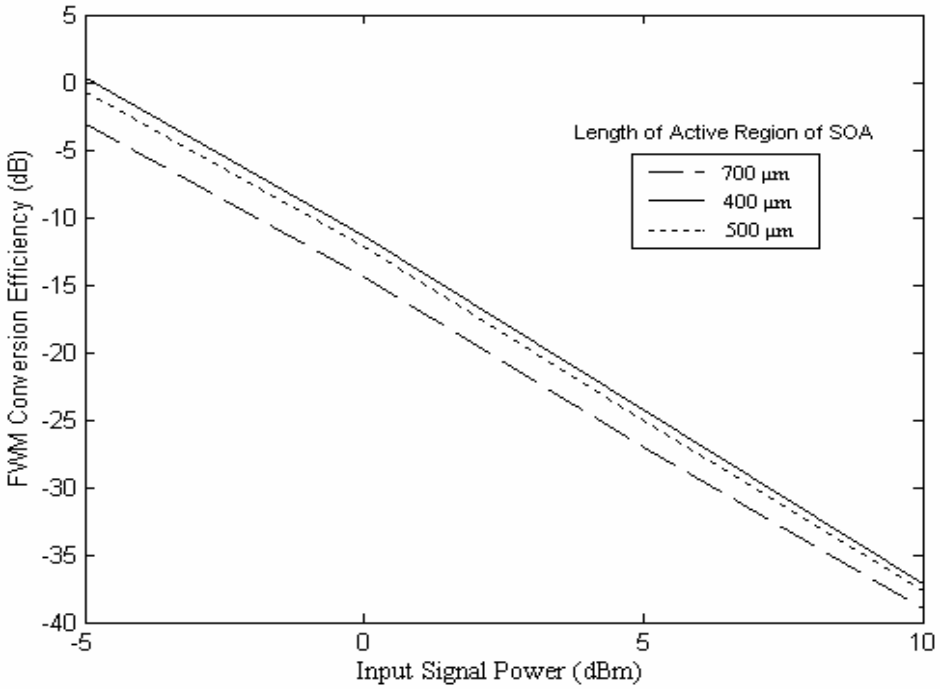

Figure 7.5: Four wave mixing conversion efficiency as the function of input signal power for different active region lengths of semiconductor optical amplifier. Taking optimized confinement factor, bias current and width of the SOA.

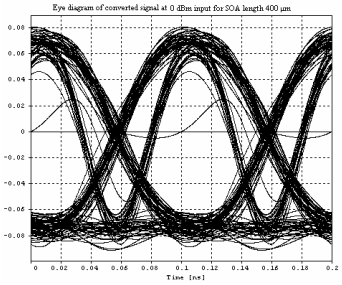

Figure 7.5a: Eye diagram of FWM signals at 400 µm.

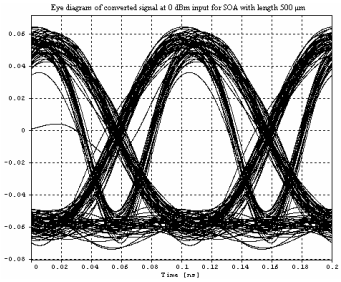

Figure 7.5b: Eye diagram of FWM signals at 500 µm.

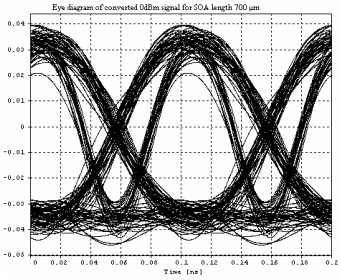

Figure 7.5c: Eye diagram of FWM signals at 700 µm.

Table 7.4

Variation of quality, jitter and conversion efficiency for FWM signals with different active region lengths of the SOA.

Length (µm)	400 µm	500 µm	700 µm
Q factor (dB)	17.23 dB	18.43 dB	22.73 dB
Jitter (ns)	0.033 ns	0.006 ns	0.005 ns
Conversion efficiency (dB)	-11.32 dB	-12.21 dB	-14.4 dB

For lower values of the active region width *i.e.* 0.12 μm or less, the FWM signals are pronounced due to gain variations in SOA. The crosstalk is generated, causing a poor eye pattern for the converted signal. But for the width of 0.15 μm, a clear eye is observed with good FWM signals. At 0.15 μm width of SOA, a good quality of 19.37 dB with lowest jitter 0.006 ns is observed for the FWM signals as shown in table (7.3).

The variation in length can be optimized by using FWM conversion efficiency. The four wave mixing conversion efficiency is given as the converted power at SOA output, divided by signal power at the SOA input.

The FWM conversion efficiency goes on decreasing with the increase in input signal. It is also observed that with an increase in active region length, the conversion efficiency of the SOA decreases. If the length of SOA is 400 μm or less, then we obtain poor quality of signal with high FWM conversion efficiency as shown in figure (7.5). For a longer active region length of 700 μm or more, we get poor FWM efficiency. But at 500 μm, good efficiency is obtained with a clear eye pattern as shown in figure (7.5b). For an active region length of 500 μm, good conversion efficiency of -12.21 dB is obtained at a sufficient quality factor of 18.43 dB with low jitter of 0.006 ns for FWM signals as shown in table (7.4). These results show that SOA optimization for enhanced FWM is possible.

The bandwidth of an optimized SOA is estimated as shown in figure (7.6). If we apply 0 dBm input signal to optimized SOA with different centre wavelengths, then approximately the same amplified output power is obtained for wavelengths from 1500 nm to 1600 nm. It implies that the gain of an optimized SOA is constant for this large band. The 3 dB bandwidth of optimized SOA is quite large. This shows good agreement with the result reported in [Yamatoya and Koyama, 2004]. Also from figure (7.6), good OSNR is observed for the entire band.

7.2.4 Single Stage Four Wave Mixing Based Wavelength Converter

In a FWM based wavelength converter, the pump signal wavelength is chosen as the average of the input and converted signal wavelengths. Therefore, the desired converted signal wavelength can be obtained by suitably choosing the wavelength of the pump signal. Figure (7.1) shows the simulation setup of wavelength converter. A Lorentzian laser source provides pump light at 1539.54 or 1559.54 nm for up and down conversions of 20 nm. The pump and signal lights are combined by a 3 dB optical coupler and launched into an optimized SOA as in section 7.2.4. At the output of SOA, an optical band pass filter with bandwidth of 60 GHz is used for selecting the converted signal.

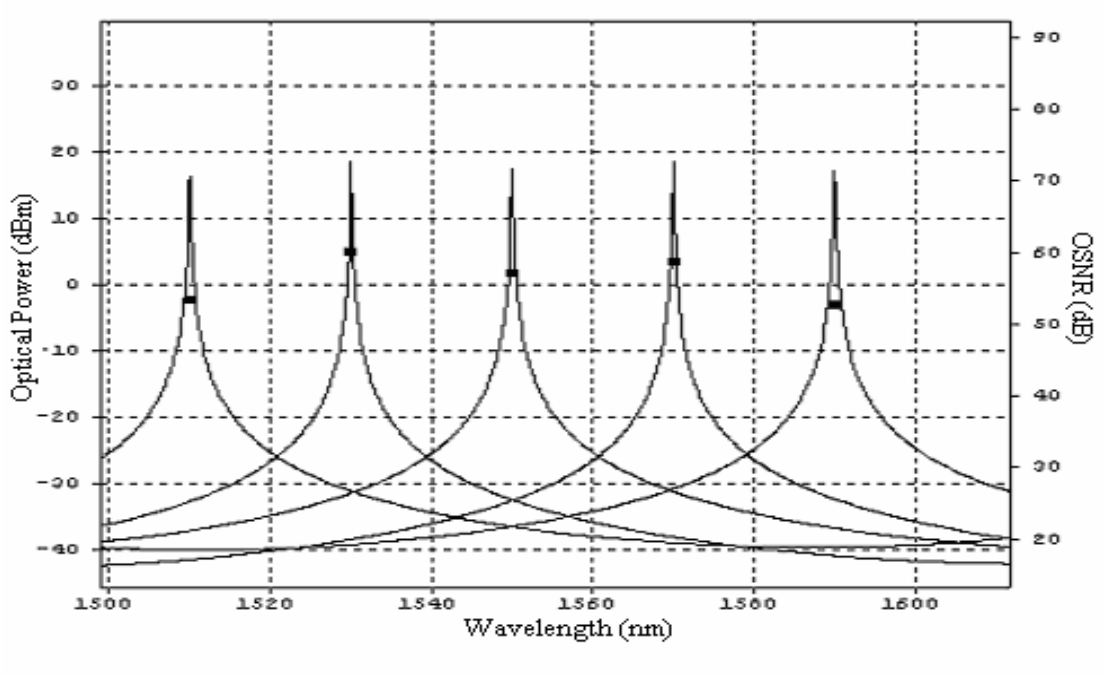

Figure 7.6: Optical output power of the SOA versus input light wavelength for 0 dBm input light power at 10 Gb/s with DPSK receiver.

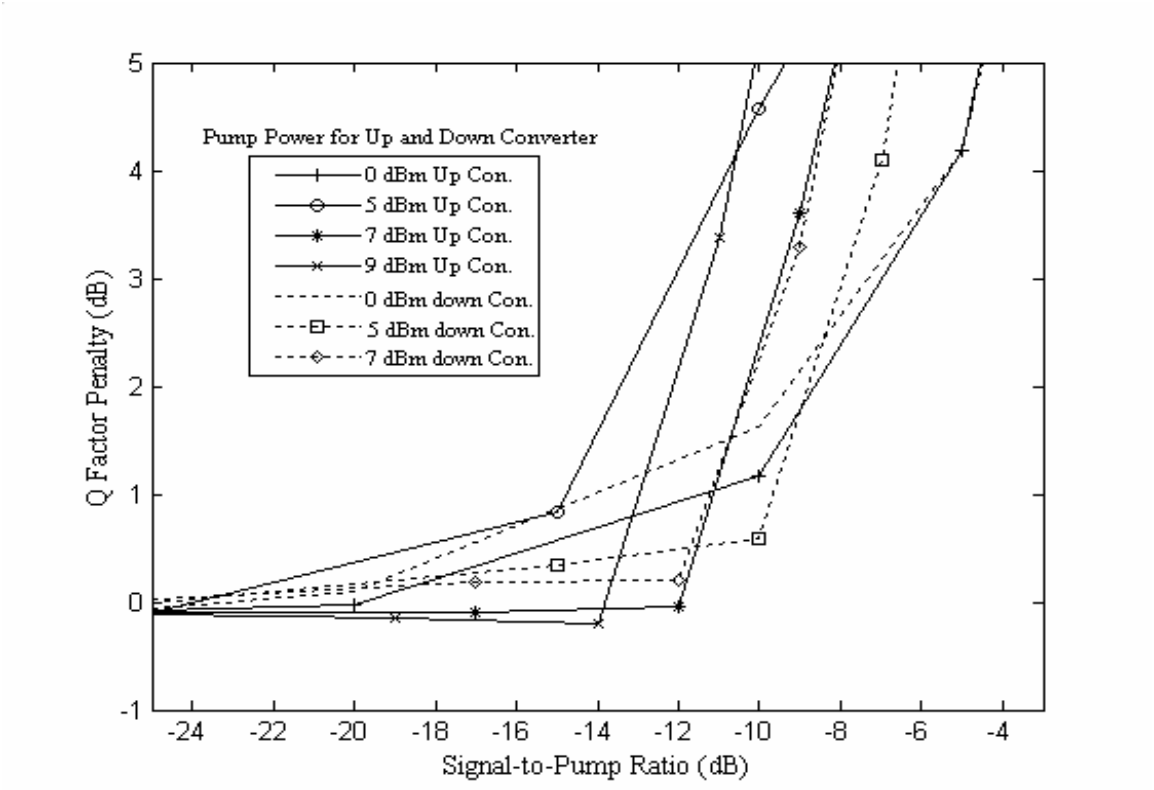

Figure 7.7: Variation of Q factor penalty with signal-to-pump ratio of different pump powers for 20 nm up and down wavelength conversion.

The signal is then fed to the SOA_1 as reported in [Singh and Kaler, Dec.2005], followed by another band pass filter with 20 GHz bandwidth for elimination of amplified spontaneous emission (ASE) noise. If a narrow optical band pass filter is used, then a good Q factor is obtained, but a large signal power drop occurs. For the detection of the converted optical signal, a DPSK receiver is used at the same 10 Gb/s bit rate of the transmitter.

If the conversion band is 50 nm or more, then the additional SOA_2 is used to improve the power level of the converted signal. For input signals from -20 dBm to +10 dBm, the unsaturated gain varies from 39.14 dB to 37.44 dB for SOA_1 or SOA_2 in-line amplifiers [Singh and Kaler, 2006]. The variable bandwidth simulations have been carried out between the lower limit and the upper limit wavelengths of 1502.97 nm and 1600.07 nm.

The optimal signal-to-pump ratio is evaluated for the wavelength converter in terms of Q factor penalty as shown in figure (7.7). The Q factor penalty is defined as the difference of quality factor before and after wavelength conversion and is an important factor to be considered. First of all, the simulation is carried out for 20 nm up and down conversions, with only SOA_1 used to amplify the weak converted signal. As shown in figure (7.7), we find the dependence of Q factor penalty at a given input signal power for different pump powers.

As we initially increase the input signal power, the Q penalty decreases for all pump levels. But if further increase the input signal, the Q penalty increases rapidly after gain saturation of SOA. As the pump power increases, the Q penalty becomes negative, which means an improved converted signal is obtained; but if we further increase the pump power, power drop of the converted signal occurs at a faster rate. The minimum Q factor penalty of -0.32 dB with signal-to-pump ratio of -45 dB for down conversion is measured. But typically, the signal-to-pump ratio needs to be maintained around -9 dB to achieve a trade off between signal OSNR and pattern effect [Lu *et al.*, 2000]. Therefore, the minimum Q factor penalty observed is 1.5 dB at -9 dB signal-to-pump ratio for down conversion at 5 dBm pump signal which is same as reported in [Li *et al.*, 2004]. The observed Q factor penalty is 3.29 dB at 7 dBm pump signal for the same converter. For the up conversion, quality improvement is observed for signal-to-pump ratio of -12 dB with pump levels 7 dBm and 9dBm. The minimum Q factor penalty observed is 1.5 dB at a signal-to-pump ratio of -9 dB at 0 dBm pump signal for up conversion which is the same as reported in [Li *et al.*, 2004].

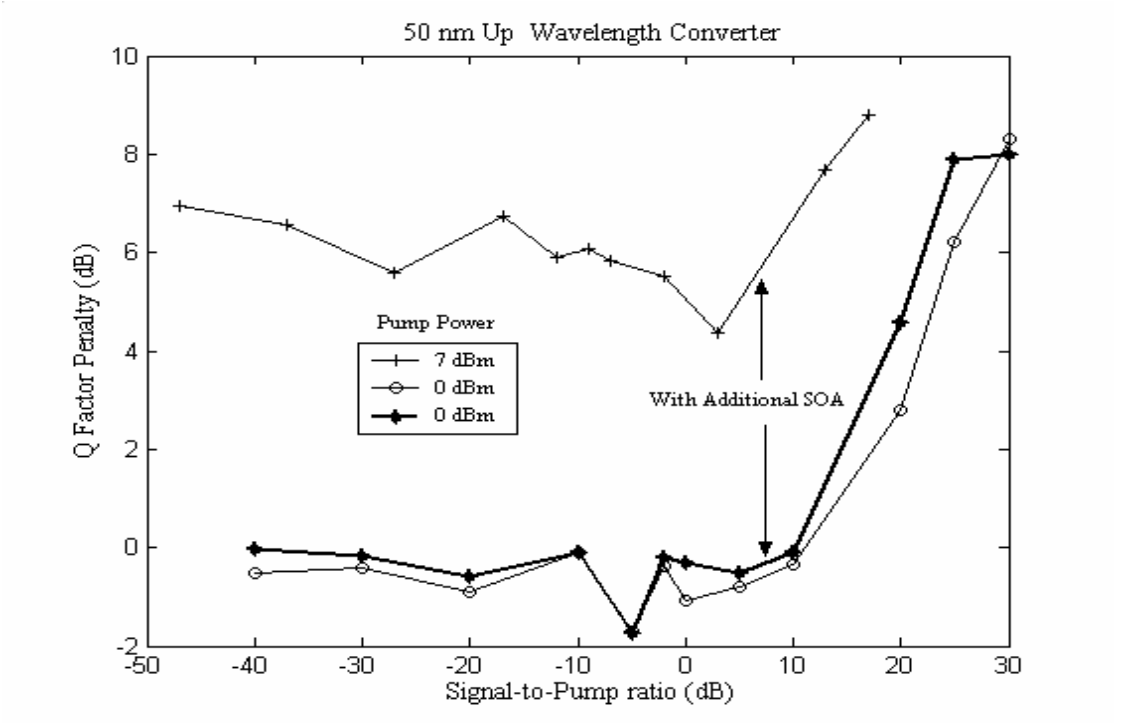

Figure 7.8a: Variation of Q factor penalty with signal-to-pump ratio of different pump powers for 50 nm up wavelength conversion.

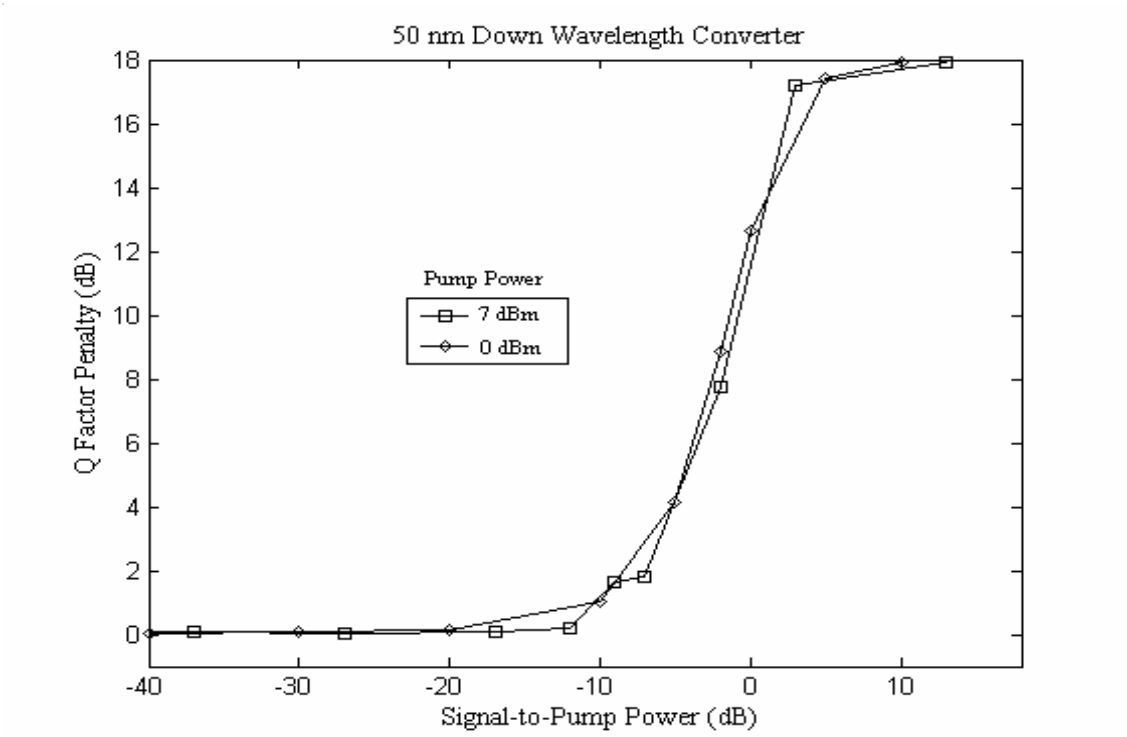

Figure 7.8b: Measured Q factor penalty as the function of signal-to-pump ratio of different pump powers for 50 nm down conversion.

The simulation is carried out for 50 nm up and down conversion with both the SOA_1 and SOA_2 used to amplify the very weak converted signal. Now, the Lorentzian laser source provides pump light at 1574.60 nm and 1524.59 nm for up and down conversion. As observed in figures (7.8a) and (7.8b), the Q penalty decreases up to the gain saturation point of the SOA. After this, the penalty increases rapidly. For down converter, the Q penalty is almost the same for pump powers from 0 dBm to +7 dBm as observed in figure (7.8b).

The minimum Q penalty is 1.65 dB for a signal-to-pump ratio of -9 dB, for both 0 dBm and 7 dBm pump power. For pump power of 7 dBm, the Q factor penalty is 2 dB, for the signal-to-pump ratio of -6 dB. It is also observed from the figure (7.8a) that minimum Q factor penalty is 6.08 dB at signal-to-pump ratio of -9 dB for up converter with pump power 7 dBm. It is investigated that the minimum Q factor penalty for up converter is -1.71 dB for the signal-to-pump ratio of -5 dB at 0 dBm pump signal, which is an improvement over the result reported in [Li *et al.*, 2004] for the small range SOA wavelength converter. The improvement observed in quality factor is 3.21 dB for this wide band wavelength converter as compared to the results reported in [Li *et al.*, 2004]. They reported the penalty of 1.5 dB for the same signal-to-pump ratio of -5 dB. Hence, the converted signal shows an improvement in quality over the applied input signal.

As shown in figures (7.9a) and (7.9b), the converted signal power increases up to gain saturation, then decreases with the increase in input signal. At 0 dBm pump power, it is observed that converted signal power is -26.6 dBm. With the addition of SOA_2 amplifier, the improvement in signal quality is 1.74 dB and the output power is improved to 8.35 dBm as shown in figure (7.9a). A clear eye pattern is also observed as shown in figure (7.9c).

The conversion efficiency of the up and down converters for different bands is also calculated. The conversion efficiency variation with input signal power is shown in figure (7.10). The additional SOA_2 amplifier is used in up conversion for high conversion efficiency over 50 nm.

The conversion efficiency decreases with the increase in input signal power. For down converter, the efficiency is less than the up converter with conversion band of 50 nm. But for conversion band of 20 nm, almost the same conversion efficiency is observed for both up and down conversions. The optical power spectrum is shown in figure (7.11) for up converted, down converted, pump and input signals.

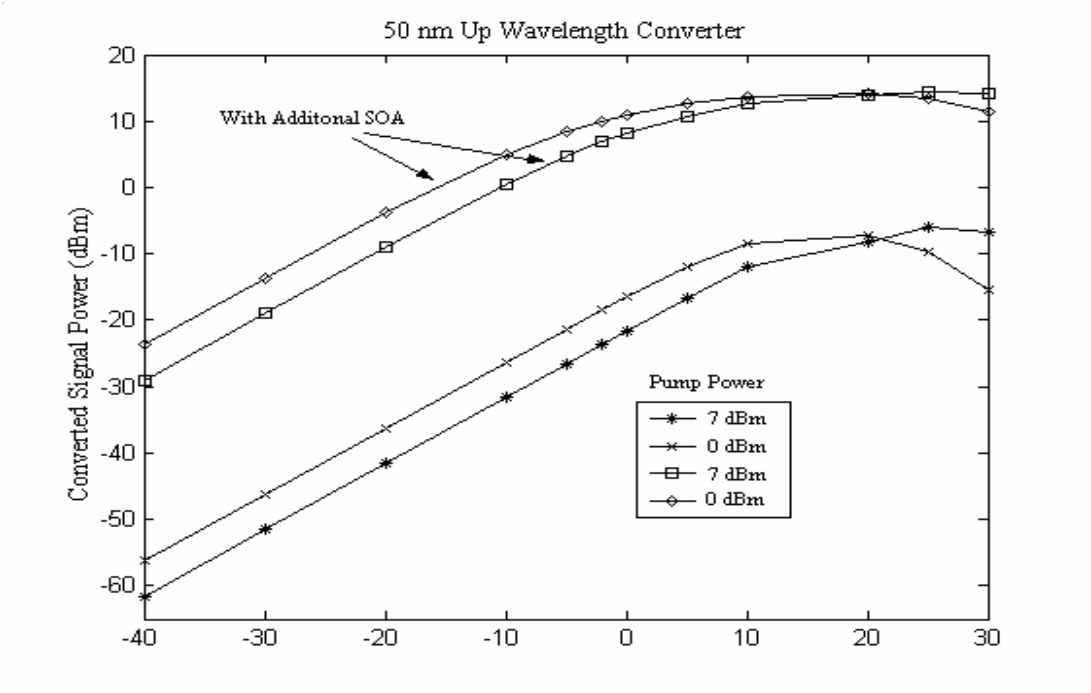

Figure 7.9a: Variation of converted signal power with input signal power of different pump powers for up converter with and without additional SOA_2.

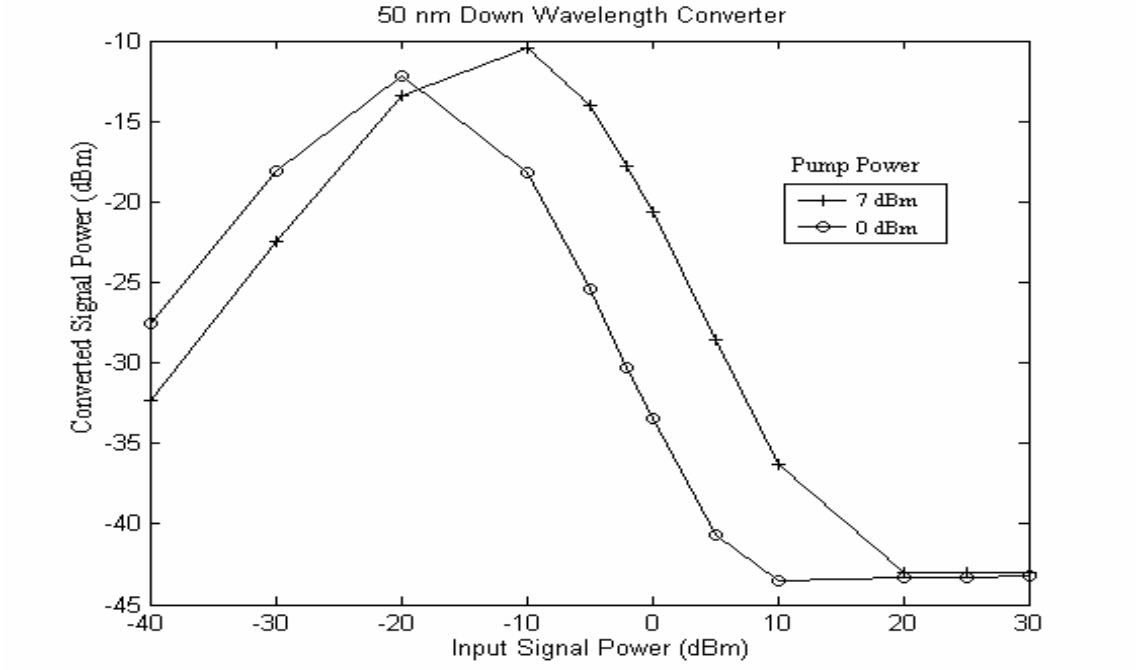

Figure 7.9b: Variation of converted signal power with input signal power of different pump powers for down converter without SOA_2 pre-amplifier.

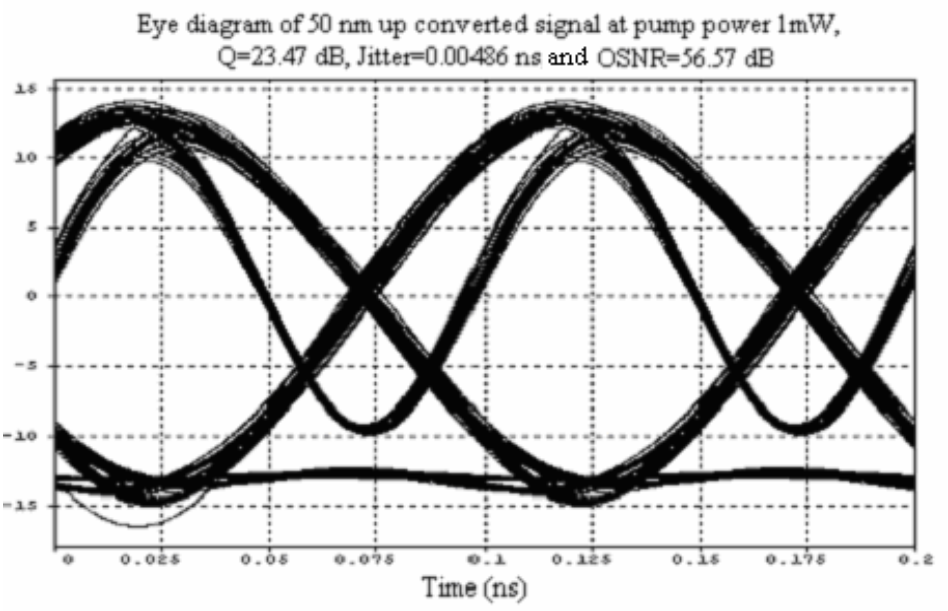

Figure 7.9c: Eye pattern of 50 nm up converted signal at 0 dBm signal-to-pump ratio.

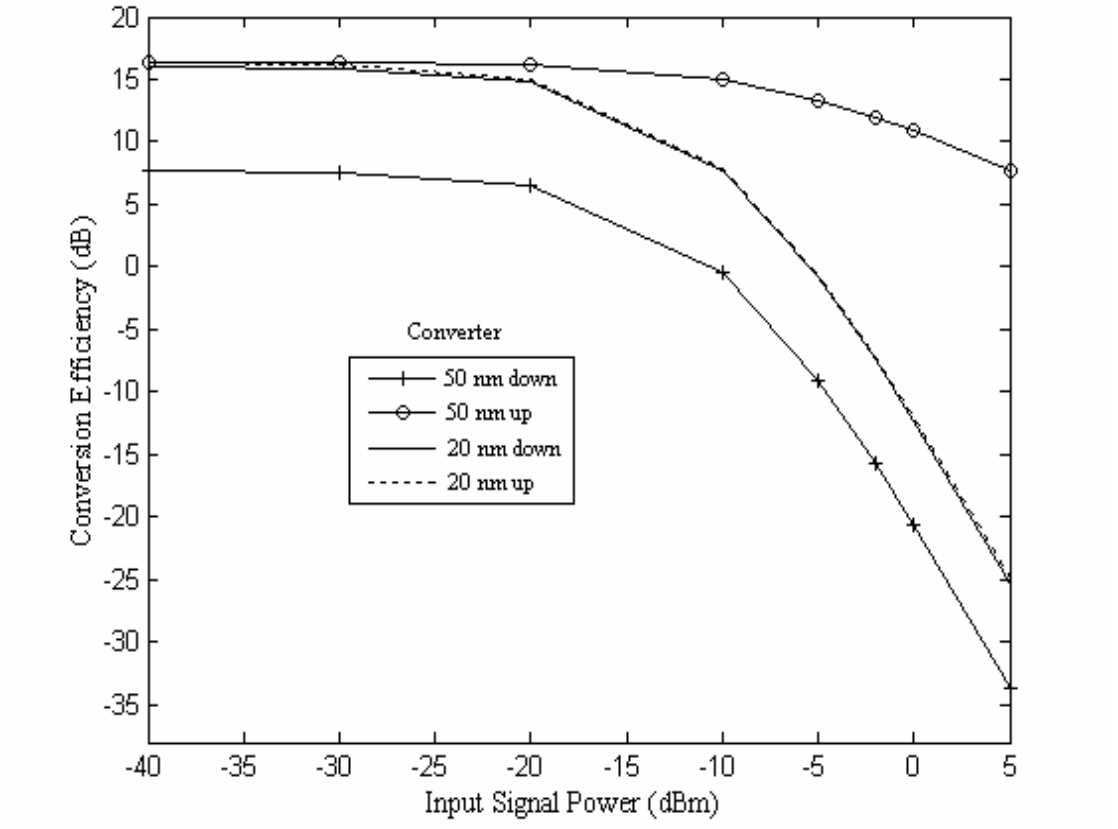

Figure 7.10: Conversion efficiency as the function of input signal power for up and down conversion with different band.

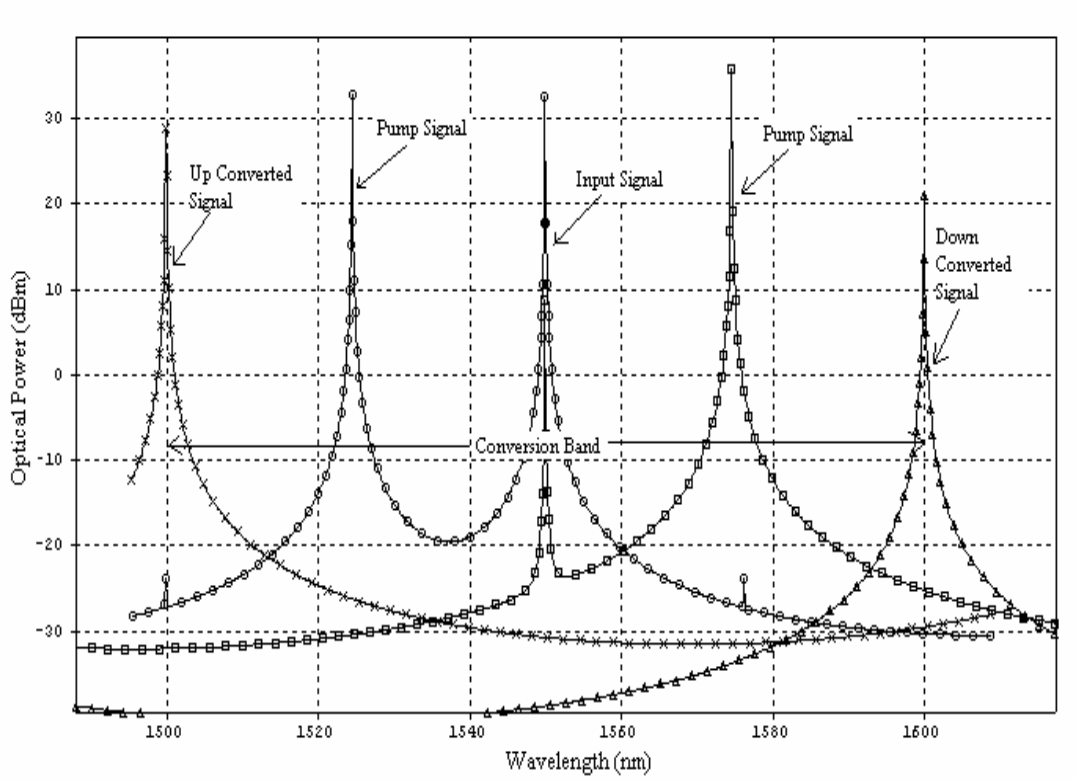

Figure 7.11: Optical spectrum for up converted, down converted, pump and input signal.

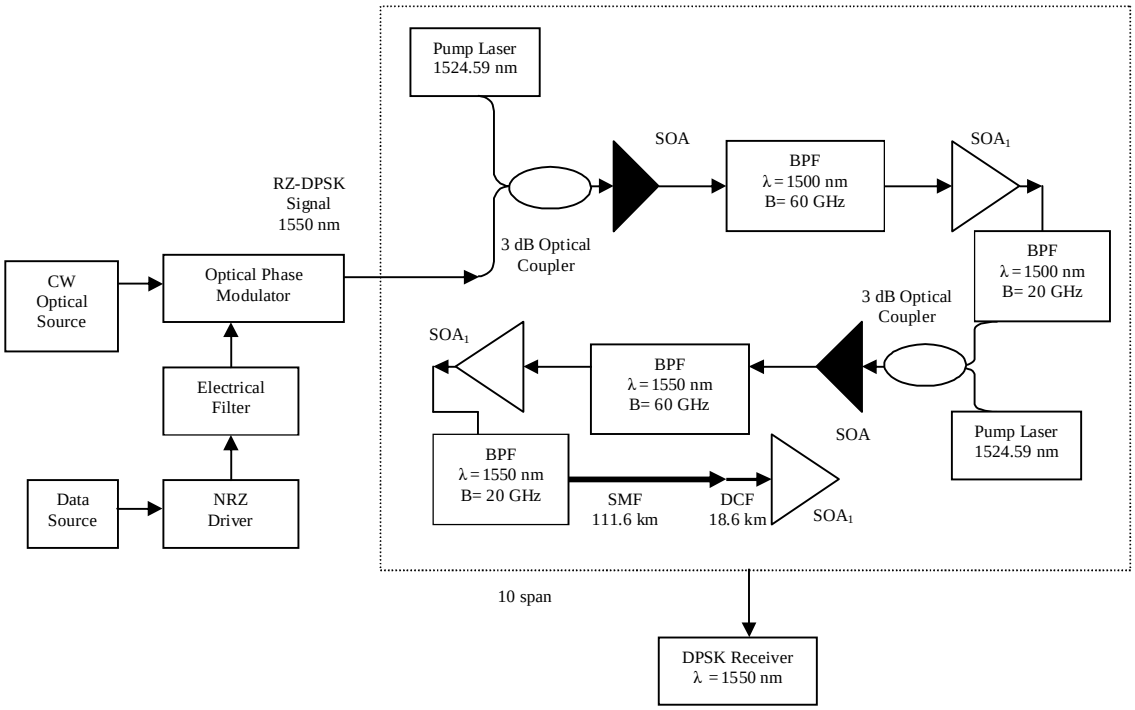

Figure 7.12: Re circulating span configuration of cascade wavelength conversion.

It is observed that the optimized SOA has large bandwidth. This is due to the constant gain for the input signal power which is less than the saturation power. The gain variation can be decreased by optimizing the SOA parameters. The quality of FWM signals is almost the same for the entire band with single SOA. But there is a power drop in converted signal for 50 nm up and down conversions. This power drop can be compensated using an SOA in-line amplifier. The conversion range measured is 100 nm for down to up conversion which is larger than that is reported in [Hsu *et al.*, 2004].

7.2.5 Cascaded Wavelength Conversion

In order to increase the capacity and flexibility of the optical networks using wavelength converter, it is essential to check the cascadability of this wavelength converter.

The same wavelength converter setup is used as above with down conversion of NRZ-DPSK signal format from 1550 nm to 1500 nm with pump power of 0 dBm. The same pump power is used for up conversion from 1500 nm to 1550 nm. Figure (7.12) represents a cascade configuration with a span count of 10 or higher for a long transmission distance of 1300 km.

The length of dispersion compensating fiber (DCF) is chosen in accordance with [Agrawal, 2002] for complete compensation ($\overline{D} = 0$). For SMF, the value of dispersion parameter D at the operating wavelength is 17 ps/km-nm. The corresponding value for DCF is six times greater with an opposite sign for the first and second order dispersion management. The loss of SMF is 0.2 dB/km and loss of DCF is 0.55 dB/km. A fully compensating system is formed. So for a transmission distance of 130.2 km, the optical input signal and output power signal are almost the same at -10 dBm with an improvement in quality of signal by using a single SOA_1 in-line amplifier.

Figure (7.12a) is produced by repetitions of transmission distance 130.2 km with SOA_1 at the end as presented in figure (7.12) for the transmission distance of 1302 km. If the input signal power is taken as -10 dBm for this system then the output power obtained is -9.96 dBm with an improvement in quality factor of 2 dB after time domain simulation.

The numerically simulated and calculated results from setup shown in figure (7.12) are presented in plot (7.13). The two curves show the variations of quality with converter stages. The previous converter [Li *et al.*, 2004] has small conversion range while this converter has wider range up to 50 nm. For the same number of stages, present cascaded wavelength conversion shows much better quality up to ten stages.

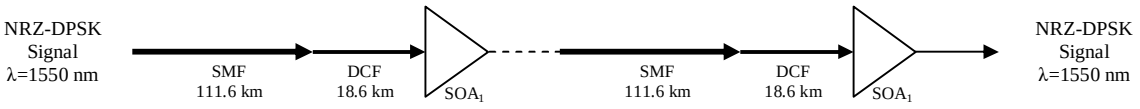

Figure 7.12a: NRZ-DPSK transmission system.

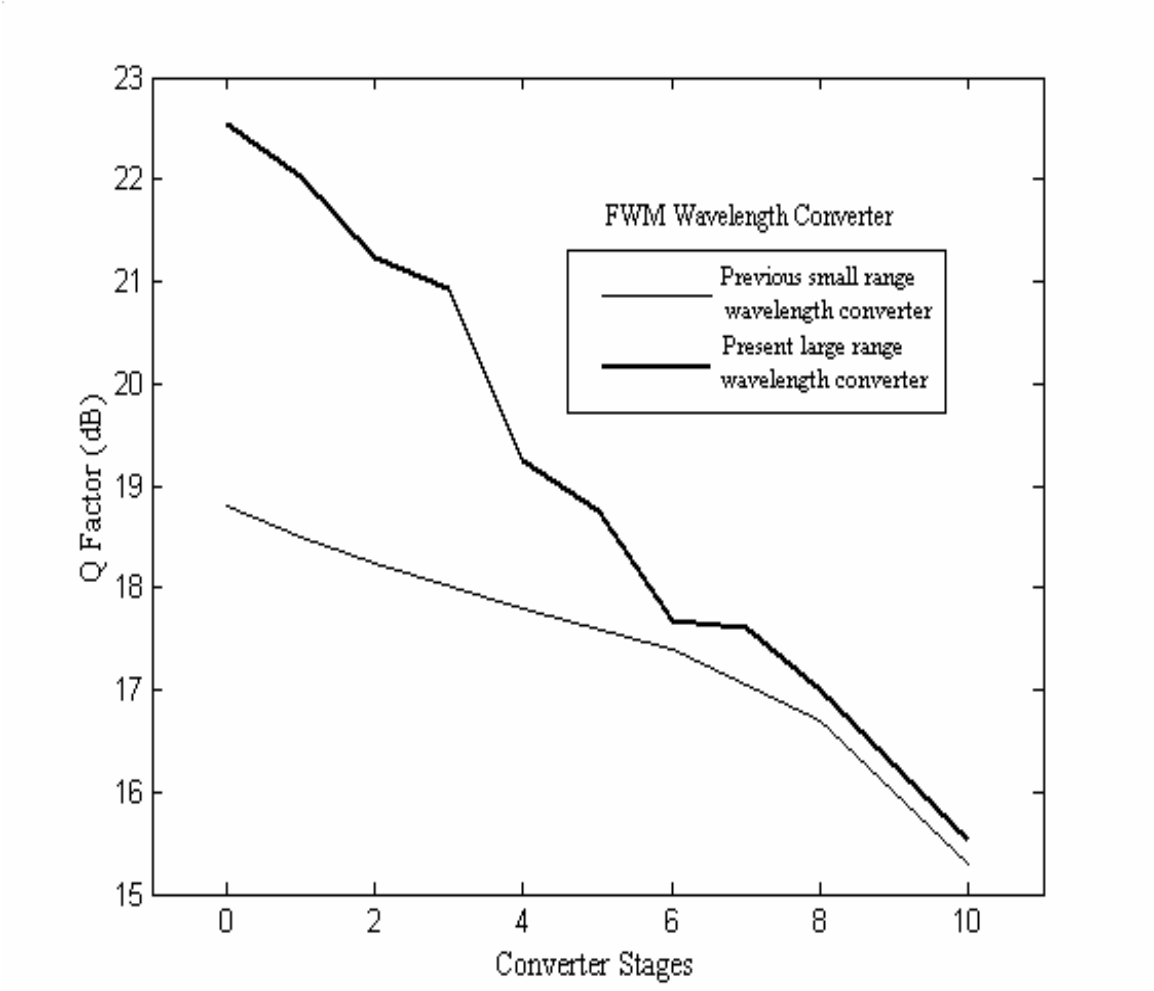

Figure 7.13: Variation of Q factor against converter stages for present (50 nm range) and previous[$] wavelength converter.

After ten stages of wavelength conversion, a Q factor of 15.53 dB is obtained. Cascaded wavelength conversion over 1302 km is possible for 10 Gb/s NRZ-DPSK format using FWM in SOA.

This wide band FWM based wavelength converter for DPSK shows high cascadability as compared to FWM based converter in OOK transmission system reported in [Li *et al.*, 2004]. The transmission distance is limited due to Q penalty. The Q penalty goes on increasing due to the increase in gain fluctuations of SOA and nonlinearities in the transmission path. The gain fluctuations in SOA increases as the input signal power approaches the saturation power. Further optimization of SOA is possible for increasing the cascadability of optical networks. This can be achieved by optimizing other parameters of SOA *i.e.* differential gain, thickness, transparency carrier density, carrier recombination time etc.

7.3 Wavelength Converters Based on Cross Phase Modulation in SOA-MZI Configuration

Wavelength conversion technique based on four wave mixing in the SOA has high bit rate capability [Ludwig and Rayton, 1994] and transparency to modulation format [Schnabel, 1994]. The wavelength conversion at 20 Gb/s and higher bit rate using FWM in SOA is possible. But conversion efficiency for this scheme is not very high. So it is difficult to retain a large signal-to-noise ratio (SNR) for converted signal in cascaded wavelength converters.

So to overcome the problems of XGM and FWM scheme, the SOA converters can be used in cross phase modulation (XPM) mode. The XPM scheme is based on the dependency of refractive index of the carrier density in the active region of the SOA. Incoming signals deplete the carrier density and modulate the refractive index. Therefore, phase modulation of a continuous wave (CW) signal is coupled into the converter. The phase modulated CW signal can be demultiplexed after the converter [Patrick and Manning, 1994].

Majumder *et al.* [2003] reported XPM based SOA Mach-Zehnder interferometer (SOA-MZ1) wavelength converter. They have optimized the bias current, optical filter bandwidth, and pump intensity in the SOA-MZI arrangements to achieve high signal-to-noise ratio. This wavelength conversion can be achieved for up and down conversions up to 2 nm for NRZ (non return to zero) signal at 10 Gb/s [Majumder *et al.*, 2005].

Song *et al*. [2004] reported the maximum up conversion efficiency of 7 dB, but this can be possible only at very low optical power. In this part, the work reported in [Patrick and Manning, 1994; Majumder *et al.,* 2003] is extended to increase the up and down wavelength conversion range. The improvement in the conversion efficiency is also reported.

7.3.1 Wavelength Converter Setup Based On XPM

The simulation setup of wavelength converter is shown in figure (7.14). The NRZ-OOK signal is produced by encoding CW signal with NRZ data with wavelength 2^{10}-1 into the amplitude modulator. For the compensation of loss, EDFA is used to amplify the signal. The EDFA have fixed gain of 25 dB with noise figure 4.5 dB.

The signal with wavelength 1552.52 nm is sent to lower port of SOA-MZI and the pump is applied at upper port with desired wavelength, which is required at the output. In order to generate the SOA-MZI configuration, two 3 dB optical coupler are used. The formation of the SOA-MZI is optimized so that maximum cross phase modulation produces the requirement inside the SOA-MZI. The upper semiconductor optical amplifier represented by SOA_1 and lower is represented by SOA_2. The output of the SOA-MZI is applied to the raised cosine band pass filter with optimized bandwidth of 20 GHz.

Then its output is detected by PIN photodiode at converted wavelength. The sensitivity of the receiver is -27 dBm and responsivity is 1 V/W. The quantum efficiency of receiver is 0.75. The simulation is carried out at centre frequency of 193.1 THz. The time domain simulation bandwidth is varied according to the conversion range.

7.3.2 SOA Parameters Validation for Enhancement of XPM

In order to enhance the XPM in the SOA-MZI configuration as shown in figure (7.14), one semiconductor optical amplifier (SOA_2) is taken as standard practical and another SOA_1 structure is optimized for enhancement of the XPM in the SOA-MZI configuration.

First of all, the input wavelength is taken as 1552.52 nm and converted wavelength chosen is 1553 nm for the validation of SOA_1. The simulation setup shown in figure (7.14) is used to validate the parameters of the SOA_1, for enhancing the XPM.

The table (7.5) shows that as the active region length of SOA_1 increases, the Q factor penalty goes on decreasing up to saturation power of SOA_1.

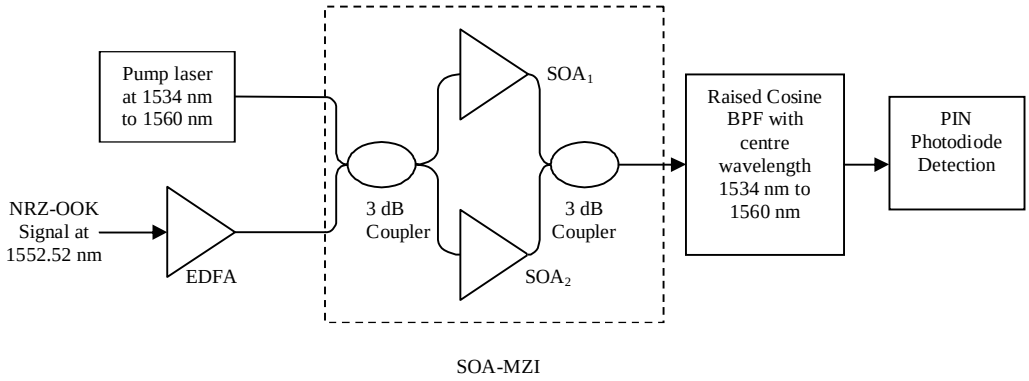

Figure 7.14: Wavelength converter setup based on cross phase modulation.

Table 7.5

Active length of the SOA_1 variation with input signal for converted signal wavelength of 1553 nm.

Active Region Length(μm) ↓	**Q Penalty (dB)**			
At different Signal input Power (dBm) →	-8 dBm	-5 dBm	-3 dBm	0 dBm
1000	15.84	8.9	6.4	6.97
1500	9	1.97	1.44	1.99
1700	8.86	1.78	1.47	2.1
1800	8.91	1.97	1.61	2.15
2000	8.91	1.97	1.61	2.15

Table 7.6

Optical filter bandwidth variation with input signal for converted signal wavelength of 1553 nm.

Optical Filter Bandwidth ↓	**Q Penalty (dB)**			
At different Signal input Power (dBm) →	-8 dBm	-5 dBm	-3 dBm	0 dBm
15	15.03	23.09	22.45	19.65
20	18.01	25.93	27.05	26.64
30	16.42	24.06	24.7	26.27
40	15.38	23.24	24.22	26.36

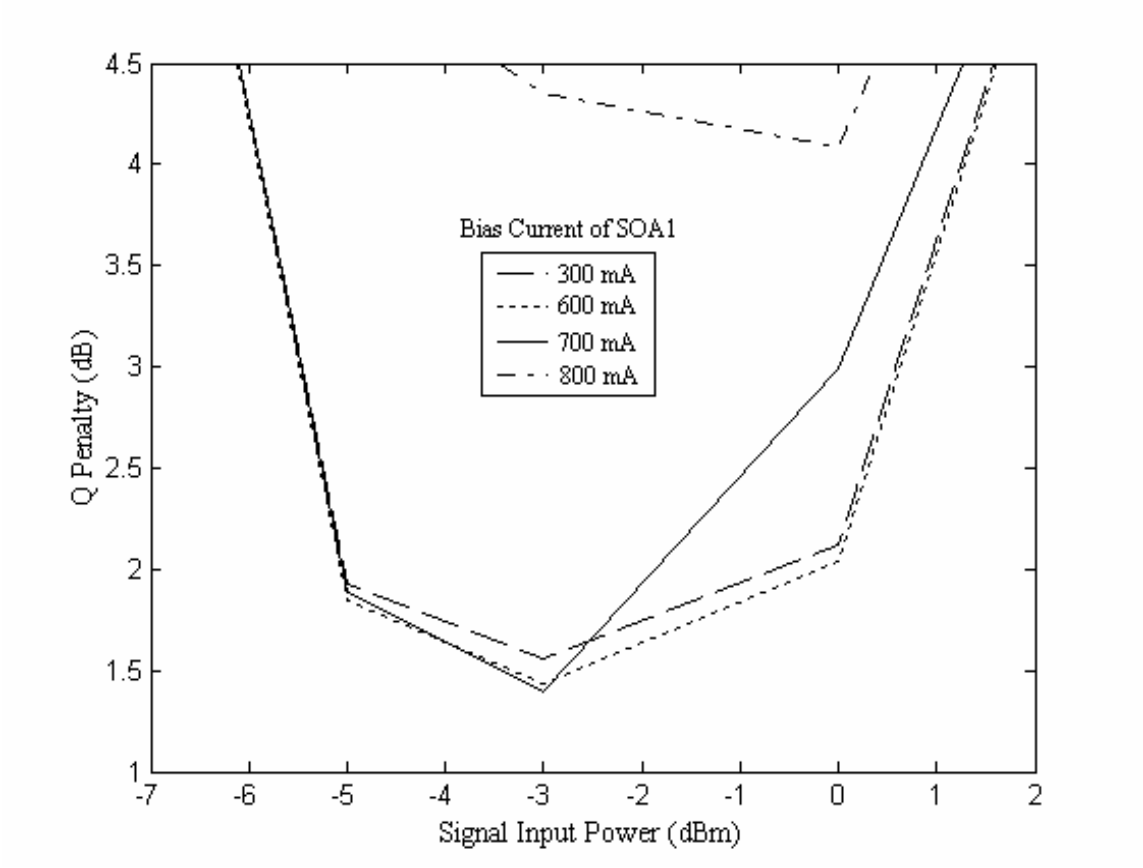

Figure 7.15: Q factor penalty variations with signal input power for different bias currents.

Table 7.7

Parameters of the SOA-MZI for wavelength converter based on XPM.

Parameters	**SOA_1**	**SOA_2**
Bias current	700 mA	400 mA
Length of the active region	1700 μm	300 μm
Width of the active region	2 μm	1.5 μm
Thickness of the active region	0.2 μm	0.2 μm
Confinement factor	0.4	0.4
Carrier lifetime	0.19 ns	0.3 ns
Transparency carrier density	1×10^{18} cm^{-3}	1×10^{18} cm^{-3}
Material gain	2.3×10^{-16} cm^2	2×10^{-16} cm^2
Line enhancement factor	3	3
Input and output coupling loss	3 dB	3 dB

From table (7.5), it is observed that the active region length of SOA_1 is 1700 μm which shows the minimum Q factor penalty.

The bias current of the SOA_1 is also optimized for boosting the XPM. As shown in figure (7.15), if the bias current increased from 300 mA to 600 mA, the Q factor penalty continuously falls. The same case is observed in [Majumder *et al.*, 2003; Majumder *et al.*, 2005]. It is observed that minimum Q factor penalty is observed at 700 mA bias current, before the saturation of the SOA_1. If there is further increase in the bias current, then large Q factor penalty is observed. The table (7.6) shows the optimized optical filter bandwidth by using optimum bias current 700 mA and length 1700 μm of SOA_1.

At 20 GHz, optical filter bandwidth of the raised cosine filter shows maximum Q factor for all input signals. Table (7.7) shows the optimized parameters of the SOA-MZI for wavelength converters based on the XPM.

It is observed that longer length of the active region and high bias current of the SOA leads to faster response and small gain variation of SOA device [Singh and Kaler, Oct. 2006]. Higher bias current of the SOA provides the best gain with wider spectrum bandwidth of the SOA.

7.3.3 Results and Discussions

In order to observe the performance of wavelength converter, the Q factor penalty versus signal input power is observed for different pump power as shown in figure (7.16). The input signal wavelength 1552.52 nm is converted to 1553 nm.

The Q factor penalty goes on decreasing with the increase in the pump power. This shows good agreement with result reported in [Durhuus *et al.*, 1996]. At 1 dBm pump power, the minimum Q factor penalty is 1.14 dB at signal-to-pump of -6 dB.

It is reported that minimum signal-to-pump power is -9 dB [Lu *et al.*, 2000]. It is also observed that as the input signal power is increased, Q factor penalty is decreased up to saturation of the SOA_1. After saturation power of the SOA_1, Q penalty goes on increasing.

The converter setup shown in figure (7.14) is also used for up and down conversion with wide band range. The time domain simulations bandwidth increases according to conversion ranges. As shown in figure (7.17), as the up conversion range increases up to 1553.1 nm for input signal 1552.52 nm.

The improvement in quality of 0.2 dB is observed at signal-to-pump of -6 dB. Hence this meets with requirements for increasing the cascadability of optical networks.

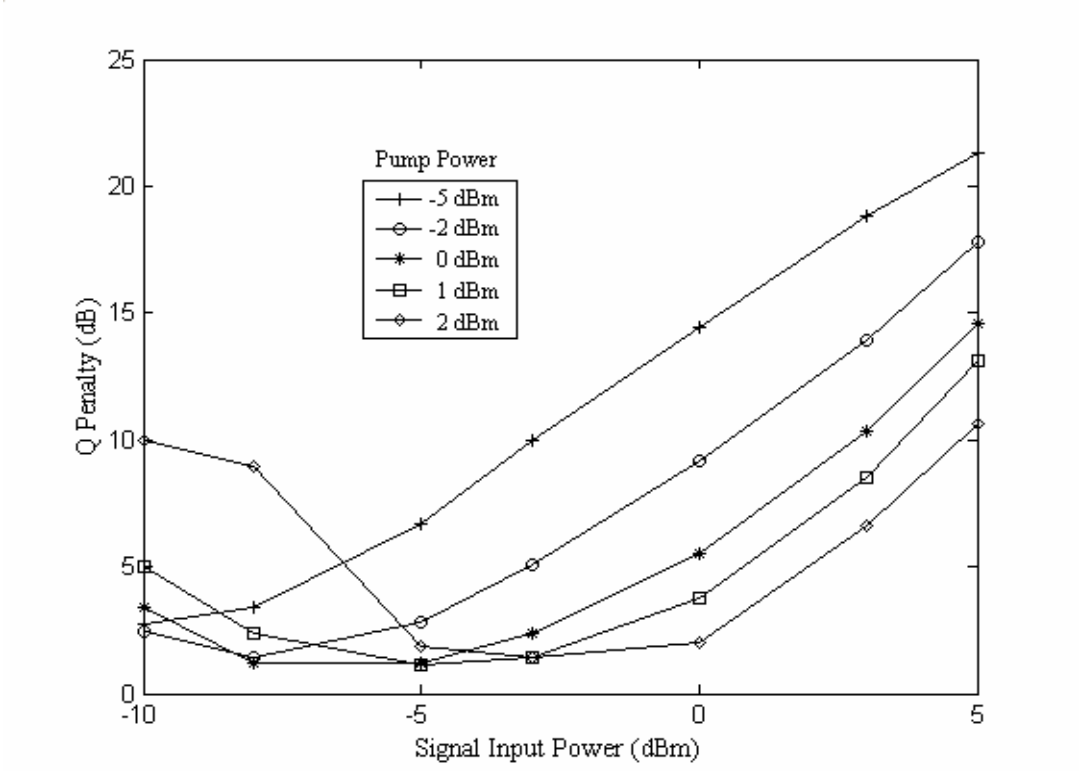

Figure 7.16: Q factor penalty variations with signal input power for pump bias currents.

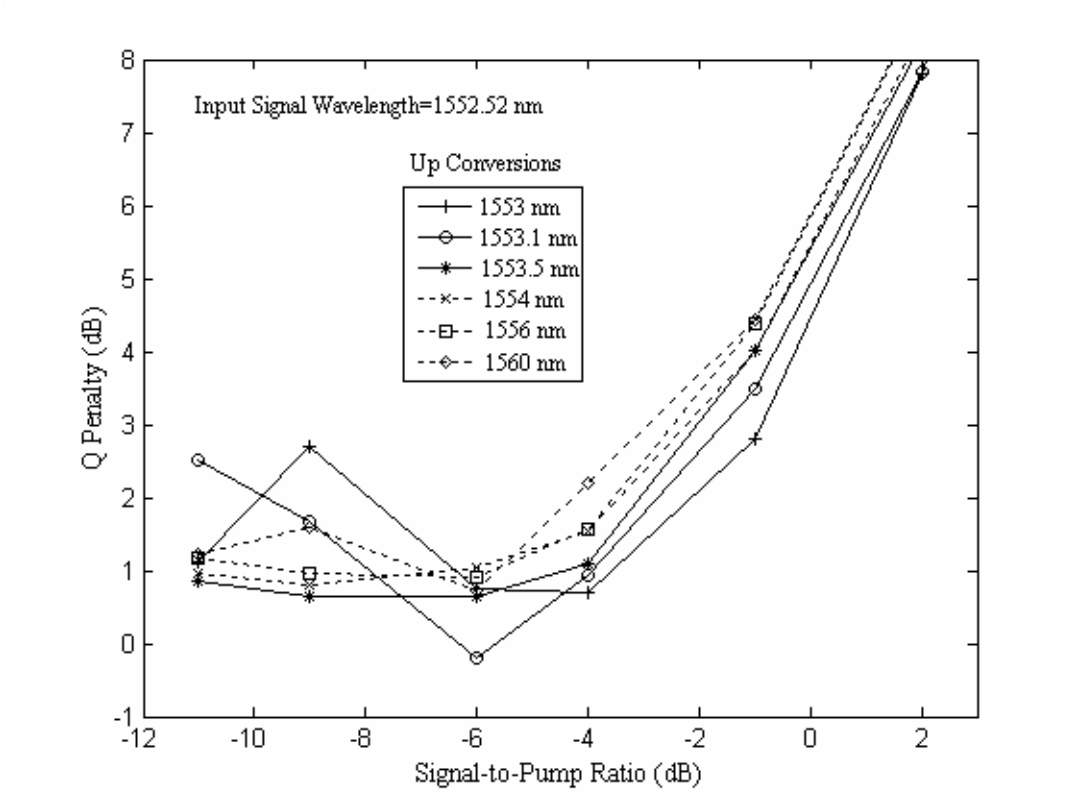

Figure 7.17: Q factor penalty variations with signal-to-pump ratio for up conversion wavelengths.

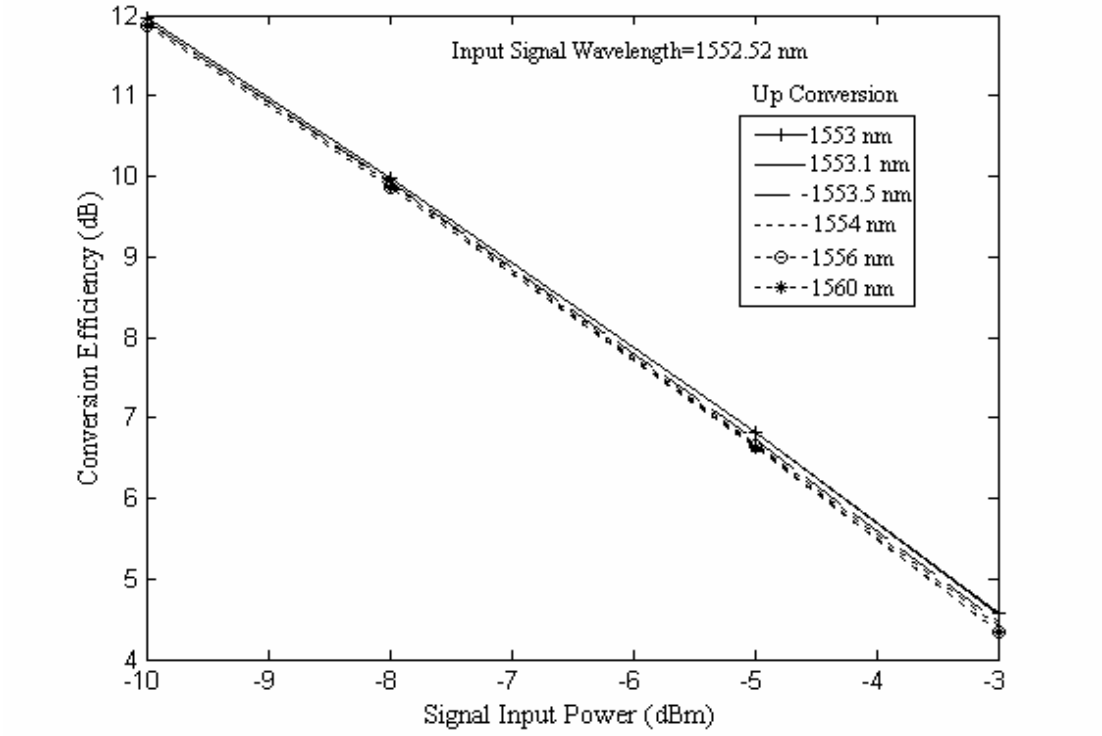

Figure 7.18: Conversion efficiency as the function of signal input power for up conversion wavelengths.

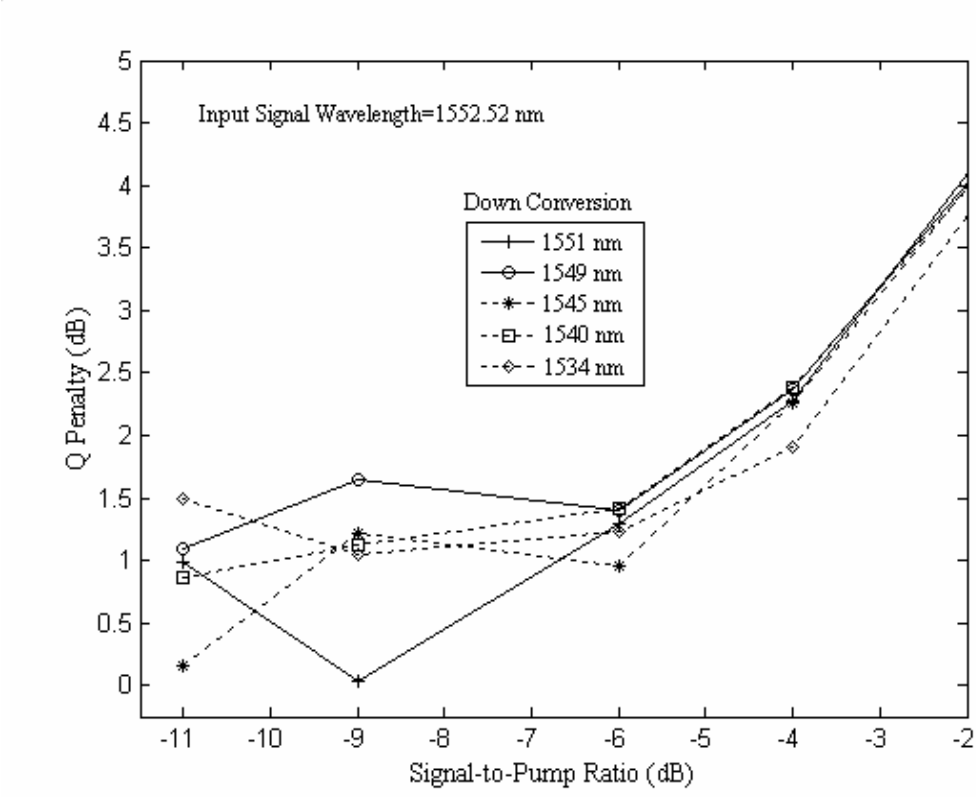

Figure 7.19: Q factor penalty variations with signal-to-pump ratio for up conversion wavelength.

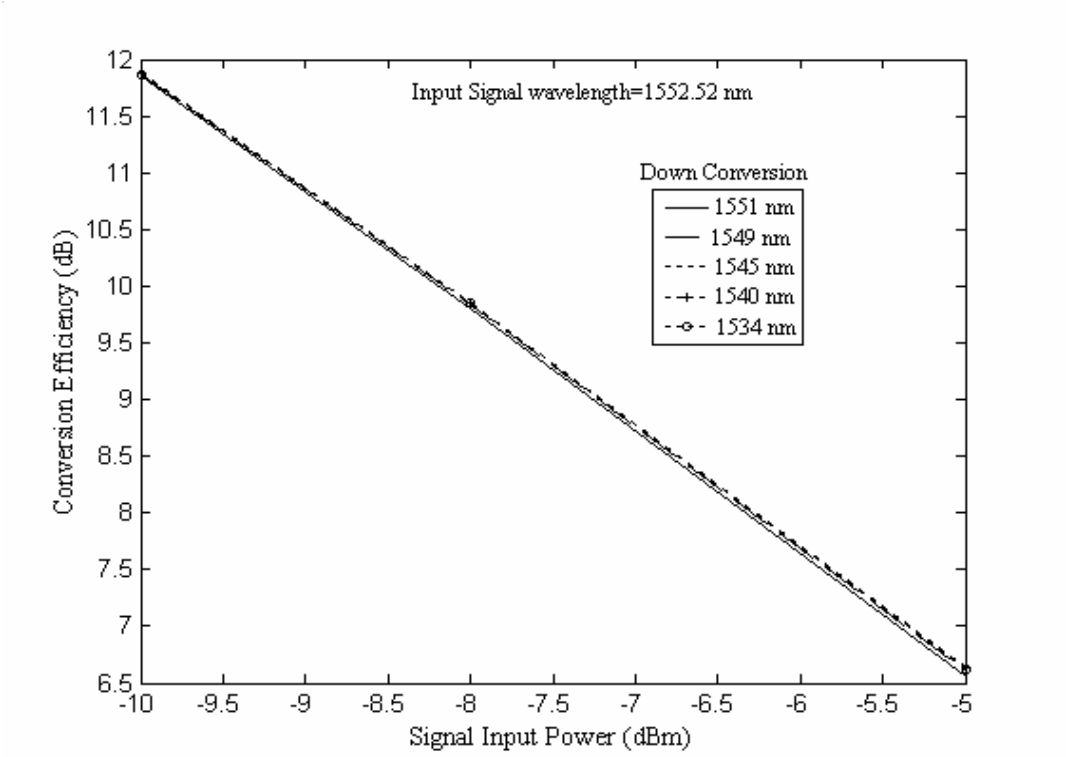

Figure 7.20: Conversion efficiency as the function of signal input power for up conversion wavelengths.

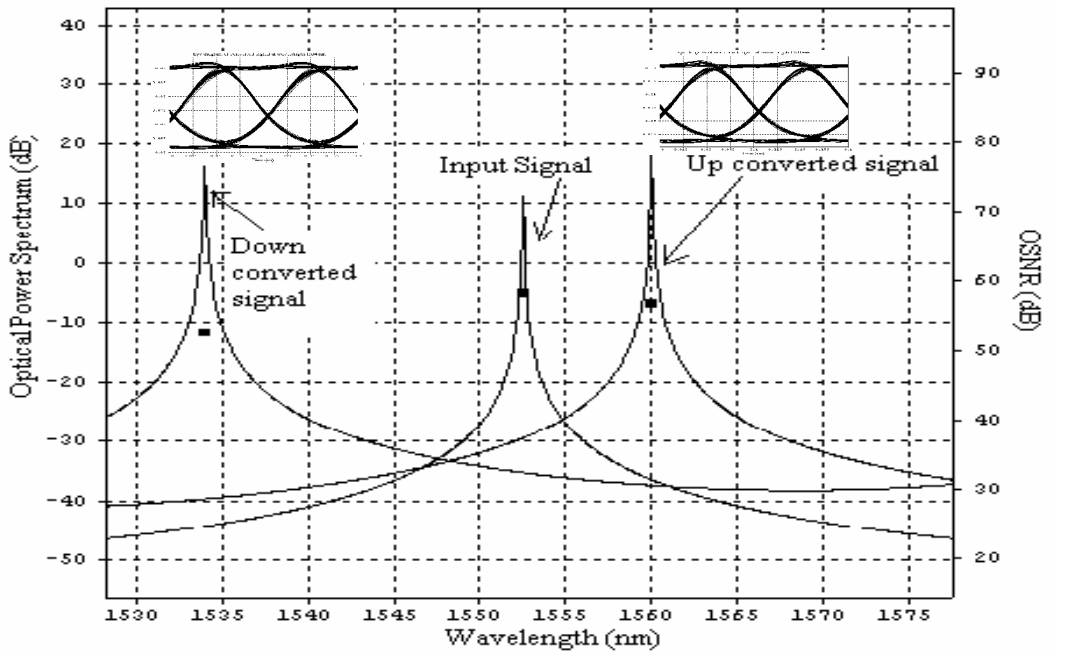

Figure 7.21: Optical power spectrum and OSNR as the function of wavelength for input, up converted, down converted signals.

Where high SNR (Q factor) is required. If the up conversion range increases more than 15 nm from input signal wavelength, the minimum Q factor penalty 0.72 dB is observed for converted signal at 1560 nm. Figure (7.18) shows the conversion efficiency as the function of signal input power for different conversion range. Almost same conversion efficiency is observed up to converted signal wavelength of 1560 nm.

The figure (7.19) shows the case of down conversion. For the converted signal wavelength 1551 nm, the minimum Q factor penalty is 0.04 dB at signal-to-pump power of -9 dB. For wideband down converted signal wavelength 1534 nm, the observed Q factor penalty is 1.05 dB for signal-to-pump power. The conversion efficiency for down converted signal is shown in figure (7.20).

The conversion efficiency for all conversion range is almost same. Figure (7.18) and (7.20) show that conversion efficiency is around 6 dB and 9 dB at minimum Q factor penalty. This shows an improvement over results reported in [Song *et al.,* 2004]. The conversion efficiency goes on decreasing with the increase in signal input power for both up and down conversion. The optical power spectrums versus conversion range more than 15 nm for both up and down conversions are shown in figure (7.21). The clear eye pattern observed at converted signal wavelength 1534 nm and 1560 nm.

7.4 Conclusions

This Chapter deals with 50 nm up and down wavelength conversion for non-return to zero differential phase shift keying (NRZ-DPSK) signal by using four wave mixing in a semiconductor optical amplifier (SOA) at 10 Gb/s. The gain fluctuations are decreased by selecting suitable parameters of the SOA to achieve sufficient quality with enhancement in four wave mixing signals. The minimum Q factor penalty observed is 1.5 dB at signal-to-pump ratio of -9 dB for both up and down conversion range of 20 nm. The Q factor improvement observed is 1.74 dB for signal-to- pump ratio of -5 dB at 0 dBm pump signal for 50 nm up converter. Ten stage cascaded wavelength conversion over 1302 km single mode transmission is possible for 10 Gb/s NRZ-DPSK format by using FWM in the SOA. Therefore, these SOA parameters can be utilized for designing of optimized SOA and wide band wavelength converter. For cascaded wavelength converter, the transmission nonlinearities in single mode fiber can be managed by using dispersion compensating fiber with second order dispersion management.

It has been also found that the wavelength conversion using XPM in the SOA-MZI configuration with the wide band more than 15 nm up and down conversions is observed

for the first time. It is observed that the high active region length and bias current in the SOA leads to XPM in the SOA-MZ1 configuration. For this, low pump power of 1 dB is observed. For up conversion range of 0.58 nm, an improvement in quality of 0.2 dB is observed at signal-to-pump power of -6 dB. This wavelength converter provides conversion band more than 15 nm for both up and down conversions. The conversion efficiency of this converter is more than 11 dB at signal-to-pump power of -9 dB.

On the whole, these wavelength converters lead to an increase in the cascadability of the wavelength converters for increasing the capacity of future optical networks.

Chapter 8
Performance Comparison of Optical Network Topologies in Presence of Optimized Semiconductor Optical Amplifiers

8.1 Introduction

This chapter investigates the performance of optical communication network topologies in presence of optimized semiconductor optical amplifiers, which is the fourth objective of this research work. The performance of bus, ring, star and tree network topologies for 10 Gb/s DPSK signal in presence of optimized semiconductor optical amplifiers is compared at low signal input power. It has been evaluated that the tree network topology offers maximum number of users with minimum utilization of SOAs and optical coupler.

The optical multiplexing and switching techniques are used for increasing the capacity [Marrachi and Dekkar, 1994]. In the WDM system, the implementations of encoders/decoders and time multiplexer /demultiplexers at Tb/s are very difficult so optical network topologies reduces the complexity. A physical broadcast topology must have minimum number of couplers, multiplexers, demultiplexers and optical amplifiers to reduce the cost in the large network. In addition, the minimum received power is required for a given the BER to maximize the number of users.

The semiconductor optical amplifier (SOA) has attracted much attention as cost effective compared to erbium doped fiber amplifier for optical transmission using the differential phase shift keying (DPSK) [Wei and Zhang, 2005]. The bus topology supported very few users (typically < 20) [Wagner, 1987]. Due to the ASE noise and gain saturation of SOAs, the number of users is limited but by use of SOAs, the single channel bus network has uniform power levels at bit rate of 20 Mb/s with repeater spacing of 0.5 km.

Ross *et al.* [1989] reported that fiber distributed data interface (FDDI) is a ring network designed with fiber. Due to power budget problem, the number of nodes in typical ring are limited to less than 6 at bit rate of 2.5 Gb/s. Willner and Hwant [1995] reported that a ring network was to accommodate 25 nodes by using (EDFA) erbium doped fiber amplifiers and novel narrow band channel dropping filter at bit rate of 2.5 Gb/s. It was demonstrated that only three node ring by using cascaded SOA for 40 km up stream transmission is possible [Iannone *et al.*, 2000].

The star topology distributes optical power equally at output ports. The number of users supported by star is less than 64 [Chen, 1992]. Many researchers have worked to reduce

the network cost by decreasing the components in star couplers as discussed in section 1.5.5 of the Chapter 1. The SOAs can be easily integrated with integrated optic implementation as transmitter or receiver chips. Therefore, the SOAs are good candidate to reduce the cost of star network. Singh *et al.* [1996] investigated that star topology supported maximum users with SOAs. At minimum transmitted power of -30 dBm, the number of users supported is limited to 4 only at 1 Gb/s. They found that pre-amplifier utilization of SOAs was efficient.

The tree network topology provides large geographical area coverage with fiber and capacity of network can be increased by use of wavelength division network (WDM). Gerla *et al.* [1988] evaluated that total number of users supported are $N_u = bn$, where b is number of branches and n is number of users per branch in the tree network. The power loss in tree network topology can be reduced by using multistage star coupler [Green, 1993]. Singh *et al.* [1997] investigated that tree network supported large number of users supported with lesser number of SOAs at 1 Gb/s, but a large transmitter power for both unsaturated and average gain saturated SOA has been taken at 1 Gb/s bit rate only. Due to increased bit rate and bandwidth demands in optical network, further work is required in order to utilize less power, less fiber, less SOAs and couplers used in various optical network topologies.

8.2 Bus Network Topology with Optimized SOAs

The schematic setup for the bus network topology is shown in figure (8.1). Each user is connected to bus through the optical coupler having output port ratio 50 to complementary output port. Every user is connected to each other by single mode fiber (SMF) and dispersion compensating fiber (DCF) through optimized SOA. The length of the dispersion compensating fiber (DCF) is chosen in accordance with [Aggarwal, 2000] for complete compensation ($\overline{D} = 0$). The total minimum fiber link is approximately 1.08 km. The placement of one SOA is done in the start of each segment in order to continue broadcasting the information from transmitter users *i.e.* segment $i-1$ shown in figure (8.1). After every SOA in segment, there are four users supporting at appropriate signal input power.

Each transmitter section consists of data source, laser source, electrical driver and optical phase modulator. The data source is non return to zero format at 10 Gb/s. The electrical driver converts binary sequence into electrical signal.

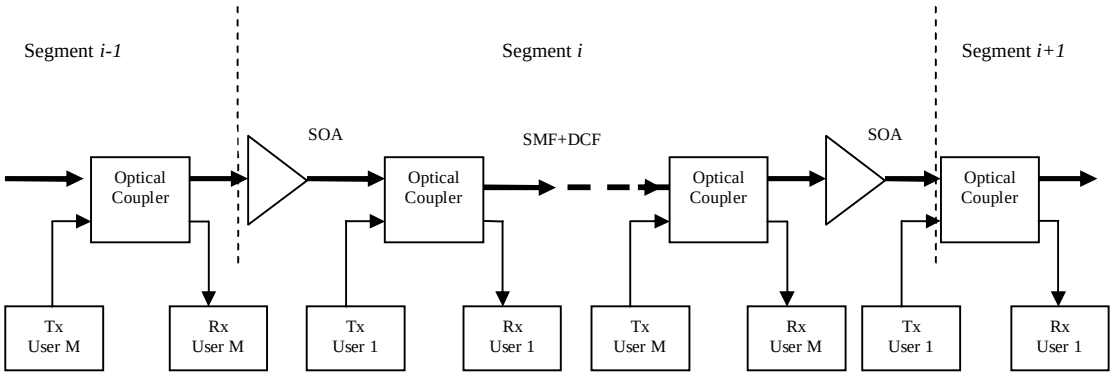

Figure 8.1: Schematic setup for broadcast bus network topology using optimized SOAs.

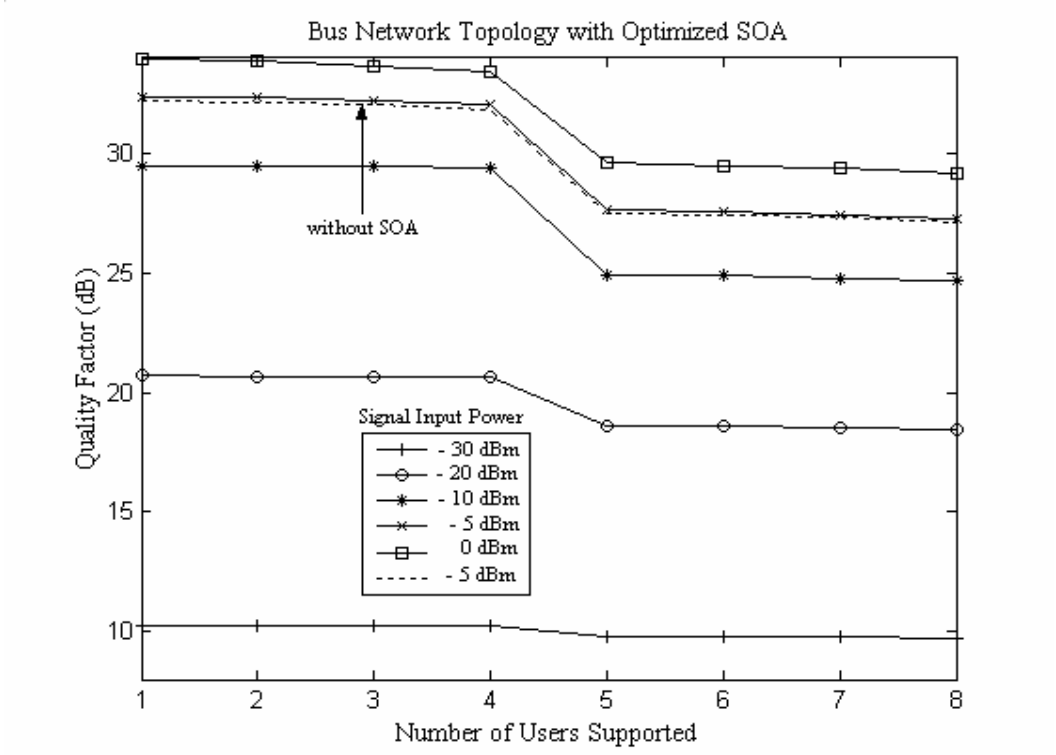

Figure 8.2: Quality factor as the function of different signal input power with given number of users supported for bus network topology in presence of optimized SOAs.

The Lorentzian laser source having wavelength of 1550.52 nm is used to modulate optical $LiNbO_3$ phase modulator with non return to zero (RZ) format and acting like transmitter. Each of the receivers has same reception wavelength as that of the transmitter in order to distribute the signal as in the segment $i-1$. The simulation is performed with simulation bandwidth 1.2 THz and centre wavelength of 1550.13 nm.

For eight users bus network topology, the simulation is performed for different signal input power by using two optimized SOAs only. As shown in figure (8.2), the quality of signal goes on decreasing with decrease in signal input power. Also, as shown in figure (8.3), the power penalty goes on increasing with the increase in the signal input power.

At low value of signal input power -30 dBm, the effect of amplified spontaneous emission (ASE) noise power is quite high [Yamatoya and Koyama, 2004]. Therefore, the quality of signal broadcast in bus network topology goes on decreasing. At high value of signal input power 0 dBm or above, the gain fluctuation occurs at high rate. Therefore, the gain of the SOA drops, causing power penalty. When the SOA is not used in the setup, there is large power penalty observed as shown in figure (8.3). Also from figure (8.3), the power received goes on decreasing from transmitting users with increase in receiver distance for different destination users. This is due to the non-uniform distribution of power among the users in bus topology network, which shows good agreement with results [Wagner, 1987]. After four users, there is increase in received power for fifth user due to the SOA.

But the quality of the signal drops due to gain saturation of the SOA as shown in figure (8.2). The performance of bus network topology is shown in figure (8.4) for number of users supported with the SOA and optical coupler for different signal input power. For the simulation of bus topology at -30 dBm signal input power, no users are supported as shown in figure (8.4). This is due to the increase in ASE noise power, which drops the quality of received signal. At -5 dBm signal input power, the effect of ASE noise power is less.

Therefore, the maximum users supported are 17. If signal input power is increased to 0 dBm, the number of users supported drops to 4 due to the gain saturation. If the output port ratio of optical couplers used is 40 then number of users supported increase up to 27. This shows an improvement over previous results.

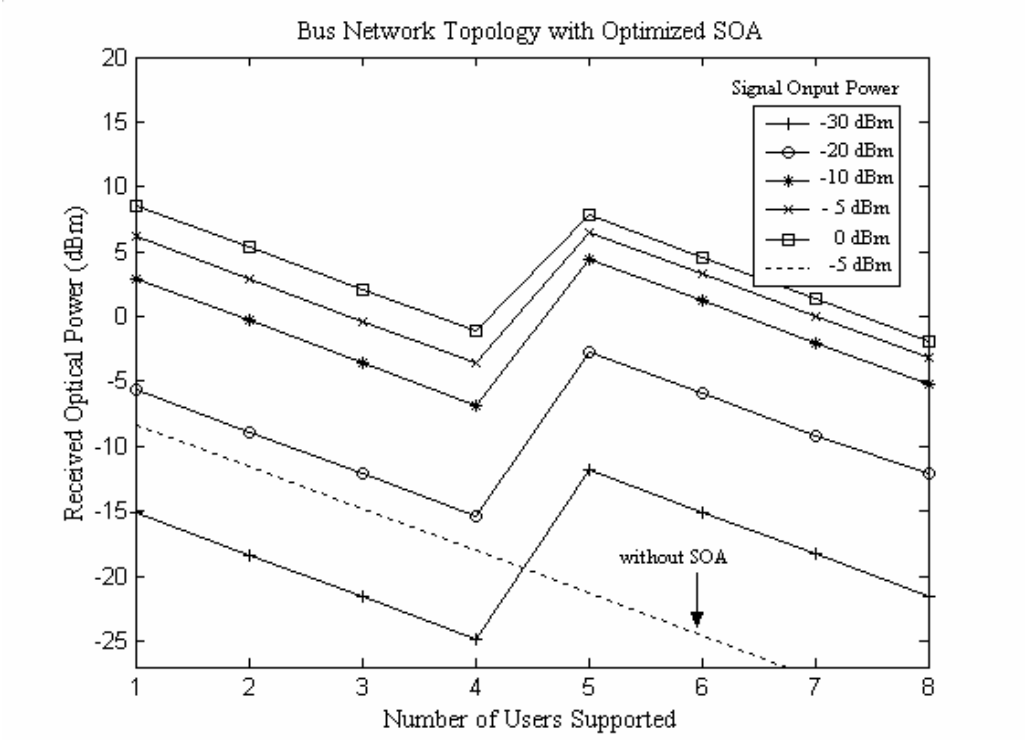

Figure 8.3: Received optical power as the function of different signal input power with given number of user supported for bus network topology in presence of optimized SOAs.

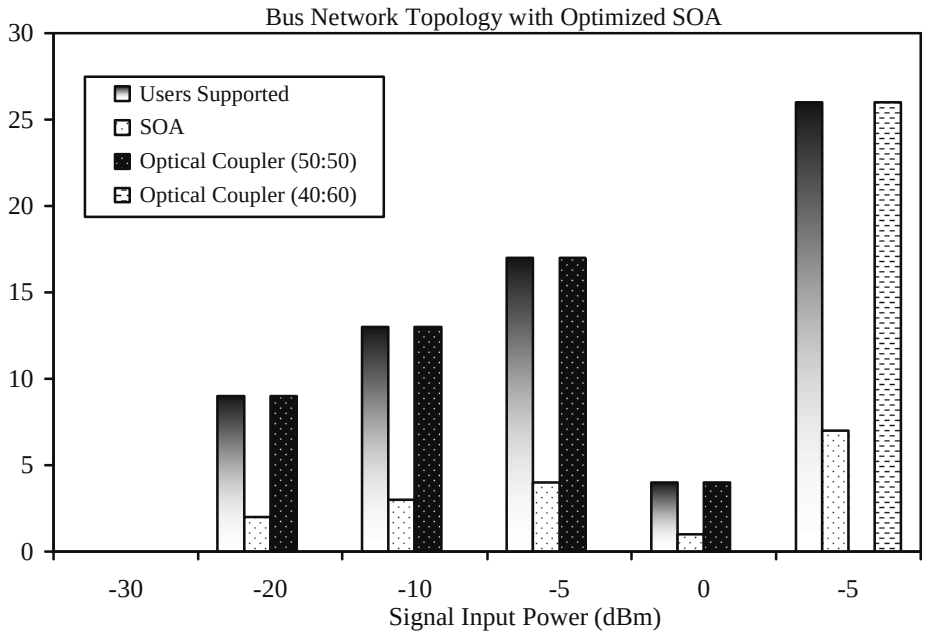

Figure 8.4: Bar graph for bus network topology in order to observe the efficiency in terms of number of user supported, SOAs, optical couplers for different signal input power.

The number of users supported increases due to adjusting the optical coupler output port ratio to 40. This will reduce the output power for next users after coupler, but reduction in power does not achieve the power penalty. This reduced power will also reduce the effect of gain saturation in the SOA. The effect of the ASE noise power is almost negligible at this condition. Therefore the users supported are increased.

8.3 Ring Network Topology with Optimized SOAs

The ring topology network is shown in figure (8.5) for different nodes. Each node is connected to other by link of fully dispersion compensating system [Aggarwal, 2002] and SOA. Each node has same transmitter and receiver with optical coupler in the bus topology network shown in figure (8.5).

Optical couplers add new channels at different wavelengths and drop the previous channel. Here, it has considered that the channel which is dropped at particular node is added at the previous node. As shown in figure (8.5a), the node N_1 adds new channel at wavelength λ_1 and drops channel from previous node N_n at wavelength λ_n. The first simulation is performed for eight number of users at bandwidth 1.6 THz and centre wavelength 1550.14 nm.

The results for different signal input power for quality and output power of received signal are observed as shown in figurers (8.6) and (8.7) with one span simulation. It is observed that sufficient received power is received at the output for all the users at different signal power as shown in figure (8.7). But, while the optimized SOA is not used in the path between nodes, there is large power penalty observed for -10 dBm input power. It is observed that the quality at -40 dBm input power is dropped for the starting users as shown in figure (8.7). This is due to outside noise effect, which is more for starting users. For all input signal power, there is sufficient quality observed for all users.

Further, the number of users is increased and the quality and received power of dropped channels for different users at small input power is observed. Here simulation is done for two spans to observe the real performance of ring topology network. As shown in figure (8.8), as the number of users increase, there is improvement in quality for both signal input power at -40 dBm and -30 dBm. For the eight number of users supported, the performance of ring topology network is poor due to single span simulation. However, for large number of users, the sufficient power and quality is observed as shown in figurers (8.8) and (8.9) for two span simulation.

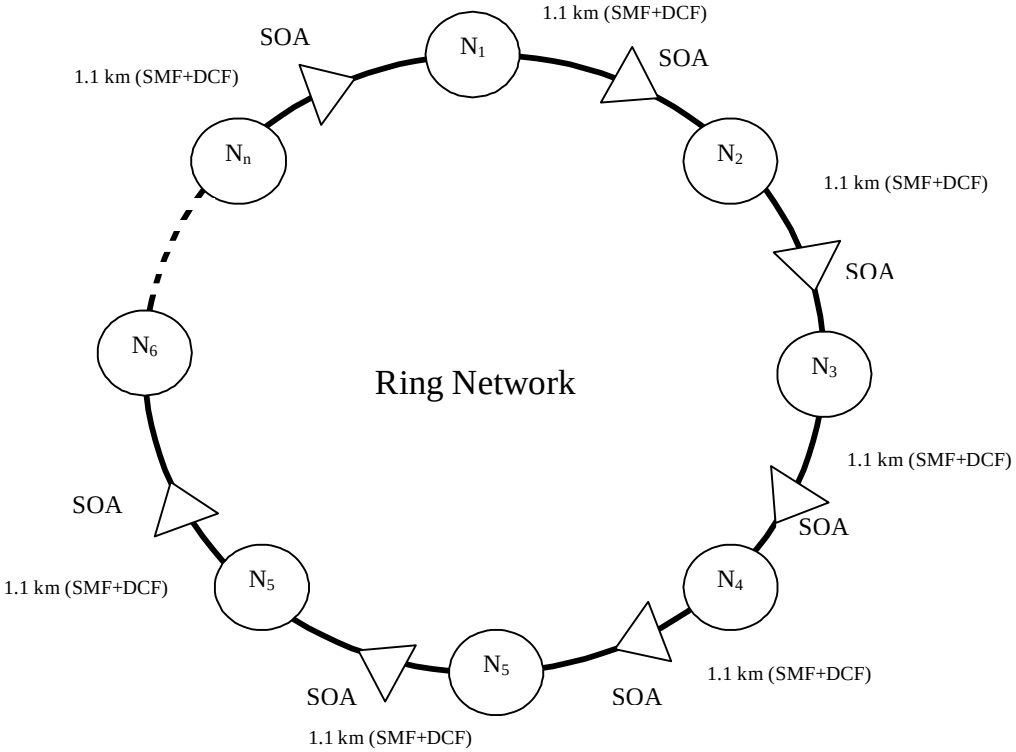

Figure 8.5: Schematic setup for ring network topology using optimized SOAs.

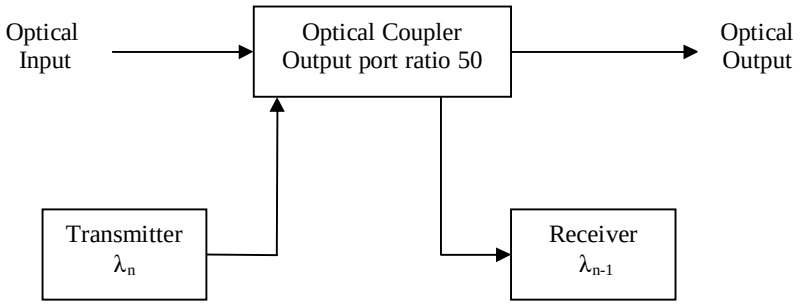

Figure 8.5a: Schematic setup for a node in ring network topology.

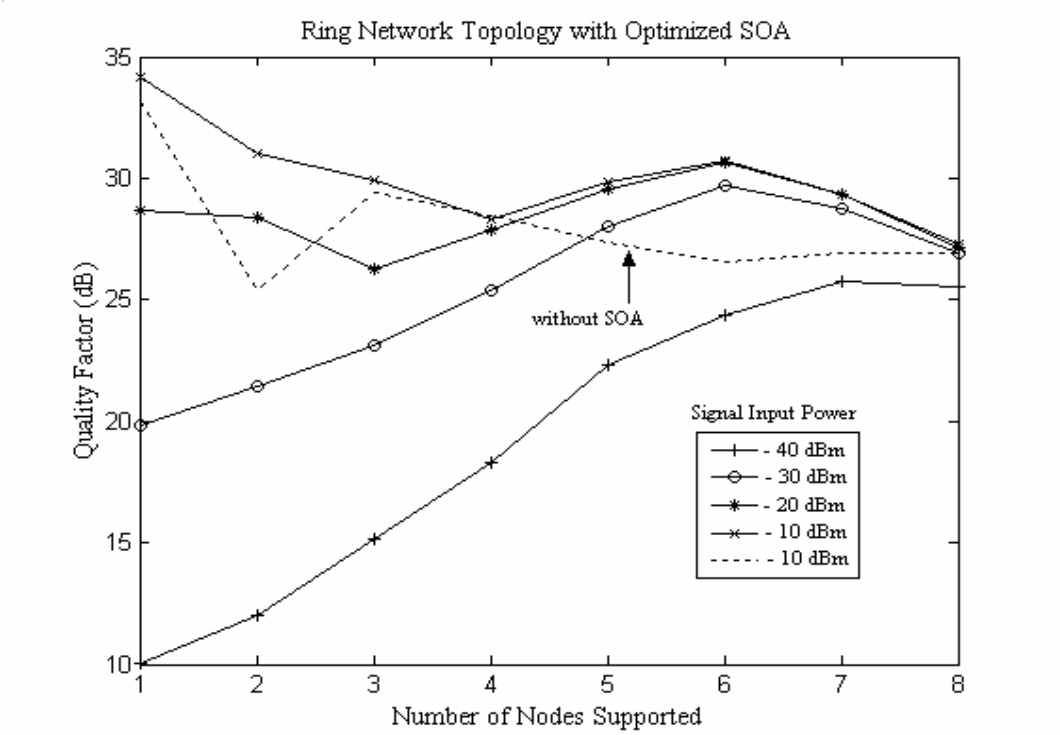

Figure 8.6: Quality factor as the function of different signal input power with given number of nodes supported for ring network topology in presence of optimized SOAs.

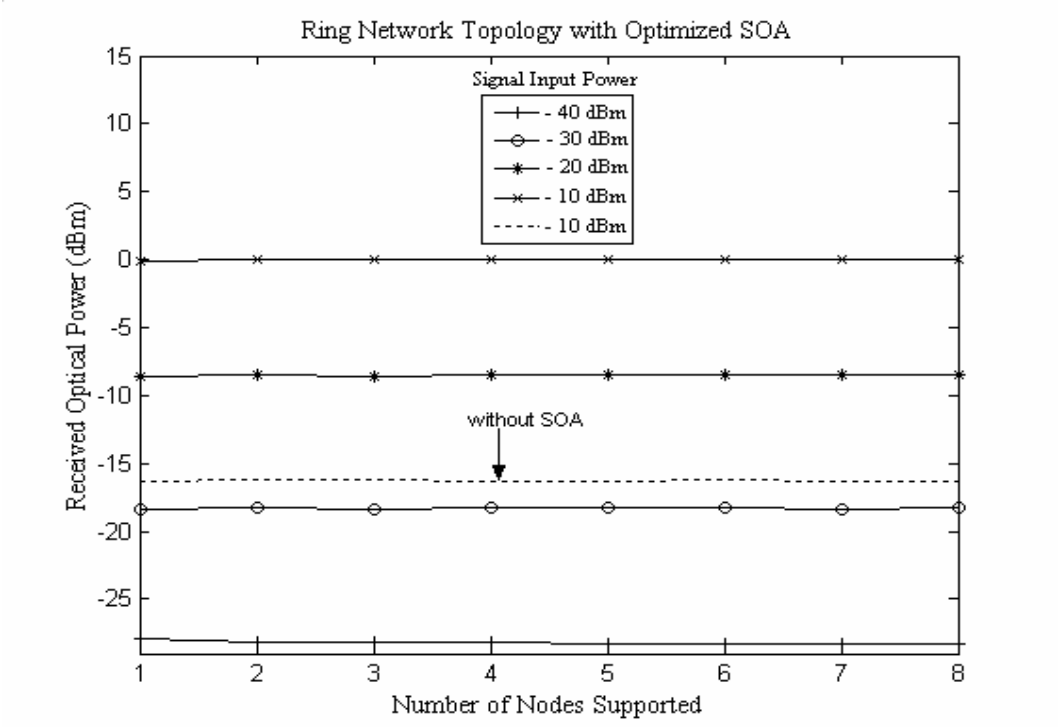

Figure 8.7: Received optical power as the function of different signal input power with given number of nodes supported for ring network topology in presence of optimized SOAs.

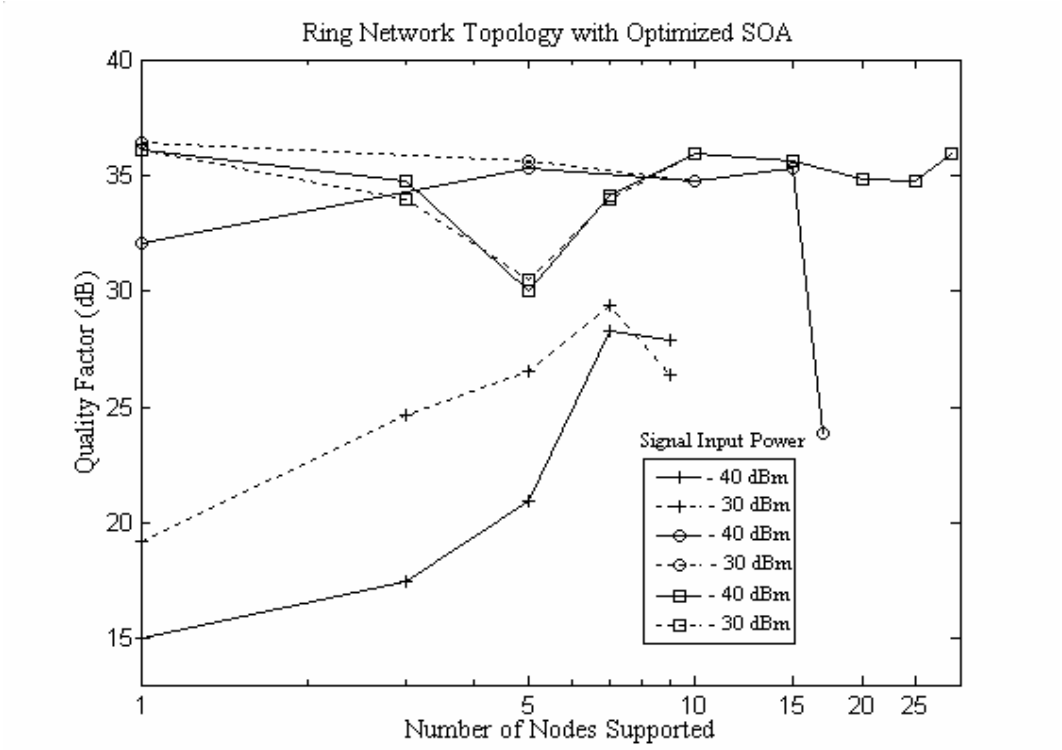

Figure 8.8: Quality factor as the function of number of nodes supported with low signal input power for ring network topology in presence of optimized SOAs.

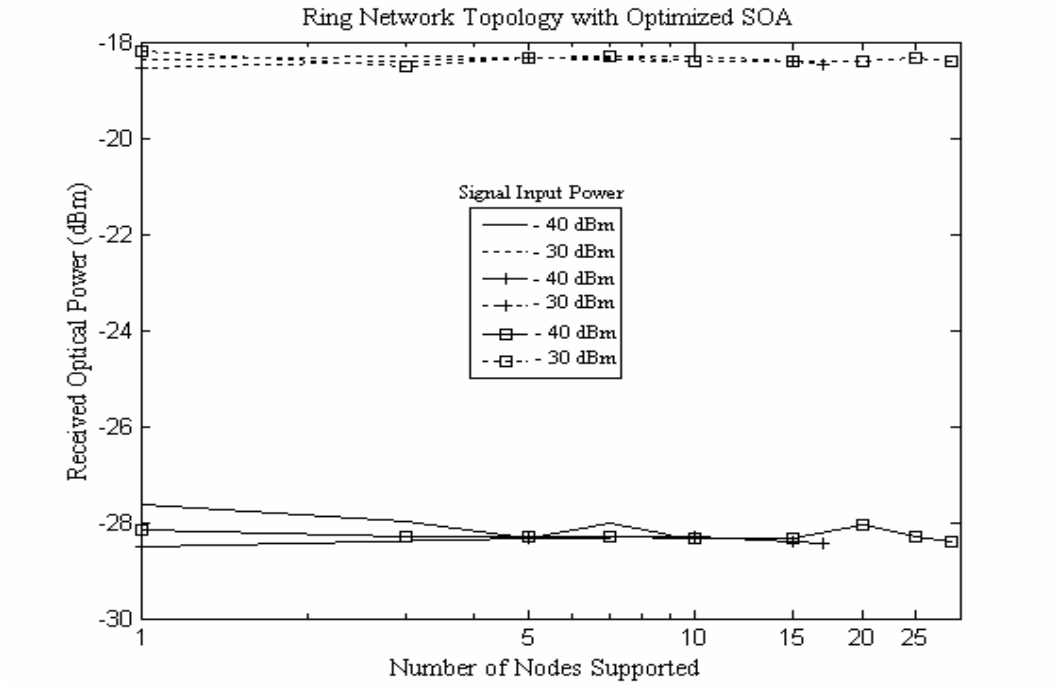

Figure 8.9: Received optical power as the function of number of nodes supported with low signal input power for ring network topology in presence of optimized SOAs.

The maximum numbers of nodes supported are 27. This result shows improvement over the results reported in [Willner and Hwant, 1995; Iannone et al., 2000].

8.4 Star network topology with optimized SOAs

The star coupler in $N_u \times N_u$ star network is made up of 2×2 optical coupler [Kobrinski *et al.*, 1987]. An 8×8 star coupler is formed by using 2×2 optical coupler as shown in figure (8.10). A $N_u \times N_u$ star coupler has $\log_2 N_u$ stages and required $(N_u/2)\log_2 N_u$ number of 2×2 optical coupler as shown in figure (8.10). Eight DPSK based transmitters are used here same as in bus network topology and connected to star coupler by using 1 km fiber links. It has been considered that the insertion loss, splice loss etc. are 1.5 dB at the each port of optical coupler in star coupler. The single mode fiber link is used to connect the users and star couplers. The simulation is done at bandwidth 2.5 THz and centre wavelength 1553.4 nm. It has been considered that transmitter user 1st passes information to receiver of 2nd user and transmitter user 2nd passes information to receiver 3rd and so on.

Figure (8.11) and (8.12) represents the quality and received power at different signal input power for eight users. The quality of received signal is decreased with the increase in signal input power of transmitter in 8×8 star coupler. This is due to the gain saturation of SOAs.

There is increase in power penalty as the signal input power increases as shown in figure (8.12). At 0 dBm signal input power, there is small power penalty observed at the receiver. When the SOAs are not using in star coupler, there is large power penalty observed as shown in figure (8.12). The number of users can be increased by using $n \times n$ star coupler configuration as shown in figure (8.13). As the numbers of users are increased, the power received goes on decreasing due to insertion and splice losses as shown in figure (8.14). For -40 dBm signal input power, the insertion loss and splice loss can be reduced to increase the number of users supported. As from figure (8.14), it is observed that eight users can be supported for minimum signal input power -40 dBm. From here, it is also found the number of SOAs and optical coupler used in $N_u \times N_u$ star coupler. The number of SOAs used is N_u. Also the number of optical coupler used is $(N_u/2)\log_2 N_u$.

The number of SOAs used = N_u

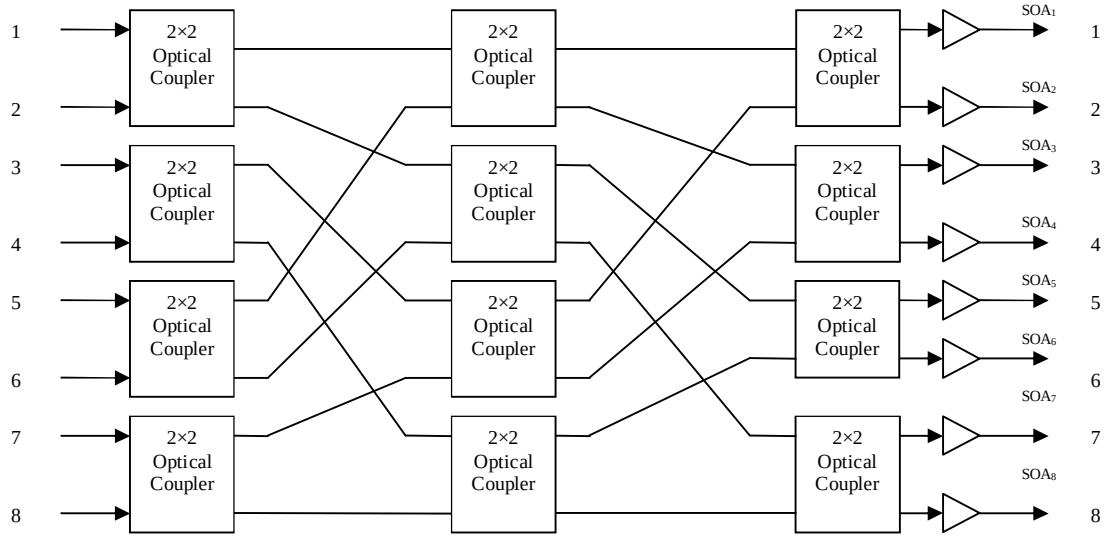

Figure 8.10: Schematic setup of 8 × 8 star coupler for star network topology in presence of optimized SOAs.

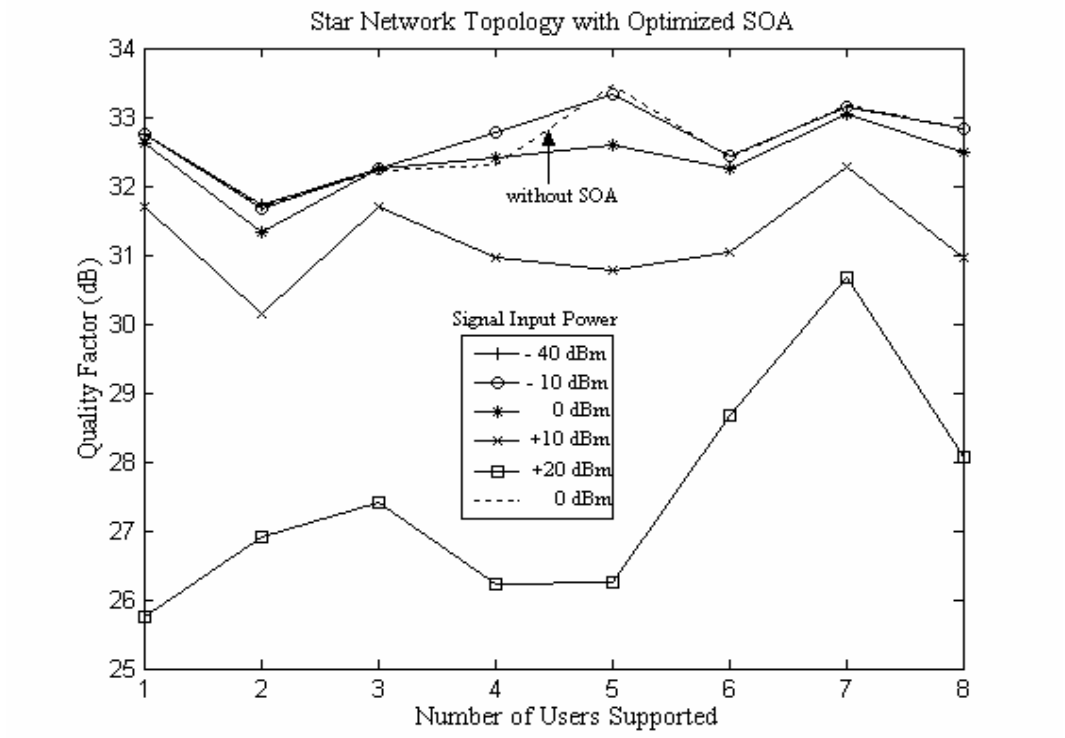

Figure 8.11: Quality factor as the function of different signal input power with given number of users supported for star network topology in presence of optimized SOAs.

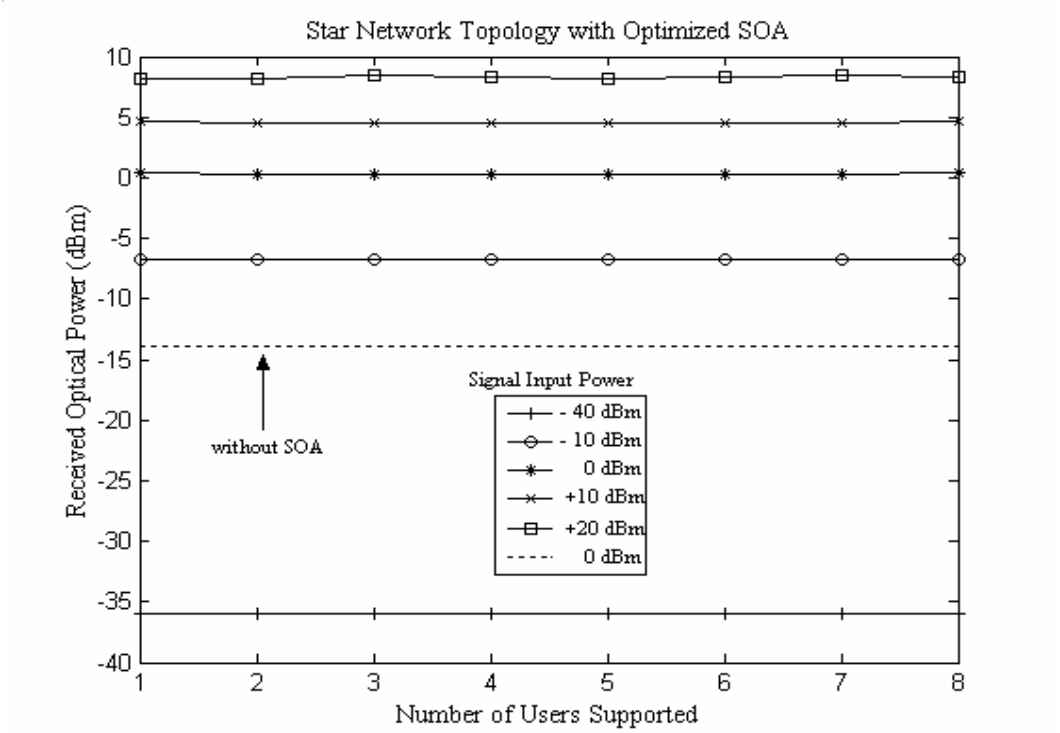

Figure 8.12: Received optical power as the function of different signal input power with given number of user supported for star network topology in presence of optimized SOAs.

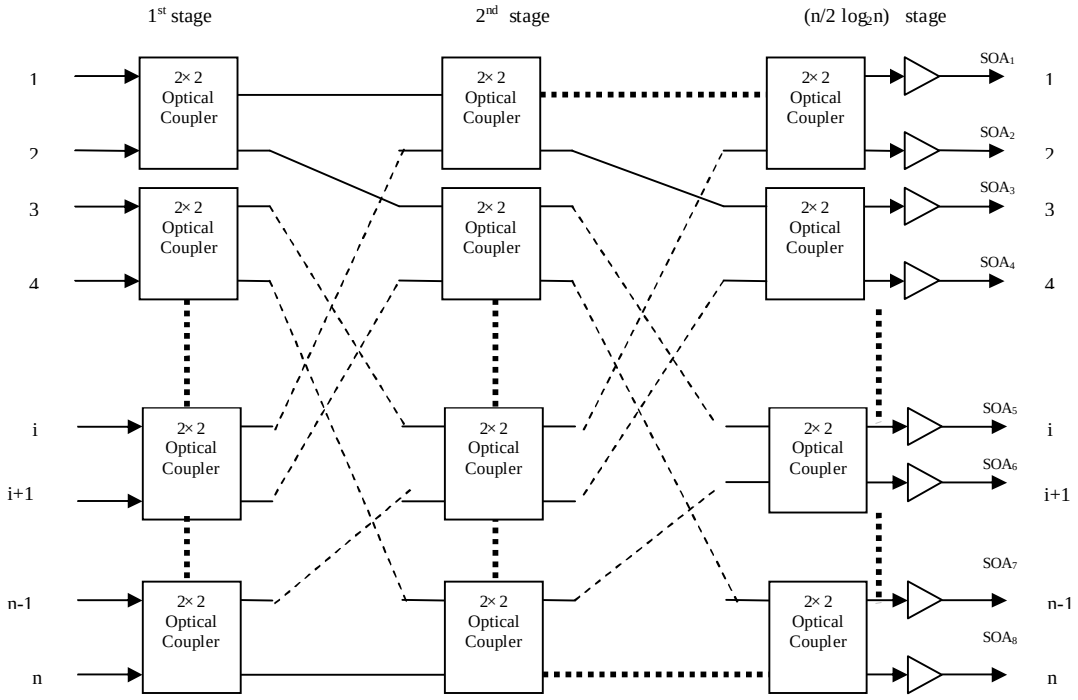

Figure 8.13: Schematic setup of n × n star coupler for n number of users star network topology in presence of optimized SOAs.

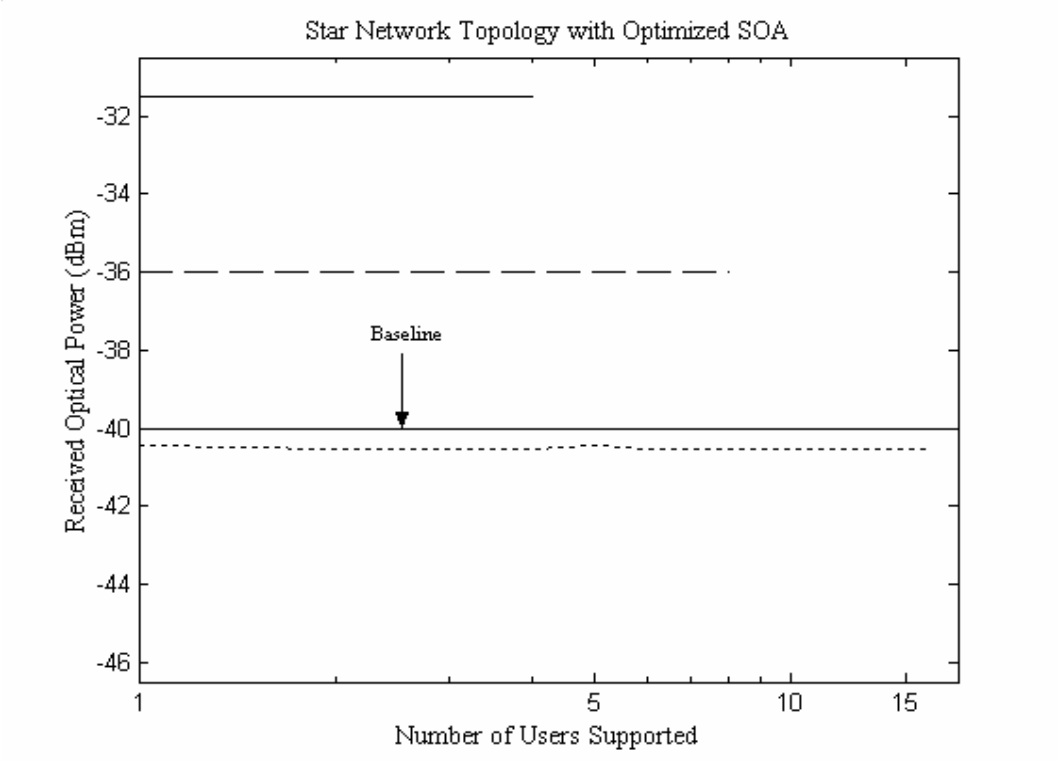

Figure 8.14: Received optical power as the function of number of users supported with -40 dBm signal input power for star network topology in presence of optimized SOAs.

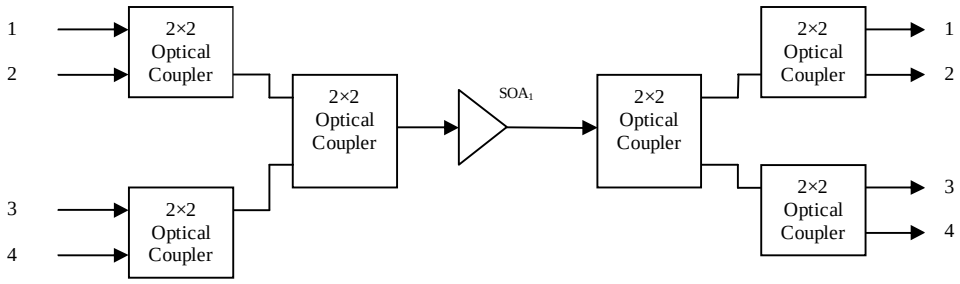

Figure 8.15: Schematic setup of 4 × 4 star coupler with one SOA for tree network topology in the presence of optimized SOAs.

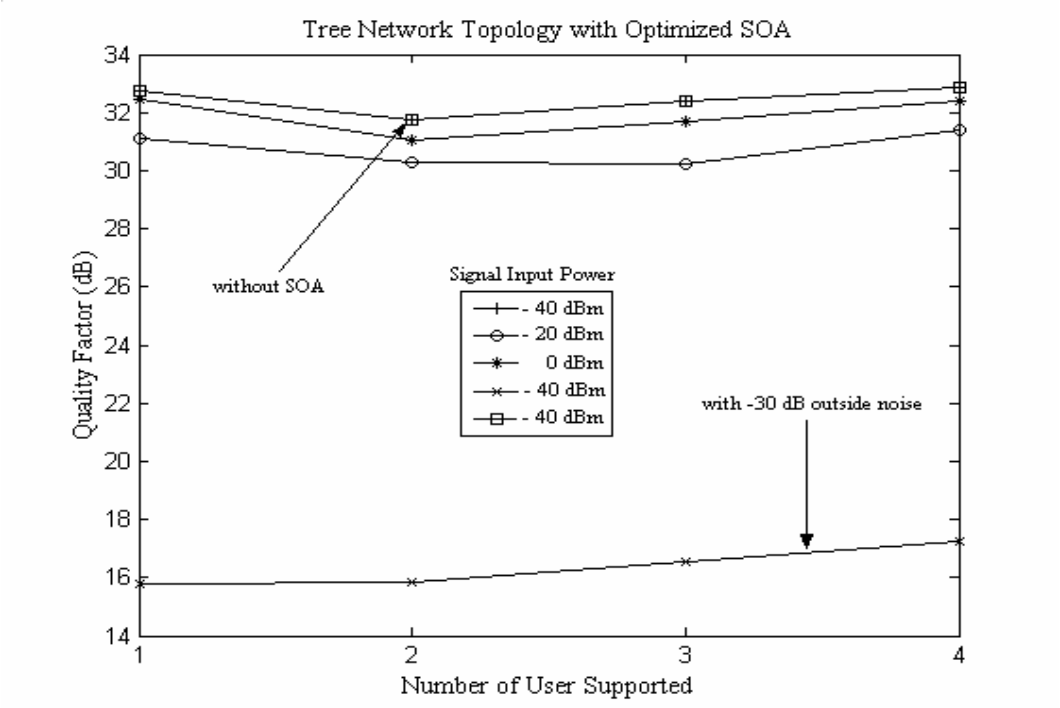

Figure 8.16: Quality factor as the function of different signal input power with given number of users supported for tree network topology in presence of optimized SOAs.

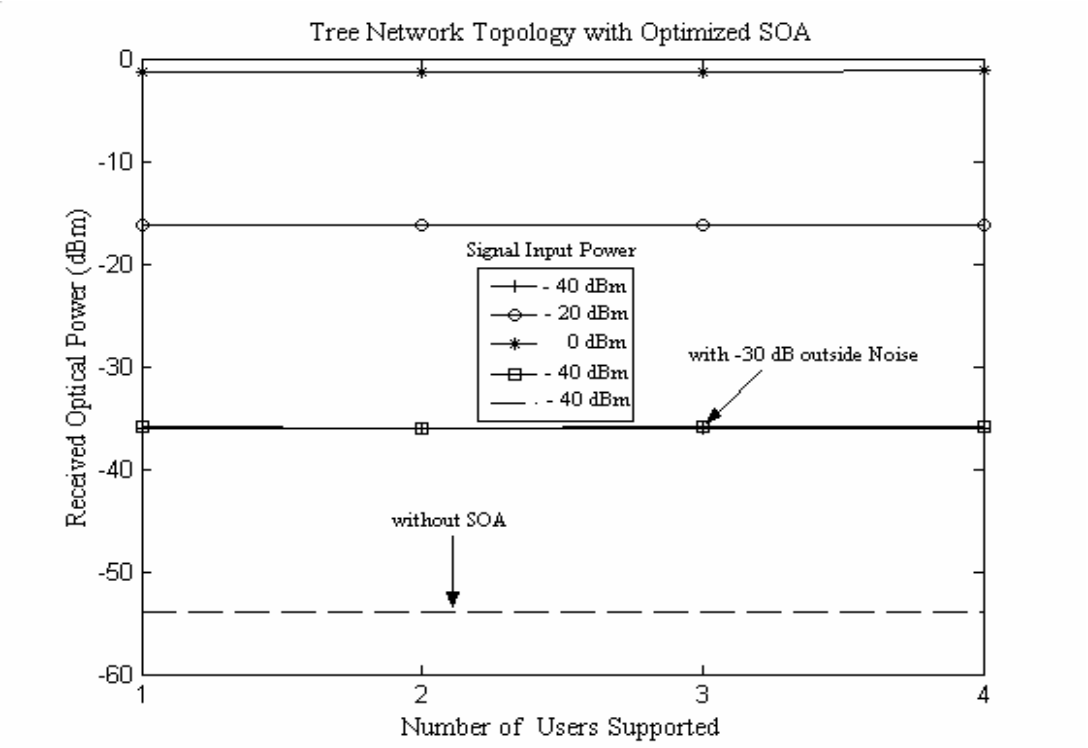

Figure 8.17: Received optical power as the function of different signal input power with given number of user supported for tree network topology in presence of optimized SOAs.

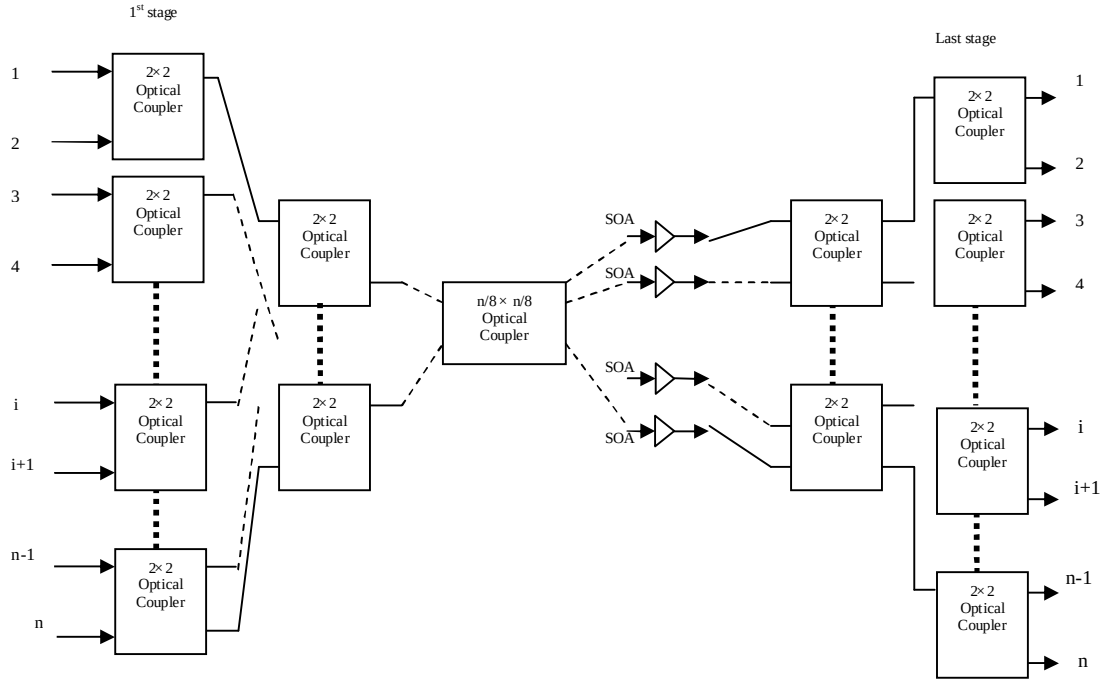

Figure 8.18: Schematic setup of n × n star coupler for n number of users in tree network topology in presence of optimized SOAs.

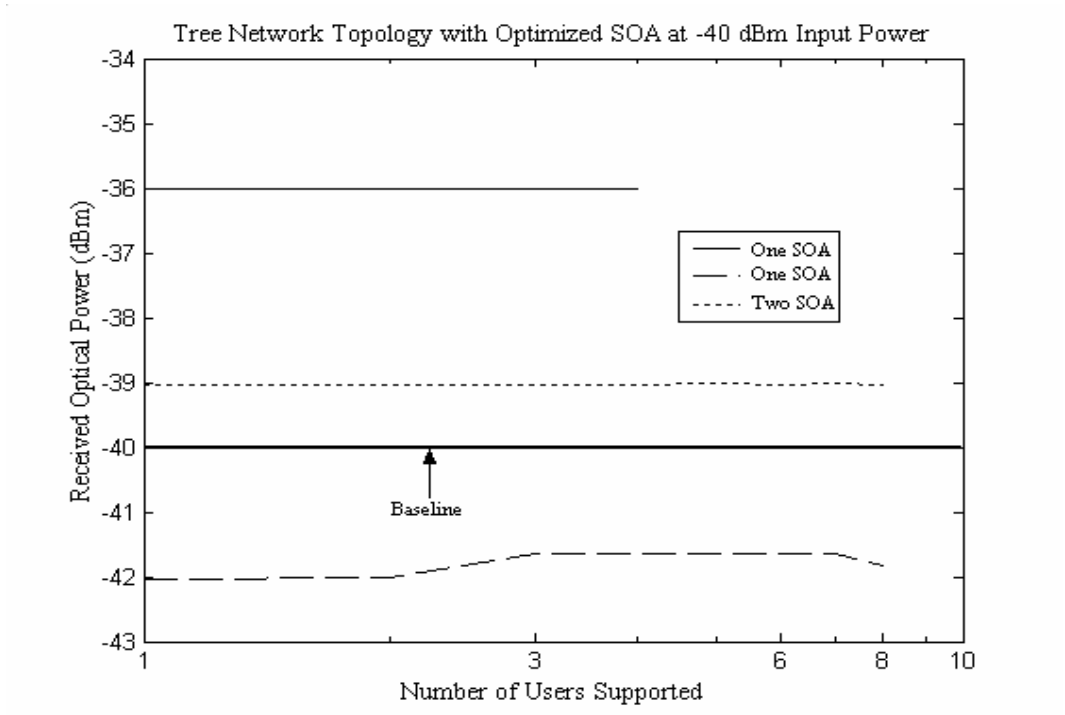

Figure 8.19: Received optical power as the function of number of users supported with -40 dBm signal input power for tree network topology in presence of optimized SOAs.

The number of Optical coupler used = $\left(\frac{N_u}{2}\right)\log_2 N_u$

8.5 Tree network topology with optimized SOAs

Tree network topology is consisted of star as main topology and folded bus as auxiliary topology. In tree net topology, the total number of users supported is $N_u = bn$ [Gerla and Fratta, 1988]. Here, b = 4 are branches and n = 1 is number of users per branch. The 4×4 star coupler with one SOA in tree net topology is shown in figure (8.15). The DPSK transmitter and receiver used here are same as used in the bus network topology. The simulation results of tree network topology for four users are shown in figures (8.16) and (8.17).

From figure (8.17), it is observed that power received goes on decreasing with increase in signal input power. However, the quality for all signal input power is almost same. While -30 dB outside noise is added in setup as shown in figure (8.15), the sufficient power is received. However, quality of received signal falls to 16 dB approximately.

If the number of users supported increases in the tree net topology then 2 dB power penalty as shown in figure (8.19). This is due to the gain saturation of the SOA and insertion loss etc. Figure (8.18) shows the setup for tree network topology for n number of users.

For eight users, two SOAs are used. The required power at the receiver is shown in figure (8.19). This shows an improvement over [Singh *et al.*, 1997], as the number of users supported for minimum signal input power at -40 dBm. It is found that for n number of users, there is need of $n/8 \times n/8$ optical star couplers required.

The number of SOAs used = $\frac{n}{8}$

The number of optical coupler required = $2\left(\frac{n}{2}+\frac{n}{4}+\frac{n}{8}\right)=\frac{7n}{4}$

8.6 Comparison of Optical Network Topologies

The performance of optical network topologies with optimized semiconductor optical amplifier at minimum signal input power is shown in figure (8.20). The performance of all optical network topologies is compared in terms of users supported, SOAs and optical couplers. For bus network topology, we need high signal input power of -5 dBm in order

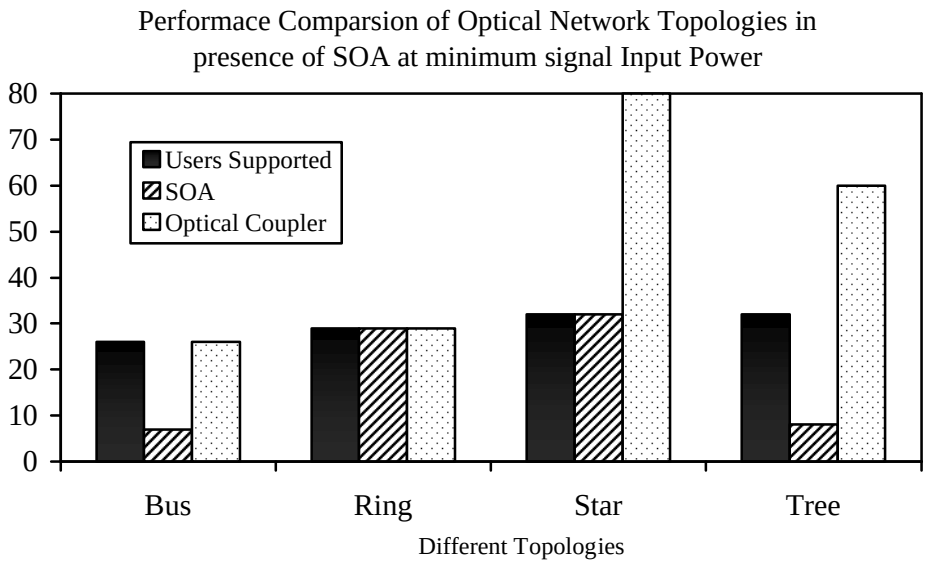

Figure 8.20: Bar graph for different network topologies in order to observe the performance in terms of number of user supported, SOAs, optical couplers at minimum signal input power.

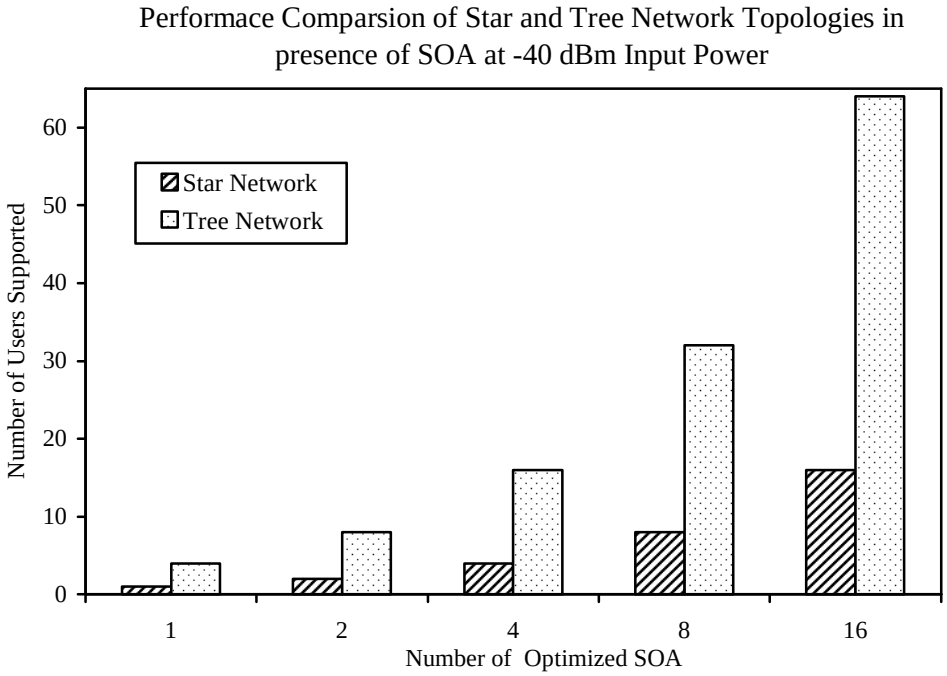

Figure 8.21: Bar graph between number of users supported and number of optimized SOAs for star and tree network topologies at -40 dBm signal input power.

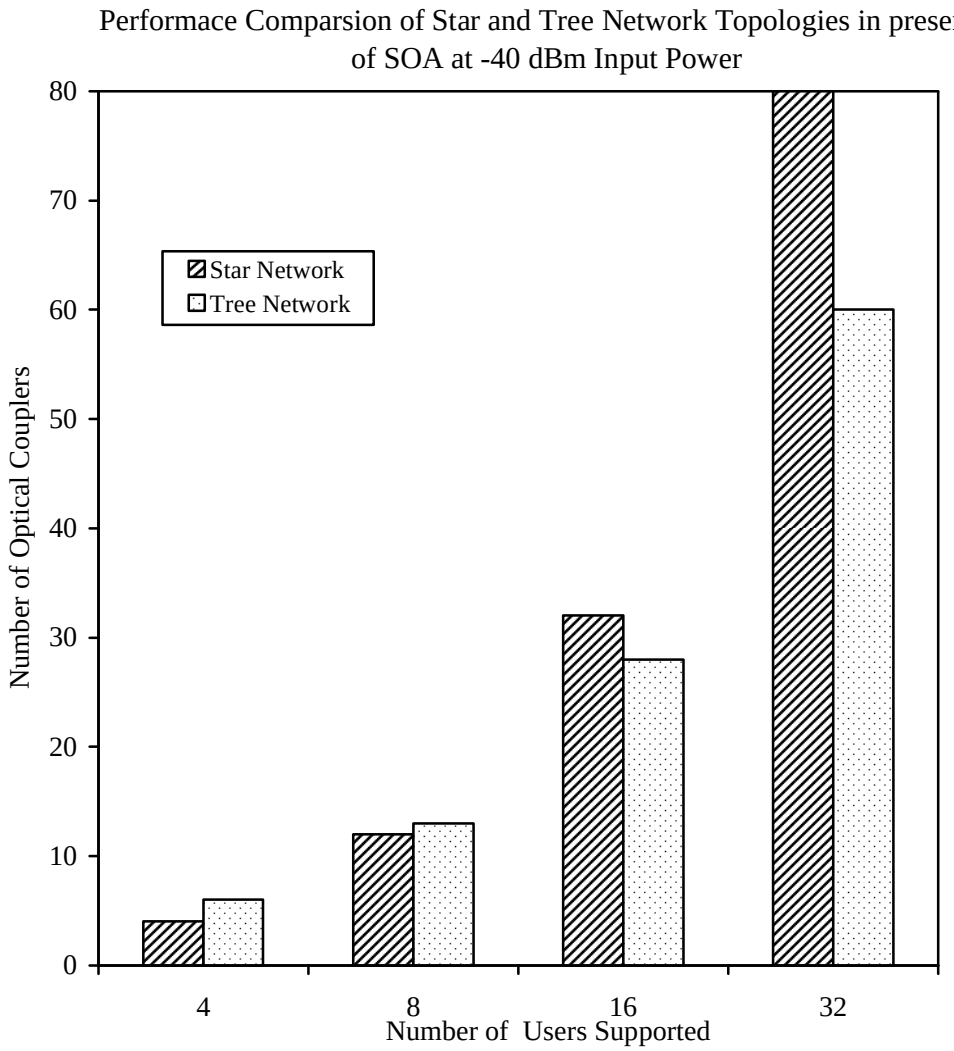

Figure 8.22: Bar graph between number of users supported and number of optical couplers for star and tree network topologies at -40 dBm signal input power.

to support maximum number of users up to 27. Even the number of optimized SOAs is 8 only. If the number of users are increased more than 27, then power penalty is found for next users. Although the number of optical couplers are same as users supported. Even then the bus network topology supports less number of users. Therefore, this topology is used in local area network.

In ring network topology, the number of users supported can be increased by using more SOAs and optical couplers. Here, the simulated results for maximum number of users are 28 only. In ring network topology, the possibility of propagation delay is more as compared to other topologies. If the 2^{nd} user is connected to 1^{st} user for clockwise ring network, then large propagation delay occurs as compared to star network topology for large number of users. The connectivity of one user to extreme users is poor in the case of ring network topology. The coverage of metro area network is possible as ring topology is the main back bone among metropolitan cities.

The star network topology can support maximum number of users, if insertion loss and splice loss be made minimum. The simulation results show that for 32 number of users, the number of optical couplers required are 80. The same number of SOAs are required as are the number of users. Hence, connectivity and propagation delay in this topology is much improved as compared to ring network topology.

Tree network topology has been also simulated for 32 users. This topology requires only eight SOAs and 56 optical couplers required. This topology has improvement over the other topologies.

The ring, star and tree network topologies can efficiently work at minimum signal input power of -40 dBm. These results show improvement over [Willner and Hwant, 1993; Gerla and Fratta, 1988; Singh *et al.*, 1997].

Further, the performance of star and tree network topologies is compared for maximum number of users at -40 dBm signal power. As shown in figure (8.21), for 16 number of optimized SOA, there are 16 users supported only. While in tree network topology, it can support 64 users. Also from figure (8.22), it is observed that the number of optical coupler required for tree network topology is 112. So tree network topology holds the maximum number of users supported at the cost of minimum utilization of the SOA. This result shows good agreement with [Singh *et al.*, 1997]. But we have obtained these results by using optimized SOA for minimum signal input power of -40 dBm.

8.7 Conclusions

It has been shown that the input power above saturation power of the SOA degrades the performance of all network topologies. In all our simulation setups, no users are supported without using SOAs. The bus network topology supported maximum 27 users with SOAs as per the setup taken in this Chapter. For ring network topology, the maximum number of nodes are more than 29. The number of users supported can be increased by decreasing splice and insertion loss in star network topology. The tree network topology offers maximum number of users with minimum utilization of SOAs and optical coupler. Hence, the tree network topology in presence of the optimized SOA provides low cost solution for connecting the large geographical area coverage.

Chapter 9

Conclusions and Scope for Future Work

9.1 Conclusions

The main motivation of this work is to increase the long haul and ultra broadband transmission distance, cascadability and flexibility of the optical networks. In order to achieve these goals, it is of utmost importance to optimize the optical amplifier and placement of OAs in optical communication systems and networks.

The semiconductor optical amplifiers (SOAs) have attracted much attention as it is cost effective as compared to the erbium doped fiber amplifiers for long haul optical communication system. But when gain saturation problems arise due to cross gain modulation (XGM), the cross phase modulation (XPM) and four wave mixing in multichannel optical system limits the system performance. Therefore, the cascaded utilization of the SOA is not possible for long transmission distance. The crosstalk and power penalty problem arises in long haul dense wavelength division multiplexing using cascaded SOA due to XGM and XPM. So there is need of proper placement of SOAs for long haul optical communication systems. Due to limited bandwidth of the SOA, there is requirement of erbium doped fiber amplifiers (EDFAs) for broadband communication systems. In past years, various techniques and methods were presented to flatten the gain of optical amplifiers to push the bit rate and transmission distance longer and longer.

Wavelength converters are the key components for increasing the flexibility and capacity of broadcast optical networks. The nonlinear effects like cross phase modulation (XPM) and four wave mixing (FWM) are the powerful elements for improving the performance of wavelength converters. All broadcast network topologies show improvement in the number of users when semiconductor optical amplifiers are placed appropriately in optical networks. But the real model of SOA utilization is not simulated in the literature for low power requirement.

This thesis focuses on the investigation of minimizing the nonlinearities in the semiconductor optical amplifiers due to XGM, XPM and gain flattening problems of EDFAs for increasing the transmission distance, capacity and flexibility of optical communication networks.

The major results obtained from this study are summarized as follows:

1. The SOA model is proposed for minimum gain fluctuation and nil power penalty for WDM multichannel transmission. For this, the SOA bias current is optimized for reduction of crosstalk with sufficient amplification. The low crosstalk of -10.314 dB and high optical gain 36.5 dB are achieved with reasonable ASE noise power. The WDM transmission of twenty channels at 10 Gb/s is achieved up to the transmission distance of 1190 km for the DPSK modulation format with channel spacing of 100 GHz. For the OOK system, the maximum transmission distance is up to 1050 km which has not been achieved yet. These results are obtained by using the optimized SOAs as in-line and pre-amplifiers. It is also observed that with the decrease in channel spacing, the quality of signal falls due to increase in cross gain modulation. The DPSK system performs best for 1190 km transmission distance with bit error rate less than 10^{-10} for all channels up to saturation power of SOA. Therefore, with the optimization of SOA, the capacity and transmission distance increases for the DPSK system. But the OOK system is best for small number of channels up to saturation of the SOA. It is concluded that DPSK system has large capacity as compared to OOK system.
2. It has been investigated for first time that the transmission of twenty-channel at 10 Gb/s DPSK signals over the transmission distance of 4340 km by using SOA as in-line and pre-amplifier at 100 GHz channel spacing. For this, the confinement factor of the SOA is optimized for reducing SOA-induced crosstalk and power penalty at sufficient amplification. Therefore, cross gain saturation of the SOA depends upon the confinement factor and the bias current. The DPSK system performs best for 4900 km transmission distance with bit error rate is less than 10^{-10} for all channels with power penalty of 1 dB.

   The optimization of differential gain of semiconductor optical amplifier at 40 Gb/s is also done. The soliton RZ-DPSK WDM signals having capacity of 0.4 Tbit/s is transmitted successfully up to the distance of 1050 km. This is achieved by using optimized semiconductor optical amplifiers with differential gain 210 atto cm^2 of the SOA and also improvement in power is more than 1.55 mW. The spectral efficiency is approaching to 0.4 bit/s/Hz for the transmission system. The cross gain saturation is further reduced by using the SOA with differential gain 200 atto cm^2. Therefore, the maximum transmission distance observed is 4550 km with good quality and nil power penalties per channel. The simulation of ten-channel 80 Gb/s WDM transmission over

910 km by using SOAs as in-line and pre-amplifier with soliton RZ- DPSK modulation format at 200 GHz channel spacing has been demonstrated.

The theoretical study of the SOA cross phase noise is proposed due to the gain saturation in WDM links. The crosstalk is found to be depending on the SOA structure parameters. The nonlinear cross phase noise is expected to be suppressed by increasing the carrier lifetime and width while reducing differential gain and confinement factor in WDM links. This SOA model may be attractive when used as pre-amplifiers and in-line amplifier for long haul links up to 5250 km for 10 × 40 Gb/s soliton DPSK WDM signals. This SOA model can offer a cost effective solution for WDM links. These results provide useful information for the designing of long WDM transmission links at high bit rate using low cost semiconductor optical amplifiers.

3. The post-power compensation method shows good performance in terms of bit error rate, eye closure penalty and received power as compared to pre- and symmetrical-power compensation methods. It is found that the pre-power compensated method in single span is best for pre-amplification of very low signal input power. The maximum transmission distance observed for post-power compensation method is 945 km.

   It has been investigated that the ten channels are used at 10 Gb/s WDM transmission 68908 km using SOAs as in-line and pre-amplifier with DPSK modulation format at 100 GHz channel spacing. In order to achieve this long haul transmission distance, the optimum span scheme is evaluated with power margin more than 24 dB. For this, the optimized SOA model is used with lower saturation power of 21.36 mW, high optical gain of 36.5 dB with reasonable ASE noise power. It has been shown that optical filter with 0.4 nm bandwidth is optimum for higher transmission distance. It is also observed that with decrease in channel spacing, the quality of signal falls due to increase in the crosstalk. For the transmission distance 17227 km, the optimum span scheme has been observed as the received quality signal is more than 27.5 dB with signal output power 0.097 dBm for channel no. 5. But for 68908 km transmission distance, optimum span scheme shows degradation in quality up to 14 dB with increase in the signal output power 0.87 dBm. It has been shown that for the optimum span scheme-1, the quality of the signal is 25.8 dB with signal power -38.5 dBm for channel no.5. This result generates power penalty of 24.5 dB for 68908 km transmission distance. It is also observed for the first time that for 50 GHz channel

spacing, the maximum transmission distance is 6650 km and for 20 GHz and maximum transmission distance 3500 km is observed by using cascaded SOAs with 10 × 10 Gb/s RZ-DPSK format.

The simulation of ten channels 10 Gb/s DWDM are performed by using cascaded SOA with the DPSK modulation format at 20 GHz channel spacing. we used optimized the SOA model for this simulation. At optimum bias current, low crosstalk and optimum bandwidth is obtained for optical phase modulator *i.e*. 5.5 GHz. Using optimum span scheme, it is possible to transmit 100 Gb/s RZ-DPSK signal at 17,227 km with maximum optical signal power up to gain saturation with BER floor less than 10^{-10}.

4. The SOA model is proposed for optical pre-amplifier for the PIN and the DPSK photoreceivers. The minimum receiver sensitivity of -69.9 dBm is observed at BER floor of 4.6×10^{-10} for PIN receiver at 10 Gb/s. An improvement in the receiver sensitivity of -19.2 dBm and -46.5 dBm is observed for the PIN receiver and the DPSK receiver at 40 Gb/s. The ASE noise power for the PIN photo detector is 22.3 µW is measured at 0.1 mW, while for the DPSK receiver is 4.1 µW which is quite lower. It has been shown that gain variation increases with increase of input light power and tolerance in input wavelength power is more than 100 nm. It is also observed that the optical gain is insensitive to polarization and remains constant. For multichannel WDM transmission links show improvement in detected power with better quality at 0.25 ns carrier lifetime.
5. In order to utilize the bandwidth of the EDFA a gain flattening approach has been illustrated. The additions gain spectrum of EDFAs makes the gain nearly flat. By using this approach, sixteen channel NRZ-DPSK signals are transmitted over the distance of 490 km at 40 Gb/s. Another approach to flatten the gain of EDFA is possible by placing the optical super Gaussian notch filter after EDFA in each span. The gain spectrum of EDFA is flattened with increase in transmission distance. Therefore, it is possible for first time that the sixteen channels NRZ-DPSK signals transmission over the distance of 504 km at 40 Gb/s. The bit rate distance product of 322.56 Tb/s km can be achieved.
6. The 50 nm up and down wavelength conversion is possible for non-return to zero differential phase shift keying (NRZ-DPSK) signal by using four wave mixing in a semiconductor optical amplifier (SOA) at 10 Gb/s. We decrease the gain fluctuations by selecting suitable parameters of the SOA to achieve sufficient quality with

enhancement in four wave mixing signals. The minimum Q factor penalty observed is 1.5 dB at signal-to-pump ratio of -9 dB for both up and down conversion range of 20 nm. The Q factor improvement observed is 1.74 dB for signal-to- pump ratio of -5 dB at 0 dBm pump signal for 50 nm up converter. Ten stage cascaded wavelength conversion over 1302 km single mode transmission is possible for 10 Gb/s NRZ-DPSK format by using FWM in SOA.

The wavelength conversion using XPM in the SOA-MZI configuration with wide band more than 15 nm up and down conversions, for the first time has also been shown. It is observed that high active region length and bias current in the SOA leads to XPM in the SOA-MZ1 configuration. For this, the low pump power of 1 dB is observed. For up conversion range of 0.58 nm, the improvement in quality of 0.2 dB is observed at signal-to-pump power of -6 dB. This wavelength converter provides conversion band of more than 15 nm for both up and down conversions. The conversion efficiency of this converter is more than 11 dB at signal-to-pump power of -9 dB. On the whole, this wavelength converter leads to an increase in the cascadability of wavelength converters for increasing the capacity of future optical networks.

7. It is observed that input power above saturation power of the SOA degrades the performance of all network topologies. The bus network topology supports maximum 27 users. For ring network topology, the maximum number of nodes are more than 29. The number of users supported can be increased by decreasing splice and insertion loss in the star network topology. The tree network topology offer maximum number of users with minimum utilization of SOAs and optical coupler. Hence, tree network topology in presence of optimized SOA provides low cost solution for connecting large geographical area coverage.

   Therefore, this study establishes that the use of optimized optical amplifiers in the optical communication networks results in revolutionary growth of internet traffic for large number of users and long transmission distance.

9.2 Recommendations

1. The SOA structural parameters are obtained by minimizing the XGM and XPM for multichannel wavelength division multiplexing system. With this SOA model, the maximum transmission distance more than 5220 km is possible for 10 × 40 Gb/s soliton RZ-DPSK WDM signals. Hence, this low cost SOA model can be

recommended for WDM transmission system as compared to complex and high cost doped fiber amplifiers. The optimum span scheme can be very useful for long haul DWDM transmission system by using cascaded optimized SOAs. The SOA model can also be applicable for low signal power to support large number of users in tree network topology.

2. The proposed gain flattening approach-III of EDFA can also be applied to more number of channels. Therefore, with this approach high bit rate distance product is achieved and applicable for wideband optical system.
3. The proposed SOA model based on enhanced FWM and XPM effects can be employed for wide range wavelength converters. The SOA parameters can be recommended for the design of optimized SOA that can be utilize for wide band wavelength converters.

9.3 Scope for Future Work

1. There is need of detailed study for the XGM, XPM, and FWM in Raman amplifier for multichannel WDM transmission system. The structural parameter optimization of EDFA and Raman Amplifier is evaluated by reducing theses nonlinearities in doped fiber amplifiers for long haul WDM transmission at higher bit rate. From this work, the optimum evaluated doped fiber has larger bandwidth as compared to SOA. The work also needs to study of self phase modulation of all optical amplifiers.
2. The research work can be extended for structural optimization of SOA for deducing efficient wavelength converter based on XGM for wideband conversion and all conversions are needed for higher bit rate as per current demands.
3. As doped fiber amplifiers having applications in wide area network (WAN) as in-line amplifiers. The placement of optimum doped fiber amplifiers (DFAs) in different optical network topologies can be studied. The doped fiber amplifier placement can also be explored in other broadcast topologies including multilevel topologies.
4. In Chapter 2, 3 and 4, the work is needed to consider the effects of polarization mode dispersion (PMD) and higher order dispersion of fiber for long distance optical communication system can be included as further scope of this study. The other type impairments like thermal noise, quantum noise

can also be added to study the combined impact for long haul transmission distance in optical communication system.

5. In chapter 7, while the wavelength converters based on FWM and XPM are used in optical network having some blocking probability, the work must progress for further to minimize the blocking probability of these wavelength converters while placing in optical networks.
6. The simulation results for DWDM systems which were carried for systems with capacity up to 100 Gb/s for maximum transmission distance of 17227 km and channel spacing 20 GHz using SOA in chapter 4 can be enhanced further.

Agrawal G.P., "*Fiber-optic communication system*," John Wiley Publisher, Singapore, pp. 06-08, 226-239 and 306-307, 2002.

Agrawal G.P., "*Applications of nonlinear fiber optics*," Academic Press, San Diego, CA, 2001.

Agrawal G.P., "*Nonlinear fiber optics*," 3rd ed. Academic Press, San Diego, CA, 2001.

Agrawal G.P. and Dutta N.K., "*Semiconductor Laser*," 2nd edition, Van Nostrand Reinhold, New York, 1993.

Agrawal G. P. and Olsson N. A., "Self-phase modulation and spectral broadening of optical pulses in semiconductor laser amplifiers", IEEE Journal of Quantum Electronics, Vol. 25, No.11, pp. 2297-2306, Nov.1989.

Aoki Y., "Properties of fiber Raman amplification and their applicability to digital optical communication system," IEEE Journal of Lightwave Technology, Vol. 6, No.7, pp. 1225-1239, 1988.

Bergano N. S., Aspell J., Davidson C.R., Trischitta P.R., Nyman B.M., Kerfoot F.W. , Holmdel N.J., "Bit error rate measurements of 14000 km 5 Gbit/s fiber-amplifier transmission system using circulating loop," Electronics Letters, Vol. 27, Issue 21, pp. 1889-1890, 1991.

Bergano N.S., "Long-haul WDM transmission using optimum channel modulation: A 160 Gb/s (32 × 5 Gb/s) 9,300km demonstration," *Proceedings of Optical Fiber communications Conferences*, paper PD-21, Feb., 1997.

Bischoff S., Buxens A., Poulsen H. N., Clausen A.T. and Mork J., "Bi-Directional Four Wave Mixing in Semiconductor Optical Amplifiers : Theory and Experiment," IEEE Journal of Light Wave Technology ,Vol.17, No. 9, pp.1617-1625, Sept. 1999.

Bjorlin E. Staffan and Bowers John E., "Noise Figure of Vertical-Cavity Semiconductor Optical Amplifiers," IEEE Journal of Quantum Electronics, Vol. 38, No. 1, pp.61-66, January 2002.

Blahut R. E., "*Theory and Practice of Error Control Codes*," Addison Wesley, 1983.

Bonati A., Chesnoy J., Erman M., Gabla P.M., Piacentin B. and Reinaudo C., "Global turnkey solutions for back-bone transmission networks," *Alcatel Telecommunications Review*, 3rd Quarter, 1999.

Bononi Alberto and Barbieri Lorenzo, "Design of Gain-Clamped Doped-Fiber Amplifiers for Optimal Dynamic Performance," IEEE Journal of Lightwave Technology, Vol. 17, No.7, pp.1229-1240, July1999.

Brackett C. A., "Dense wavelength division multiplexing networks: principles and applications," IEEE Journal on Selected Areas in Communications, Vol.8, No.6, pp.948-964, August 1990.

Carena A., Curri V. and Poggiolini P., "On the Optimization of Hybrid Raman/Erbium-Doped Fiber Amplifiers," IEEE Photonics Technology Letters, Vol. 13, No.11, pp. 1170-1172, Nov.2001.

Chen Y. K., "Amplified distributed reflective optical star couplers," IEEE Photonics Technology Letters, Vol.4, No.6, pp.570-573, June 1992.

Chen Yung-Kuang, Chi S. and Guo Wann-Yih, "High-flexibility configurations of amplified star coupler for optical networks," Journal of Optical Communications, Vol.15, No.2, pp.56-62, 1994.

Cho P.S., Gtigoryan V.S., Godin Y.A., Salamon A. and Achiam Y. , "Transmission of 25 Gb/s RZ-DPSK signals with 25 GHz channel spacing over 1000 km SMF-28 fiber. Photonics Technology Letters, vol. 15, pp. 473-475, 2003.

Cho P.S. and Khurgin J.B., "Suppression of cross-gain modulation in SOA using RZ-DPSK modulation formats," IEEE Photonics Technology Letters, Vol. 15, No.1, pp.162–164, Jan., 2003.

Choi W., Hur S., Lee J., Kim Y., and Jeong J., "Transmission performance analysis of 8 × 10 Gb/s WDM signals using cascaded SOAs due to signal wavelength displacement," IEEE Journal Lightwave Technology, vol. 20, pp. 1350-1356, Aug. 2002.

Chung H.S. and Chung Y.C., "Transmission of 8 × 40 Gb/s WDM channels with 100 GHz spacing using short-period dispersion-managed fiber," Journal of Optics Communications, Vol. 250, pp. 286-291, 2005.

Cockrane P., "Future directions in long haul fiber optic system," British Telecom Technology Journal, Vol. 8, No.2, pp. 5-17, 1990.

Chraplyvy A. R., Delavaux, J.M., Derosier R. M., Ferguson G. A., Fishman D. A., Giles C. R., Nagel J. A., Nyman B. M., Sulhoff J. W., Tench R. E., "1420 km transmission of sixteen 2.5 Gb/s channels using silica-fiber-based EDFA repeaters," IEEE Photonics Technology Letters, Vol. 6, No. 11, pp. 1371-1373, Nov. 1994.

Dagenais M., Heim P., Saini S., Wilson S., Leavitt R., Yu A., Horton T., Luciani V., Stone D., and Hu Y., "High power C-band semiconductor booster optical amplifier," *Optical Fiber Communication Conf. OFC 2003*, Atlanta, GA, Vol. 1, pp. 85-87, March 23–28, 2003.

Desurvire E., Giles C.R. and Simpson J.R., "Gain saturation effects in high speed, multichannel erbium doped fiber amplifiers at λ= 1.53 μm," IEEE Journal of Lightwave Technology, Vol. 7, pp. 2095-2104,1989.

Diagonnet M.J.F., "*Rare-earth doped fiber laser and amplifier*," Marcel Dekker, New York, 1993.

Dreyer K., Joyner C. H., Pleumeekers J. L., Burrus C. A., Dentai A., Miller B. I., Shunk S., Sciortino P., Chandrasekhar S., Buhl L., Storz F., and Farwell M., "High-gain mode-adapted semiconductor optical amplifier with 12.4-dBm saturation output power at 1550 nm," IEEE Journal of Lightwave Technology, Vol. 20, pp. 718–721, 2002.

Durhuus T., Mikkelsen B., Joergensen C., Danielsen S. L. and Stubkjaer K. E., "All-optical wavelength conversion by semiconductor optical amplifiers," IEEE Journal of Lightwave Technology, Vol. 14, pp. 942-954, 1996.

Duthie P. J., Wale M. J. and Bennion I., "A New Architecture for Large Integrated Optic Switch Arrays," *Proceedings of First Topical Meeting on Photonic Switching*, Incline Village, Nevada, Photonic Switching, Springer-Verlag, March 18-20, 1987.

Erwan Pincemin, Oliver Audouin, Bruno Dany and Stefan Wabnitz., "Stability of synchronous intensity modulation control of 40 Gb/s dispersion managed soliton transmission," IEEE Journal of Lightwave Technology, vol. 19, no. 5, pp 624-635, May 2001.

Fiddy Michael, "Artificial Materials for Optical Switches and Buffers," *Proceeding of PAK-US International Symposium on 'High Capacity Optical Networks and Enabling Technologies'*, Islamabad, Pakistan, Dec.19-21, 2005.

Franz J. and Jain V.K., *"Fiber-optic communication system,"* pp. 279-303, Narosa Publisher, India, 1996.

Geraghty D.F., Lee R.B., Verdilt M., Ziari M., Mathur A. and Vahala K.J., "Wavelength conversion for WDM communication system using four-wave mixing in semiconductor optical amplifiers", IEEE Journal Select. Topics Quantum Electronics, Vol. 3, pp. 1146-1155, May 1997.

Gerla M. and Fratta L., “Tree Structured Fiber Optic MANs,” IEEE J. Selected Areas in Communications, Vol.6, No.6, pp.934-943, July 1988.

Giles C.Randy and Desurvire Ennanuel, “ Modeling erbium doped fibre amplifier,” IEEE Journal of Lightwave Technology, Vol. 9, No 2, pp.271-283, Feb 1991.

Gimlett J.L., “A new low noise 16 GHz PIN/HEMT optical receiver,” *ECOC’88 (Post Deadline Session)*, Brighton, pp.13-16, Sept., 1988.

Girardin F., Guekos G., and Houbavlis A., “Gain recovery of bulk semiconductor optical amplifiers,” IEEE Photonics Technology Letters, Vol.10, pp.784-786, 1998.

Giuliani G. and Alessandro D. D’, “Noise analysis of conventional and gain-clamped semiconductor optical amplifiers,” IEEE Journal of Lightwave Technology, Vol. 18, pp. 1256–1263, Sept. 2000.

Gnauck A. H. and Giles C. R., “2.5 and 10 Gb/s transmission experiments using a 137 Photon/bit erbium-fiber preamplifier receiver,” IEEE Photonics Technology Letters, Vol. 4, pp.80-82, 1992.

Goldstein E., “Optical ring networks with distributed amplification,” IEEE Photonics Technology Letters, Vol.3, No.4, pp.390-393, April 1991.

Green P. E., “Fiber Optic Networks,” Prentice Hall, India, 1993.

Gustavsson M., Lagerstrom B., Thylen L., Janson M., Lundgren L., Morner A. C., Rask M., Stoltz B., “Monolithically integrated 4 × 4 InGaAsP/InP laser amplifier gate switch arrays,” Electron. Letter, Vol. 28, Issue 4, pp. 2223-2225, 1992.

Hsu D., Lee S.L., Gong P.M., Y.M. Lin, Lee S.S.W. and Yuang M.C., “High efficiency wide-band SOA-based wavelength converter by using dual-pumped FWM and an assist beam,” IEEE Photonics Technology Letters, Vol. 16, pp. 1903-1905, 2004.

Hwang Seongtaek and Cho Kyuman, “Gain tilt control of L-band erbium-doped fiber amplifier by using a 1550-nm band light injection,” IEEE Photonics Technology Letters, Vol. 13, No. 10, pp.1070-1072, Oct. 2001.

Huang W. and Jain F. , “Integrated InGaAs-InP quantum wire laser-modulators for 1.55-μm applications,” Journal of Optical Engineering, Vol. 43, Issue 3, pp. 667-672, March 2004.

Iannone E., Sabella R., Stefano L. de, and Valeri F., “All-optical wavelength conversion in optical multi carrier networks,” IEEE Trans. Communication, Vol. 44, pp. 942-954, 1996.

Iannone P.P., Reichmann K.C., Smiljanic A., Frigo N.J., Gnauck A.H., Spiekman L.H., and Derosier R.M., "A transparent WDM network featuring shared virtual rings," IEEE Journal of Lightwave Technology, Vol. 18, No. 12, 1955-1963, Dec. 2000.

Irshid M. I. and. Kavehrad M, "Expansion of FDM/WDM star networks using high-power erbium-doped fiber amplifiers," Journal of Optical Communications, Vol.14, No.3, pp.114-119, 1993.

Jain Faquir and Huang W., "1.55 mm InGaAs-InP quantum wire optical modulators: optimization of wire width to maximize absorption and index of refraction changes due to excitonic transitions", International Journal of Infrared and Millimeter Waves, vol. 22, pp. 1009-1018, Jul. 2001.

Jennen Jean, Waardt H. de, and Acket G., "Modeling and performance analysis of WDM transmission links employing semiconductor optical amplifiers," IEEE Journal of Lightwave Technology, Vol. 19, pp. 1116-1124, Aug.2001.

Joergensen C., Danielsen S. L., Stubkjaer K. E., Schilling M., Daub K., Doussiere P., Pommerau F., Hansen P. B., Poulsen H. N., Kloch A., Vaa M., Mikkelsen B., Lach E., Laube F., Idler W., and Wunstel L., "All-optical wavelength conversion at bit rates above 10 Gb/s using semiconductor optical amplifiers," IEEE Journal Select. Topics Quantum Electronics, Vol.3, pp. 1168-1180, 1997.

Kartalopoulos S.V., "*Introduction to DWDM technology*", IEEE and SPIE Optical Engineering Press, USA, 2000.

Kasamatsu T., Yano Y. and Ono T., "Laser-diode-pumped highly efficient gain-shifted thulium-doped fiber amplifiers operating in the 1480-1510nm band," IEEE Photonics Technology Letters, Vol.13, pp.506-508, 2001.

Kasper B.L., "An APD/FET optical receiver operating at 8 Gb/s," IEEE Journal of Lightwave Technology, Vol. LT-5, No.3, pp. 344-347, 1987.

Kelly A. E., Lealman I. F., Rivers L. J., Perrin S. D. and Silver M., "Polarization insensitive, 25-dB gain semiconductor laser amplifier without antireflection coatings," Electronic Letters, Vol. 32, no. 19, pp. 1835-1836,2000.

Kikuchi K., Zah C.E. and Lee T.P., "Measurement and analysis of phase noise generated from semiconductor optical amplifiers", IEEE Journal of Quantum Electronics, Vol. 27, No.3, pp. 416-422, March 1991.

Kim Y., Jang H., Kim Y., Lee J., Jang D., and Jeong J., " Transmission performance of 10 Gb/s 1550-nm transmitters using semiconductor optical amplifiers as booster

amplifiers," IEEE Journal of Lightwave Technology, Vol. 21, No.2, pp. 476-481, Feb. 2003.

Kim H. K., Chandrasekhar S., Srivastava A., Burrus C. A., and Buhl L., "10 Gb/s based WDM signal transmission over 500 km of NZDSF using semiconductor optical amplifier as the in-line amplifier," Electronic Letters, Vol. 37, No. 3, pp.185-187, 2001.

Koai K. T. and Olshansky R., "Nonregenerative photonic dual bus with optical amplifiers," IEEE Photonics Technology Letters, Vol.4, No.4, pp.482-485, April 1993.

Kobrinski H., Bulley R.M., Goodman M.S., Vechi M.P. and Brackott C.A., "Demonstration of high capacity in the lambdanet architecture: Multiwavelength Optical Networks," Electronic Letters, Vol.23, No.18, pp. 824-826, July 1987.

Koestner C.J. and Snitzer E.A., "Amplification in a fiber laser," Journal of Applied Optics, Vol. 3, pp. 1182-1187, 1964.

Kovacevic M. and Acampora A., "Benefits of wavelength translation in all optical clear channel networks," IEEE Journal of Selected Area in comm., Vol. 14, pp. 69-79, 1996.

Li Z., Yi D., Mo J., Wang Y. and Lu C., " 1050-km WDM transmission of 8 × 10.709 Gb/s DPSK Signal using cascaded in-line semiconductor optical amplifier," IEEE Photonics Technology Letters, Vol. 16, No. 7, pp. 1685-1687, July 2004.

Ludwig R. and Raybon G., "BER measurement of frequency converted signals using four-wave mixing in semiconductor laser amplifier at 1,2.5,5 and 10Gbit/s", Electronic Letters, Vol. 30, pp. 338-339, Jan. 1994.

Lu L., Dong Y., Wang H., Cai W., and Xie S., "Bit-error-rate performance dependence on pump and signal powers of the wavelength converter based on FWM in semiconductor optical amplifiers", IEEE Photonics Technology Letters, Vol. 12, pp. 855–857, July 2000.

Lyons M.H., Jonsen K.D. and Hawker I., "Traffic scenanos for the 21st century," British Telecom Technology Journal, Vol. 11, No. 4, pp. 73-84, Oct. 1993.

Mahony M. J. O', "Semiconductor laser optical amplifiers for use in future fiber systems," IEEE Journal of Lightwave Technology, Vol. 6, pp. 531-544, 1988.

Majumder S.P., Sarkar B.C. and Yoshino T., "Performance analysis of an all optical wavelength converter based on XPM in SOAs," Journal of Optics and Laser Technology, Vol. 35, pp.261-265, 2003.

Majumder S.P., Sarkar B.C. and Yoshino T., "Performance evaluation of a wavelength converter based on SOA as a symmetrical-MZ1 configuration," Journal of Optical Fiber Technology, Vol. 11, pp.146-158, 2005.

Marrakchi Abdellatif and Dekker Marcel, "Photonic Switching and Interconnects," Eds., 1994.

Mason B., Chandrasekhar S., Ougazzaden A., Lentz C., Geary J. M., Buhl L. L., Peticolas L., Glogovsky K., Freund J. M., Reynolds L., Przybylek G., Walters F., Sirenko A., Boardman J., Kercher T., Rader M., Grenko J., Monroe D., and Ketelsen L., "Photonic integrated receiver for 40 Gbit/s transmission," Electronic Letters, Vol. 38, pp. 1196–1197, 2002.

Matsuda T., Kotanigawa T., Kataoka T. and Naka A., "54 × 42.7 Gb/s L- and U-band WDM signal transmission experiments with in-line hybrid optical amplifiers," Electronics Letters, Vol. 40, No. 6, pp. 380-381, 2004.

Mecozzi A., "Soliton transmission control with semiconductor amplifiers," Opt. Letter, Vol. 20, pp. 1616-1618, 1995.

Mollenauer L.F., "Soliton transmission speeds greatly multiplied by sliding-frequency guiding filters," Optics and Photonics News, Vol. 5, Issue 4, pp.15-19, April 1994.

Morgan T. J., Tucker R.S. and Lacey J.P.R., "All-optical wavelength translation over 80 nm at 2.5 Gb/s using four wave mixing in semiconductor optical amplifiers," IEEE Photonics Technology Letters, Vol. 11, pp. 982-984, 1999.

Morito K., Ekawa M., Watanabe T., and Kotaki Y., "High-output-power polarization-insensitive semiconductor optical amplifier," IEEE Journal of Lightwave Technology, Vol. 21, No.1, pp. 176–181, January 2003.

Morito K., Ekawa M., Watanabe T., Fujii T. and Kotaki Y., "High saturation output power (+17 dBm) 1550 nm polarization insensitive semiconductor optical amplifier," *26th Europ. Conf. Optical Communication ECOC 2000*, Munich, Germany, pp. 39-41, September 3–7, 2000.

Miyamoto et al., "8 × 40 Gb/s WDM transmission over 367 km zero dispersion flattened line with 120 km repeater using carrier suppressed RZ pulse format," *Tech. digest OAA'99.*, Nara, post-Deadline paper PDP4, 999.

Mynbaev D.H. and Scheiner L.L., "*Fiber-optic communications technology*," Pearson Education, 4th Ed., pp. 546-547, 2004.

Nakano H., Tsuji S., Sasaki S., Uomi K. and Yamashita K., " 10 Gb/s, 4-channel wavelength division multiplexing fiber transmission using semiconductor optical

amplifier modules," IEEE Journal of Lightwave Technology, Vol. 11, No. 4, pp. 612-617 ,April 1993.

Nakazawa M., Kubota H., Suzuki K., Yamada E., Sahara A., " Ultrahigh-speed long-distance TDM and WDM soliton transmission technologies," IEEE Journal of Selected Topics in Quantum Electronics, Vol. 6, Issue: 2, pp. 363-396, Mar/Apr 2000.

Nielsen T. N., Stentz A. J., Rottwitt K., Vengsarkar D. S., Chen Z. J., Hansen P. B., Park J. H., Feder K. S., Strasser T. A., Cabot S., Stulz S., Peckham D.W., Hsu L., Kan C. K., Judy A.F., Sulhoff J., Park S. Y., Nelson L. E., and Gruner-Nielsen L., "3.28 Tbit/s (82 x 40Gb/s) transmission over 3 x 100 km nonzero-dispersion fiber using dual C and L-band hybrid Raman/Erbium-doped inline amplifiers," *Proceeding of OFC 2000*, Baltimore, post-deadline paper 23, 2000.

Novak S. and Moesle A., "Analytic model for gain modulation of EDFA," IEEE Journal of Lightwave Technology, Vol. 20, No. 6, pp. 975-985, 2002.

Nuyts R.J., Park Y.K., Gallison P., **"**Performance improvement of 10 Gb/s standard fiber transmission systems by using the SPM effect in the dispersion compensating fiber," IEEE Photonics Technology Letters, Vol. 8, pp. 1406-1408, 1996.

Oberg M. G. and Olsson N. A., "Crosstalk between intensity-modulated wavelength-division multiplexed signals in a semiconductor laser amplifier," IEEE Journal of Quantum Electronics, Vol. 24, pp. 52-59, 1998.

Olsson N.A., "Light wave systems with optical amplifiers," IEEE Journal of Lightwave Technology, Vol. 7, pp. 1071-1082, 1989.

Olsson N.A and Ziel J.P. Vander, "characteristics of semiconductor laser pumped Brillouin amplifier with electronically controlled bandwidth," IEEE Journal of LightWave Technology, Vol. Lt-5, No.1, pp. 147-153, Jan 1987.

Onishchukov G., Lokhnygin V., Shipulin A., and Golles M., "Differencial binary phase-shift keying transmission using cascaded semiconductor optical amplifier," *Proceedings of CLEO/Pacific Rim'99*, Vol. 2, pp. 513-514, 1999.

Ono H., Yamada M., Kanamori T., Sudo S., and Ohishi Y., "1.58-μmband gain-flattened erbium-doped fiber amplifiers for WDM transmissions systems," IEEE Journal of Lightwave Technology, Vol. 17, pp. 490-496, Nov. 1999.

Otani T., Kawazawa T., Goto K., Tapeeda N. and Akiba S., "16 Channels 2.5 Gb/s WDM train experiment over 9000 km by using gain equalized amplifier repeaters," Electronics Letters, Vol. 33, No. 4, pp.309-310, Feb 1997.

Patrick D.M. and Manning R.J., “20 Gb/s wavelength conversion using semiconductor nonlinearity,” Electronic Letters, Vol.30, pp.252-253, Feb. 1994.

Payne D.N, Mears R.J., Reekie L. and Jauncey I.M., “Low-noise erbium-doped fiber amplifier at 1.54 μm,” Electron Letters, Vol. 23, pp. 1026-1028, 1987.

Pedersen B., Bjarklev A., Povlsen J. H., Dybdal K. and Larsen C. C., “ The design of erbium-doped fiber amplifiers,” IEEE Journal of Lightwave Technology, Vol. 9, No. 9, pp. 1105-1112, 1991.

Perino J.S., Wiesenfield J. M., Glance B., “Fiber transmission of 10 Gbit/s signals following wavelength conversion using a traveling -wave SOA”, Electronic Letters, Vol. 30, No. 3, pp. 256-258, Feb. 1994.

Pincemin E., Lourec P.L., Audouin O., Dany B., Wabnitz S., “Analysis of synchronous intensity modulation control of 40 Gbit/sdispersion-managed soliton transmissions,” *Optical Fiber Communication Conference, 2000*, Vol. 1, Issue 2000,pp. 45- 47, 2000.

Pizzinat Anna, Santagiustina Marco, and Schivo Cristian, “Impact of hybrid EDFA-distributed Raman amplification on a 4 × 40-Gb/s WDM optical communication system,” IEEE Photonics Technology Letters, Vol. 15, pp. 341-343, 2003.

Rasmussen C., Fjelde T., Bennike J., Liu F., Dey S., Mikkelsen B., Mamyshev P., Serbe P., Wagt P., Akasaka Y., Harris D., Gapontsev D., Ivshin V., and Reeves-Hall P. , “DWDM 40G transmission over trans-pacific distance (10 000 km) using CSRZ-DPSK, enhanced FEC, and all-Raman-amplified 100-km ultra wave fiber spans,” IEEE Journal of Lightwave Technology, Vol. 22, No.1, pp. 203-207, January 2004.

Ross F. E., “FDDI: A tutorial,” IEEE Communication Magazine, Vol. 24, No.5, pp.10-17, May 1986.

Ross F. E., “An overview of FDDI: the fiber distributed interface,” IEEE Journal on Selected Areas in Communications, Vol. 7, No. 7, pp.1043-1051, Sept.1989.

Rothnie D.M., Midwinter J.E., “Improved standard fiber performance by positioning the dispersion compensating fiber,” Electronic Letters, Vol. 32, No. 20, pp1907-1908, Sept.1996.

Rottwitt Karsten, Provisen Jørn Headegaard and Bjarklev Anders, “Long distance transmission through distributed erbium-doped fibers,” IEEE Journal of Lightwave Technology, Vol. 11, No. 12, pp.2105-2115, Dec.1993.

Saito T., Sunohara Y., Fukagai K., Ishikawa S., Henmi N., Fujita S., and Aoki Y., "High receiver sensitivity at 10 Gb/s using an Er-doped fiber preamplifier pumped with a 0.98 μm laser diode," IEEE Photonics Technology Letters, Vol. 3, pp. 551-553, 1991.

Saleh B. and Teich M., "*Fundamental of Photonics*," chapter 15 and 16, John Wiley Publisher, New York, 1991.

Schnabel R., "Polarization insensitive frequency conversion of a 10 channel OFDM signal using FWM in SOA," IEEE Photonics Technology Letters, Vol.6, pp.56-58, Jan. 1994.

Senior J.M., "*Optical fiber communications*," Prentice Hall, New York, 1992.

Seo Y.K., Choi C.S and Choi W.Y, "All optical signal up conversion for radio to fiber application using cross gain modulation in semiconductor optical amplifier," IEEE Photonics Technology Letters, Vol.14, pp.1448-1450, Oct.2002.

Settembre Marina, Mater Francesco a, H¨agele Volker, Gabitov Idar Mattheus, Arnold W., and Turitsyn Sergei K., "Cascaded optical communication systems with in-line semiconductor optical amplifiers," IEEE Journal of Lightwave Technology, Vol. 15, No.6, pp. 962-967, June 1997.

Sharma Ajay K., Sinha R.K., and Agarwala R.A, "Higher order Dispersion Compensation by Differential Time Delay," Journal of Optical Fiber Technology, Vol. 4, pp. 135-143, 1998.

Sharma Ajay K., Sinha R.K., and Agarwala R.A., "Improved Analysis of Dispersion Compensation using Differential Time delay for High-speed Long-span Optical Link," Fiber and Integrated Optics incorporating International Journal on Optoelectronics, Vol. 16, no. 4, Oct. 1997.

Sharma Ajay K., Sinha R.K., and Agarwala R.A, "On Differential Time Delay governing higher order terms," International Journal of Light and Electron Optics, Optik Vol. 111, No. 7, pp. 310-313, 2000.

Singh S. and Kaler R.S., "1190 km WDM transmission of 20 × 10 Gb/s RZ-DPSK signals using cascaded in-line semiconductor optical amplifier," *Proceedings of International Conference on Optics and Optoelectronics, ICOL-05*, PP-FIO-42, Dec. 2005.

Singh S. and Kaler R.S.," Minimization of cross gain saturation in wavelength division multiplexing by optimizing differential gain in semiconductor optical amplifiers,"

Fiber and Integrated Optics incorporating International Journal on Optoelectronics, Vol. 25, Issue 4, pp. 287-303 June 2006.

Singh S. and Kaler R.S., "Transmission performance of 20 × 10 Gb/s WDM signals using cascaded optimized SOAs with OOK and DPSK modulation formats", Journal of Optics Communication, Vol. 266, Issue 1, pp. 100-110, October 2006.

Singh Y. N., Jain V. K. and Gupta H. M., "Semiconductor optical amplifiers in WDM star networks," *IEE proceedings-Optoelectronics,* Vol.143, No.2, pp.144-152, April 1996.

Singh Y. N., Jain V. K. and Gupta H. M., "Semiconductor optical amplifiers in WDM tree-net," IEEE Journal of Lightwave Technology, Vol. 15, No.2, pp. 252-260, February, 1997.

Sinha R.K. , Garg S. and Deori K.L. , "Design of a Thin-Film-Based Optical Filter for Broadband Multichannel Communication Systems," Czechoslovak Journal of Physics, Vol. 53, No. 5, pp. 417-424, May 2003.

Song H. J., Lee J.S. and Song J.I., "Signal up conversion by using a cross phase modulation in all optical SOA-MZ1 wavelength converter," IEEE Photonics Technology Letters, Vol.16, No.2, pp. 593-595, Feb. 2004.

Spiekman L. H., "Applications of semiconductor optical amplifier," *Proceeding of ECOC-IOOC* vol. 5, Tutorial We1.3, 2003.

Spiekman L. H., Wiesenfeld J. M., Gnauck A. H., Garrett L. D., Hoven G. N. van de, Dongen T. van, Sander-Jochem M. J. H., and Binsma J. J. M., "Transmission of 8 DWDM channels at 20 Gb/s over 160 km of SMF using a cascade of SOA," IEEE Photonics Technology Letters, Vol. 12, pp. 717-719, June 2000.

Storkfelt N., Mikkelsen B., Olesen D.S., Yamaguchi M. and Stubkjaer K.E., "Measurement of carrier life time and line enhancement factor for 1.5 μm ridge waveguide laser amplifier," IEEE Photonics Technology Letters, Vol.3, pp.632-634, 1991.

Sun Y., Srivastava A. K., Banerjee S., and Sulhoff J. W., "Error-free transmission of 32 × 2.5 Gbit/s DWDM channels over 125 km using cascaded inline semiconductor optical amplifiers," Electronic Letters, Vol. 35, pp.1863-1865, 1999.

Taga H., Edagawa N., Yoshida Y., Yamamoto S. and Wakabayashi H., "IM-DD long-distance multichannel WDM transmission experiments using Er-doped fiber amplifiers," ," IEEE Journal of Lightwave Technology, Vol.12, No.8 pp.1448-1454, 1994.

Takahashi N., Hirono T., Akashi H., Takahashi S. and Sasaki.T., "An output power stabilized erbium doped fiber amplifier with automatic gain control,". IEEE Journal of selected topic in Quantum Electronics, Vol. 3, No. 4, pp. 1019-1025, 1997.

Tancevski L. and Rush L.A., "Sub microsecond transient time responses in cascades of EDFAs," *International Conference on Application of Photonics Tech.(Photonics North)*, Vol. SPIE 3491, pp 553-568, 1998.

Vareille G. Petel F., Uhel R., Bassier, G., Collet J.P., Bourret G., Marcerou J.F., "340 Gb/s (34 x 10Gb /s, 50GHz spacing DWDM) straight line transmissions over 6380 km with full system implementation assessment," *Proceedings of Optical Fiber Communications Conferences*, paper PD18, Feb., 1999.

Willner A.E. and Hwant S.M., "Transmission of many WDM channels through a cascade of EDFA' s in long distance links and ring networks," IEEE Journal of Lightwave technology, Vol.13, No. 5, pp. 802-816, May 1995.

Wagner S. S., "Optical amplifier applications in fiber optic local networks," IEEE Transactions on Communications, Vol. 35, No. 4, pp.419-426, April 1987.

Wei X. and Zhang L., "Analysis of phase noise in saturated SOAs for DPSK applications," IEEE Journal of Quantum Electronics, Vol. 41, No. 4, pp. 554-561, April 2005.

Wei X., Su Y., Liu X., Leuthold J. and Chandrasekhar S., "10 Gb/s RZ-DPSK transmitter using a saturated SOA as a power booster and limiting amplifier," IEEE Photonics Technology Letters, Vol. 16, No. 6, pp. 1582-1584, June 2004.

Wolfson D., Danielsen S. L., Joergensen C., Mikkelsen B., and Stubkjaer K.E., "Detailed theoretical investigation of the input power dynamic range for gain-clamped semiconductor optical amplifier gates at 10 Gb/s," IEEE Photonics Technology Letters, Vol. 10, pp. 1241-1243, Sept.1998.

Wysocki P.F., Judkins J.B., Espindola R.P., Andrejco M., Vengsarkar A.M. and Walker K., "Broad-band erbium-doped fiber amplifier flattened beyond 40 nm using long-period grating filter," IEEE Photonics Technology Letters, Vol. 9, No.10, pp. 1343-1345, 1997.

Xu C., Liu X., Mollenauer L. F., and Wei X., "Comparison of return-to-zero differential phase-shift keying and on-off keying in long-haul dispersion managed transmission," IEEE Photonics Technology Letters, Vol. 15, pp. 617-619, Apr. 2003.

Xu Shuangmei, Khurgin J.B., Vurgaftman I. and Meyer J.R., "Reducing crosstalk and signal distortion in wavelength-division multiplexing by increasing carrier lifetimes in semiconductor optical amplifiers," IEEE Journal of Lightwave Technology, Vol. 21, No. 6, pp. 474-1485, 2003.

Xu Shuangmei and Khurgin J. B., "A dispersion management scheme for reducing SOA-induced crosstalk in WDM links," IEEE Journal of Lightwave Technology, Vol. 22, No. 2, pp. 417-422, Feb.2004.

Yamatoya T. and Koyama F., "Novel optical preamplifier with inverted ASE signal of semiconductor optical amplifier," *in Proc. ECOC'01*, Vol. 2, 2001, pp. 176–177.

Yamatoya T. and Koyama F., "Optical preamplifier using optical modulation of amplified spontaneous emission in saturated semiconductor optical amplifier," IEEE Journal of Lightwave Technology, Vol. 22, pp. 1290-1295, 2004.

Yeh C. H., Chien H. C., Lee C. C. and Chi S., "Gain-clamping erbium doped waveguide amplifier module using optical feedback technique," Journal of Optics Communications, Vol. 246, pp. 73-77, 2005.

Yoneda, S. and Okshi, T., "Erbium-doped fiber amplifiers for all fiber video distribution systems," IEICE Transaction on Communication, E-75B9, pp. 850-861, 1992.

Zhao Mingshan, Morthier Geert and Baets Roel, "Analysis and optimization of intensity noise reduction in spectrum-sliced WDM systems using a saturated semiconductor optical amplifier," IEEE Photonics Technology Letters, Vol. 14, No. 3, pp.390-392, March 2002.

Zimmerman Donald R. and Spiekman Leo H., "Amplifiers for the masses: EDFA, EDWA, and SOA amplets for metro and access applications," IEEE Journal of Lightwave Technology, Vol. 22, No.1, pp. 66-70, January 2004.

Papers in International Refereed Journals:

1. Surinder Singh and R.S.Kaler, "Wide Band Optical Wavelength Converter Based on Four Wave Mixing Using Optimized Semiconductor Optical Amplifier," Fiber and Integrated Optics incorporating International Journal on Optoelectronics, *Taylor and Francis,* UK, vol. 25, Issue 3, pp. 213-230, May 2006.
2. Surinder Singh and R.S.Kaler, "Minimization of Cross Gain Saturation in Wavelength Division Multiplexing by Optimizing Differential Gain in Semiconductor Optical Amplifiers," Fiber and Integrated Optics incorporating International Journal on Optoelectronics, *Taylor and Francis,* UK, vol. 25, Issue 4, pp. 287-303, July 2006.
3. Surinder Singh and R.S.Kaler, "Receiver Sensitivity Improvement Using Polarization Insensitive Semiconductor Optical Amplifier," International Journal of Optical Engineering, Vol. 45, Issue 6, pp. 65007-1-6, *SPIE*, OE 050772, USA, *(available online: spie .org)*.
4. Surinder Singh and R.S.Kaler, "Gain Flattening Approach to Physical EDFA for 16 × 40 Gb/s NRZ-DPSK WDM Optical Communication Systems," Fiber and Integrated Optics incorporating International Journal on Optoelectronics, *Taylor and Francis*, UK**,** Vol. 25, Issue 5, pp. 363-374, September, 2006.
5. Surinder Singh and R.S.Kaler, "Transmission Performance of 20 × 10 Gb/s WDM signals using Cascaded Optimized SOAs with OOK and DPSK Modulation Formats," Journal of Optics Communication, Vol. 266, Issue 1, pp. 100-110, October 2006, Netherlands *(available online: sciencedirect.com)*.
6. Surinder Singh and R.S.Kaler,"Simulation of DWDM signals using optimum span scheme with cascaded optimized semiconductor optical amplifiers," optik-International Journal for Light and Electron Optics, Vol. 118, Issue 2, pp. 74-82, Jan. 2007, Germany, *(available online: sciencedirect.com).*
7. Surinder Singh and R.S.Kaler," All Optical Wavelength Converters Based on Cross Phase Modulation in SOA-MZI Configuration," optik-International Journal for Light and Electron Optics, Vol. 118, Issue 8, pp. 390-394, Aug. 2007, Germany, *(available online: sciencedirect.com)*.

8. Surinder Singh and R.S.Kaler, "Analysis and Minimization of Cross Phase Modulation in Semiconductor Optical Amplifiers for Multichannel WDM Optical Communication Systems," International Journal of Optics Communication, Vol. 274, Issue 1, pp. 105-115, June 2007, Netherlands *(available online: sciencedirect.com).*
9. Surinder Singh and R.S.Kaler," Placement of Optimized Semiconductor Optical Amplifier in Fiber Optical Communication Systems," *Article in Press for* publication in optik-International Journal for Light and Electron Optics, Ref. IJLEO 50308, Germany, *(available online: sciencedirect.com).*

Papers published in International Conferences:

10. Surinder Singh and R.S.Kaler, "NRZ to RZ Modulation Format Conversion Using SOA," presented and published in proceeding of International Conference on Optics & Optoelectronics organized Instruments Research & Development Establishment, Dehradun, Uttaranchal (INDIA) and Paper No. PP-OPD-4, 12-15th December 2005.
11. Surinder Singh and R.S.Kaler, "1190 Km WDM Transmission of 20 × 10 Gb/s RZ-DPSK signals using Cascaded In-line Semiconductor Optical Amplifier," presented and published in proceeding of International Conference on Optics & Optoelectronics organized by Instruments Research & Development Establishment, Dehradun, Uttaranchal (INDIA), Paper No.PP-FIO-42, 12-15th December 2005.
12. Surinder Singh and R.S.Kaler, "Transmission performance of 16 × 40 Gb/s NRZ-DPSK signals using cascaded gain saturable EDFA," presented and published in proceeding of International Conference on Optics & Optoelectronics organized by Instruments Research & Development Establishment, Dehradun, Uttaranchal (INDIA), Paper No. PP-FIO-43, 12-15th December 2005.
13. Surinder Singh, H. K. Sidhu and R. S. Kaler, "Performance Analysis of EDFA Physical Model in Optical Fiber communication systems," published in International conference on Active and Passive optical components for WDM Communication at Boston, USA, 2006.
14. Surinder Singh and R. S. Kaler, "Power Budget Improvement of WDM Optical Communication Systems by Using Gain Flattening of EDFA for 16 × 40 Gb/s," presented and published in Indo-UK Workshop on "Recent Advances in Fiber Optics and Photonics - RAFOP 2006, pp. 125-128, IIT, Roorkee, India.

(a) Analysis of Gain in Multichannel WDM System

The equation (15) is solved by taking the variation of time. As time varies the position of the power and carrier density changes in SOA accordingly and hence gain changes. For the variation of time and position, we assume that

$$\int_{-\infty}^{t_1} P(t,z)dt = P(t_1,z_1)$$

$$\int_{-\infty}^{t_2} P(t,z)dt_2 = \int_{-\infty}^{t_1} P(t_1,z_1)dt_1 = P(t_2,z_2)$$

So on

$$\int_{-\infty}^{t_n} P(t,z)dt_n = \int_{-\infty}^{t_{n-1}} P(t_1,z_1)dt_{n-1} = \cdot\ \cdot\ \cdot\ \cdot\ \cdot\ \cdot\ \cdot\ \cdot\ \cdot\ \cdot = P(t_n,z_n) \quad \text{(A1)}$$

By applying the above assumption from equation (A1) into equation (15), we get

$$g(t_1,z_1) = \exp\left(-\frac{P(t_1,z_1)}{\tau}\right)\left\{\int_{-\infty}^{t_1}\left[\frac{a\Gamma}{\tau}\left[\frac{I\,\tau}{wqt_a} - N(t,z)L\right]\exp\left(\frac{P(t_1,z_1)}{\tau}\right)dt\right]\right\} \quad \text{(A2)}$$

Due to nature of the SOA, we also take another assumption of time varying as

$$\int_{-\infty}^{t_1} \exp\left(\frac{P(t,z)}{\tau}\right)dt = \frac{\exp\left(\frac{P(t_1,z_1)}{\tau}\right)}{\partial P(t_1,z_1)/\tau\partial t} \quad \text{A3)}$$

The time rate of change of power is small and life time is also low. These parameters have negligible affect on optimization of confinement factor. For simplicity, we considered these parameters are constant.

$$P_{L_0} = \frac{\partial P(t_1,z_1)}{\tau\partial t}$$

and

$$P_{L_1} = \frac{\partial P(t_2,z_2)}{\tau\partial t} \quad \text{(A4)}$$

As variation in parameters from P_{L_0} to P_{L_1} is too small, we can write it as

$$P_{L_0} = P_{L_1} = P_L \quad \text{(A5)}$$

We are applying the conditions and assumptions from equations (A3), (A4) and (A5) into (A2). After solving, we get

$$g(t_1,z_1)=\frac{a\Gamma}{\tau P_L}\exp\left(-\frac{P(t_1,z_1)}{\tau}\right)\left[\begin{array}{l}\frac{I\tau}{wqt_a}\exp\left(\frac{P(t_2,z_2)}{\tau}\right)\\+\sum_{n=1}^{M}\frac{(-1)^n}{P_L^{n-1}}L\,\overline{N}^n(t_n,z_n)\exp\left(\frac{P(t_{n+1},z_{n+1})}{\tau}\right)\end{array}\right] \quad \text{(A6)}$$

Where $\overline{N}^n=\partial N(t_n,z_n)/\partial t_1^n$ is the rate of change of carrier density with time. From equation (A6), we considered the power variations as

$$P(t_2,z_2)\text{-}P(t_1,z_1)=\Delta P_1$$

and $$P(t_{n+1},z_{n+1})\text{-}P(t_1,z_1)=\Delta P_n \quad \text{(A7)}$$

Then equation (A6) can be written as

$$g(t_1,z_1)=\frac{a\Gamma}{\tau P_L}\left[\frac{I\tau}{wqt_a}\exp\left(\frac{\Delta P_1}{\tau}\right)+\sum_{n=1}^{M}\frac{(-1)^n}{P_L^{n-1}}L\,\overline{N}^n(t_n,z_n)\exp\left(\frac{\Delta P_n}{\tau}\right)\right] \quad \text{(A8)}$$

(b) Analysis of Gain Variation in Multichannel WDM System

By applying equation (A1) to equation (19), then equation becomes

$$\Delta g(t_1,z_1)=\exp\left(-\frac{P(t_2,z_2)}{\tau}\right)\left[\begin{array}{l}\int_{-\infty}^{t_1}\frac{a\Gamma}{\tau}\left[\frac{I\tau}{wqt_a}-N(t,z)L\right]\exp\left(\frac{P(t_2,z_2)}{\tau}\right)dt_1\\-g(t,z)\int_{-\infty}^{t_1}\frac{P(t,z)}{\tau}\exp\left(\frac{P(t_2,z_2)}{\tau}\right)dt_1\end{array}\right] \quad \text{(A9)}$$

As from equation (17), the gain is constant. Considered the variation in gain is

$$\Delta g(t_1,z_1)=I_1+I_2 \quad \text{(A10)}$$

By applying the equations (A3), (A4) and (A5) into (A10), we have

$$I_1=\frac{a\Gamma}{\tau P_L}\exp\left(-\frac{P(t_2,z_2)}{\tau}\right)\left[\begin{array}{l}\frac{I\tau}{wqt_a}\exp\left(\frac{P(t_3,z_3)}{\tau}\right)\\+\sum_{n=1}^{M}\frac{(-1)^n}{P_L^{n-1}}L\,\overline{N}^n(t_n,z_n)\exp\left(\frac{P(t_{n+2},z_{n+2})}{\tau}\right)\end{array}\right] \quad \text{(A11)}$$

$$I_2=\sum_{n=1}^{M}\frac{(-1)^n}{\tau P_L^n}g(t,z)\,\overline{P}^{n-1}(t_{n-1},z_{n-1})\exp\left(-\frac{P(t_2,z_2)}{\tau}\right)\exp\left(\frac{P(t_{n+2},z_{n+2})}{\tau}\right) \quad \text{(A12)}$$

Where $\overline{P}(t_1,z_1)=\partial P(t,z)/\partial t$ is the rate of change of power with time. Also $\overline{N}^{n}=\partial N(t_n,z_n)/\partial t_1^n$ is the rate of change of carrier density with time. Substituting equations (A11) and (A12) into equation (A10) and also by using equation (A7), we have

$$\begin{aligned}\Delta g(t_1,z_1)=&\frac{a\Gamma I}{wqt_a P_L}\exp\left(\frac{\Delta P_1}{\tau}\right)\\&+\frac{1}{\tau}\sum_{n=1}^{M}\frac{(-1)^n}{P_L^n}\exp\left(\frac{\Delta P_n}{\tau}\right)\left[a\Gamma L\,\overline{N}^{n}(t_n,z_n)-g\,\overline{P}^{n-1}(t_{n-1},z_{n-1})\right]\end{aligned}\tag{A13}$$

Substituting the gain coefficient of equation (10) into (A13), then gain variation is

$$\Delta g(t_1,z_1)=\frac{a\Gamma}{\tau P_L}\left[\frac{I\tau}{wqt_a}\exp\left(\frac{\Delta P_1}{\tau}\right)+\sum_{n=1}^{M}\frac{(-1)^n}{P_L^{n-1}}L\exp\left(\frac{\Delta P_n}{\tau}\right)\times\left[\overline{N}^{n}(t_n,z_n)-(N(t,z)-N_t)\overline{P}^{n-1}(t_{n-1},z_{n-1})\right]\right]\tag{A14}$$